学位論文

Development of Boron Carriers Equipped with Mono- and Dimeric Macrocyclic Polyamines and Their Zinc(II) Complexes for Boron Neutron Capture Therapy

（ホウ素中性子捕捉療法のための大環状ポリアミン単量体、二量体およびその亜鉛錯体を有するホウ素キャリアーの開発）

Doctoral Thesis

Tokyo University of Science

２０２２年（令和４年）３月

Hiroki Ueda

(Supervisor: Prof. Shin Aoki)

Contents

Abbreviation

aq.	aqueous
$ATB^{0,+}$	amino acid transporter system $B^{0,+}$
ATR	attenuated total reflection
A549 cells	human caucasian lung carcinoma
B	boron
^{10}B	boron-10
^{11}B	boron-11
$BF_3 \cdot OEt_2$	trifluoroborane diethylether complex
$B(OH)_3$	boric acid
Boc	*tert*-butoxycarbonyl
Borax	sodium tetraborate
brs	broad signal
BNCT	boron neutron capture therapy
BPA	L-4-boronophenylalanine
BPO	benzoyl peroxide
BSH	disodium mercaptoundecahydrododecaborate
***n*-BuLi**	*n*-butyllithium
ca.	circa, about
CCDC	cambridge crystallographic data center
CIF	crystallographic information file
cm^{-1}	wavenumber(s)
ctDNA	calf thymus DNA
dA	adenine
dT	thymidine
d(TpT)	thymidyl(3′–5′)thymidine

DMEM	Dulbecco's modified Eagle medium
DMSO	dimethyl sulfoxide
DNA	deoxyribonucleic acid
EPR	enhanced permeability and retention
eq	equation
equiv	equivalent
ESI	electrospray ionization
et at.	and others
Et_2O	diethyl ether
EtOH	ethanol
f	femto
FBS	fetal bovine serum
^{18}F-BPA	L-4-borono-3-[^{18}F]fluorophenylalanine
GLUT	glucose transporter
HeLa S3 cells	human cervical carcinoma
HEPES	4-(2-hydroxyethyl)-1-piperazineethanesulfonic acid
HRMS	high resolution mass spectrometry
Hz	hertz
IMR-90 cells	normal human fibroblast
ICP-MS	inductively coupled plasma mass spectrometry
IC_{50}	half-maximum inhibitory concentration
IR	infrared
Jurkat cells	human T lymphocyte cells
KURNS	the Institute for Integrated Radiation and Nuclear Science, Kyoto University
K_d	dissociation constant
LAT	L-type amino acid transporter

LET	linear energy transfer
m-	meta
m/z	mass-to-charge ratio
M^+	parent molecular ion
Me	methyl
MeCN	acetonitrile
MEM	minimum essential medium
MeOH	methanol
MeV	mega electron volt
min	minute(s)
mL	milliliter
mM	millimolar
mol	mole(s)
mp	melting point
MRI	magnetic resonance imaging
MS	mass spectrometry
MTT	3-(4,5-di-methylthiazol-2yl)-2,5-diphenyltetrazolium bromide
MβCD	methyl-beta-cyclodextrin
n	neutron(s)
n_{th}	thermal neutron(s)
N	normality
NBS	*N*-bromosuccinimide
NMR	nuclear magnetic resonance
ORTEP	Oak Ridge Thermal-Ellipsoid Plot Program
o-	ortho
p-	para
PBS	phosphate buffered saline

PCPB	*p*-carboxyphenylboronic acid
PDT	photodynamic therapy
PepT1	peptide transporter
PET	positron emission tomography
Ph.D.	Doctor of Philosophy
PTS	polyamine transport system
quant.	quantitative
RNA	ribonucleic acid
rt	room temperature
rpm	revolutions per minute
SD	standard deviation
SDS	sodium dodecyl sulfate
SQAG	sulfoquinovosyl acyl glycerol
SPD	spermidine
SPM	spermine
$t_{1/2}$	half-life
T_m	thermal melting
T/B	tumor to blood
T/N	tumor to normal cell
TFA	trifluoroacetic acid
THF	tetrahydrofuran
TK1	thymidine kinase 1
TLC	thin-layer chromatograpy
TMS	tetramethylsilane
TSP	3-(trimethylsilyl)propionic-2,2,3,3-d_4 acid sodium
UV	ultraviolet
vis	visible

[9]aneN$_3$	1,4,7-triazacyclononane (tacn)
[12]aneN$_4$	1,4,7,10-tetraazacyclododecane (cyclen)
[15]aneN$_5$	1,4,7,10,13-pentaazacyclopentadecane
Å	angstrom(s)
°C	degrees Celsius
μ	micro
σ	barn
γ	gamma

Chapter 1.

General Introduction

[1-1] General introduction of boron neutron capture therapy

As of 2020, the numbers of cancer incident and mortality have increased to almost 19.3 million and 10.0 million cases, respectively, and it is predicted that the burden of new cancer cases is going to increase to 28.4 million in 2040.[1] In several decades, the cancer therapy has been developed due to the understandings of cancers and can be classified into three main groups; surgery, chemotherapy, and radiation therapy.[2] In surgery, tumor tissues are removed from the patients in a physical manner using laparoscopic and robotic surgery, lasers, and so on. However, these invasive methods may cause pain in the bodies during and after treatments and not applicable to infiltrative cancers.

The chemotherapy could be effective against cancer cells spread to whole the body. In addition, various types of anti-cancer agents have been developed including small ~ large molecules, which could be stably provided on a large scale and a consistent quality. However, this treatment may induce side effects such as fatigue feeling, hair loss and so on, due to the unexpected cell death in healthy cells.

The last method is the radiotherapy which has been established as non-invasive methods for cancer treatment using X-ray, γ-ray, proton, and heavy ions. Theoretically, it is possible to selectively irradiate various type of tumors with minimum damage to normal cells. One of the disadvantages of radiation therapy, however, is side effect such as mouth and throat problem and dysfunction of target organs due to irradiation with adjacent normal tissues.

Although combinations of these methods are generally used according to tumor types, tumor size and location, age, genetic reasons, and some related situations, these options are sometimes not sufficient for the treatment of multiple tumor types such as lung, breast, liver, stomach, and colon and rectum, which are the most common causes of cancer death. In this context, the development of more effective and safer methods is highly desirable.

Boron neutron capture therapy (BNCT) is one of a radiotherapy based on the nuclear reaction ($^{10}B(n, \alpha)^{7}Li$) between boron-10 (^{10}B)-containing drugs and thermal neutrons (^{1}n), giving high linear energy transfer (LET), alpha (α, (^{4}He)) particle and lithium (^{7}Li) nuclei (eq. 1-1).[2,3]

$$^{10}B + n_{th} \longrightarrow [^{11}B] \begin{cases} \xrightarrow{6\%} {}^{4}He + {}^{7}Li + 2.79\ MeV \\ \xrightarrow{94\%} {}^{4}He\ (1.47\ MeV) + {}^{7}Li\ (0.84\ MeV) + \gamma\ (0.48\ MeV) \end{cases} \quad \text{(eq. 1-1)}$$

It is known that the reactivity of ^{10}B nuclei with low energy thermal neutrons is much higher than that of the nucleus constituting biological molecules listed in Table 1-1.[2,4] In addition, the generated two heavy particles induce an excitation and ionization of molecules within short path length of 5-9 μm, suggesting that the developments of ^{10}B delivery agents/systems would achieve for the selective treatment of a single cells containing ^{10}B species.

Table 1-1. Thermal neutron capture cross-sections of the elements in tissues and boron (^{10}B and ^{11}B).

Nuclide	Cross-section σ_{th} (barn)[a]	Weight% in mammal tissues
^{1}H	0.333	10.00
^{12}C	0.0035	18.00
^{14}N	1.83	3.00
^{16}O	0.00019	65.00
^{23}Na	0.43	0.11
^{24}Mg	0.0053	0.04
^{31}P	0.18	1.16
^{32}S	0.53	0.2
^{35}Cl	32.68	0.16
^{39}K	2.1	0.20
^{40}Ca	0.4	2.01
^{56}Fe	2.57	0.01
^{10}B	3838	none
^{11}B	0.0055	none

[a] Barn (1 barn = 10^{-24} cm^2) is a unit of thermal neutron cross-section, which mean the reactivity of each atom with thermal neutrons.

The typical procedure of BNCT has been established in the following manners: (i) cancer patients are treated with cancer-specific ^{10}B agents; (ii) after accumulation of ^{10}B atoms into cancer cells, the target region are irradiated with thermal or epithermal neutrons, which is generated from an accelerator-based system in a medical institute; and (iii) ^{10}B-containing cells are selectively induced the cytotoxic effect due to two heavy particles because a single cell size is approximately 10~20 μm (Scheme 1-1).[5]

One of the main advantages of this binary system is that it provides radiation dose contrast between normal and cancer cells by using a combination of low toxic thermal neutrons and ^{10}B drugs. In 2020, this method has been approved for the treatment of

recurrent head and neck cancer by the Ministry of Health, Labor and Welfare of Japan.[6] Besides, it is expected that BNCT would be applied to the treatment of refractory cancer such as lung, liver, and breast cancer if the development of boron delivery agents could be successfully proceeded in the near future (Scheme 1-2).[7]

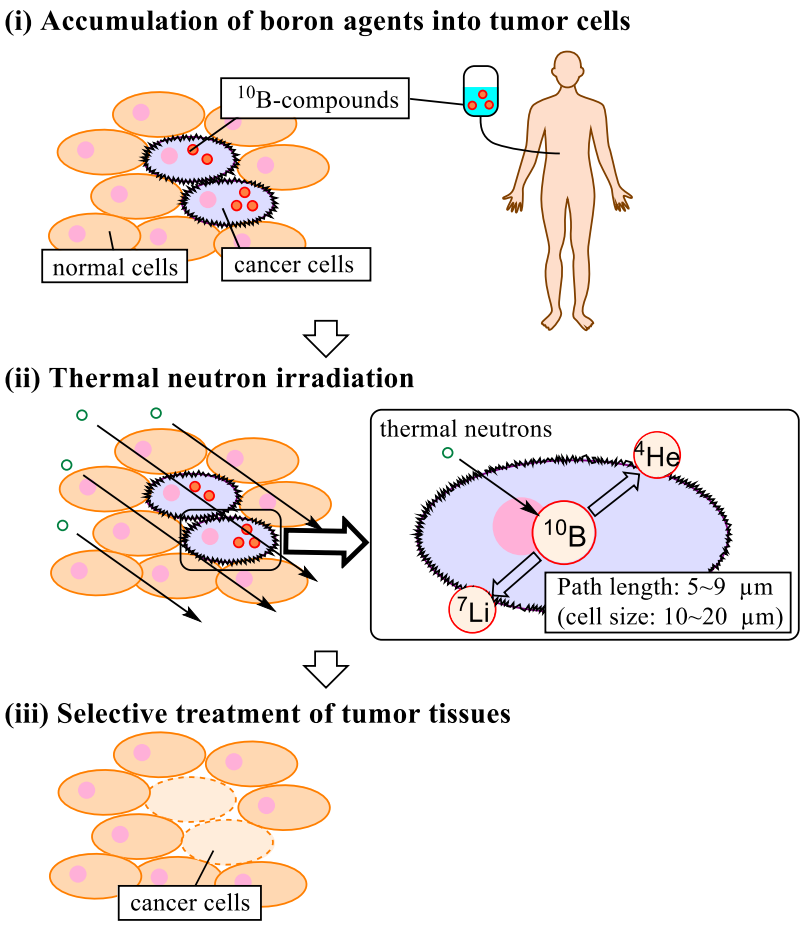

Scheme 1-1. Typical procedure of boron neutron capture therapy.

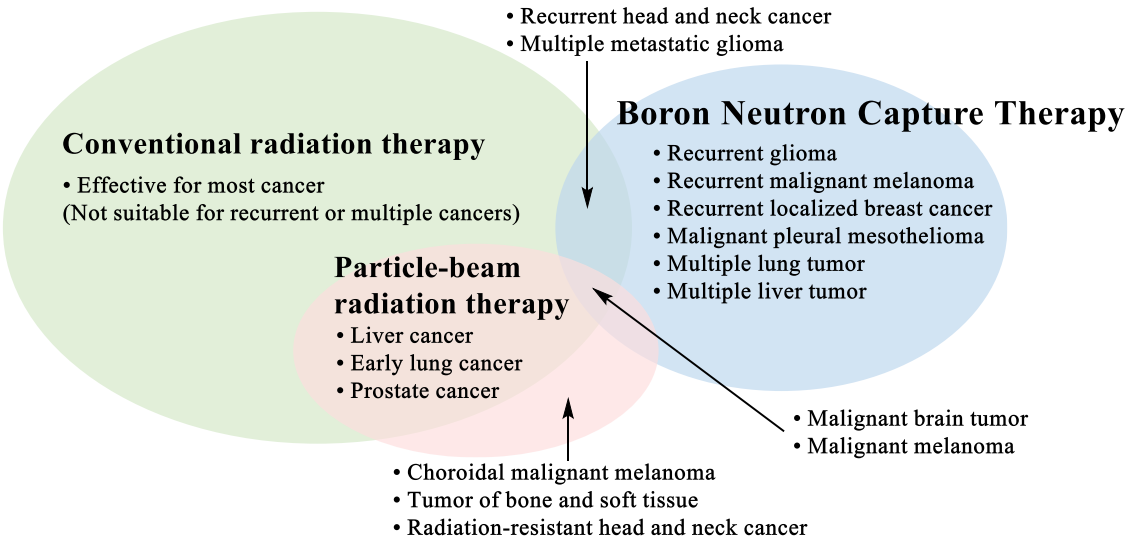

Scheme 1-2. Classification of tumor types of radiotherapy.

[1-2] Clinically used BNCT agents and BNCT drug candidates

Since selective and high accumulation of ^{10}B-containing drugs into cancer cells are highly required for successful BNCT, the design of BNCT drugs demands for the following criteria: (1) low toxic and higher uptake into tumor cells than in healthy cells (tumor to blood (T/B) ratios should be greater than 3); (2) ^{10}B atoms must be retained in the tumor tissue but also be rapidly cleared from blood and normal tissues; and (3) the ^{10}B concentration inside or near tumor cells must be $\geq 10^9$ ^{10}B atoms/cell (20–35 μg/gram of tumor tissue).[8]

In 1938, Kruger and colleagues performed the first in vivo BNCT experiment using boric acid ($B(OH)_3$) at the University of Illinois.[2,9] Sweet and coworkers carried out the clinical BNCT trials for the treatment of brain tumor using sodium tetraborate (borax) **1**, *p*-carboxyphenylboronic acid (PCPB) **2**, and sodium decahydrodecaborate **3** in 1951–1961 (Scheme 1-3).[10] The results suggested that these boron compounds were not effective for cancer treatment due to their weak retention in tumor tissues, resulting in the suspension of the project in the United States in 1961. It should be note that neutron

beam quality generated from reactors for the research purpose was insufficient for BNCT.

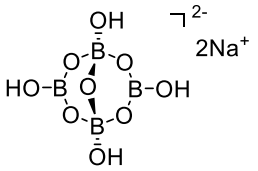

Borax
1

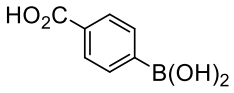

p-Carboxyphenylboronic acid (PCPB)
2

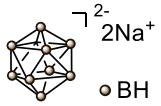

Decahydrodecaborate ($B_{10}H_{10}Na_2$)
3

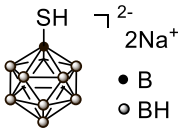

Mercaptoundecahydrododecaborate (BSH)
4
J. Am. Chem. Soc. **1964** (Ref. 11)

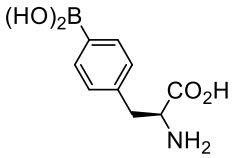

L-*p*-Boronophenylalanine (BPA)
5
J. Am. Chem. Soc. **1958** (Ref. 14)

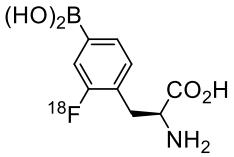

4-Borono-2-[^{18}F]fluoro-L-phenylalanine (^{18}F-BPA)
6
Appl. Radiat. Isot. **1991** (Ref. 19)

Scheme 1-3. Clinically used BNCT agents in the past and present.

To solve this problem, Soloway and Hatanaka reported on the development of disodium mercaptoundecahydrododecaborate (BSH) **4** (Scheme 1-3),[11] which showed weak toxicity and selective accumulation into malignant glioma (T/B: ca. 8.0).[12] In 1968, ^{10}B-enriched BSH (^{10}B-BSH) was used for the clinical BNCT trials for the treatment of brain tumors irradiated with thermal neutrons from the Hitachi Nuclear Reactor in Japan, and then sufficient evidences including 120 cases of malignant brain tumors during 1968–1992 were reported by Hatanaka et al.[13] However, a availability of BSH for cancer treatment by BNCT is restricted due to low accumulation activity into various tumor types.

For selective cancer treatment, Mishima and coworkers utilized the tyrosine analogue, L-4-boronophenylalanine (BPA) **5**[14] for the treatment of malignant melanoma, considering the large amounts consumption of tyrosine for the synthesis of melanin.[15] The first clinical BNCT treatment using ^{10}B-BPA (hydrochloride salts) was carried out in 1987, resulting in the success which initiated the related BNCT studies worldwide.[16] In 2001, Ono and coworkers conducted the clinical BNCT trials of recurrent head and neck cancers using ^{10}B-BPA (used as a complex with D-fructose to improve the solubility)[17] for the application to other types of cancers.[18] In addition, ^{18}F-labeled BPA (^{18}F-BPA) **6**[19] was developed for the detection of the accumulation of BPA into tumor tissues by means of positron emission tomography (PET).[20] In subsequent studies, it has been proposed that BPA **5** and ^{18}F-BPA **6** are transferred into cells through the amino acid transporters such as L-type amino acid transporter (LAT1) and amino acid transporter system $B^{0,+}$ ($ATB^{0,+}$), which are highly expressed in some type of cancer cells.[21,22] Although these findings suggested the successful application of BNCT, some problems are still remained such as the retention of BPA in tumor tissues and application to a multi-type of cancers. To improve the effectiveness, Ono and coworkers used a combination of BSH **4** and BPA **5**, indicating that novel boron agents having different accumulation pathway would be desirable for the combination with BPA.[23]

Over the past 30 years, the discovery of boron drugs has been attempted worldwide in order to satisfy the aforementioned criteria for the establishment of safer and more effective BNCT. Typical examples are boron-conjugate analogues such as porphyrins, nucleosides, polyamines, amino acids, and carbohydrates, as shown in Scheme 1-4. These compounds were designed and synthesized to selectively target cancer cells based on enhanced proliferation activity and/or upregulated proteins on cell membrane such as transporters, receptors, and so on (Table 1-2).

First, it is known that porphyrins and related macrocycles have a selective accumulation activity into tumor tissues.[24] In 1990, Kahl and coworkers reported on the

development of a boronated porphyrin, tetrakis-carborane carboxylate of 2,4-bis (*α*,*β*-dihydroxyethyl)-deutero-porphyrin IX (BOPP) **7**,[25] which is selectively accumulated into tumor tissues of tumor-bearing mice (Scheme 1-4).[26] However, in vitro BNCT studies suggested that BNCT activity of BOPP **7** is much weaker than that of BPA.[27] Besides, the application to photodynamic therapy (PDT) was interrupted in Phase I clinical trial due to the low selectivity to tumor tissues (T/B ratio : ca. 0.2) and much slower clearance ($t_{1/2}$ = 16.8 days) of BOPP **7** and their metabolites, which induced phototoxicity.[28]

Second, it is reported that the high expression of thymidine kinase 1 (TK1) which catalyze the phosphorylation of thymidine and 2′-deoxyuridine for RNA and DNA synthesis is observed in various type of tumors such as lung, breast, and prostate.[29,30] Therefore, it is expected that boron containing thymidine analogues would be accumulated into tumor cells after conversion to the anionic monophosphate.[31] To date, the design and synthesis of boron-containing biochemical precursors of nucleic acids were widely conducted, and one of the promising candidates, 3-[5-(2-(2,3-dihydroxyprop-1-yl)-*o*-carboran-1-yl)pentan-1-yl]thymidine (N5-2OH) **8**, was reported in 2002 by Barth and Tjarks groups.[31,32] Although the mean survival times of glioma-bearing rat was prolonged by BNCT using 3-carboranyl thymidine analogue (N5-2OH) **8**,[33] the clinical application has not been reported.

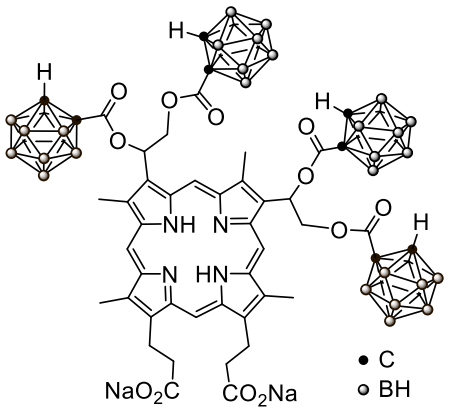

Boronated porphyrin (BOPP)
7
J. Chem. Soc., Chem. Commun. **1990** (Ref. 25)

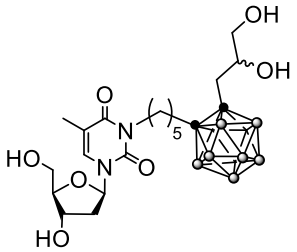

N-3-Substituted carboranyl thymidine (N5-2OH)
8
J. Med. Chem. **2002** (Ref. 32)

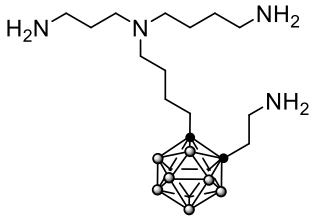

Carboranyl spermidine (ASPD-5)
9
J. Med. Chem. **1999** (Ref. 38)

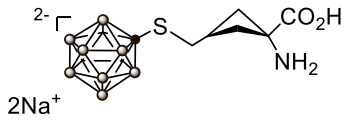

BSH conjugated amino acid (ACBC-BSH)
10
Amino Acids **2014** (Ref. 39)

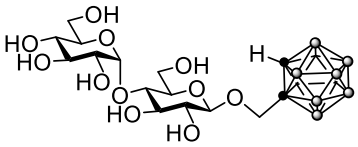

ortho-Carboranyl bisglycoside
11
Chem. Eur. J. **1998** (Ref. 43)

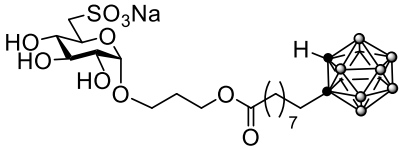

Carboranyl sulfoquinovosyl acyl glycerol (SQAG)
12
Chem. Pharm. Bull. **2017** (Ref. 46)

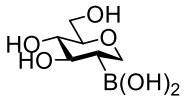

2-boryl-1,2-dideoxy-D-glucose
13
Bioorg. Med. Chem. **2018** (Ref. 47)

Scheme 1-4. Typical examples of boron-containing molecules.

Next, polyamine analogues has been considered to be one of the promising molecules for cancer treatment, because polyamine level in cancer cells is increased due to activated polyamine transport system (PTS) and biosynthesis.[34–37] In 1999, Soloway et al. reported on the development of boron-containing spermidine (SPD) and spermine (SPM) analogues as a new BNCT agents.[38] Although most promising compound, carboranyl polyamine analogue (ASPD-5) **9**, selectively accumulated into tumor tissues (T/B ratio: ca. 6.3), the boron concentration was not enough for BNCT, resulting that the development of boron-containing polyamine derivatives was suspended.

Recently, Hattori and coworkers reported that BSH-containing α,α-cycloalkylamino acids (ACBC-BSH) **10** inhibited the proliferation of cancer cells after thermal neutron irradiation due to moderate boron uptake via LAT1.[39] Besides, the mean survival time of tumor bearing rats was prolonged by BNCT utilizing a combination of ACBC-BSH **10** with BPA.[40] These results prospect that cyclic amino acid would be potential scaffold for boron delivery agents. Kabalka et al. has been also developed some cyclic amino acid analogues containing boronic acid group, which possess the selective accumulation activity into tumor tissues while their BNCT activity has not been reported.[41]

Finally, it is well known that tumor cells exhibit high glucose consumption and overexpression of glucose transporters (GLUTs) for their activated proliferation, which is known as Warburg effect.[42] To data, the design and synthesis of boron-containing carbohydrates such as **11** have been performed, while their biological potential such as tumor accumulation activity and BNCT effect has not been reported.[43–45] In addition, Tanaka, Itoh and coworkers previously designed and synthesized sulfoquinovosyl acyl glycerol (SQAG) derivative **12** and 2-boryl-1,2-dideoxy-D-glucose derivative **13** which possess the moderate intracellular uptake activity while their BNCT effect was not satisfying.[46,47]

In the last few decades, boron delivery agents based on peptides,[48] liposomes,[49] nanoparticles,[50] and anti-body[51] have been also investigated. However, these strategies

hardly reach the clinical application. Therefore, the discovery of novel boron carriers has been highly required for improvement of the BNCT effectiveness.

Table 1-2. Examples of boron delivery agents and their proposed mechanism.

Type of carriers	Proposed mechanism	References
Porphyrins	Accumulates via endosomal accumulation and leaky vasculature	24–28
Nucleosides	Accumulation in cancer cells by thymidine kinase mediated trapping	31–33
Polyamines	Activated polyamine transport system (PTS)	37,38
Amino acids	High expression of L-type amino acid transporter (LAT1)	39–41,52
Carbohydrates	Enhanced glycolysis, High expression of glucose transporter (GLUTs)	43–47
Peptides	High expression of peptide transporter (PepT1) interaction with cancer-specific protein, and so on.	48
Liposomes	Accumulation into tumor tissues via enhanced permeability and retention (EPR) effect[53]	49
Nanoparticles	Accumulation into tumor tissues via EPR effect	50
Anti-bodies	Recognition of cancer-specific proteins on the cell membrane	51

[1-3] Aim and contents of thesis

In this Ph.D. thesis, we report on the development of boron-containing monomeric- and dimeric macrocyclic polyamine derivatives and the corresponding zinc(II) complexes as novel boron carriers for BNCT. In Chapter 2, we describe the design, synthesis, and biological evaluation of monomeric-type macrocyclic polyamine derivatives **14**–**22** containing boron in natural abundant ratio ($^{10}B/^{11}B$ = 19.9/80.1) (Scheme 1-5). Moreover, three promising compounds **17b**, **18b**, and **19a** are selected, and their ^{10}B-enriched forms are also prepared for in vitro BNCT experiment (Scheme 1-6).

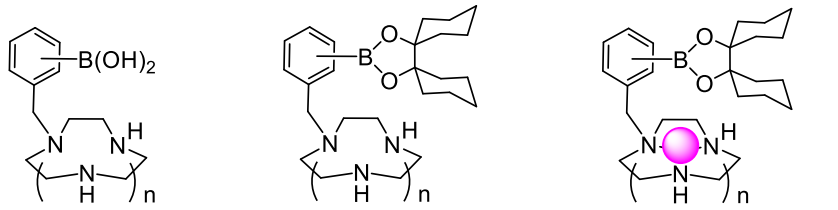

14a : n = 1, *p*-form
14b : n = 1, *m*-form
14c : n = 1, *o*-form
15a : n = 2, *p*-form
15b : n = 2, *m*-form
15c : n = 2, *o*-form
16a : n = 3, *p*-form
16b : n = 3, *m*-form
16c : n = 3, *o*-form

17a (L^1): n = 1, *p*-form
17b (L^2): n = 1, *m*-form
18a (L^3): n = 2, *p*-form
18b (L^4): n = 2, *m*-form
19a (L^5): n = 3, *p*-form
19b (L^6): n = 3, *m*-form
19c (L^7): n = 3, *o*-form

20a (ZnL^1): n = 1, *p*-form
20b (ZnL^2): n = 1, *m*-form
21a (ZnL^3): n = 2, *p*-form
21b (ZnL^4): n = 2, *m*-form
22a (ZnL^5): n = 3, *p*-form
22b (ZnL^6): n = 3, *m*-form
22c (ZnL^7): n = 3, *o*-form

Scheme 1-5. Structure of monomeric macrocyclic polyamines and their Zn^{2+} complexes.

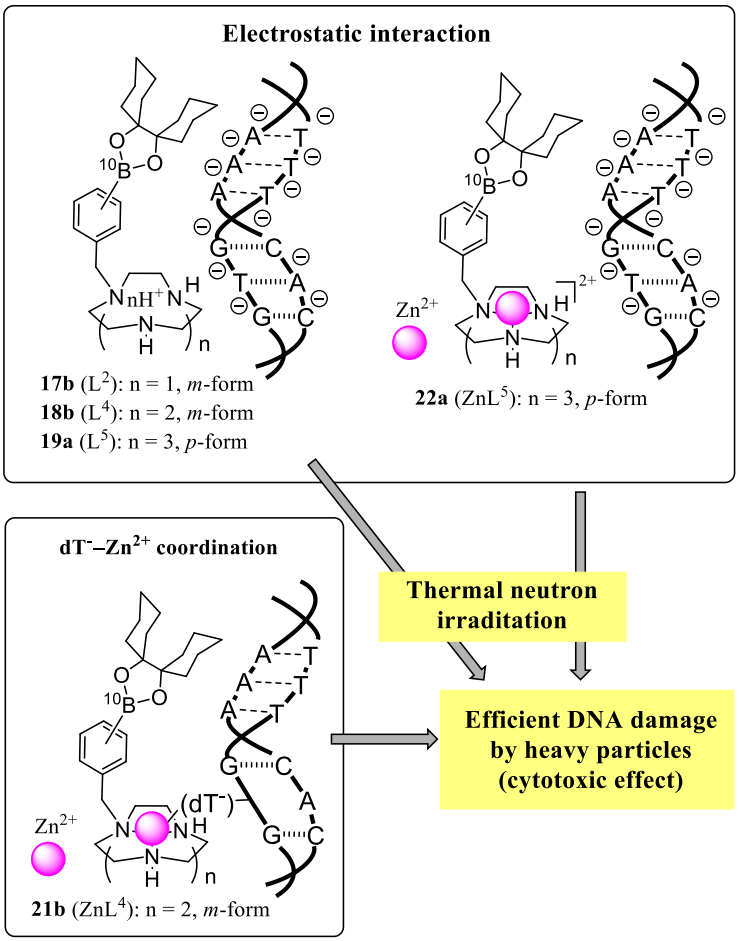

Scheme 1-6. Design and synthesis of monomeric macrocyclic polyamines for BNCT.

In Chapter 3, we report on the development of macrocyclic polyamine dimers **23**–**32** and the corresponding zinc(II) complexes **33**–**48** for the use in BNCT (Scheme 1-7). Their interaction with calf-thymus DNA (ctDNA) are examined, and their BNCT activities are evaluated using their ^{10}B-enriched forms (Scheme 1-8). Chapter 4 concludes this Ph.D. thesis with the prospects about the use of these macrocyclic polyamine derivatives for cancer treatment and application to medicinal chemistry and related fields.

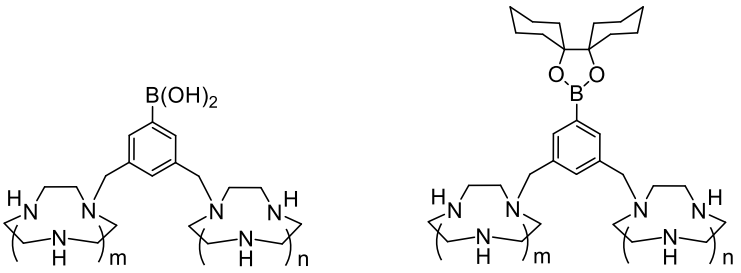

23 (L^8): m = 2, n = 1
24 (L^9): m = 2, n = 2
25 (L^{10}): m = 2, n = 3
26 (L^{11}): m = 3, n = 1
27 (L^{12}): m = 3, n = 3

28 (L^{13}): m = 2, n = 1
29 (L^{14}): m = 2, n = 2
30 (L^{15}): m = 2, n = 3
31 (L^{16}): m = 3, n = 1
32 (L^{17}): m = 3, n = 3

Zn^{2+} (1 or 2 equiv)

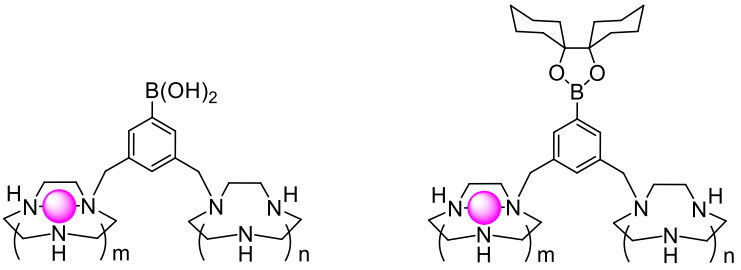

33 (ZnL^8): m = 2, n = 1
34 (ZnL^{10}): m = 3, n = 2
35 (ZnL^{11}): m = 3, n = 1

36 (ZnL^{13}): m = 2, n = 1
37 (ZnL^{15}): m = 3, n = 2
38 (ZnL^{16}): m = 3, n = 1

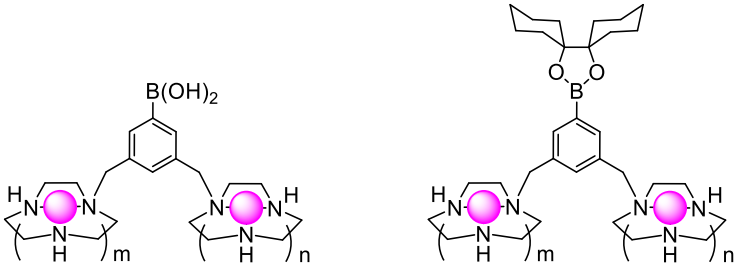

39 (Zn_2L^8): m = 2, n = 1
40 (Zn_2L^9): m = 2, n = 2
41 (Zn_2L^{10}): m = 2, n = 3
42 (Zn_2L^{11}): m = 3, n = 1
43 (Zn_2L^{12}): m = 3, n = 3

44 (Zn_2L^{13}): m = 2, n = 1
45 (Zn_2L^{14}): m = 2, n = 2
46 (Zn_2L^{15}): m = 2, n = 3
47 (Zn_2L^{16}): m = 3, n = 1
48 (Zn_2L^{17}): m = 3, n = 3

Scheme 1-7. Structure of dimeric macrocyclic polyamines and their Zn^{2+} complexes.

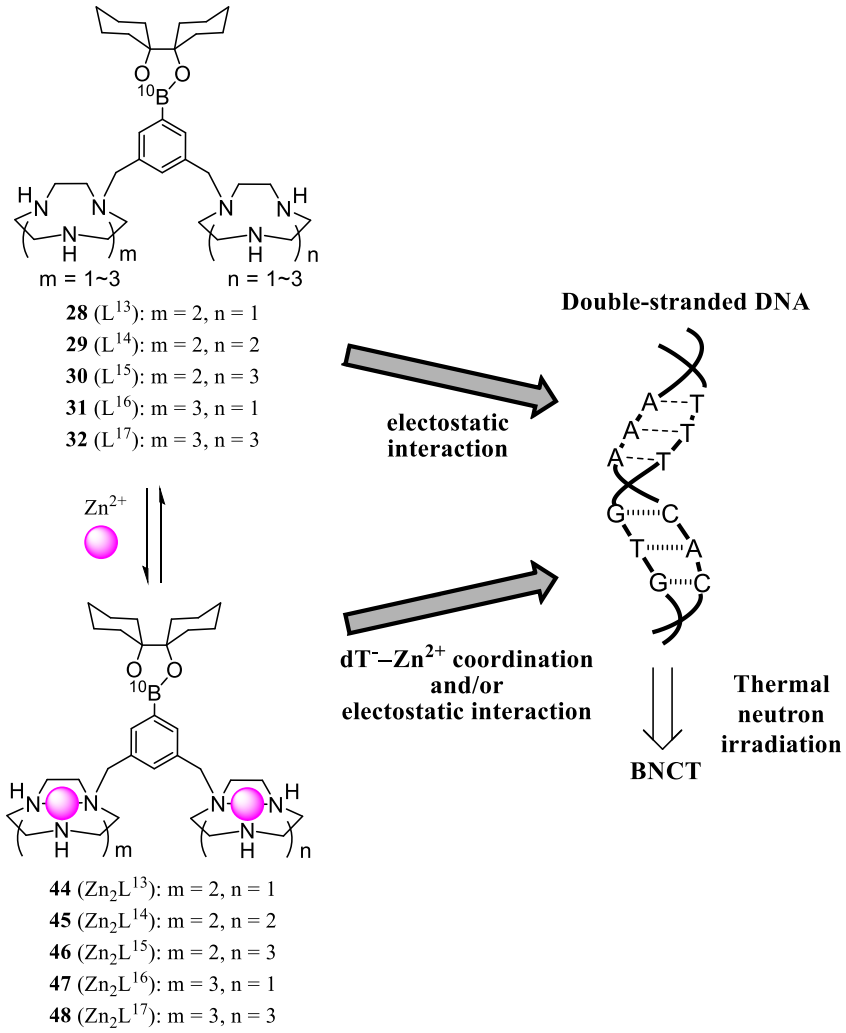

Scheme 1-8. Design and synthesis of dimeric macrocyclic polyamines for BNCT.

Chapter 2.

Design, Synthesis, and Biological Evaluation of Boron-Containing Macrocyclic Polyamines and Their Zinc(II) Complexes for Boron Neutron Capture Therapy

（ホウ素中性子捕捉療法のための
含ホウ素大環状ポリアミン誘導体と亜鉛錯体の
設計・合成および生物学的評価）

[2-1] Introduction

Boron neutron capture therapy (BNCT) is a potential radiotherapy based on the nuclear reaction between boron-10 (^{10}B) atoms and thermal neutrons (^{1}n). The neutron capture reaction [$^{10}B(n, \alpha)^{7}Li$] generates high linear energy transfer (LET) α particles and lithium ions that have destructive effects and short path lengths in the 5–9 μm range. Therefore, it is expected that cancer cells containing ^{10}B species would be selectively destroyed with minimal effects on healthy tissues.[2,3]

For successful BNCT, a high level of accumulation and selective delivery of ^{10}B into cancer cells are required. The design of effective BNCT agents requires the following criteria: (1) low systemic toxicity and higher uptake in tumor tissue than in normal tissue (tumor to blood (T/B) ratios should be greater than 3); (2) ^{10}B must be retained in the tumor tissue but also be rapidly cleared from blood and normal tissues; and (3) the concentration of boron inside or near tumor cells must be $\geq 10^{9}$ ^{10}B atoms/cell (20–35 μg/gram of tumor tissue).[8] In this context, only two compounds, disodium mercaptoundecahydrododecaborate (BSH) **4**[11–13] and L-4-boronophenylalanine (BPA) **5**[14–22] (used as a complex with D-fructose) have been used for the clinical treatment of cancers such as malignant glioma, malignant melanoma, and recurrent head and neck cancer, which are not enough for treatment of multiple tumor types (Scheme 2-1).[7]

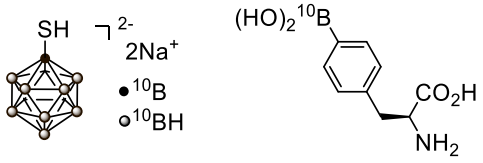

^{10}B-BSH
4

^{10}B-BPA
5
(used as a complex with D-fructose)

Scheme 2-1. Structures of representative BNCT agents.

It is also known that polyamines including spermidine **49** and spermine **50** are essential for numerous cellular functions such as DNA replication and protein synthesis.[34] The increase in polyamine concentrations in cancer cells is associated with the activation of cell proliferation and regulated by the promoted polyamine transport system (PTS) and biosynthesis.[35] Therefore, polyamine derivatives could serve as potentially useful scaffolds for the delivery of boron-containing drugs into cancer cells, as represented by the spermidine derivatives **51** and **52** (Scheme 2-2).[36–38] To the best of our knowledge, however, the use of these derivatives in BNCT has not been reported.

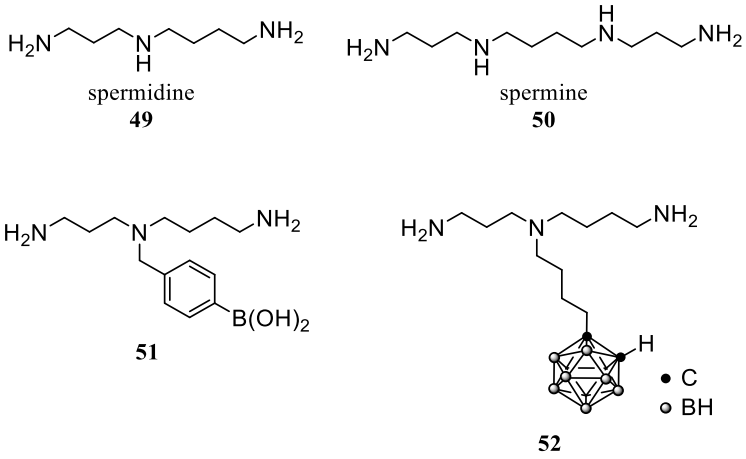

Scheme 2-2. Structures of polyamines and boron-containing spermidine derivatives **51** and **52**.

We previously reported on the design and synthesis of phenylboronic (*ortho*-form) acid-pendant cyclen (1,4,7,10-tetraazacyclododecane, [12]aneN$_4$) **18c** for the sensing of metal cations such as zinc (Zn^{2+}), iron (Fe^{2+}), copper (Cu^{2+}), and cobalt (Co^{2+}) (Scheme 2-3).[54] It was found that the carbon–boron bond at the *o*-position of the (2-boronophenyl)methyl side chain in **18c** is hydrolyzed upon complexation with these metal ions to give **53**, resulting in a shift of the ^{11}B NMR signal from ca. 30 ppm to ca. 20 ppm, which corresponds to B(OH)$_3$. In addition, we also found that **18c** was efficiently transferred into cancer cell lines (Jurkat, A549 and HeLa S3 cells).[47,54] In subsequent

studies, the decomposition of *ortho*-carborane-polyamine conjugates upon metal complexation was discovered and applied to the magnetic resonance imaging (MRI) of Cu^{2+} in solutions.[55]

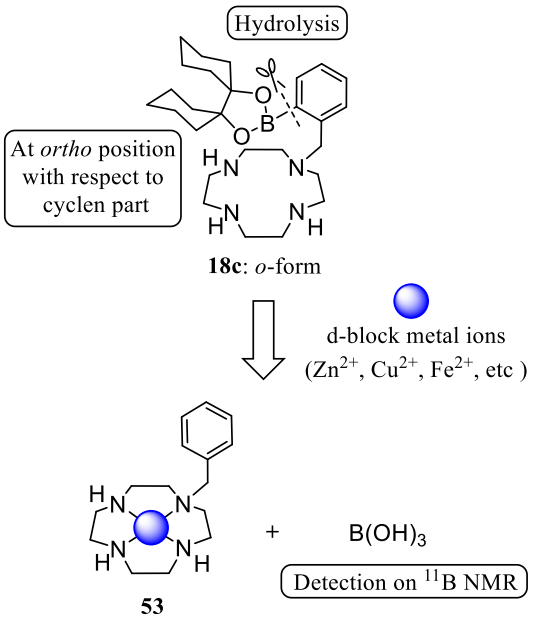

Scheme 2-3. Hydrolytic cleavage of C–B bond of **18c**.

The aforementioned background and the high intracellular uptake of **18c** in cancer cells prompted us to examine the development of boron carriers equipped with macrocyclic polyamine scaffolds such as [9]aneN$_3$ (1,4,7-triazacyclononane) **54** (L^{18}), [12]aneN$_4$ (cyclen) **55** (L^{19}), and [15]aneN$_5$ (1,4,7,10,13-pentaazacyclopentadecane) **56** (L^{20}) (Scheme 2-4). In this work, we designed and synthesized the phenylboronic acid-pendant macrocyclic polyamines **14**–**16**, their corresponding boronic acid ester analogues **17**–**19** (L^1–L^7), and Zn^{2+} complexes **20**–**22** (ZnL^1–ZnL^7). It was expected that the cationic charge of **17**–**19** due to the protonation of macrocyclic polyamine groups (**17**–**19**·nH^+, n = 1 or 2) would facilitate their intracellular uptake.[35,56,57] We hypothesized that the protonated form of these boron-polyamine conjugates (**17**–**19**) would be restricted

to mono- or dicationic forms (n = 1, 2) (**17a**,**b**·nH^+, **18a**,**b**·nH^+, and **19a**–**c**·nH^+ forms in Scheme 2-4) due to the deprotonation constants of the macrocyclic polyamines, **54**,[58] **55**,[59] and **56**,[60] as described below.

It is also well known that macrocyclic polyamines form stable complexes with intracellular metal ions such as Zn^{2+}, Cu^{2+}, and Ni^{2+} in aqueous solutions at physiological pH (Scheme 2-4),[61–63] and these complexes are much more stable than Zn^{2+} complexes of linear polyamines such as spermidine **49** and spermine **50**. In addition, it was reported that the cytotoxicity of macrocyclic polyamines is reduced by the complexation with Zn^{2+}.[64] It is well established that Zn^{2+}-cyclen complexes such as **57** (ZnL^{19}) bind to thymidines (dT) in DNA to form stable complexes **58** through the coordination bonding between the deprotonated imide moiety of dT (dT^-) and Zn^{2+} in aqueous solution at neutral pH (Scheme 2-5).[65] Therefore, we expected that the neutron irradiation of **20**–**22** when located in close proximity to DNA would effectively induce DNA damage. In this study, we report on the cytotoxicity and intracellular uptake activity of **14**–**19** and the corresponding Zn^{2+} complexes **20**–**22** in several cancer cell lines. These agents were first prepared as ligands containing boron in a natural abundance ratio ($^{10}B/^{11}B$ = 19.9/80.1). After the biological assessment of these $^{10}B/^{11}B$ agents, three promising compounds were chosen among them and the corresponding ^{10}B-enriched compounds and their Zn^{2+} complexes were synthesized and used in BNCT experiments.

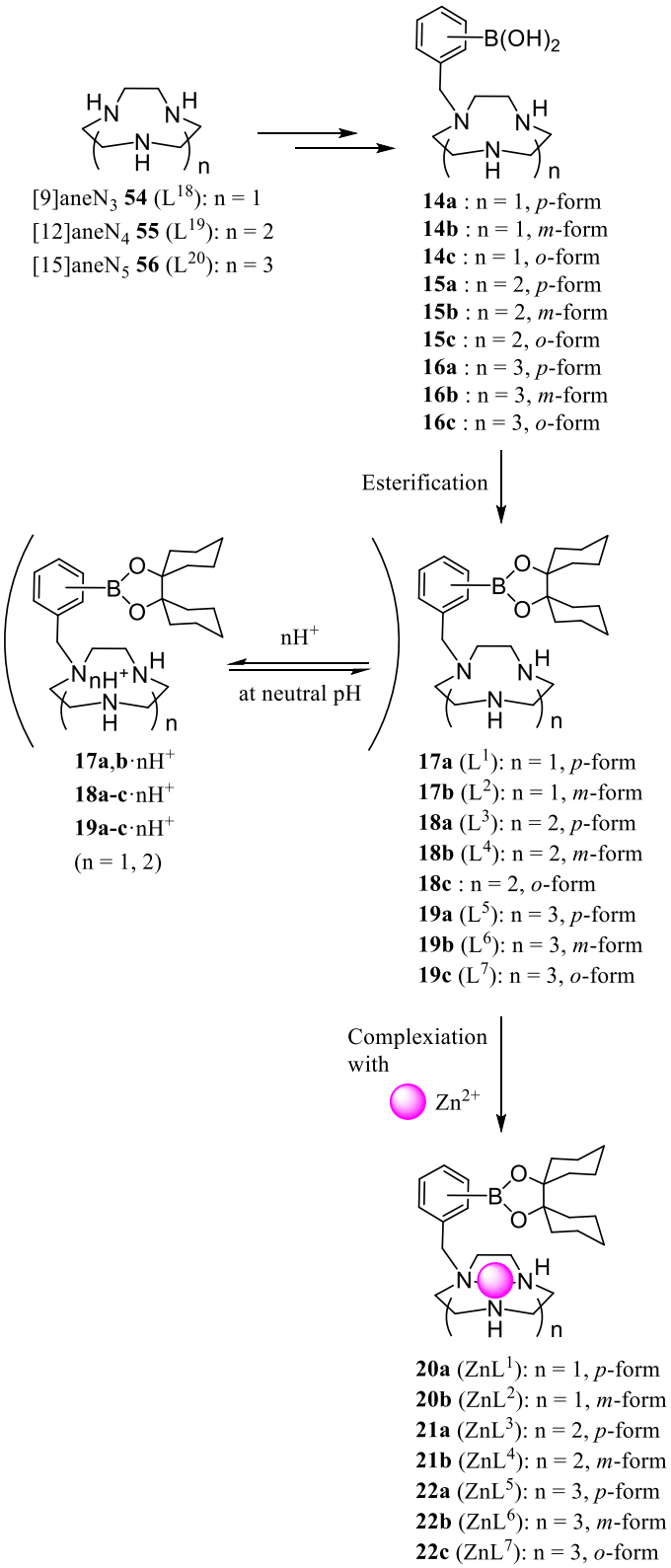

Scheme 2-4. Structures of macrocyclic polyamine derivatives and their Zn^{2+} complexes synthesized in this work.

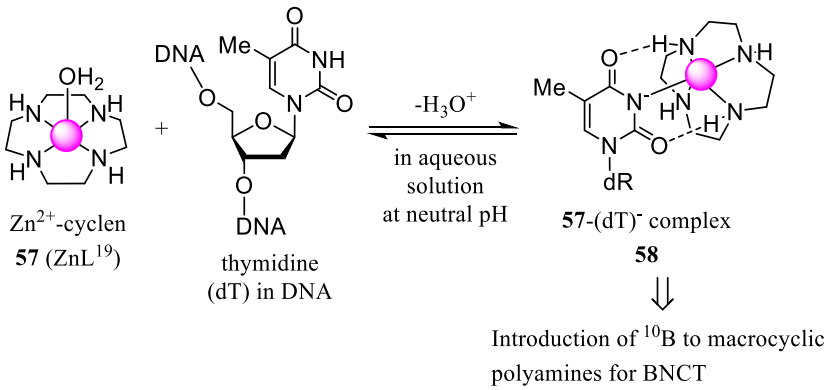

Scheme 2-5. Complexation of Zn^{2+}-cyclen **57** (ZnL^{19}) with the deprotonated thymidine (dT^{-}) in aqueous solution at neutral pH.

[2-2] Results and discussion

[2-2-1] Synthesis of boron-containing macrocyclic polyamine derivatives and the X-ray single crystal structure analysis of 21a

The synthesis of the macrocyclic polyamine derivatives is shown in Schemes 2-6, 2-7, and 2-8. The boron-containing BNCT agents were initially synthesized using naturally abundant ratio of boron ($^{10}B/^{11}B$ = 19.9/80.1), in order to evaluate their intracellular uptake, from which more potent candidates were selected and the corresponding ^{10}B-enriched compounds were synthesized for use in BNCT experiments.

The 9-membered macrocyclic polyamine **54** ([9]aneN$_3$)[66] was treated with $(Boc)_2O$ to give **59**,[67] which was then reacted with 4-(bromomethyl)phenylboronic acid **60a**[68] to afford **61a** (Scheme 2-6). After removing the Boc groups of **61a** by treatment with trifluoroacetic acid (TFA) to give **14a** as the 2TFA salt, the reaction of **14a** with bicyclohexyl-1,1′-diol **62**[69] gave **17a**. The synthesis of the *m*-isomer **17b** was carried out in a similar manner.[70] The *o*-isomers of **14** and **17** (**14c** and **17c**) were not obtained, due to the cleavage of their C–B bonds in aqueous solution even in the absence of metal ions. The complexation of **17a** and **17b** with Zn^{2+} was conducted *in situ* before the biological evaluation.

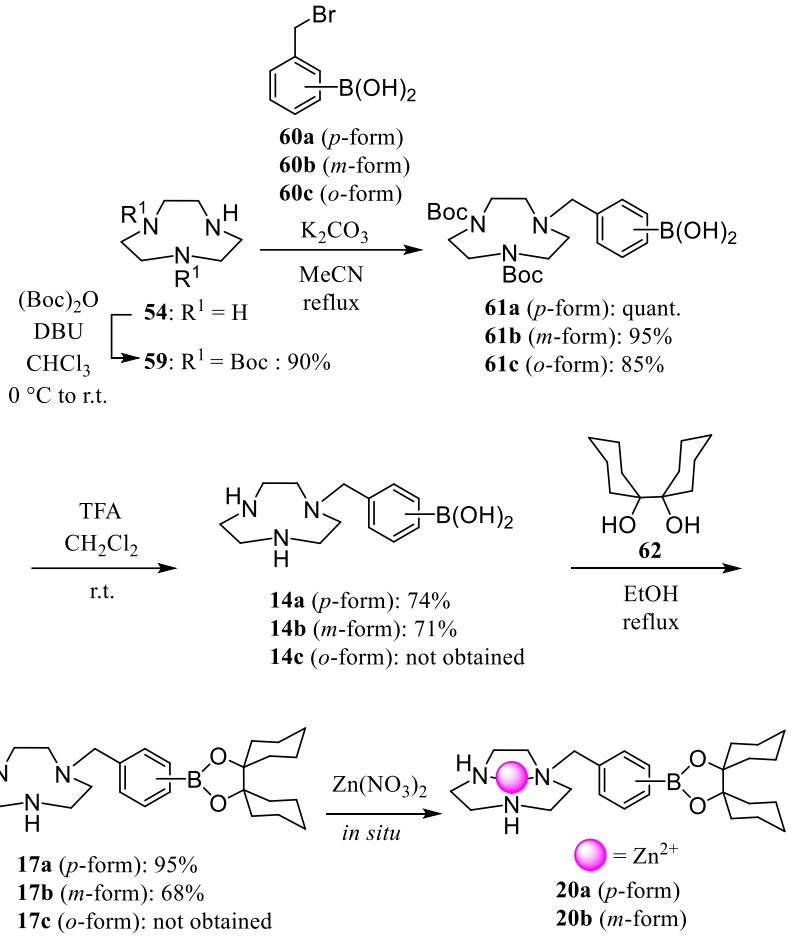

Scheme 2-6. Synthesis of **14a**,**b**, **17a**,**b**, and **20a**,**b**.

The synthesis of the 12-membered tetraamine (cyclen) ([12]aneN$_4$) derivatives **18a**,**b** and the 15-membered pentaamine ([15]aneN$_5$) derivatives **19a**–**c** was carried out, as shown in Schemes 2-7 and 2-8.[66–73] The deprotection of **64a** and **66a**–**c** with TFA afforded **15a** and **16a**–**c** 2TFA and 3TFA salts, respectively, as determined by elemental analysis.

The Zn^{2+} complexes of **18a** and **18b** (**21a** and **21b**) were isolated and those of **19a**–**c** (**22a**–**c**) were prepared *in situ* for use in biological experiments. The structure of **21a** was confirmed by a single-crystal X-ray structure analysis, as shown in Figure 2-1. The Zn^{2+} complex of the *o*-form **18c** was not obtained due to the carbon–boron bond cleavage that occurred upon complexation with Zn^{2+}, as previously described.[54] In contrast, the

C–B bond in **22c** (Zn^{2+}-**19c** complex) was hydrolyzed very slowly (approximate half-life is 24 h) as observed by ^{11}B-NMR, possibly due to the higher pK_a value of the Zn^{2+}-bound water in the Zn^{2+}–[15]aneN$_5$ complex than that of **21c**, which is a Zn^{2+} complex of the [12]aneN$_4$-type ligand **18c**.[73]

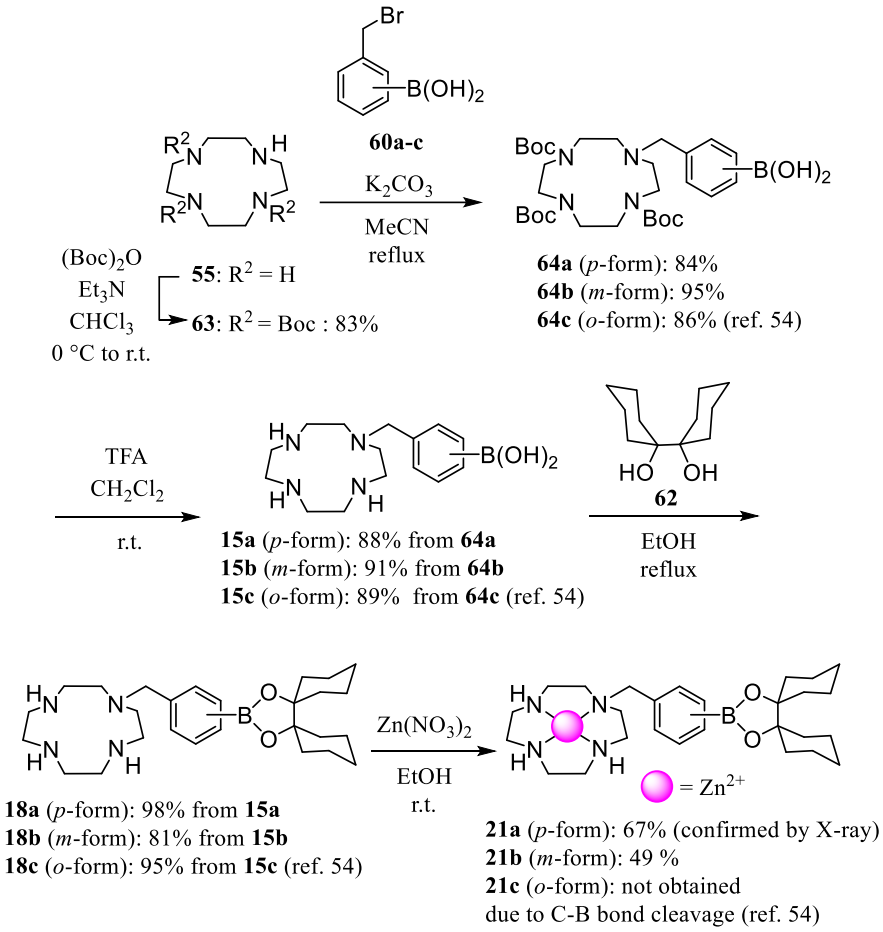

Scheme 2-7. Synthesis of **15a**,**b**, **18a**–**c**, and **21a**,**b**.

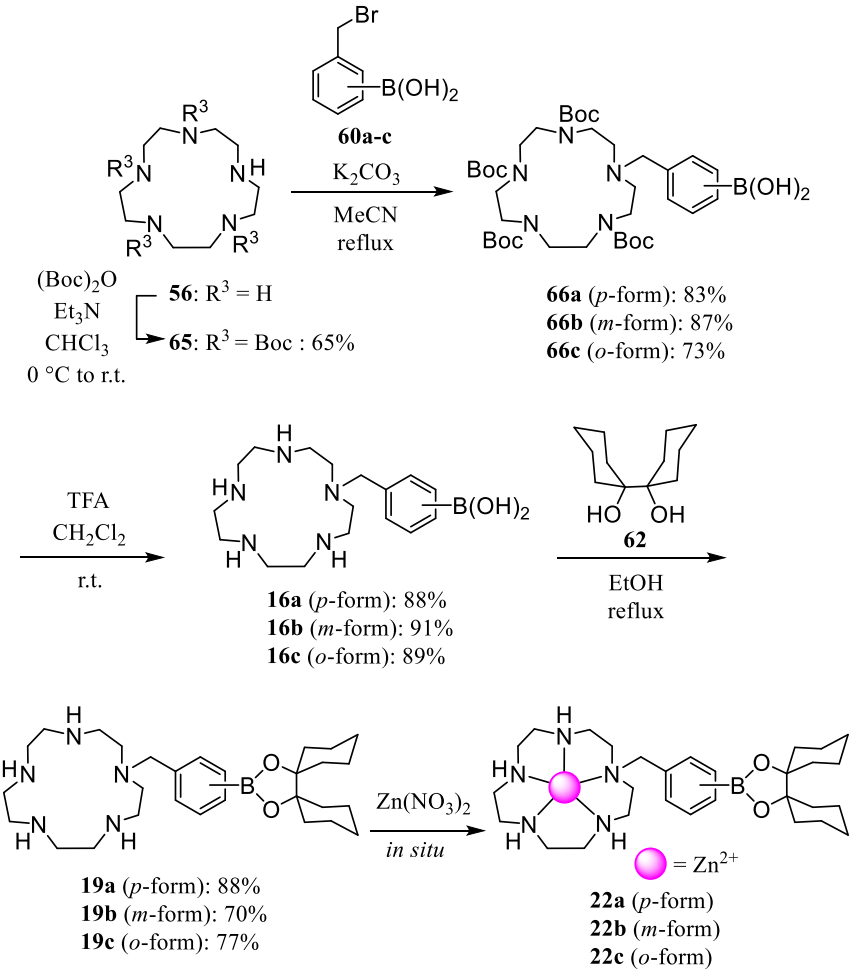

Scheme 2-8. Synthesis of **16a**–**c**, **19a**–**c**, and **22a**–**c**.

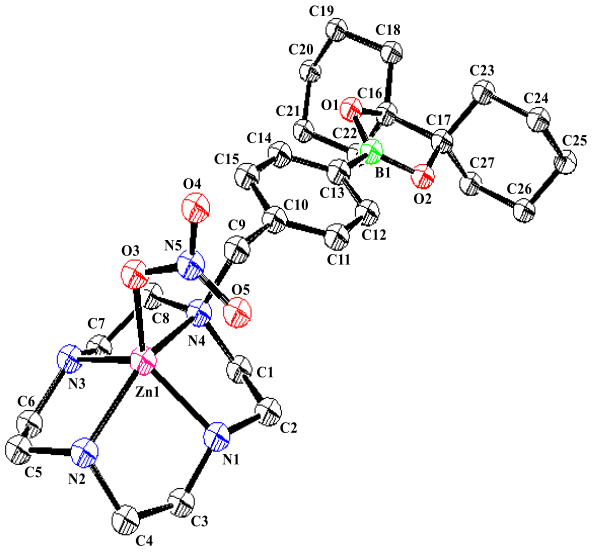

Figure 2-1. ORTEP drawing of **21a** (ZnL^3) with a Zn^{2+}–bound NO_3^-. Selected bond

lengths: Zn(1)–N(1) 2.059 Å, Zn(1)–N(2) 2.167 Å, Zn(1)–N(3) 2.091 Å, Zn(1)–N(4) 2.962 Å, Zn(1)–O(3) 1.999 Å, C(13)–B(1) 1.561 Å, B(1)–O(1) 1.363 Å, and B(1)–O(2) 1.366 Å. One external nitrate anion, ethanol and hydrogen atoms were omitted for clarity.

[2-2-2] Evaluation of the cytotoxicity of boron-containing macrocyclic polyamine derivatives against HeLa S3, A549, and IMR-90 cells

The cytotoxicity of the boron-containing macrocyclic polyamine derivatives **14**–**19** and their corresponding Zn^{2+} complexes **20**–**22** against HeLa S3 (human cervical carcinoma), A549 (human caucasian lung carcinoma), and IMR-90 (normal human fibroblast) cells was examined by an MTT (3-(4,5-di-methylthiazol-2yl)-2,5-diphenyltetrazolium bromide) assay in comparison with those of BSH (**4**) and BPA-D-fructose complex (**5**). The cells (1×10^4 cells/well) were incubated with boron compounds **4**, **5**, and **14**–**22** (0–200 μM) in culture medium containing 10% fetal bovine serum (FBS) for 24 h at 37 °C under 5% CO_2, and then treated with the MTT reagent to evaluate cell viability.

The results are presented in Figures 2–2, 2–3, and 2–4 and the IC_{50} values of these agents are summarized in Table 2-1. The findings indicated that **14**–**22** are somewhat more toxic than **4** and **5**, and that **17a**, **18a**, and **19a** are more toxic than **14a**, **15a**, and **16a**, possibly due to the hydrophobicity of the boronic acid ester group. It should be noted that the cytotoxicity of Zn^{2+} complex **21b**, **22b**, and **22c** is lower than the corresponding Zn^{2+}-free ligands **18b**, **19b**, and **19c**, while the Zn^{2+}-free ligands **17a**, **17b**, **18a**, **19a**, and their Zn^{2+} complexes **20a**, **20b**, **21a**, and **22a** have a similar toxicity. The similar toxicity between **17a** and **20a** and **17b** and **20b** would be due to the weak Zn^{2+} complexation of **17a** and **17b**, which have only three nitrogen atoms in the [9]aneN_3 ring group.

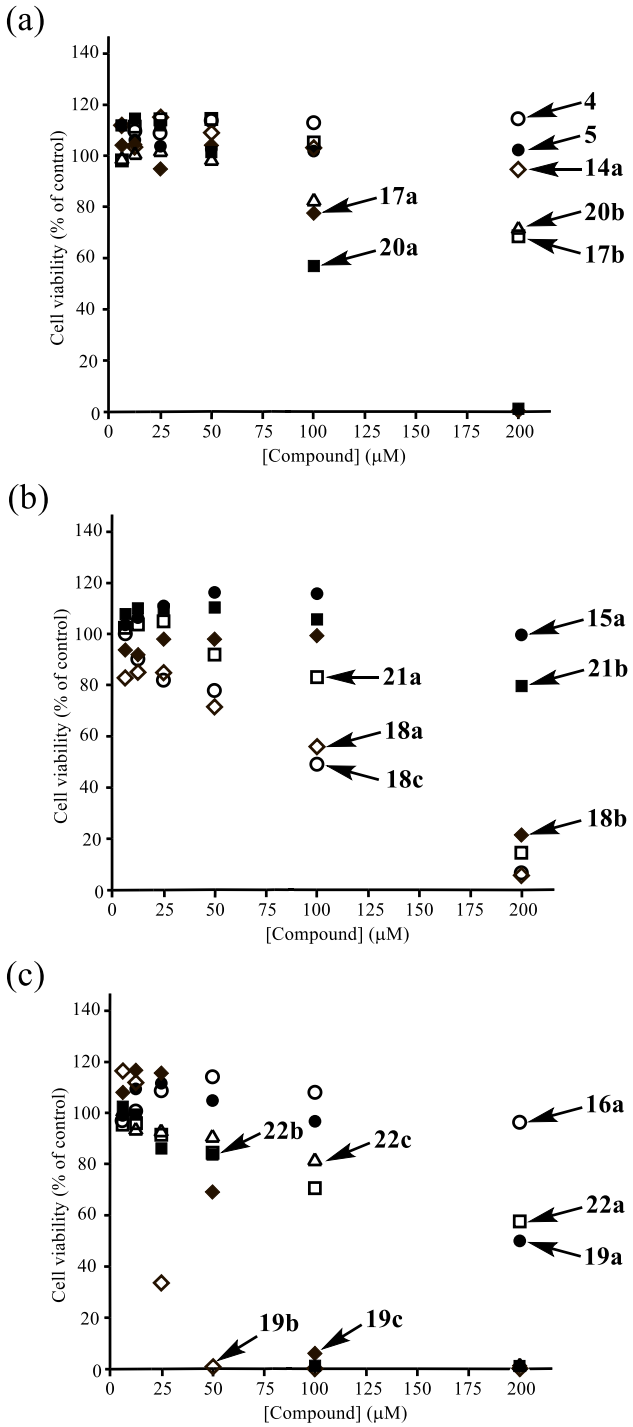

Figure 2-2. Results of MTT assays for boron compounds **4**, **5**, and **14**–**22** against HeLa S3 cells. Cell viability of HeLa S3 cells (% of control; in the absence of boron compound) in the presence of boron compounds (a) **4** (○), **5** (●), **14a** (◇), **17a** (◆), **17b** (□), **20a** (■) and **20b** (△), (b) **15a** (●), **18a** (◇), **18b** (◆), **18c** (○), **21a** (□) and **21b** (■), (c) **16a** (○), **19a** (●), **19b** (◇), **19c** (◆), **22a** (□), **22b** (■) and **22c** (△) [0–200 μM] at 37 °C for 24 h.

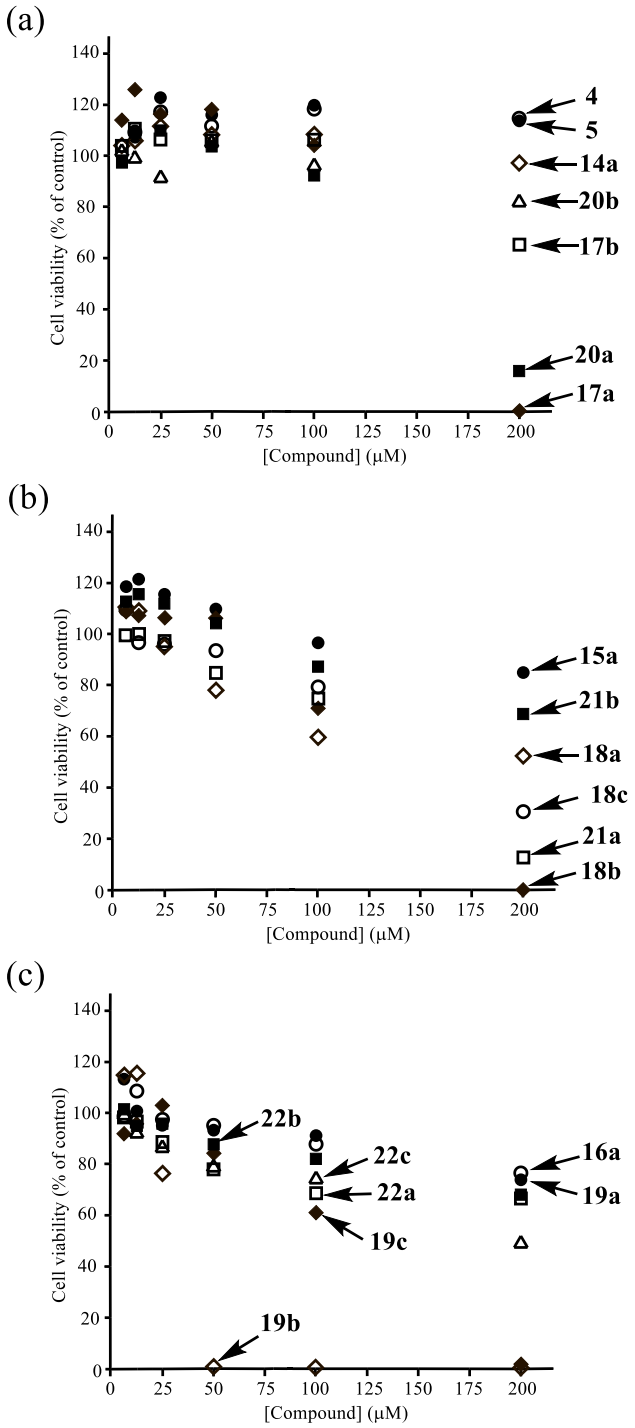

Figure 2-3. Results of MTT assays for boron compounds **4**, **5**, and **14**–**22** against A549 cells. Cell viability of A549 cells (% of control; in the absence of boron compound) in the presence of boron compounds (a) **4** (○), **5** (●), **14a** (◇), **17a** (◆), **17b** (□), **20a** (■) and **20b** (△), (b) **15a** (●), **18a** (◇), **18b** (◆), **18c** (○), **21a** (□) and **21b** (■), (c) **16a** (○), **19a** (●), **19b** (◇), **19c** (◆), **22a** (□), **22b** (■) and **22c** (△) [0–200 μM] at 37 °C for 24 h.

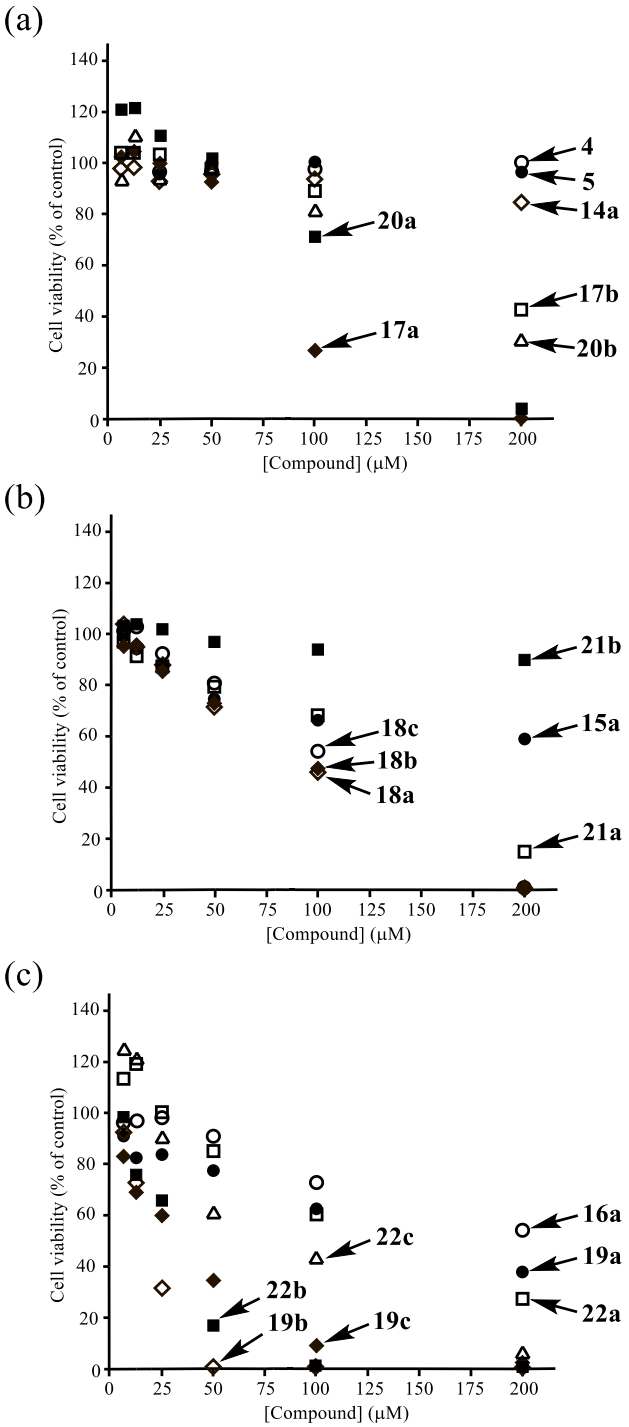

Figure 2-4. Results of MTT assays for boron compounds **4**, **5**, and **14**–**22** against IMR-90 cells. Cell viability of IMR-90 cells (% of control; in the absence of boron compound) in the presence of boron compounds (a) **4** (○), **5** (●), **14a** (◇), **17a** (◆), **17b** (□), **20a** (■) and **20b** (△), (b) **15a** (●), **18a** (◇), **18b** (◆), **18c** (○), **21a** (□) and **21b** (■), (c) **16a** (○), **19a** (●), **19b** (◇), **19c** (◆), **22a** (□), **22b** (■) and **22c** (△) [0–200 μM] at 37 °C for 24 h.

Table 2-1. The IC_{50} values of boron compounds **4**, **5**, and **14**–**22** [0–200 μM] against HeLa S3, A549, and IMR-90 cells after the treatment for 24 h.

Compound (Ligands)	HeLa S3 (μM)	A549 (μM)	IMR-90 (μM)	Compound (Zn complexes)	HeLa S3 (μM)	A549 (μM)	IMR-90 (μM)
4 (BSH)	> 200	> 200	> 200				
5 (BPA)	> 200	> 200	> 200				
18c	100	162	108				
14a	> 200	> 200	> 200				
15a	> 200	> 200	> 200				
16a	> 200	> 200	> 200				
17a (L^1)	131	151	83	**20a** (ZnL^1)	112	155	130
17b (L^2)	> 200	> 200	187	**20b** (ZnL^2)	> 200	> 200	162
18a (L^3)	112	> 200	94	**21a** (ZnL^3)	148	139	95
18b (L^4)	163	128	135	**21b** (ZnL^4)	> 200	> 200	> 200
19a (L^5)	> 200	> 200	151	**22a** (ZnL^5)	> 200	> 200	129
19b (L^6)	22	34	18	**22b** (ZnL^6)	71	> 200	32
19c (L^7)	65	117	35	**22c** (ZnL^7)	138	197	83

[2-2-3] Intracellular uptake of boron-containing macrocyclic polyamine derivatives into HeLa S3, A549, and IMR-90 cells, as determined by inductively coupled plasma mass spectrometry

The intracellular uptake of the boron compounds into HeLa S3, A549, and IMR-90 cells was evaluated by inductively coupled plasma mass spectrometry (ICP-MS), as shown in Scheme 2-9. The cells (5×10^5 cells/well) were seeded on 6-well plates and incubated in culture medium containing 10% FBS for 1 day at 37 °C in a 5% CO_2 environment (20% O_2) and then treated with boron compounds **4**, **5**, and **14**–**22** (30 μM) under same conditions. This concentration (30 μM) of **4**, **5**, and **14**–**22** (lower concentrations are better to reduce their toxicity) was carefully determined based on the consideration of a balance between their IC_{50} values (toxicity) and intracellular uptake

values that are listed in Table 2-1 and Figure 2-5. After incubating the cells for 24 h, they were washed with PBS and broken down with nitric acid overnight, and the amount of boron atoms (total amount of ^{10}B and ^{11}B) was quantitatively determined by ICP-MS and normalized as the amount of per cell because some compounds have weak toxicity.

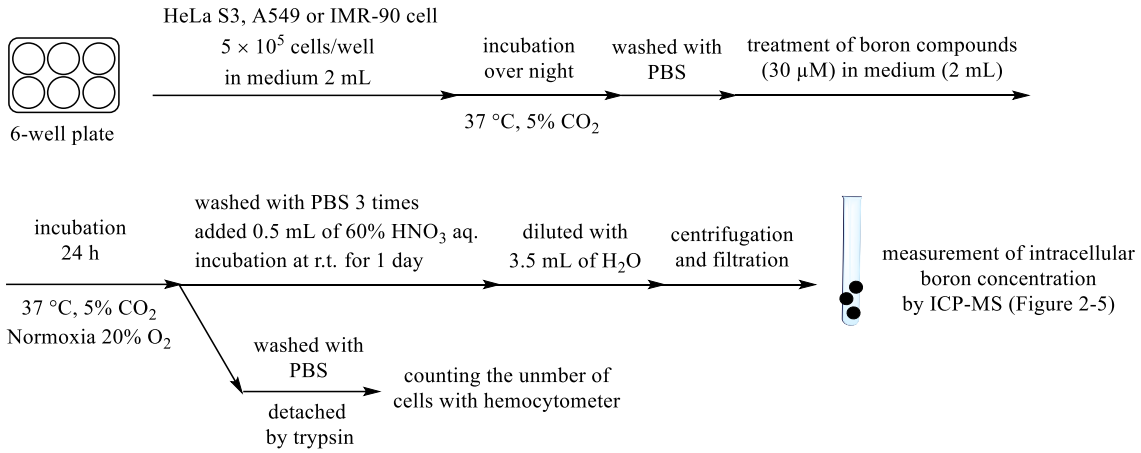

Scheme 2-9. Typical procedure used for measuring the intracellular uptake of boron compounds in living cells.

As shown in Figure 2-5a, the intracellular uptake of **17**–**19** is higher than that of reference compounds BSH **4** comprised of twelve ^{10}B and BPA **5**, possibly because cell-membrane permeability is improved by their boronic acid ester group. In addition, it was found that intracellular uptake of the 9-membered triamine derivatives **17a**,**b** and **20a**,**b** into A549 cells was higher than **18a**,**b** and **19a**–**c**, and their Zn^{2+} complexes **21a**,**b** and **22a**–**c** exhibited a lower intracellular uptake (Figure 2-5b), suggesting that the 9-membered triamine group in **17a** and **17b** is better for the intracellular uptake into A549 cells.

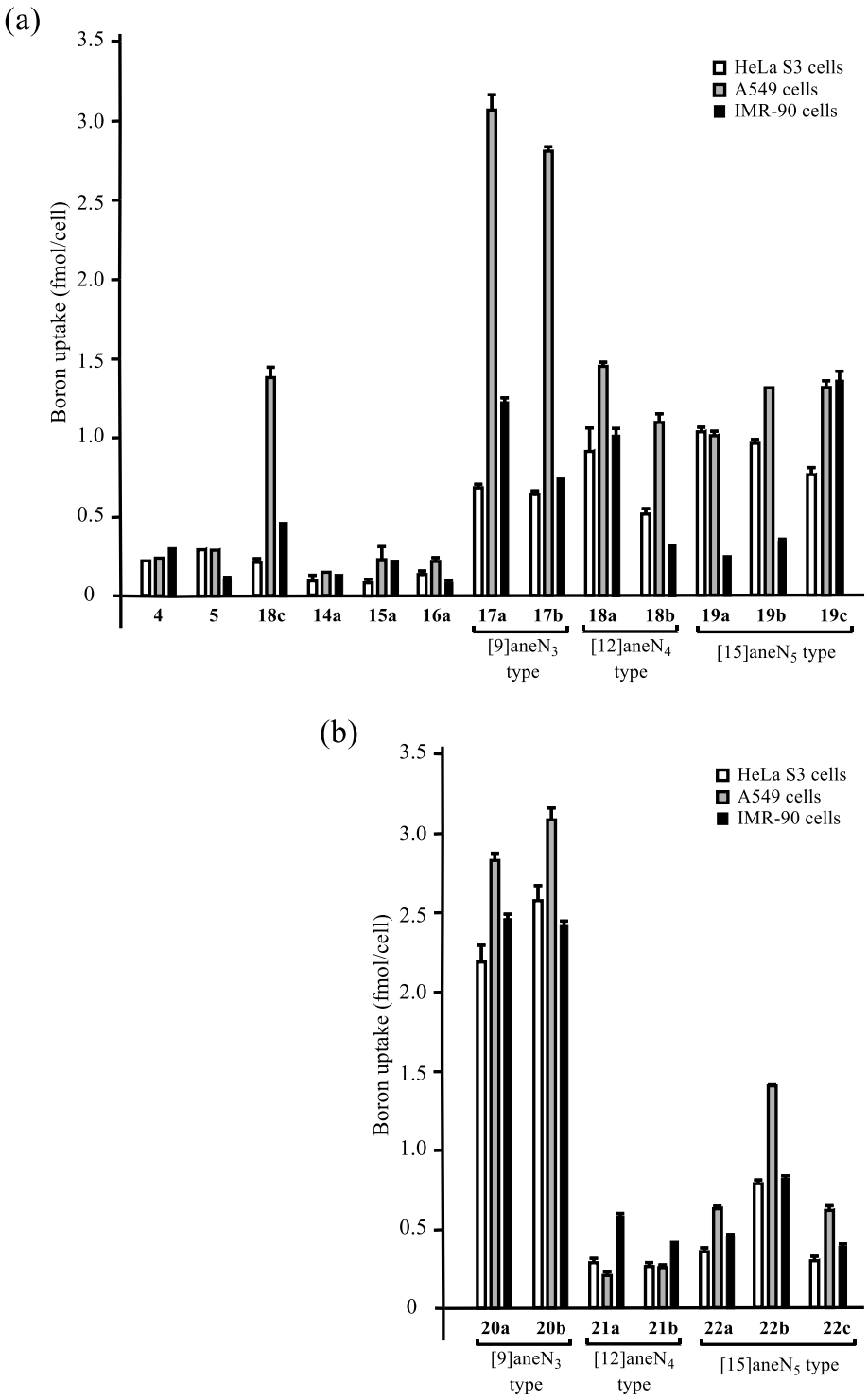

Figure 2-5. Comparison of intracellular boron atoms against HeLa S3 (open bars), A549 (shaded bars) and IMR-90 (closed bars) cells as determined by ICP-MS. All cells were treated with boron compounds (a) **4**, **5**, **14**–**19**, and (b) **20**–**22** (30 μM) in culture medium at 37 °C for 24 h. Data represent the mean ± SD of at least three replicates.

The tumor/normal cell (T/N) ratios with respect to the intracellular uptake of the boron compounds (**4**, **5**, and **14**–**22**) were calculated using equation (1), and their intracellular boron uptake (in HeLa S3 cells and A549 cells)–T/N ratio profiles are shown in Figures 2-6a and 2-6c. The boron uptake–IC_{50} value (indicating the toxicity) profiles are plotted in Figures 2-6b (HeLa S3 cells) and 2-6d (A549 cells). These data suggest that **19a** has a higher boron uptake (> 2.5 fmol/cell) and T/N selectivity (ca. 4) and a rather low toxicity against HeLa S3 cells (Figures 2-6a and 2-6b) and that **17b**, **18b**, and **19a** exhibit better boron uptake, higher T/N ratios (over 3), and lower toxicity against A549 cells and normal cells (IC_{50} > 100 μM) (Figures 2-6c and 2-6d), although the reasons for their selective uptake to cancer cells are yet to be studied.

$$\text{T/N ratio} = \frac{[\text{B } (^{10}\text{B and } ^{11}\text{B}) \text{ uptake in HeLa S3 or A549 cells (fmol/cell)}]}{[\text{B } (^{10}\text{B and } ^{11}\text{B}) \text{ uptake in IMR-90 cells (fmol/cell)}]} \quad \cdots(1)$$

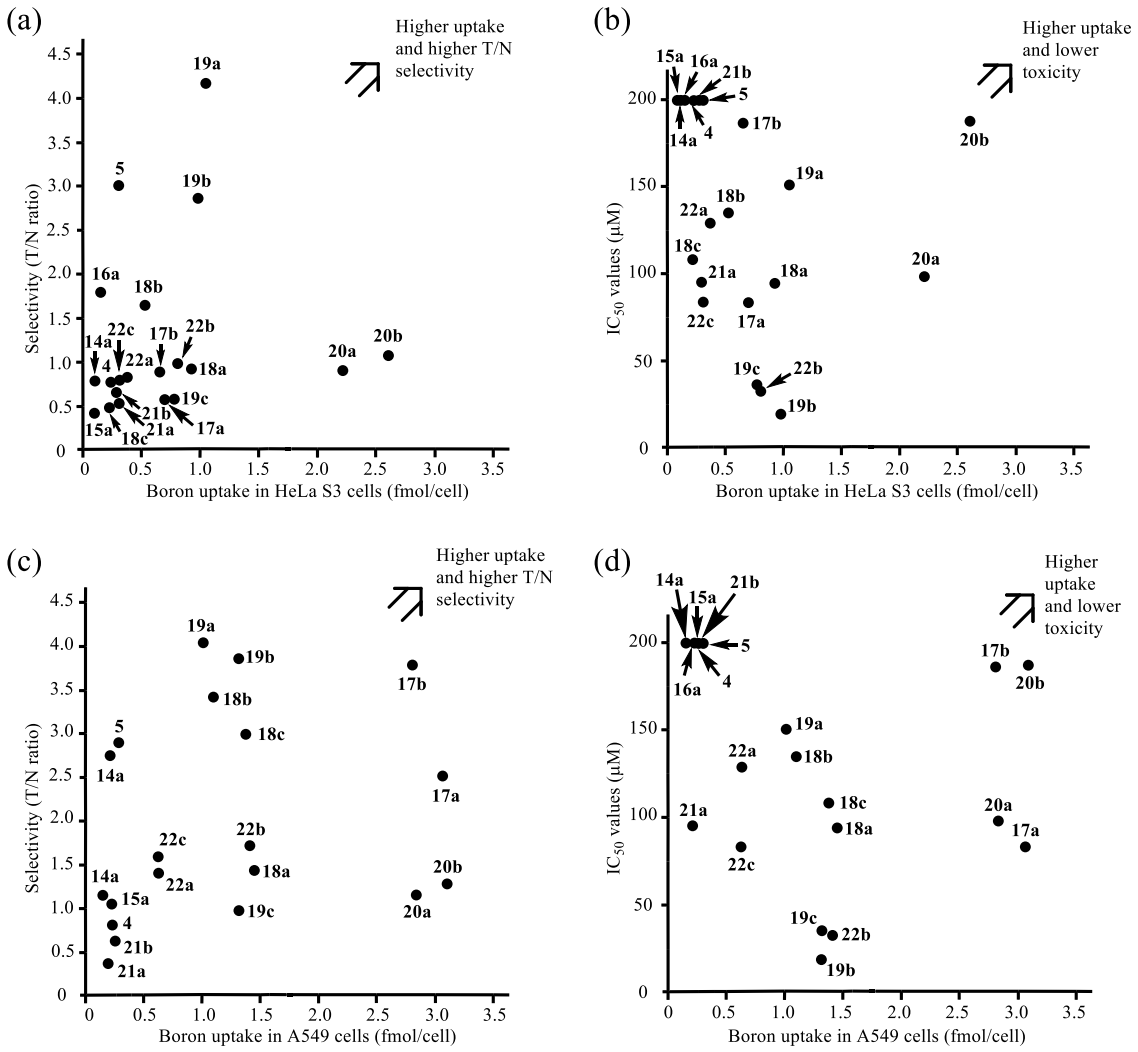

Figure 2-6. Intracellular boron uptake–T/N selectivity profiles (a, c) and intracellular boron uptake–IC_{50} value against normal cell profiles (b, d) of boron compounds **4**, **5**, and **14**–**22**. (a, c) Selectivity (T/N ratio) to HeLa S3 cells (a) and A549 cells (c) were calculated from the results for the intracellular uptake of the boron compounds into HeLa S3 and A549 cells in comparison to the uptake into IMR-90 cells, respectively. (b, d) IC_{50} values (μM) of boron compounds **4**, **5**, and **14**–**22** against IMR-90 cells and boron uptake (fmol/cell) into HeLa S3 cells (b) and A549 cells (d).

Concerning the relationship of these data and the protonation properties of the aforementioned boron-macrocyclic polyamine conjugates, the deprotonation constants (pK_a values) of unmodified macrocyclic polyamines **54**, **55**, and **56** are summarized in Scheme 2-10.[58–60] It is likely that the major forms of **54** (the amine moieties of **17a**,**b**) at neutral pH are diprotonated (**54**·$2H^+$) and monoprotonated (**54**·H^+) forms, and those of **55** (the amine moieties of **18a**,**b**) and **56** (the amine moieties of **19a**–**c**) are diprotonated forms (**55**·$2H^+$ and **56**·$2H^+$, respectively). These findings regarding the intracellular uptake of **17a**,**b**, **18a**,**b**, and **19a**–**c** (Figure 2-5) suggest that the diprotonated and/or monoprotonated forms of these boron-polyamine conjugates are preferable for effective intracellular uptake and that the monoprotonated form might be more favorable. The intrinsic stability constants (log K_{ZnL}) of the Zn^{2+} complexes **57**, **67**, and **68** (ZnL^{18}–ZnL^{20}) are also described in Scheme 10. The similar intracellular uptake of [9]aneN_3-type **17a,b** and **20a,b** in A549 cells and higher uptake of **20a,b** than that of **21a,b** and **22a**–**c** (Figure 2-5) can be explained by a smaller log K_{ZnL} value for **67** (ZnL^{18}) than those for **57** (ZnL^{19}) and **68** (ZnL^{20}) (less stability of **67** than **57** and **68**), although the reasons for higher intracellular uptake of **20a,b** than **17a,b** in HeLa S3 cells and IMR-90 cells are yet to be studied. The relationship of these complexation properties and the results of BNCT experiments of **17**, **18**, and **19** will be discussed below.

Consideration of protonation/deprotonation situations in Scheme 2-10 suggest that [9]aneN_3 (**54**) and [15]aneN_5 (**56**) would exist as **54**·$2H^+$ and **56**·$3H^+$ forms as well as **54**·H^+ and **56**·$2H^+$ forms, respectively, under (slightly) acidic conditions in cancer cells, so that exclusion of these drugs form the cells through the hydrophobic cell membrane would be somewhat disturbed. This point might be one of advantages of these boron-polyamine agents. It is unlikely that **54**, **55**, and **56** exist as **54**·$3H^+$, **55**·$3H^+$, **55**·$4H^+$, **56**·$4H^+$, and **56**·$5H^+$ forms, respectively, under physiological conditions, because their pK_{a1} values (and pK_{a2} values for **55** and **56**) are very low (less than 2).

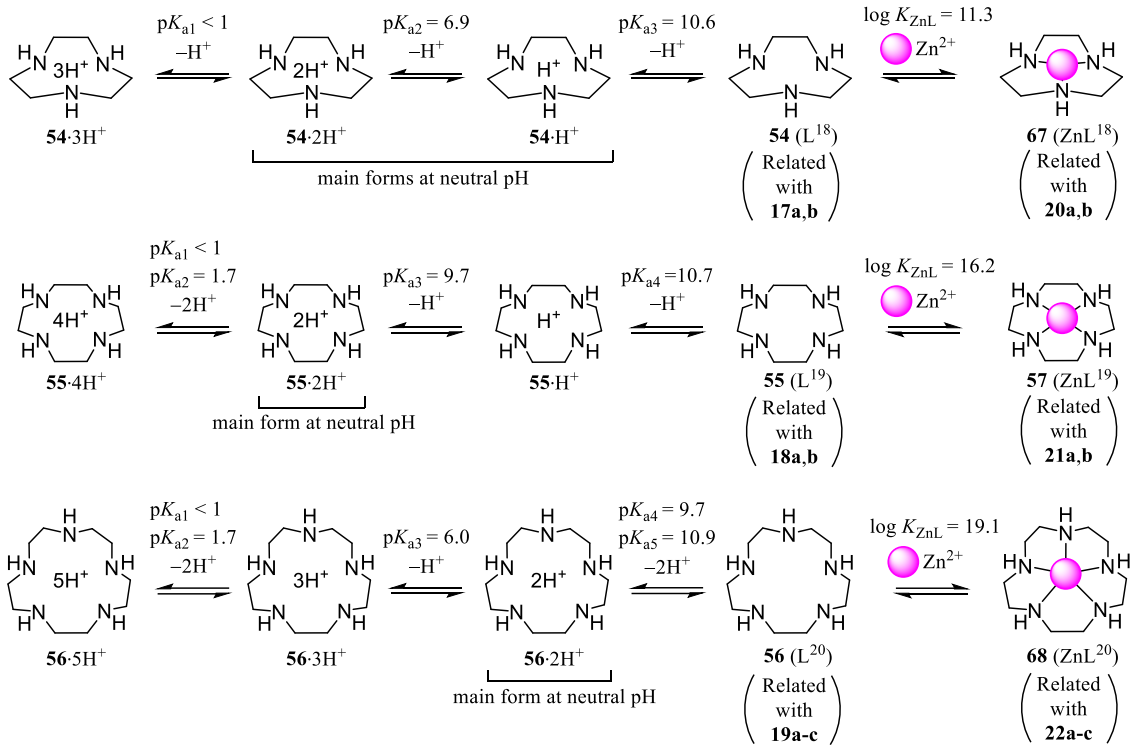

Scheme 2-10. Reported deprotonation constants (pK_a) of macrocyclic polyamines **54**–**56** (L^{18}–L^{20})[58–60] and stability constants (log K_{ZnL}) of their Zn^{2+} complexes **57**, **67**, and **68** (ZnL^{18}–ZnL^{20}) in aqueous solution at 25 °C.[61]

Next, the mechanism responsible for the intracellular uptake of **17a**, **18a**, and **19a** into HeLa S3 and A549 cells was examined. As shown in Figures 2-7a and 2-7b, the intracellular uptake of **17a**, **18a**, and **19a** was inhibited to a considerable extent at 4 °C, suggesting that the transfer of **17a**, **18a**, and **19a** into the cells is due to an energy-dependent process.

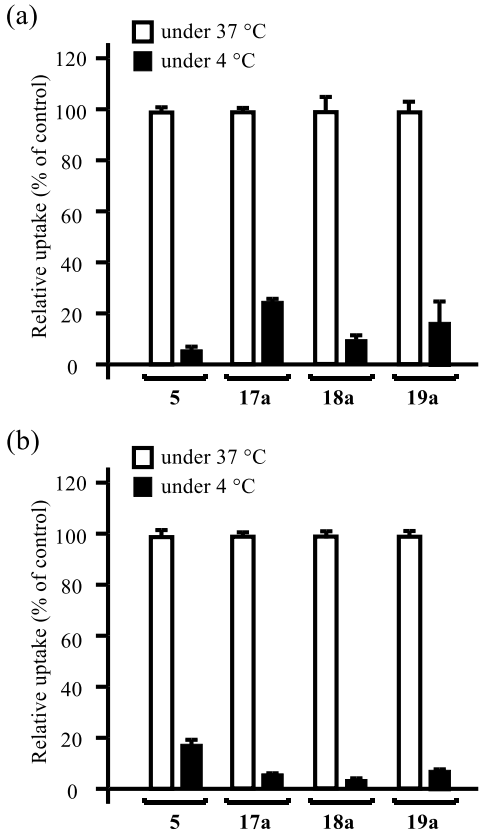

Figure 2-7. Effect of low temperature on the intracellular uptake of boron compounds **5** and **17a**–**19a** (30 μM) into HeLa S3 (a) and A549 cells (b) at 37 °C (open bars) or 4 °C (closed bars) for 1 h. Data represent the mean ± SD of at least three replicates.

It is known that the polyamine transporter system (PTS) in mammalian cells is associated with the endocytosis pathway of linear polyamines such as spermidine **49** and spermine **50** (Scheme 2-2).[35] In addition, methyl-beta-cyclodextrin (MβCD) **69** was reported to inhibit the caveola-endocytosis pathway due to the depletion of cholesterol,[74] and dynasore **70** and amiloride **71** are used as inhibitors of clathrin-endocytosis[75] and micropinocytosis,[76] respectively (the chemical structures of these inhibitors are shown in Scheme 2-11). As shown in Figure 2-8, the intracellular uptake of **19a** into HeLa S3 cells is inhibited to a considerable extent by dynasore **70** and spermidine **49**, suggesting that **19a** is transferred into the cells via the clathrin-endocytosis pathway, possibly including PTS.[35] A similar inhibitory effect of spermidine **49** on the intracellular uptake

of **19a** into A549 cells was observed, as shown in Figure 2-9. We assume that the weak inhibition of the uptake of **5** and **19a** by MβCD **69** is due to the inclusion of these boron compounds in the inner cavity of MβCD. It is reported that amiloride **71** inhibits the Na^+/H^+ exchanger and hence lower the intracellular Na^+ concentration. It is assumed that this Na^+ deficiency would be compensated by the Na^+ uptake via sodium-dependent amino acid transporters such as $ATB^{0,+}$ (amino acid transporter system $B^{0,+}$) that had been reported to mediate the co-transport of Na^+ with phenylalanine analogue **5**.[21] This assumption may explain the increased intracellular uptake of **5** in the presence of amiloride.

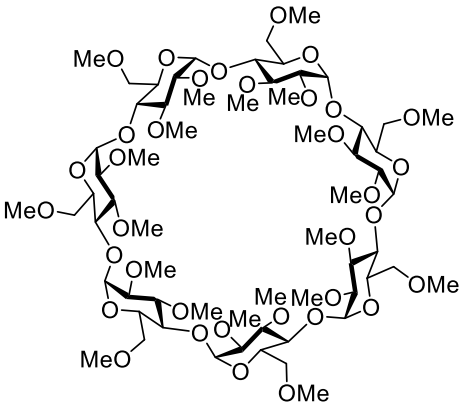

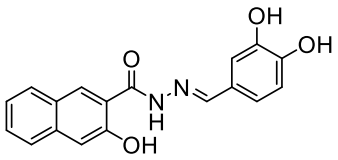

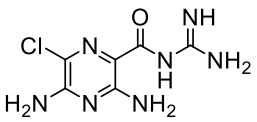

Scheme 2-11. Structures of endocytosis inhibitors.

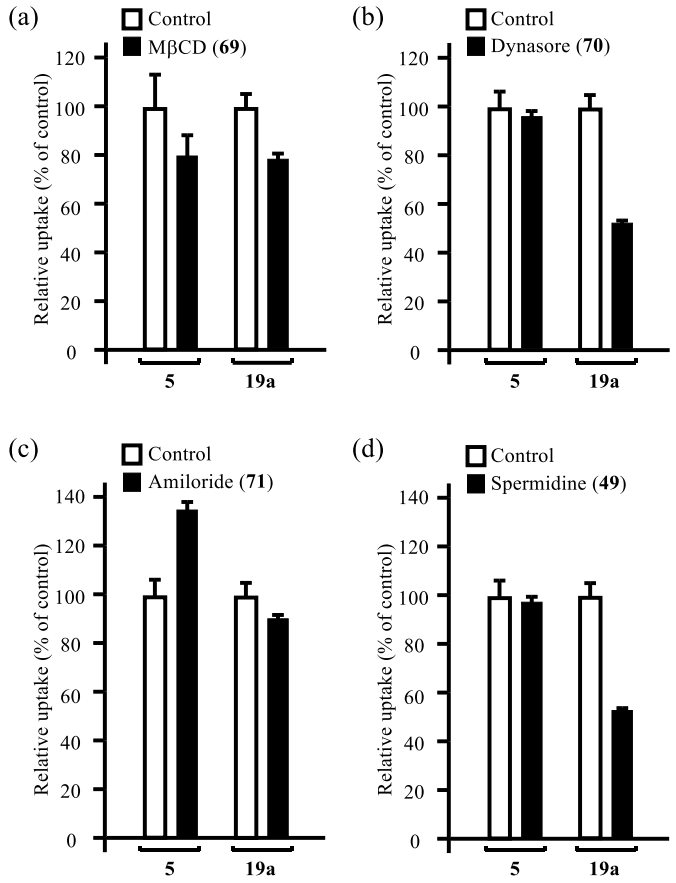

Figure 2-8. Relative uptake of **5** and **19a** (30 μM) into HeLa S3 cells in the absence (open bars) and presence of inhibitors (closed bars), 1.5 mM of MβCD **69** (a), 80 μM of dynasore **70** (b), 2 mM of amiloride **71** (c), and 2 mM of spermidine **49** (d). After pretreatment with the inhibitors for 1 h, the cells were incubated with **5** and **19a** at 37 °C for 1 h in the presence of inhibitors. Data represent the mean ± SD of at least three replicates.

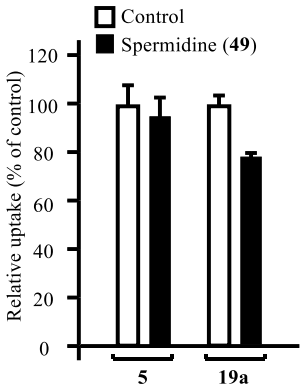

Figure 2-9. Relative uptake of **5** and **19a** (30 μM) into A549 cells in the absence (open

bars) and presence of **49** (2 mM) (closed bars). After preincubation with **49** for 1 h, the cells were incubated with **5** and **19a** at 37 °C for 1 h in the presence of **49**. Data represent the mean ± SD of at least three replicates.

[2-2-4] Evaluation of the cytotoxic effect of the selected boron-containing macrocyclic polyamine derivatives with thermal neutron irradiation by a colony formation assay

Based on the aforementioned results, we decided to choose **17b** (L^2), **18b** (L^4), and **19a** (L^5) for the BNCT, in which ^{10}B and ^{11}B are contained in a natural abundance ratio ($^{10}B/^{11}B$ = 19.9/80.1), and synthesized the corresponding ^{10}B-enriched compounds **^{10}B-17b**, **^{10}B-18b**, and **^{10}B-19a**, as shown in Scheme 2-12.

The ^{10}B-enriched forms of **60a** and **60b** (**^{10}B-60a** and **^{10}B-60b**) were prepared by the reaction of **72a**,**b** with ^{10}B-enriched trimethylborate (> 99.5% of ^{10}B), followed by hydrolysis with aqueous HCl to give **^{10}B-73a** and **^{10}B-73b** and bromination with *N*-bromosuccinimide (NBS). The reaction of **^{10}B-60a** and **^{10}B-60b** with **59**, **63**, and **65** and the following conversions were conducted as described in Schemes 2-6, 2-7 and 2-8 to obtain **^{10}B-17b**, **^{10}B-18b**, and **^{10}B-19a**, respectively.

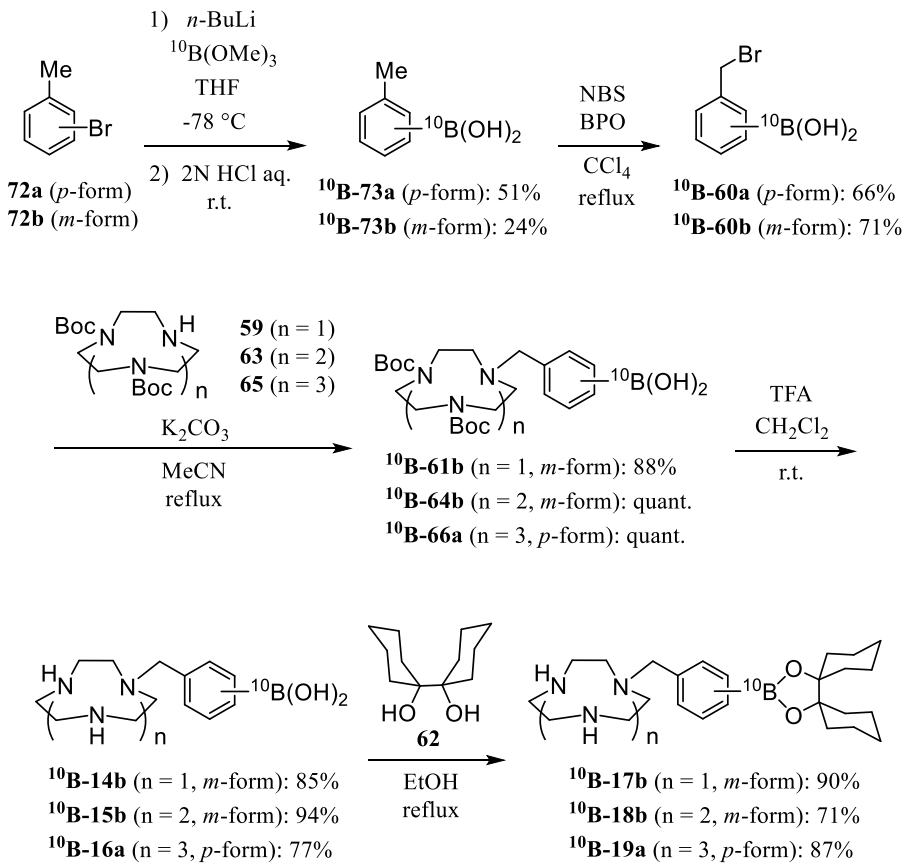

Scheme 2-12. Synthesis of ^{10}B-enriched **17b**, **18b**, and **19a** (**^{10}B-17b**, **^{10}B-18b**, and **^{10}B-19a**).

BNCT experiments using A549 cells in the presence of the aforementioned B-containing drugs (^{10}B/^{11}B and ^{10}B-enriched compounds) were conducted at the Institute for Integrated Radiation and Nuclear Science, Kyoto University (KURNS). As shown in Scheme 2-13, A549 cells were incubated with the boron compounds (30 μM) for 24 h and suspensions (5×10^4 cells/mL) of these cells were irradiated with thermal neutrons [average thermal neutron flux: $(1.5 \pm 0.1) \times10^9$ n/cm^2·s] at room temperature for various times (0, 15, 30, and 45 min). The irradiated cells were seeded on the 12-well plate (3×10^3 cells/well), incubated for 7 days, fixed with EtOH, and stained with crystal violet to produce visualizable images (Figure 2-10). The surviving fractions were calculated as the stained colony area using the "ImageJ-plugin Colony Area"[77] software and

normalized by comparing the results with those for non-irradiated cell samples (Figure 2-11).

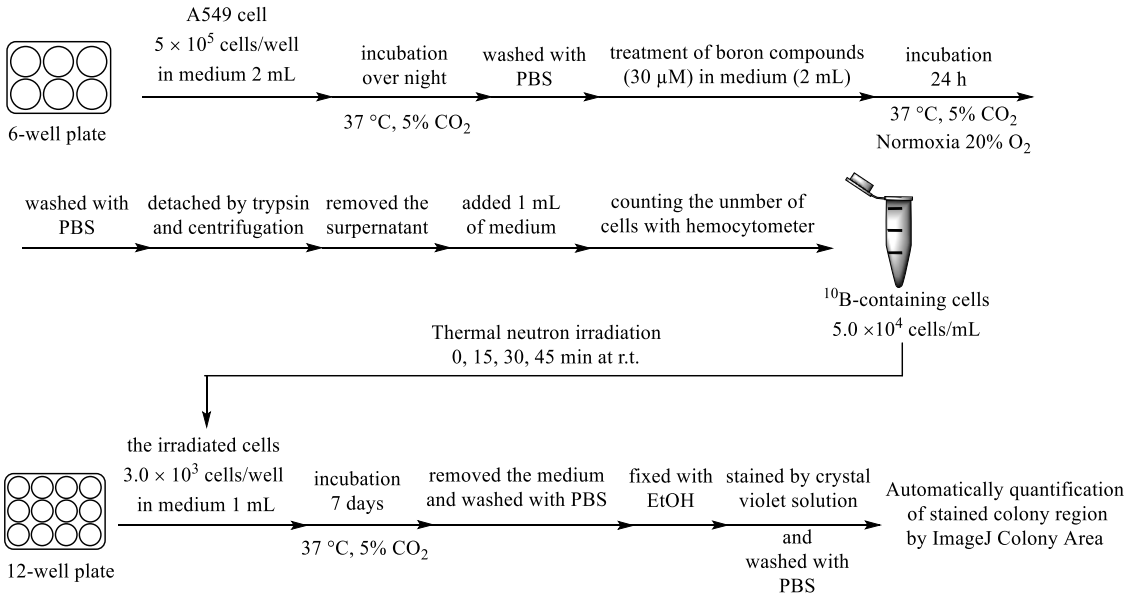

Scheme 2-13. Evaluation of the anti-tumor effect of boron compounds in an in vitro BNCT study.

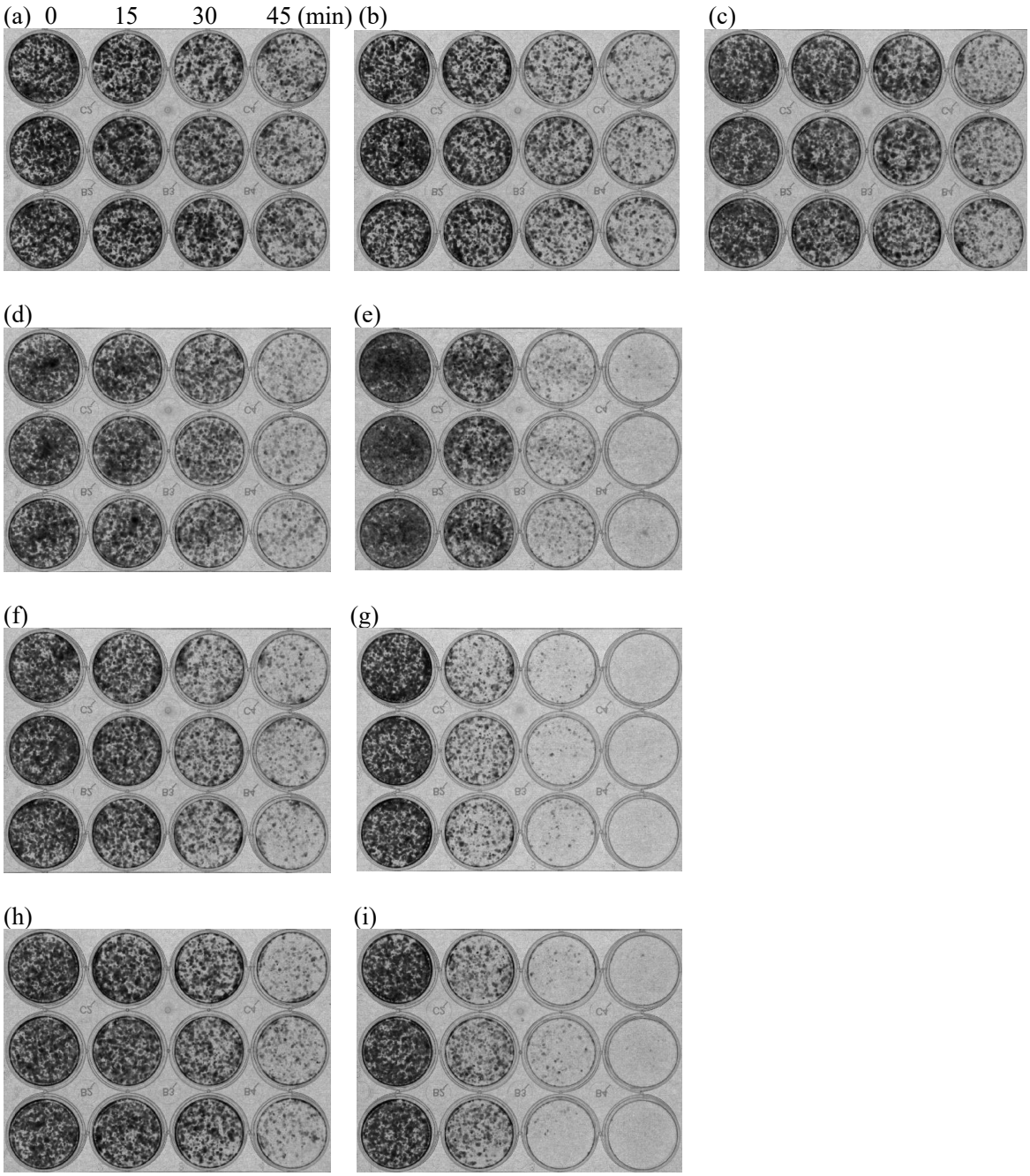

Figure 2-10. Typical images of colony formation assay of A549 cells after thermal neutron irradiation in the presence of (a) none, (b) ^{10}B-BSH (**4**), (c) ^{10}B-BPA (**5**), (d) **17b**, (e) **^{10}B-17b**, (f) **18b**, (g) **^{10}B-18b**, (h) **19a**, and (i) **^{10}B-19a** ([B-containing compounds] = 30 μM) (taken by Bio-Rad ChemiDoc^{TM} MP Imaging System (Bio-Rad)).

The results for the anti-tumor effect of boron compounds against A549 cells are summarized in Figure 2-11, which suggests the following points:

(1) The cytotoxic activity of **^{10}B-17b**, **^{10}B-18b**, and **^{10}B-19a** against A549 cells is higher than that for **4** (^{10}B-BSH) and **5** (^{10}B-BPA).

(2) The cytotoxic activity of the ^{10}B-enriched analogues is more potent than that of the ^{10}B/^{11}B derivatives (**^{10}B-17b** vs **17b**, **^{10}B-18b** vs **18b**, and **^{10}B-19a** vs **19a**) apparently due to the enrichment of ^{10}B.

(3) The BNCT activity of **^{10}B-20b**, **^{10}B-21b**, and **^{10}B-22a**, which are Zn^{2+} complexes of **^{10}B-17b**, **^{10}B-18b**, and **^{10}B-19a**, is also displayed in Figure 2-11. It was found that metal-free **^{10}B-18b** and **^{10}B-19a** exhibit a higher BNCT effect than **^{10}B-21b** and **^{10}B-22a**, possibly because of their higher intracellular uptake than that of stable **^{10}B-21b** and **^{10}B-22a**, which are very stable (see Figure 2-5 and Scheme 2-10).

(4) The BNCT effect of **^{10}B-17b** and its Zn^{2+} complex **^{10}B-20b** were nearly the same, possibly due to rather low stability of **^{10}B-20b**, as indicated by a relatively small log K_{ZnL} value (11.3) for **67** (ZnL^{18}) in Scheme 2-10.

(5) The relationship between the intracellular boron uptake (from Figure 2-5) and the BNCT effect (from Figure 2-11) is summarized in Figure 2-12. The BNCT effect of **^{10}B-18b** and **^{10}B-19a** was more potent than that of **^{10}B-17b**, while the intracellular uptake of the metal-free **^{10}B-18b** and **^{10}B-19a** was lower than that of **^{10}B-17b**.

(6) As presented in Figures 2-7 and 2-8, intracellular uptake of boron-containing macrocyclic polyamines is considerably inhibited at 4 ℃ and in the presence of endocytosis inhibitor and spermidine. Besides, the BNCT effect of ^{10}B-enriched agents is not parallel to their intracellular uptake, as shown in Figure 2-12, which suggests their close interaction with DNA in living cells. Therefore, it is likely that B-macrocycles are transferred into living cells via an energy-dependent process such as endocytosis and then make a close contact to DNA, resulting in an efficient BNCT effect, although the possibility of the partial distribution of these boron agents in the cell membrane cannot

be denied.

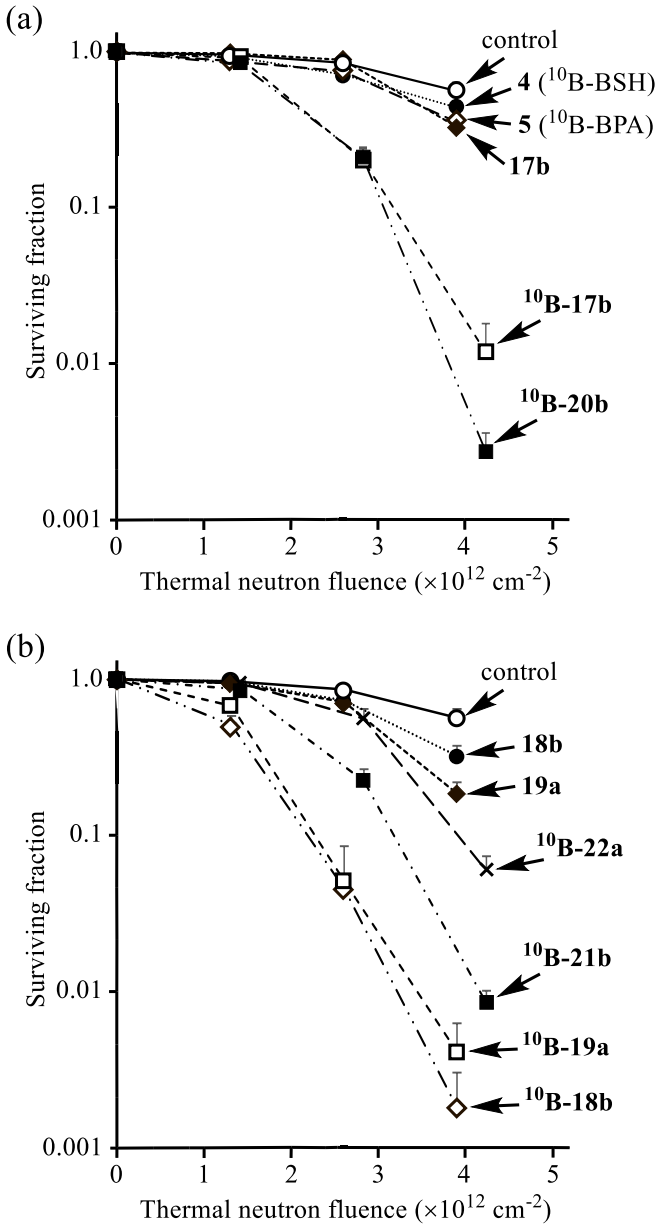

Figure 2-11. Anti-tumor effect of boron compounds **4**, **5**, **17b**, **^{10}B-17b**, **18b**, **^{10}B-18b**, **19a**, **^{10}B-19a**, **^{10}B-20b, ^{10}B-21b**, and **^{10}B-22a** (30 μM) against A549 cells was examined by a colony formation assay: (a) control (in the absence of boron compound) (○), **4** (●), **5** (◇), **17b** (◆), **^{10}B-17b** (□), and **^{10}B-20b** (■). (b) control (○), **18b** (●), **^{10}B-18b** (◇), **19a** (◆), and **^{10}B-19a** (□), and **^{10}B-21b** (■), and **^{10}B-22a** (×). After treatment with the boron compound for 24 h, the cells were irradiated with thermal neutrons for 0, 15, 30, and 45 min and then incubated without neutron irradiation for 7 days. Averaged

thermal neutron flux was 1.4 × 10^9 n/cm^2·s for control (in the absence of boron compound), **4**, **5**, **17b**, **18b**, **^{10}B-18b**, **19a** and **^{10}B-19a** and 1.6 × 10^9 n/cm^2·s for **^{10}B-17b**, **^{10}B-20b, ^{10}B-21b** and **^{10}B-22a**, respectively. The survival fraction was determined by ImageJ-plugin Colony Area. Data represent the mean ± SD of at least three replicates.

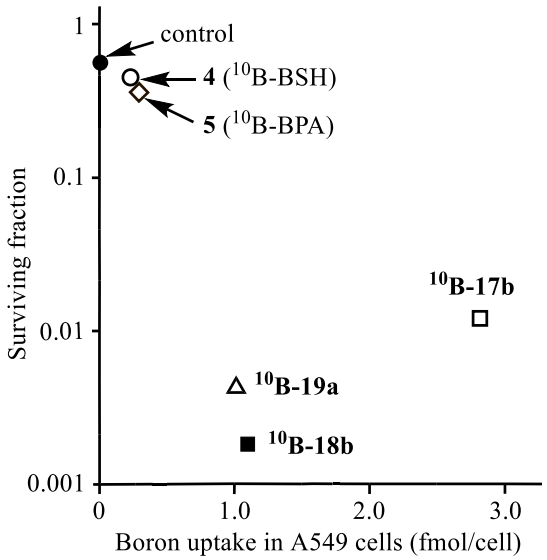

Figure 2-12. Relationship between the intracellular uptake of boron compounds **4** (○), **5** (◇), **^{10}B-17b** (□), **^{10}B-18b** (■), **^{10}B-19a** (△) (30 μM) and control (in the absence of boron compound) (●) into A549 cells after incubation for 24 h and their BNCT effect (Surviving fractions after irradiation with thermal neutrons for 45 min; thermal neutron fluence: 4.1 ± 0.1 × 10^{12} n/cm^2).

These experimental data allow us to propose two possibilities for the BNCT effect of **^{10}B-17b**, **^{10}B-18b**, and **^{10}B-19a**, as presented in Scheme 2-14. One possible explanation would be that cytotoxicity is dependent on the close interaction of metal-free macrocyclic polyamines with DNA via the ionic interaction (**74** in Scheme 2-14) and the amount of double-strand breaks in DNA by ^{4}He and/or ^{7}Li generated by the [^{10}B(n, α)^{7}Li] reaction.[2,78] More plausible possibility would be the breakdown of DNA via the interaction with metal complexes **^{10}B-20b**, **^{10}B-21b**, and **^{10}B-22a** (**75** and **76** in Scheme 2-14), because it is very likely that these B-containing macrocyclic polyamines would

form complexes with metal cations contained in the media and/or in living cells.

As described in the Introduction (Scheme 2-5), we expected that the Zn^{2+} complexes **^{10}B-20b**, **^{10}B-21b**, and **^{10}B-22a** would interact with deprotonated dT (dT^{-}) in DNA and that the DNA would be efficiently damaged upon thermal neutron irradiation (**76** in Scheme 2-14) (it had been reported that Cu^{2+}, Ni^{2+} and Fe^{2+} complexes of cyclen negligibly interact with DNA).[65c] These data allow us to consider that the metal-free **^{10}B-17b**, **^{10}B-18b**, and **^{10}B-19a** (possibly the diprotonated form, as speculated in Scheme 2-10) are transferred into cancer cells efficiently and form complexes with intracellular Zn^{2+} and recognize dT in DNA, resulting in an efficient BNCT effect.

In order to obtain experimental data for this hypothesis, we measured the melting temperature (T_m) of the double-stranded calf-thymus DNA (ctDNA) (50 μM in phosphate) in the presence of **18b** (L^4), **21b** (ZnL^4), **19a** (L^5), **22a** (ZnL^5), and **49** (for the reference).[65d,e,79] As shown in Table 2-2 and Figure 2-13, the T_m value of ctDNA was raised by **18b**, **19a**, and **49** (ΔT_m = +6 °C and +8 °C for **18b** and **19a**, respectively, at r = 5.0 and ΔT_m = +12 °C for **49** at r = 0.2, where r = [**18b**, **19a**, or **49**]/[ctDNA(P)]) due to stabilization of the double-stranded structure of ctDNA (**74** in Scheme 2-14). On the other hand, the T_m value was lowered in the presence of **21b** (ΔT_m = –6 °C at r = 1.0), possibly due to the destabilization of ctDNA by the interaction of its Zn^{2+}-[12]aneN$_4$ complex part with dT units in DNA (Scheme 2-5 and **76** in Scheme 2-14) (the breakdown of the hydrogen bondings between dT and adenine (dA) in double-stranded DNA was previously checked by the disappearance of imino proton signals of dT in the presence of Zn^{2+}-[12]aneN$_4$ complexes in ^{1}H NMR measurements).[79c]

An interesting finding was that the T_m value was raised by **22a** (ΔT_m = +6 ºC at r = 1.0), suggesting that **21b** and **22a** interact with ctDNA in different modes. It should be noted that coordination sites of Zn^{2+}, whose general coordination number is 4~6 (or 7),[63b,73,80] would be almost occupied by the coordination of five nitrogens from its [15]aneN$_5$ ring unit of **22a** and hence Lewis acidity of the Zn^{2+} ion would be considerably reduced.

Therefore, it is considered that these factors would hamper the coordination of **22a** with dT^- sites in DNA and that **22a** interacts with ctDNA mainly by the electrostatic interaction to stabilize the DNA double-strand, as shown in **75** of Scheme 2-14.[81,82] These data support the efficient DNA damage induced by **^{10}B-18b**, **^{10}B-21b**, **^{10}B-19a**, and **^{10}B-22a** at the close position upon neutron irradiation, as proposed in Scheme 2-14.

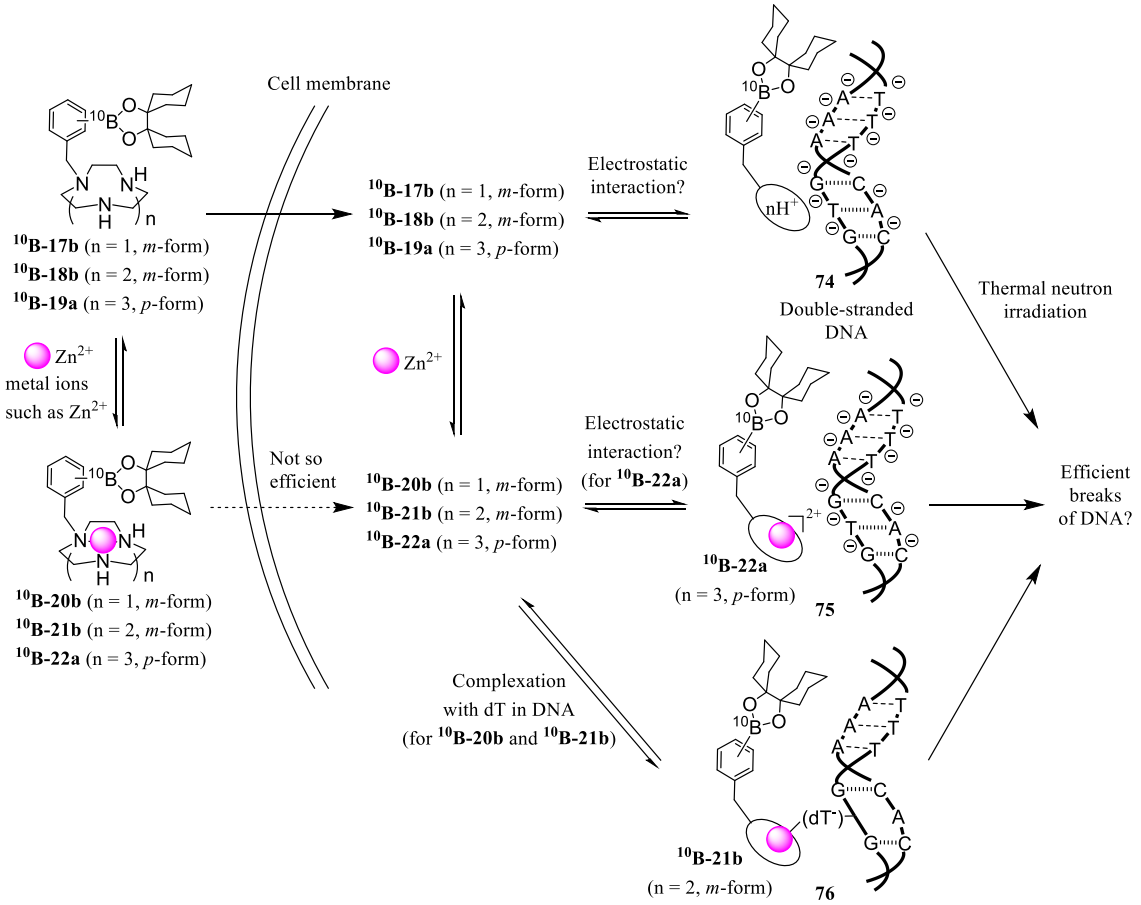

Scheme 2-14. Proposed scheme for BNCT effect of **^{10}B-17b**, **^{10}B-18b**, **^{10}B-19a**, and their Zn^{2+} complexes.

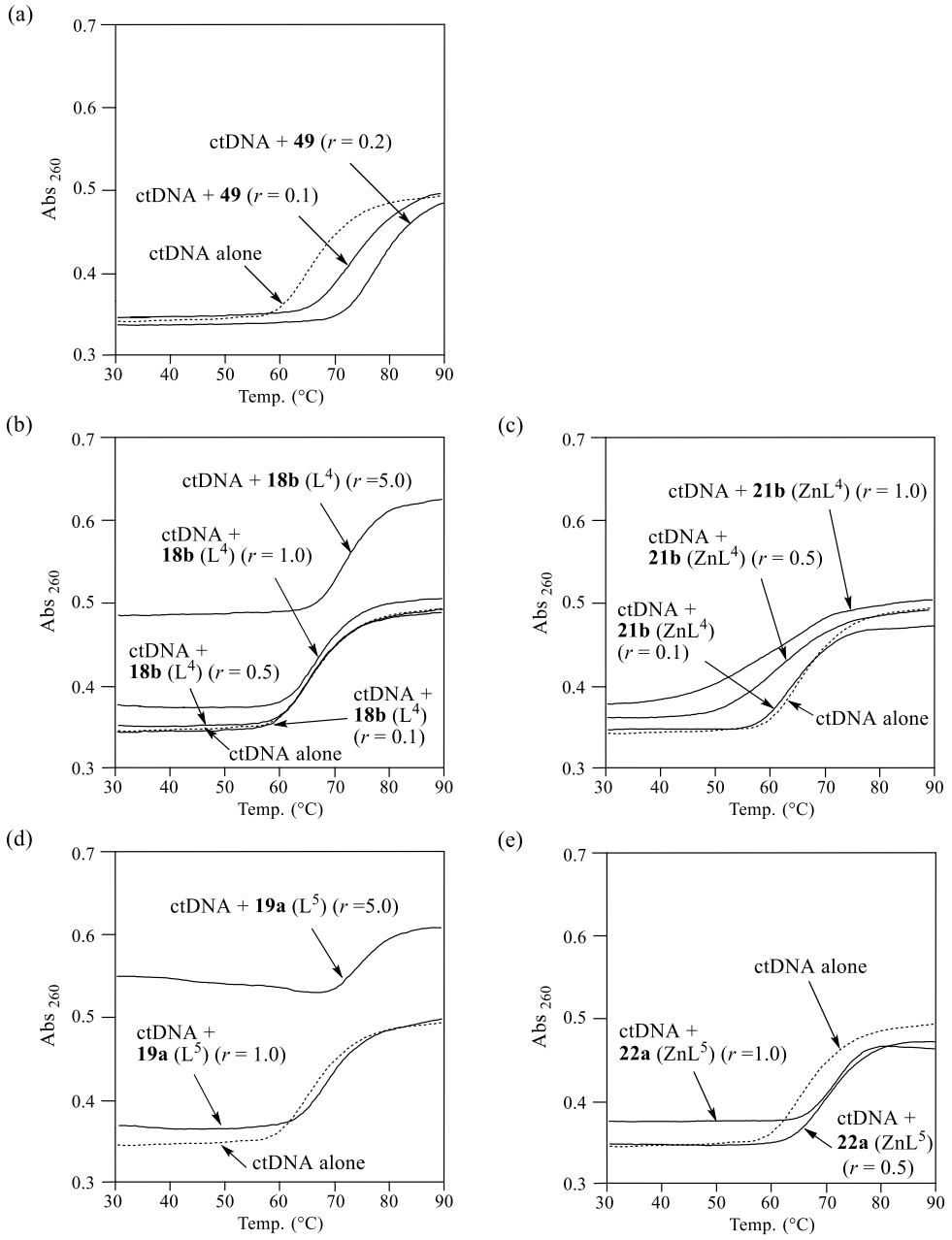

Figure 2-13. Change in thermal melting (T_m) curves of ctDNA (at [ctDNA(P)] = 50 μM) in the absence (dash line) and presence of (a) spermidine **49**, (b) **18b**, (c) **21b**, (d) **19a**, and (e) **22a** (plain line) at pH 7.4 (10 mM HEPES with I = 0.02 ($NaNO_3$), (r = [**49**, **18b**, **21b**,**19a**, or **22a**]/[ctDNA(P)])

Table 2-2. T_m values of ctDNA in the presence of **49**, **18b**, **21b**, **19a**, and **22a** (r = [**49**, **18b**, **21b**, **19a**, or **22a**]/[ctDNA(P)]) ([ctDNA(P)] = 50 μM in phosphate)

Additives (Zn complexes)	r	T_m (°C)	ΔT_m (°C)
none		66	
Spermidine (**49**)	0.1	73	+7
	0.2	78	+12
18b (L^4)	0.1	66	
	0.5	66	
	1.0	67	+1
	5.0	72	+6
21b (ZnL^4)	0.1	64	-2
	0.5	62	-4
	1.0	60	-6
19a (L^5)	1.0	69	+3
	5.0	74	+8
22a (ZnL^5)	0.5	71	+5
	1.0	72	+6

[2-3] Conclusions

In conclusion, we report on the design and synthesis of boron-containing macrocyclic polyamine derivatives as novel boron delivery agents for BNCT. The results of biological studies suggest that the intracellular uptake of **17**–**19**, especially, the 9-membered triamine derivatives **17a** and **17b**, into cancer cells is higher than that of **4** and **5**, and that **17b**, **18b**, and **19a** are selectively transferred into A549 cells. The results of BNCT experiments using A549 cells in the presence of **17b**, **18b**, and **19a** including boron in a natural abundance $^{10}B/^{11}B$ ratio and their ^{10}B-enriched derivatives **^{10}B-17b**, **^{10}B-18b**, and **^{10}B-19a** suggest that metal-free forms of these boron carriers inhibit the proliferation of A549 cells to a considerable extent after irradiation with thermal neutrons and that this inhibition is stronger than that for **4** and **5**. In addition, it was suggested that [12]aneN_4-type **^{10}B-18b** and [15]aneN_5-type **^{10}B-19a** exhibit a higher BNCT effect than [9]aneN_3-type derivatives, possibly due to the formation of the corresponding Zn^{2+} complexes (**^{10}B-21b** and **^{10}B-22a**) in cancer cells that would interact with DNA, although **^{10}B-21b** and **^{10}B-22a** interact with DNA in different modes. It should also be noted that macrocycles containing boron in a natural abundance $^{10}B/^{11}B$ ratio are capable of inducing cell death in BNCT to some extent and hence can be used as ^{11}B MRI probes to detect their distribution in living bodies as well as BNCT agents.

We believe that these findings provide useful information for the further development of BNCT for cancer treatment. The design and synthesis of more efficient and safer (high T/N ratio) boron carriers are currently underway in our laboratory.

Chapter 3.

Design, Synthesis and Biological Evaluation of Boron-Containing Macrocyclic Polyamine Dimers and Their Zinc(II) Complexes for Boron Neutron Capture Therapy

（ホウ素中性子捕捉療法のための
含ホウ素大環状ポリアミン二量体と亜鉛錯体の
設計・合成および生物学的評価）

[3-1] Introduction

Boron neutron capture therapy (BNCT) is a powerful method for cancer therapy and is based on the irradiation of cancer cells with thermal neutrons (^{1}n). The nuclear reaction of ^{10}B with thermal neutrons (^{1}n) (^{10}B(n, α)^{7}Li) generates two heavy particles, α particles and lithium ions, which induce the ionization and excitation of biologically essential molecules, such as proteins, RNA and DNA within a relatively short range of around 5–9 μm, resulting in the induction of cell death in ^{10}B-containing cells.[2,3] Therefore, specific delivery of such boron agents to cancer cells is required for selective cancer treatment with minimal effects on healthy tissues. Although two BNCT agents, disodium mercaptoundecahydrododecaborate (BSH) **4**[11–13] and L-4-boronophenylalanine (BPA) **5**[14–22] (used as a complex with D-fructose) have been clinically used for the cancer therapy for recurrent head and neck cancer and malignant gliomas, they are not sufficiently specific to permit them to be used for the treatment of various tumor types (Scheme 3-1).[7] Therefore, the development of more efficient and less toxic boron carriers will be needed for the treatment of multiple tumor types.

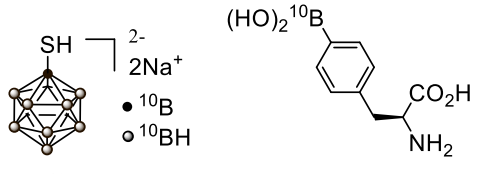

^{10}B-BSH
4

^{10}B-BPA
5
(used as a complex with D-fructose)

Scheme 3-1. Structures of representative BNCT agents.

To date, various boron carrier candidates based on amines,[37,38] amino acids,[39–41,52] carbohydrates,[43–47] biochemical precursors of nucleic acids,[31–33] porphyrins,[24–28] liposomes,[49] peptides,[48] and monoclonal antibodies have been proposed.[51] These boron compounds can be classified into four categories based on their targets: (1) boron-

containing molecules with no cell targeting; (2) cancer cell selective compounds; (3) binding only to the cell nucleus, and (4) tumor cell selective and binding to the cell nucleus.[83] It is well known that the selective and high accumulation of boron-containing molecules into cancer cells are required for successful BNCT (20–35 μg/gram of ^{10}B inside and/or near tumor tissues).[8] In addition, if it were possible to fix the position of such boron carriers close to DNA molecules by introducing DNA-binding units into their structures, then it would be possible to reduce the dose of the carriers.[2]

It is known that polyamines such as spermidine **49** and spermine **50** play important roles in various cellular events, including the regulation of gene expression, maintenance of chromatin structure and membrane stability due to ionic interaction with DNA, RNA, proteins and phospholipids.[34] It should be also noted that the enhancement of the growth of cancer cells is associated with increased polyamine levels, a process that is controlled by the activated polyamine transport system (PTS) and biosynthesis.[35] These issues suggest that polyamine scaffolds would be suitable for use in cancer-selective and DNA-binding boron carriers, as represented by the spermidine derivatives **51** and **52** (Scheme 3-2),[37,38] although evaluations of their BNCT effect have not been reported.

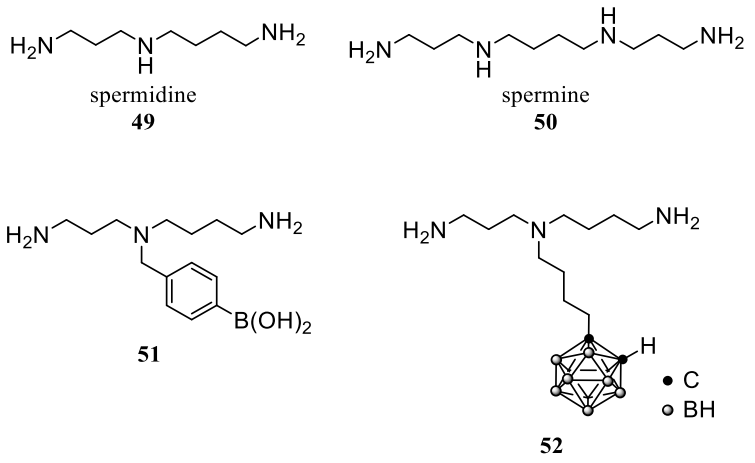

Scheme 3-2. Structures of polyamines and boron-containing spermidine derivatives **51** and **52**.

As described in Chapter 2, we recently reported on the design and synthesis of boron-containing macrocyclic polyamines **17b**, **18b**, and **19a** (L^2, L^4, and L^5) and their Zn^{2+} complexes **20b**, **21b**, and **22a** (ZnL^2, ZnL^4, and ZnL^5) (Scheme 3-3). Our findings indicated that **17b**, **18b**, and **19a** are transferred into cancer cells (A549 and HeLa S3 cells) more efficiently than into IMR-90 cells, a model of normal cells. The results of BNCT studies using ^{10}B-enriched forms of **17b**, **18b**, and **19a** suggested that [12]aneN_4-type **^{10}B-18b** and [15]aneN_5-type **^{10}B-19a** inhibit the proliferation of A549 cells to a considerable extent after thermal neutron irradiation, and that the inhibition effect is stronger than that for **4**, **5**, and [9]aneN_3-type **^{10}B-17b**.

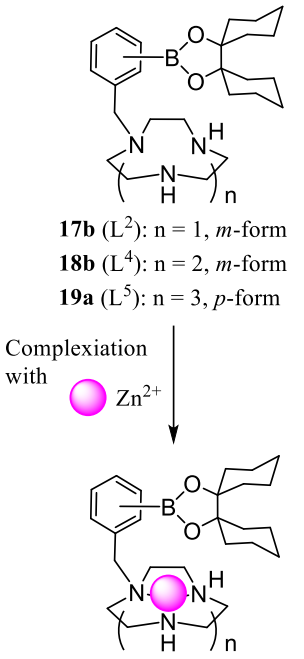

17b (L^2): n = 1, *m*-form
18b (L^4): n = 2, *m*-form
19a (L^5): n = 3, *p*-form

20b (ZnL^2): n = 1, *m*-form
21b (ZnL^4): n = 2, *m*-form
22a (ZnL^5): n = 3, *p*-form

Scheme 3-3. Structures of macrocyclic polyamine derivatives **17b**, **18b**, and **19a** (L^2, L^4, and L^5) and their Zn^{2+} complexes **20b**, **21b**, and **22a** (ZnL^2, ZnL^4, and ZnL^5).

It has also been well established that Zn^{2+}-cyclen complexes such as **57** (ZnL^{19}) interact selectively with thymidine (dT) parts in DNA at physiological pH in aqueous solution, yielding a fairly stable complex **58**, which is formed by coordination bonding

between the deprotonated imide moiety of dT (dT^-) and Zn^{2+} and hydrogen bonding between the N-H and carbonyl groups of dT^- (Scheme 3-4a).[65] Melting temperature (T_m) measurements of the double-stranded calf-thymus DNA (ctDNA) in the absence and presence of **18b**, **19a**, **21b** and **22a** suggested that the main interaction mode of **18b**, **19a**, and **22a** (L^4, L^5 and ZnL^5) is electrostatic interactions with ctDNA to stabilize its double-stranded structure (**74** and **75** in Scheme 3-5) and that **21b** (ZnL^4) destabilizes the double-stranded DNA, possibly via the interaction of its Zn^{2+}-cyclen complex part with dT in DNA (**76** in Scheme 3-5). Therefore, it was concluded that metal-free **^{10}B-18b** (^{10}B-L^4) is efficiently transferred into cancer cells and form complexes with intracellular Zn^{2+}, and that **^{10}B-18b** interacts with DNA by the electrostatic interactions between polyanionic DNA and the cationic polyamine part of **^{10}B-18b** (**74** in Scheme 3-5). On the other hand, the Zn^{2+} complex of **^{10}B-18b**, **^{10}B-21b** (^{10}B-ZnL^4), recognizes dT^- in DNA by the complexation of its Zn^{2+}-[12]aneN_4 part with dT^- in DNA. Regarding the [15]aneN_5 derivatives **^{10}B-19a** (^{10}B-L^5) and its Zn^{2+} complex **^{10}B-22a** (^{10}B-ZnL^5), it was suggested that both of them interact with DNA by the electrostatic interactions by means of the cationic [15]aneN_5 part of **^{10}B-19a** (**74** in Scheme 3-5) or the Zn^{2+}-[15]aneN_5 unit of **^{10}B-22a** (**75** in Scheme 3-5), resulting in effective DNA damage upon thermal neutron irradiation (Scheme 3-5).

(a)

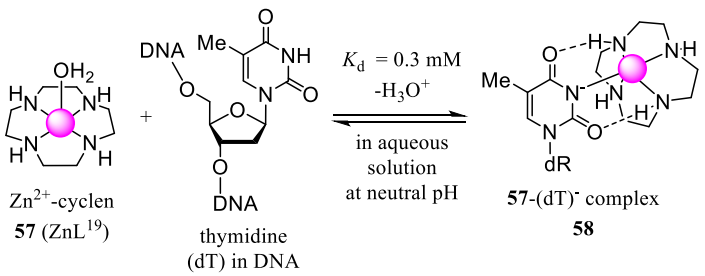

(b)

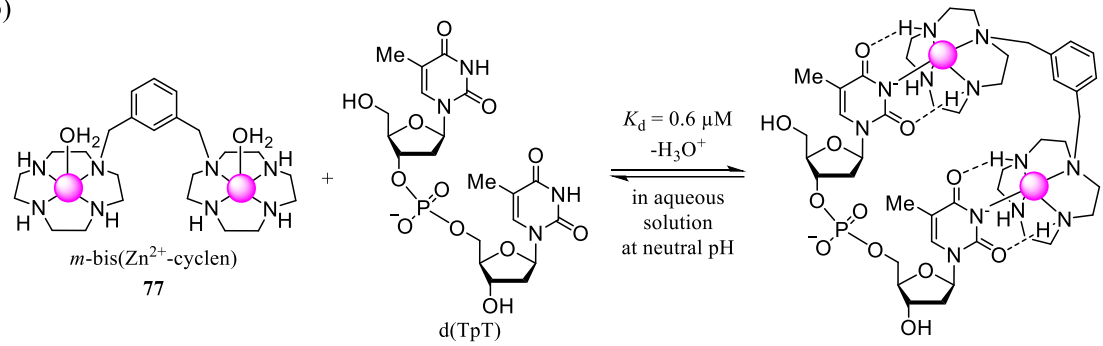

Scheme 3-4. Complexation of (a) Zn^{2+}-cyclen **57** (ZnL^{19}) with the deprotonated form of thymidine (dT^-) and (b) bis(Zn^{2+}-cyclen) **77** with $d(T^-pT^-)$ **78** in aqueous solution at neutral pH.

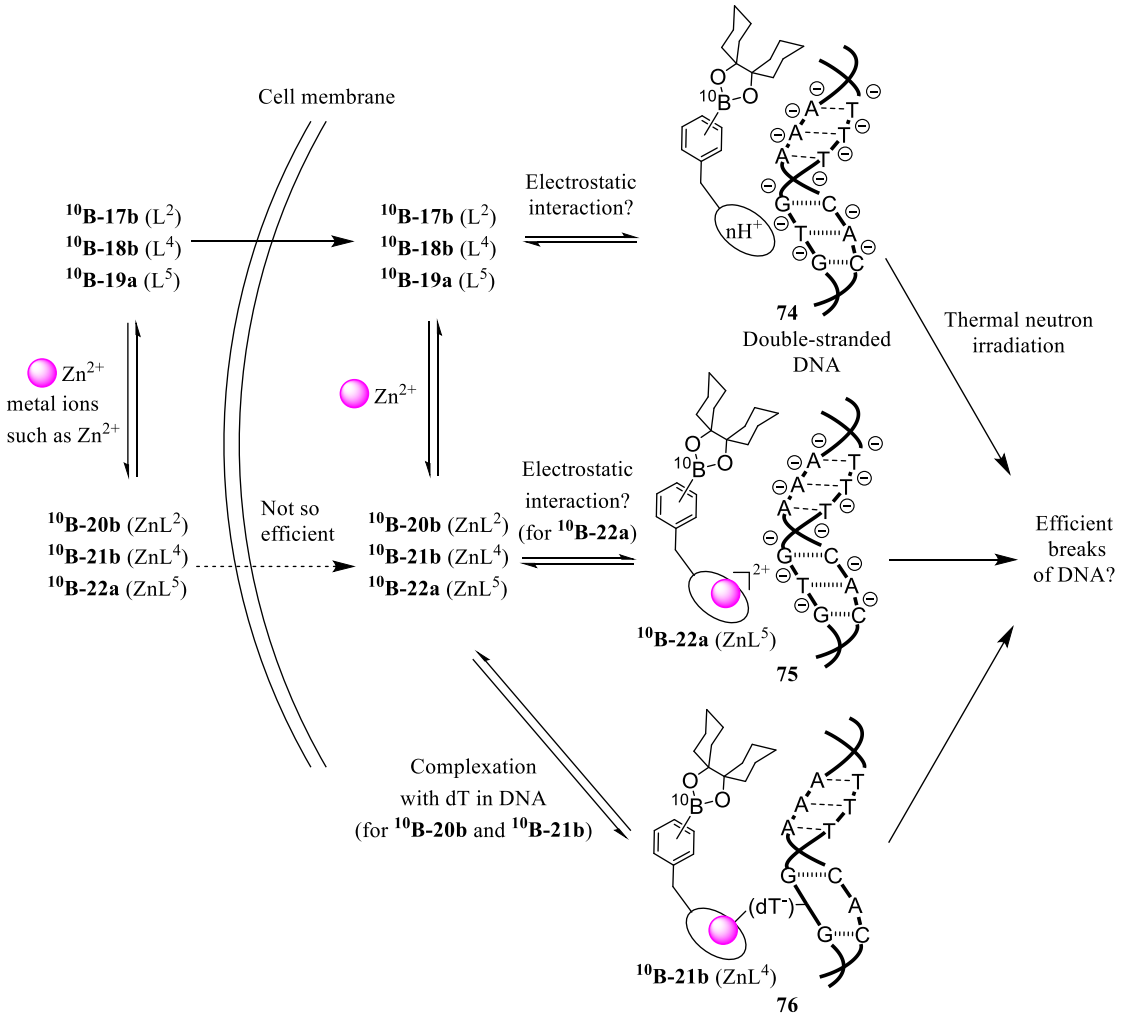

Scheme 3-5. Proposed scheme for the interaction of **^{10}B-17b**, **^{10}B-18b**, and **^{10}B-19a**, and their Zn^{2+} complexes with DNA for BNCT.

The aforementioned results prompted us to design and synthesize the conjugated compounds of boron with homo- and hetero-dimers of [9]aneN$_3$, [12]aneN$_4$ (cyclen) and [15]aneN$_5$. Aoki and Kimura reported that bis(Zn^{2+}–cyclen) complexes such as **77** (*m*-bis(Zn^{2+}–cyclen)) strongly interact with the thymidyl(3′–5′)thymidine dimer (d(TpT)) **78** to form a 1:1 complex **79**, which is more stable than that of **58** (Scheme 3-4b).[84] The dissociation constant (K_d) for **79** (1:1 **77**–d(T$^-$pT$^-$) complex) was determined to be 0.6 μM in aqueous solution at neutral pH, while the K_d value for a 1:1 complex of dT$^-$ with **57** (ZnL^{19}) (**58**) was 0.3 mM under the same conditions.[84] In this work, therefore, we designed and synthesized the boron-containing macrocyclic polyamine dimers **23**–**32** (L^8–L^{17}) and their corresponding monozinc(II) complexes **33**–**38** (ZnL^8–ZnL^{16}) and dizinc(II) complexes **39**–**48** (Zn$_2$L^8–Zn$_2$L^{17}), which contain phenylboronic acid or the corresponding boronic acid ester groups (Scheme 3-6). We hypothesized that the interaction of ditopic macrocyclic polyamines and their corresponding monozinc(II) and dizinc(II) complexes with DNA would be stronger than that of the monomers such as **21b** (ZnL^4) and that a higher BNCT effect would be observed. In this study, we report on the synthesis of these boron carriers, their interaction with double-stranded DNA (calf-thymus DNA, ctDNA), and biological studies including cytotoxicity and intracellular uptake activity against several cell lines (HeLa S3, A549, and IMR-90 cells). The BNCT effect of the ^{10}B-enriched macrocyclic polyamine dimers and their Zn^{2+} complexes are also reported.

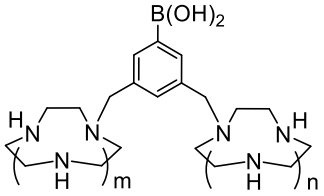

23 (L^8): m = 2, n = 1
24 (L^9): m = 2, n = 2
25 (L^{10}): m = 2, n = 3
26 (L^{11}): m = 3, n = 1
27 (L^{12}): m = 3, n = 3

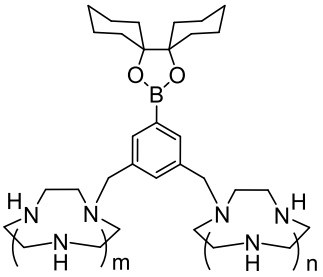

28 (L^{13}): m = 2, n = 1
29 (L^{14}): m = 2, n = 2
30 (L^{15}): m = 2, n = 3
31 (L^{16}): m = 3, n = 1
32 (L^{17}): m = 3, n = 3

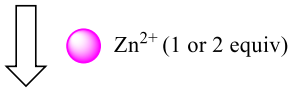

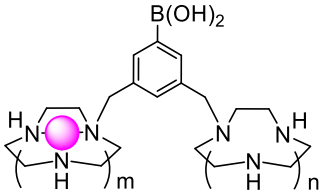

33 (ZnL^8): m = 2, n = 1
34 (ZnL^{10}): m = 3, n = 2
35 (ZnL^{11}): m = 3, n = 1

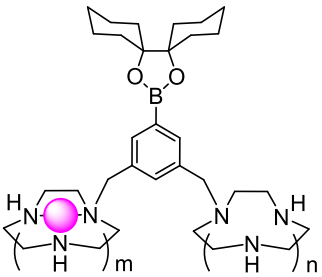

36 (ZnL^{13}): m = 2, n = 1
37 (ZnL^{15}): m = 3, n = 2
38 (ZnL^{16}): m = 3, n = 1

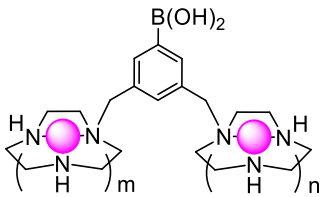

39 (Zn_2L^8): m = 2, n = 1
40 (Zn_2L^9): m = 2, n = 2
41 (Zn_2L^{10}): m = 2, n = 3
42 (Zn_2L^{11}): m = 3, n = 1
43 (Zn_2L^{12}): m = 3, n = 3

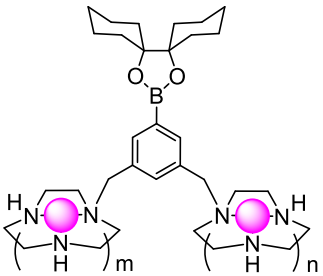

44 (Zn_2L^{13}): m = 2, n = 1
45 (Zn_2L^{14}): m = 2, n = 2
46 (Zn_2L^{15}): m = 2, n = 3
47 (Zn_2L^{16}): m = 3, n = 1
48 (Zn_2L^{17}): m = 3, n = 3

Scheme 3-6. Structures of boron-containing macrocyclic polyamine dimers **23**–**32** (L^8–L^{17}) and their Zn^{2+} complexes **33**–**48** (ZnL^8–ZnL^{16} and Zn_2L^8–Zn_2L^{17}) that were synthesized in this work.

[3-2] Results and discussion

[3-2-1] Synthesis of boron-containing macrocyclic polyamine dimers and their zinc(II) complexes

The synthesis of the boron-containing macrocyclic polyamine dimers **23**–**32** (L^8–L^{17}) and their Zn^{2+} complexes **33–48** (ZnL^8–ZnL^{16} and Zn_2L^8– Zn_2L^{17}) is shown in Schemes 3-7 and 3-8. 3,5-Dimethylphenylboronic acid **80** was treated with pinacol to give **81**[85], which was reacted with *N*-bromosuccinimide (NBS) to obtain **82** (Scheme 3-7).[86] The reaction of **82** with **63**[72] and **65**[73] afforded **83** and **84**, respectively. The heterodimers **23**, **25** and **26** (L^8, L^{10}, and L^{11}) were prepared by the reaction of **83** and **84** with Boc-protected macrocyclic polyamines **59**[67] and **65**, followed by the deprotection of pinacol ester and Boc groups using aqueous HBr and EtOH solution. The HBr salts of **23**, **25** and **26** (L^8, L^{10}, and L^{11}) were converted to their corresponding acid-free forms using an anionic ion exchange resin column (Amberlite IRA-400, OH^- form) and then treated with bicyclohexyl-1,1′-diol **62**[69] to give **28**, **30** and **31** (L^{13}, L^{15}, and L^{16}), respectively. The complexation of these ligands with Zn^{2+} (1 or 2 equiv) was conducted *in situ* prior to their biological evaluation. Because it is well known that the stability of Zn^{2+} complexes is dependent on the number of nitrogen atoms in the macrocyclic rings, the order of the complexation constants is Zn^{2+}-[15]aneN_5 (**22a** in Scheme 3-3) > Zn^{2+}-[12]aneN_4 (**21b**) > Zn^{2+}-[9]aneN_3 (**20b**).[61] Therefore, it is very likely that the heterodimer-type ligands **23** (L^8), **25** (L^{10}), **26** (L^{11}), **28** (L^{13}), **30** (L^{15}) and **31** (L^{16}) form monozinc(II) complexes as indicated in **33**–**38** (Scheme 3-6).

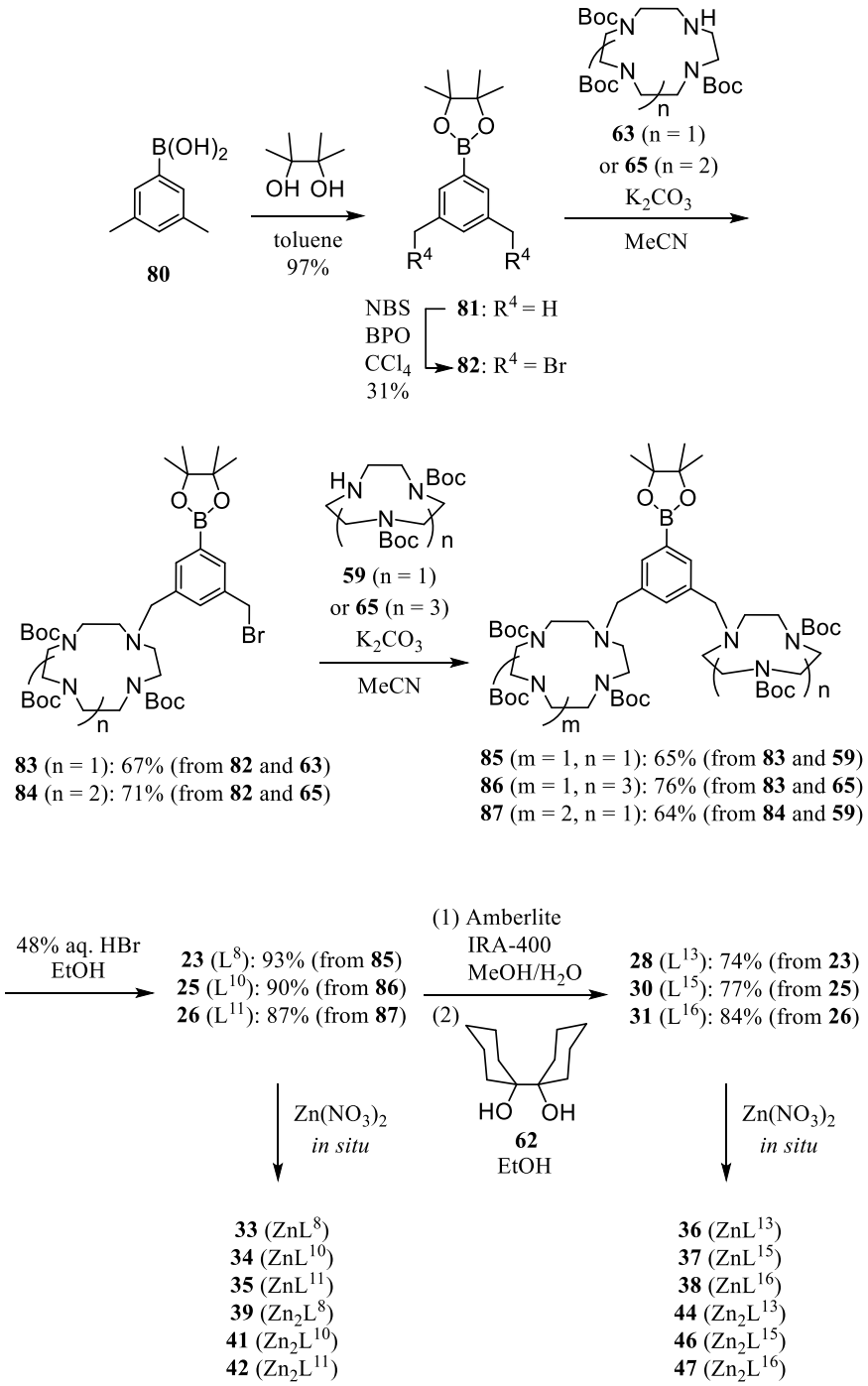

Scheme 3-7. Synthesis of heterodimers and their Zn^{2+} complexes.

The homodimers **24** and **27** (L^9 and L^{12}) were synthesized from **82** via the intermediates **88** and **89**, and the following conversion were carried out in a similar manner to give **29** and **32** (L^{14} and L^{17}), as presented in Scheme 3-8. Their dizinc(II) complexes, **40**, **43**, **45**, and **48** (Zn_2L^9, Zn_2L^{12}, Zn_2L^{14}, and Zn_2L^{17}), were also prepared *in situ* before their evaluation.

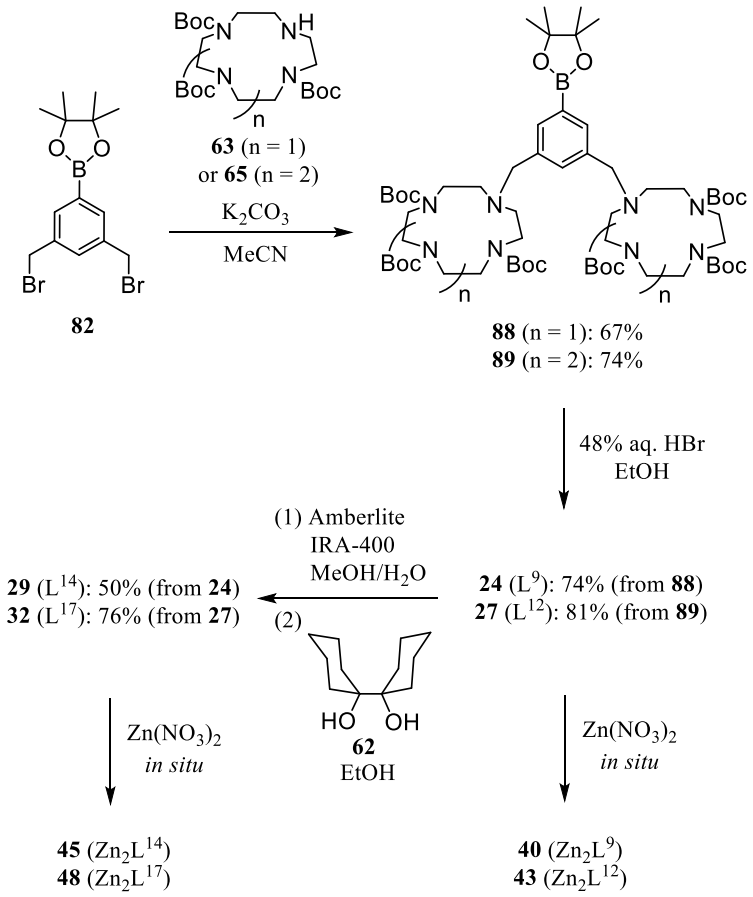

Scheme 3-8. Synthesis of homodimers and their Zn^{2+} complexes.

[3-2-2] Effect of boron-containing macrocyclic polyamine dimers and their zinc(II) complexes on the melting temperature (T_m) of calf thymus DNA

The interaction of macrocyclic polyamine dimers **28**–**32** (L^{13}–L^{17}) and their Zn^{2+} complexes **37**, **44**–**46** and **48** (ZnL^{15}, Zn_2L^{13}–Zn_2L^{15} and Zn_2L^{17}) with double-stranded DNA (dsDNA) was evaluated by measurement of the T_m values of the double-stranded calf-thymus DNA (ctDNA) (50 μM in phosphate) by following its UV absorption change at 260 nm as a function of the temperature.[79] The T_m value of ctDNA alone was first determined to be 66 °C in the absence of additive (r = 0, where r = [additives]/[ctDNA(P)]), as shown in Figures 3-1a–d and Table 3-1. At increasing concentrations of **28**–**32** (L^{13}–L^{17}), the T_m value of ctDNA was raised (ΔT_m = +8 °C, +14 °C, +15 °C, +10 °C and +15 °C for **28**, **29**, **30**, **31**, and **32**, respectively, at r = 0.2, where r = [**28**–**32** (L^{13}–L^{17})]/[ctDNA(P)]) due to stabilization of the double-stranded structure of ctDNA (Figure 3-1 and Table 3-1). On the other hand, a decrease in the T_m value was observed in the presence of **44** and **45** (Zn_2L^{13} and Zn_2L^{14}) (ΔT_m = –2 °C and –7 °C for **44** and **45**, respectively, at r = 0.2), which means the destabilization of double-stranded structure of ctDNA, possibly due to the cleavage of hydrogen bondings between dT and adenine (dA) by the coordination of its Zn^{2+}–cyclen complex moieties with dT^- units in DNA. A negligible effect of **46** (Zn_2L^{15}) on the T_m value of ctDNA was observed, while an increase in the T_m value was observed in the presence of **37** (ZnL^{15}), which is a monozinc(II) complex of **30** (L^{15}). In our previous studies, decreases and increases in the T_m value of ctDNA were observed in the presence of **21b** and **22a** (ZnL^4 and ZnL^5), respectively (ΔT_m = –6 °C and +6 °C for **21b** and **22a**, respectively, at r = 1.0), suggesting that **21b** and **22a** would interact with DNA via different modes. In the X-ray crystal structure of the Zn^{2+}-[15]aneN$_5$ complex **68** (ZnL^{20}) reported by Notni et al.,[87] five nitrogens of the [15]aneN$_5$ ring unit coordinate to Zn^{2+} and one nitrogen atom coordinates to Zn^{2+} at the almost apical site of its pseudo-tetragonal-pyramidal coordination structure (Scheme 3-9). This structure suggests that the Lewis acidities of the Zn^{2+} of **22a** (ZnL^5)

and **68** (ZnL^{20}) are lower than that of the Zn^{2+} complex of [12]aneN_4(cyclen)-type ligand (**21b**) and hence the coordination with dT^- in DNA is weakened. Therefore, the Zn^{2+} complex of the [15]aneN_5-type ligand (**22a**) interacts with ctDNA mainly by electrostatic interactions, resulting in the stabilization of the double-stranded ctDNA. These backgrounds allowed us to consider that **46** (Zn_2L^{15}) interacts with DNA by two interactions, namely, by coordination between Zn^{2+}-[12]aneN_4 with the dT^- unit that lowers T_m values and by electrostatic interactions between its Zn^{2+}-[15]aneN_5 complex unit with anionic DNA that raises T_m values, resulting in a negligible or small change in the T_m value of ctDNA. Besides, it was found that an increase in the T_m value of ctDNA (ΔT_m = +15 °C for **48** at r = 0.2) was observed in the presence of dizinc(II) complex **48** (Zn_2L^{17}), possibly due to the stabilization of the double-stranded ctDNA by the electrostatic interactions with two Zn^{2+}-[15]aneN_5 complex units of **48**.

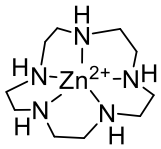

Zn^{2+}-[15]aneN_5 complex
68 (ZnL^{20})

Scheme 3-9. X-ray crystal structure of the Zn^{2+}-[15]aneN_5 complex **68** (ZnL^{20}).[87]

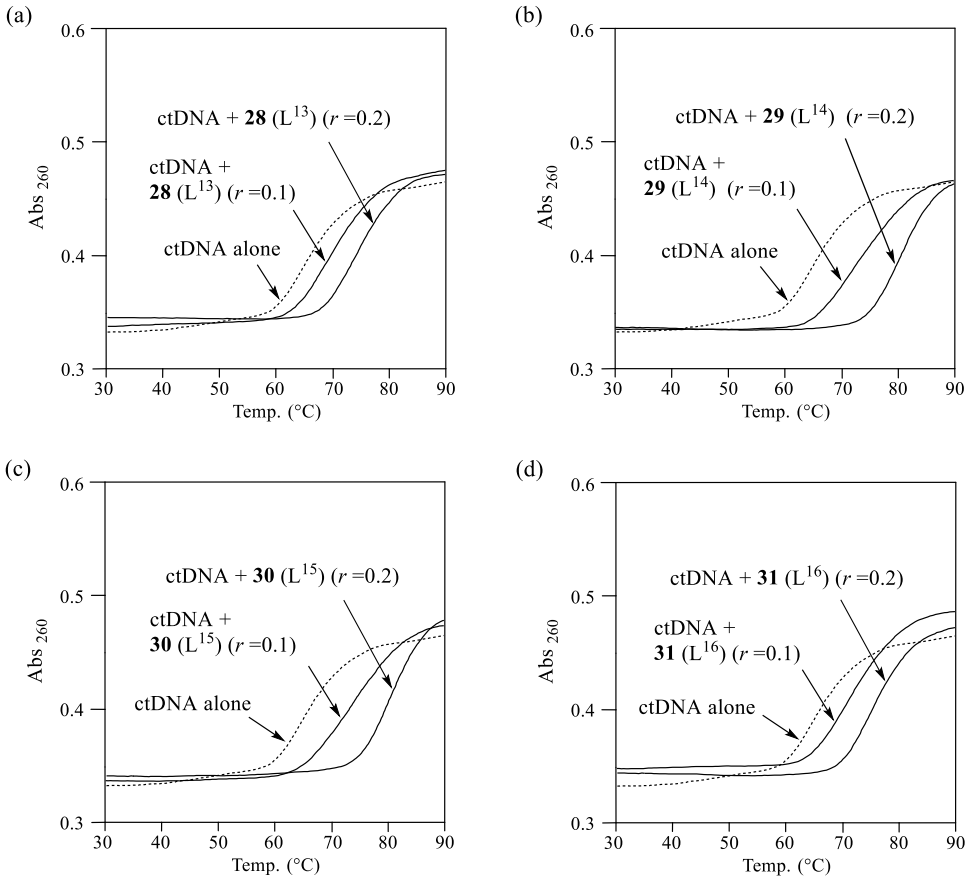

Figure 3-1. Thermal melting (T_m) curves for ctDNA (at [ctDNA(P)] = 50 μM) in the absence (dash curves) and presence of (a) **28** (L^{13}), (b) **29** (L^{14}), (c) **30** (L^{15}), and (d) **31** (L^{16}) (plain curves) at pH 7.4 (10 mM HEPES with I = 0.02 ($NaNO_3$), (r = [ligand]/[ctDNA(P)]).

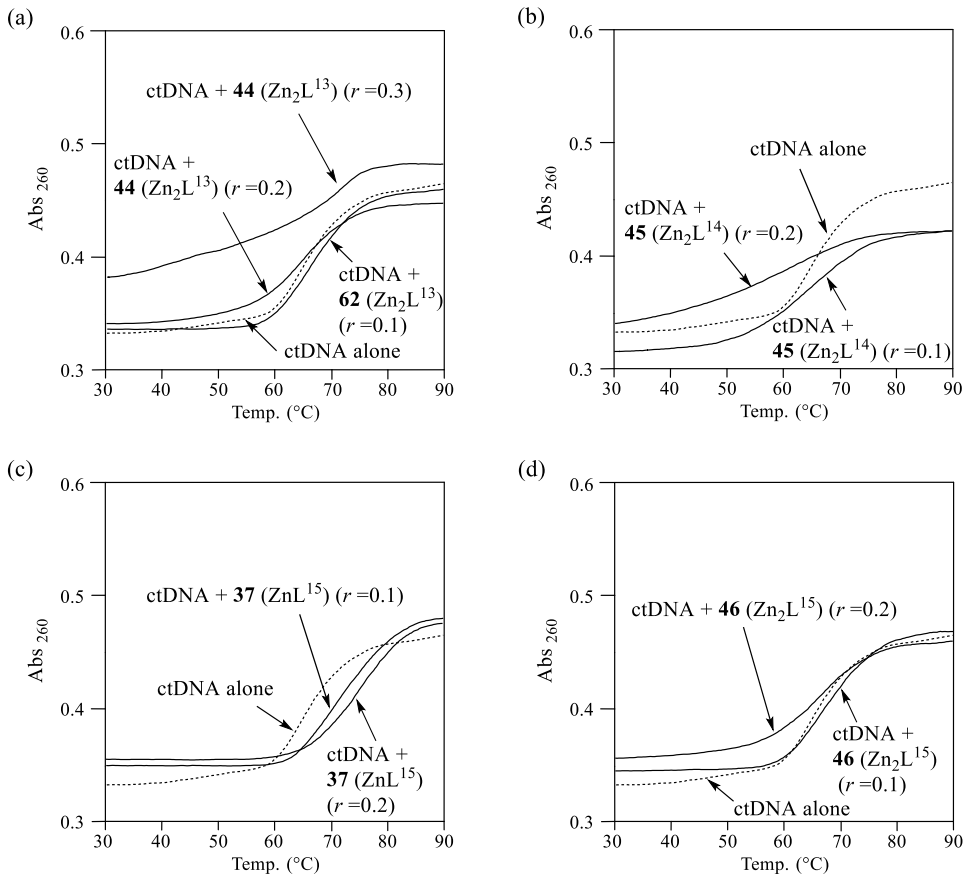

Figure 3-2. Thermal melting (T_m) curves for ctDNA (at [ctDNA(P)] = 50 μM) in the absence (dash curves) and presence of (a) **44** (Zn_2L^{13}), (b) **45** (Zn_2L^{14}), (c) **37** (ZnL^{15}) and (d) **46** (Zn_2L^{15}) (plain curves) at pH 7.4 (10 mM HEPES with I = 0.02 ($NaNO_3$), (r = [Zn^{2+} complex]/[ctDNA(P)]).

Table 3-1. Change in the T_m values of ctDNA by **28**–**32** (L^{13}–L^{17}), **37**, **44**–**46**, and **48** (ZnL^{15}, Zn_2L^{13}–Zn_2L^{15}, and Zn_2L^{17}) (r = [**28**–**32**, **37**, **44**–**46**, and **48**]/[ctDNA(P)]) ([ctDNA(P)] = 50 μM in phosphate).

Additives (Ligands)	r	T_m (°C)	ΔT_m (°C)	Additives (Zn complexes)	r	T_m (°C)	ΔT_m (°C)
none		66					
49[a]	0.1	73	+7				
	0.2	78	+12				
18b (L^4)[a]	0.5	66		**21b** (ZnL^4)[a]	0.1	64	-2
	1.0	67	+1		0.5	62	-4
	5.0	72	+6		1.0	60	-6
19a (L^5)[a]	1.0	69	+3	**22a** (ZnL^5)[a]	0.5	71	+5
	5.0	74	+8		1.0	72	+6
28 (L^{13})	0.1	70	+4	**44** (Zn_2L^{13})	0.1	66	
	0.2	74	+8		0.2	64	-2
					0.3	disappeared	
29 (L^{14})	0.1	73	+7	**45** (Zn_2L^{14})	0.1	64	-2
	0.2	80	+14		0.2	59	-7
30 (L^{15})	0.1	73	+7	**37** (ZnL^{15})	0.1	71	+5
	0.2	81	+15		0.2	75	+9
				46 (Zn_2L^{15})	0.1	67	+1
					0.2	66	
31 (L^{16})	0.1	72	+6				
	0.2	76	+10				
32 (L^{17})[b]	0.1	75	+9	**48** (Zn_2L^{17})[b]	0.1	75	+9
	0.2	81	+15		0.2	80	+14

[a] From Chapter 2. [b][ctDNA(P)] = 30 μM

[3-2-3] Evaluation of the cytotoxicity of boron-containing macrocyclic polyamine dimers and their zinc(II) complexes against HeLa S3, A549, and IMR-90 cells

The cytotoxicity of **23**–**48** (L^8–L^{17}, ZnL^8–ZnL^{16}, and Zn_2L^8–Zn_2L^{17}) against cancer cell lines, HeLa S3 (human cervical carcinoma) and A549 (human caucasian lung carcinoma), and a model of normal cells, IMR-90 (normal human fibroblast) cells, was evaluated by an MTT (3-(4,5-di-methylthiazol-2yl)-2,5-diphenyltetrazolium bromide) assay. The cells (1×10^4 cells/well) were treated with **23**–**48** (0–400 μM) in cell culture medium for 24 h at 37 °C under an atmosphere of 5% CO_2, and cell viability was examined using the MTT reagent. The results are shown in Figures 3-3, 3-4, and 3-5 and the IC_{50} values of these boron compounds are summarized in Table 3-2. For comparison, the IC_{50} values of **5**, **17b**, **18b**, **19a**, **20b**, **21b**, and **22a** (L^2, L^4, L^5, ZnL^2, ZnL^4, and ZnL^5) are also listed in Table 3-2.

These results indicate that the cytotoxicity of the dimeric ligands **23**, **24**, **26** and **28**–**31** (L^8, L^9, L^{11} and L^{13}–L^{16}) are much weaker than that of the monomeric polyamines **17b**, **18b**, and **19a** (L^2, L^4, and L^5), and that **25**, **27**, and **32** (L^{10}, L^{12}, and L^{17}) are somewhat more toxic than **17b**, **18b**, and **19a** (L^2, L^4, and L^5). It was also found that Zn^{2+} complexes **33**–**38**, **40**, **41**, **45**, and **46** possess very weak cytotoxicity. It has been reported that the cytotoxic effect of macrocyclic polyamines is decreased by complexation with Zn^{2+} ion.[64] On the other hand, the dizinc(II) complexes **39**, **42**, **44**, and **47** (Zn_2L^8, Zn_2L^{11}, Zn_2L^{13} and Zn_2L^{16}) are more toxic than the corresponding metal-free ligands **23**, **26**, **28**, and **31** (L^8, L^{11}, L^{13} and L^{16}), and monozinc(II) complexes **33**, **35**, **36**, and **38** (ZnL^8, ZnL^{11}, ZnL^{13}, and ZnL^{16}), possibly due to the weak Zn^{2+} complexation of their [9]aneN_3 part.

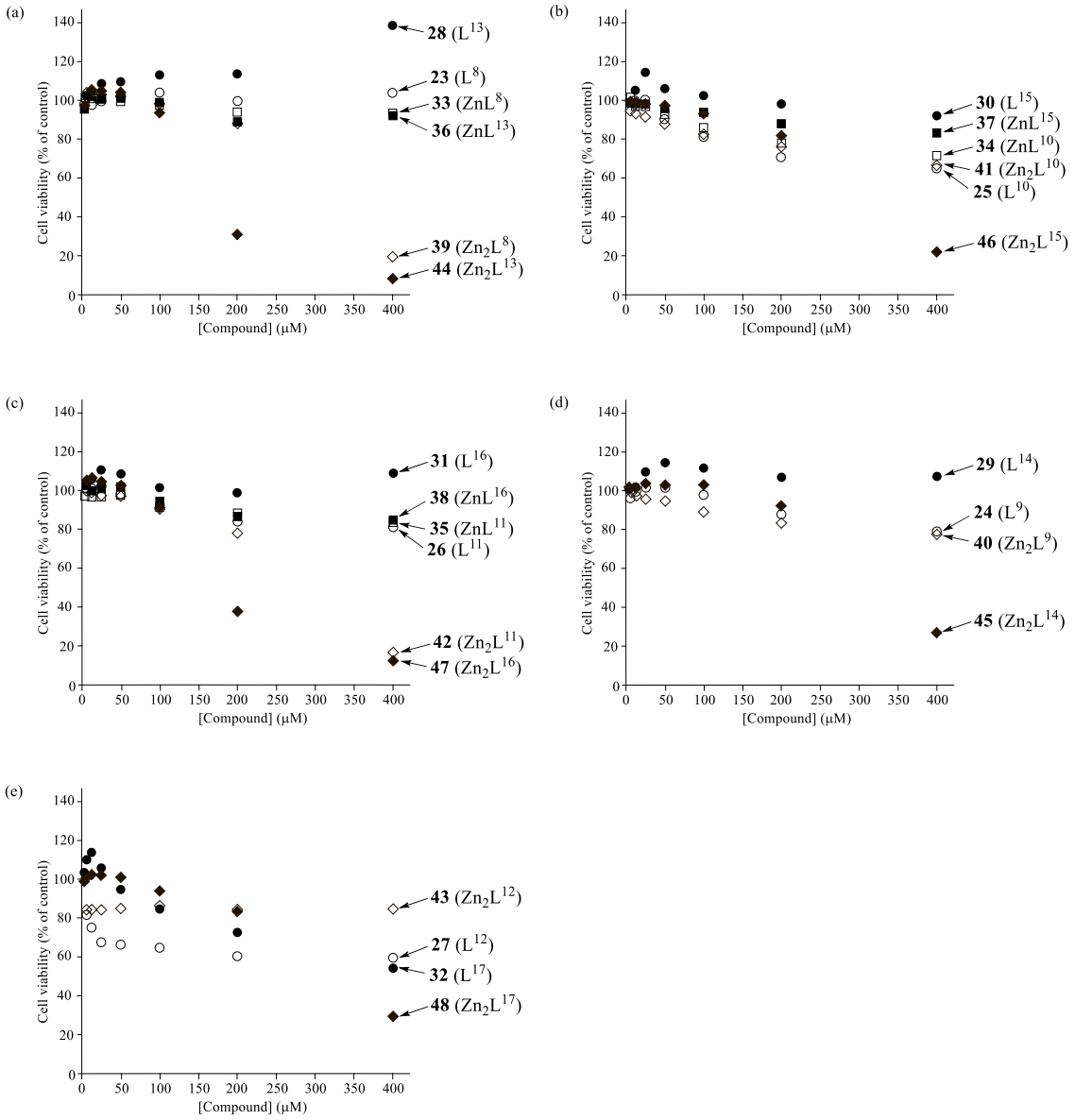

Figure 3-3. Results of MTT assays for boron compounds (0–400 μM) against HeLa S3 cells. Cell viability of HeLa S3 cells (% of control; in the absence of boron compound) in the presence of (a) **23** (○), **28** (●), **33** (□), **36** (■), **39** (◇) and **44** (◆), (b) **25** (○), **30** (●), **34** (□), **37** (■), **41** (◇), and **46** (◆), (c) **26** (○), **31** (●), **35** (□), **38** (■), **42** (◇) and **47** (◆), (d) **24** (○), **29** (●), **40** (◇) and **45** (◆), (e) **27** (○), **32** (●), **43** (◇) and **48** (◆) at 37 °C for 24 h.

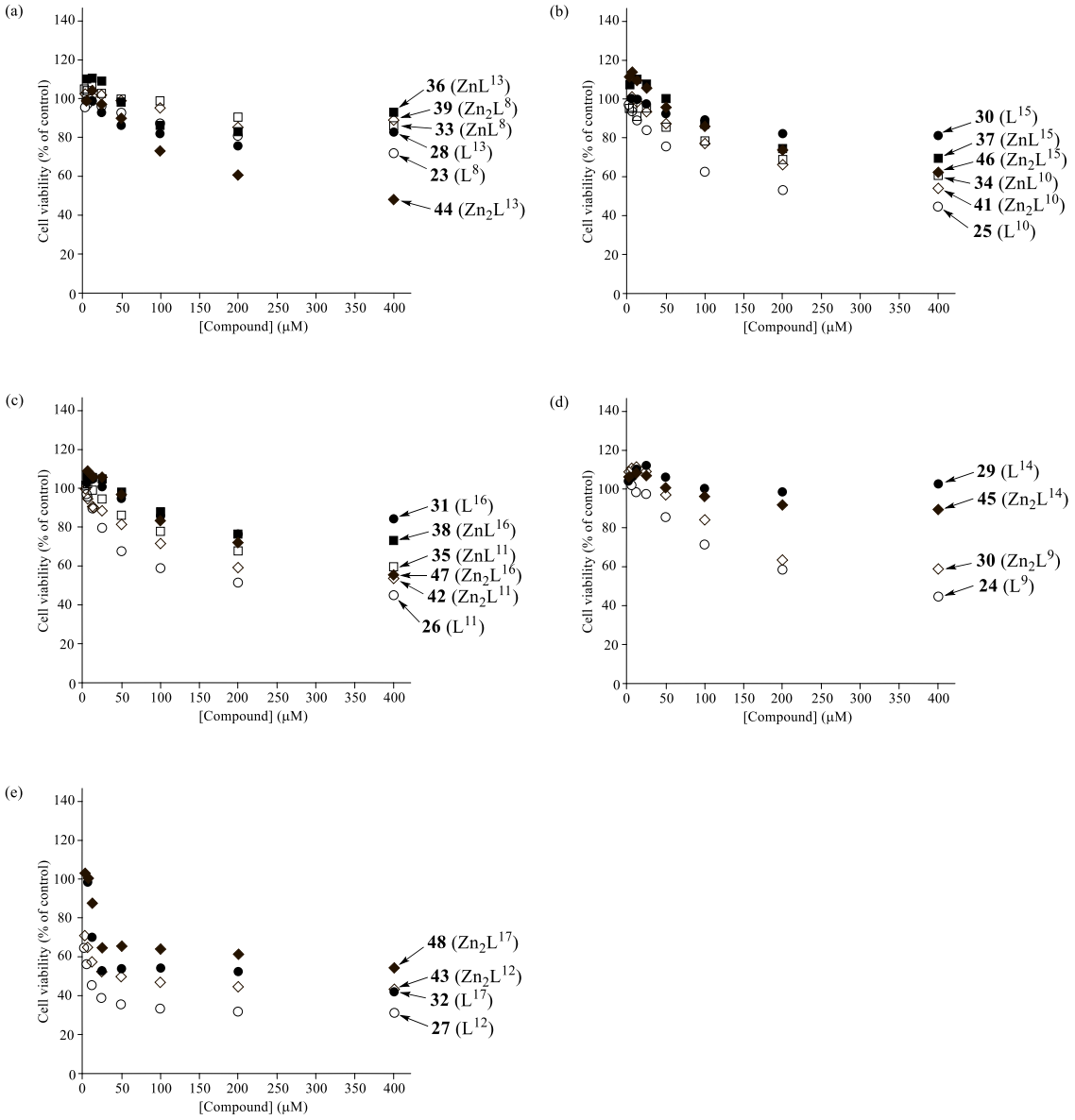

Figure 3-4. Results of MTT assays for boron compounds (0–400 μM) against A549 cells. Cell viability of A549 cells (% of control; in the absence of boron compound) in the presence of (a) **23** (○), **28** (●), **33** (□), **36** (■), **39** (◇) and **44** (◆), (b) **25** (○), **30** (●), **34** (□), **37** (■), **41** (◇), and **46** (◆), (c) **26** (○), **31** (●), **35** (□), **38** (■), **42** (◇) and **47** (◆), (d) **24** (○), **29** (●), **40** (◇) and **45** (◆), (e) **27** (○), **32** (●), **43** (◇) and **48** (◆) at 37 °C for 24 h.

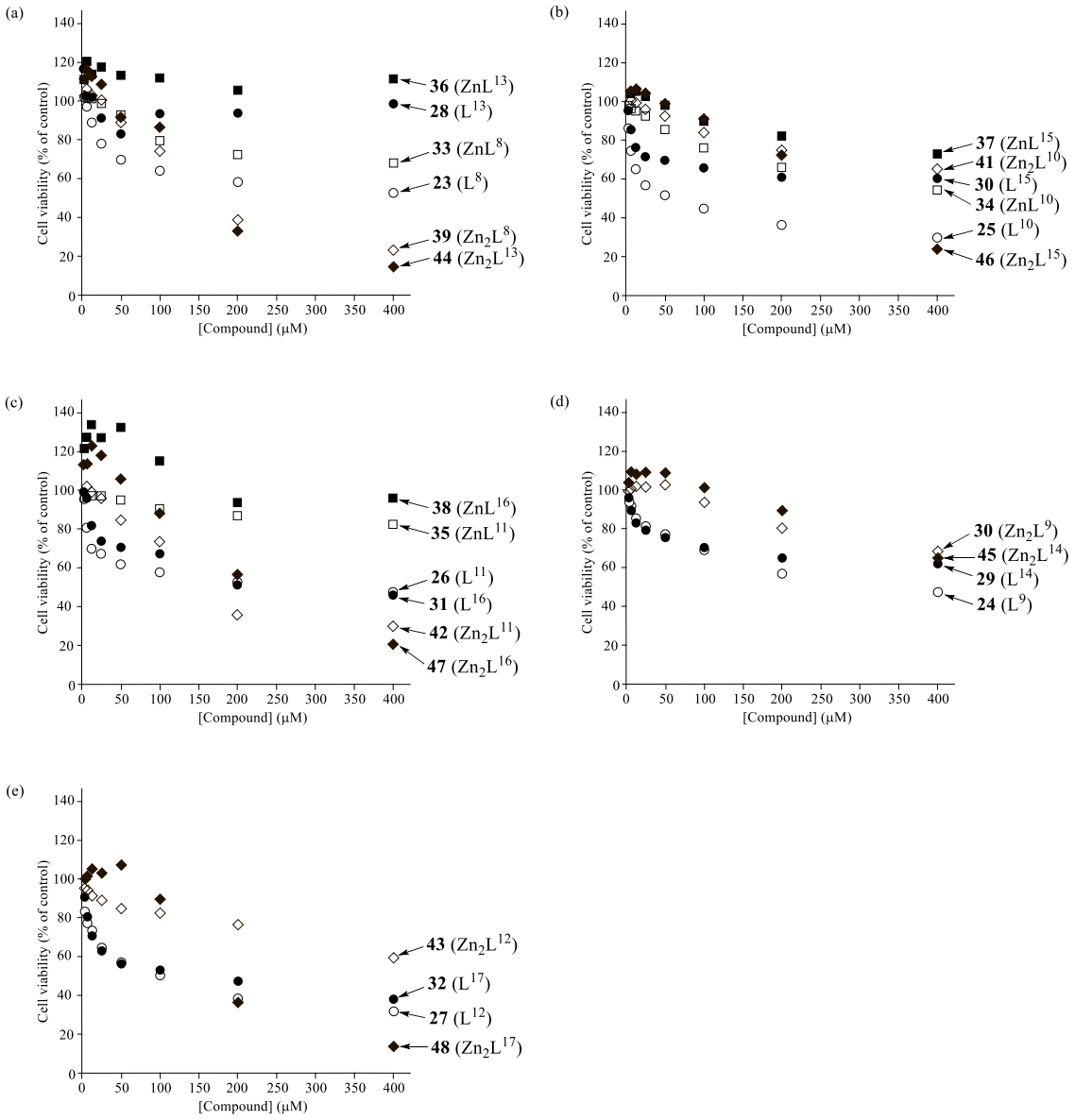

Figure 3-5. Results of MTT assays for boron compounds (0–400 μM) against IMR-90 cells. Cell viability of IMR-90 cells (% of control; in the absence of boron compound) in the presence of (a) **23** (○), **28** (●), **33** (□), **36** (■), **39** (◇) and **44** (◆), (b) **25** (○), **30** (●), **34** (□), **37** (■), **41** (◇), and **46** (◆), (c) **26** (○), **31** (●), **35** (□), **38** (■), **42** (◇) and **47** (◆), (d) **24** (○), **29** (●), **40** (◇) and **45** (◆), (e) **27** (○), **32** (●), **43** (◇) and **48** (◆) at 37 °C for 24 h.

Table 3-2. IC_{50} values of boron compounds **5**, **17b** (L^2), **18b** (L^4), **19a** (L^5), **20b** (ZnL^2), **21b** (ZnL^4), and **22a** (ZnL^5) [0–200 μM], and **23**–**48** (L^8–L^{17}, ZnL^8–ZnL^{16}, and Zn_2L^8–Zn_2L^{17}) [0–400 μM] against HeLa S3, A549 and IMR-90 cells after the treatment for 24 h.

Compound (Ligands)	HeLa S3 (μM)	A549 (μM)	IMR-90 (μM)	Compound (Zn complexes)	HeLa S3 (μM)	A549 (μM)	IMR-90 (μM)
5 (BPA)	> 200	> 200	> 200				
17b (L^2)	> 200	> 200	187	**20b** (ZnL^2)	> 200	> 200	162
18b (L^4)	163	128	135	**21b** (ZnL^4)	> 200	> 200	> 200
19a (L^5)	> 200	> 200	151	**22a** (ZnL^5)	> 200	> 200	129
23 (L^8)	> 400	> 400	> 400	**33** (ZnL^8)	> 400	> 400	> 400
				39 (Zn_2L^8)	312	> 400	168
24 (L^9)	> 400	325	322	**40** (Zn_2L^9)	> 400	> 400	> 400
25 (L^{10})	> 400	276	62	**34** (ZnL^{10})	> 400	> 400	> 400
				41 (Zn_2L^{10})	> 400	> 400	> 400
26 (L^{11})	> 400	252	309	**35** (ZnL^{11})	> 400	> 400	> 400
				42 (Zn_2L^{11})	292	> 400	163
27 (L^{12})	> 400	10	106	**43** (Zn_2L^{12})	> 400	51	> 400
28 (L^{13})	> 400	> 400	> 400	**36** (ZnL^{13})	> 400	> 400	> 400
				44 (Zn_2L^{13})	171	373	168
29 (L^{14})	> 400	> 400	> 400	**45** (Zn_2L^{14})	329	> 400	> 400
30 (L^{15})	> 400	> 400	> 400	**37** (ZnL^{15})	> 400	> 400	> 400
				46 (Zn_2L^{15})	307	> 400	292
31 (L^{16})	> 400	> 400	268	**38** (ZnL^{16})	> 400	> 400	> 400
				47 (Zn_2L^{16})	177	> 400	236
32 (L^{17})	> 400	250	160	**48** (Zn_2L^{17})	324	> 400	175
				$Zn(NO_3)_2$ [a]	297	633	305

[a] The effect of $Zn(NO_3)_2$ (0–800 μM) on cell viability were also evaluated.

[3-2-4] Intracellular uptake of boron compounds into A549 cells, as determined by ICP-MS

We next measured the intracellular uptake of the macrocyclic polyamine dimers and their Zn^{2+} complexes **23**–**48** (L^8–L^{17}, ZnL^8–ZnL^{16}, and Zn_2L^8–Zn_2L^{17}) into A549 cells. A549 cells (5×10^5 cells/well) were incubated in cell culture medium containing boron compounds **5**, **18b** (L^4) and **23**–**48** (100 μM) at 37 °C in a 5% CO_2 environment (20% O_2) for 24 h. After washing the cells with PBS, they were broken down with nitric acid overnight, and the amount of boron (^{10}B and ^{11}B) was quantitatively analyzed by inductively coupled plasma mass spectrometry (ICP-MS). As summarized in Figure 3-6, the intracellular uptake of **23**–**48** is lower than that of **18b**, and the boron uptake of **40** and **44** is similar to that of **5** (BPA).

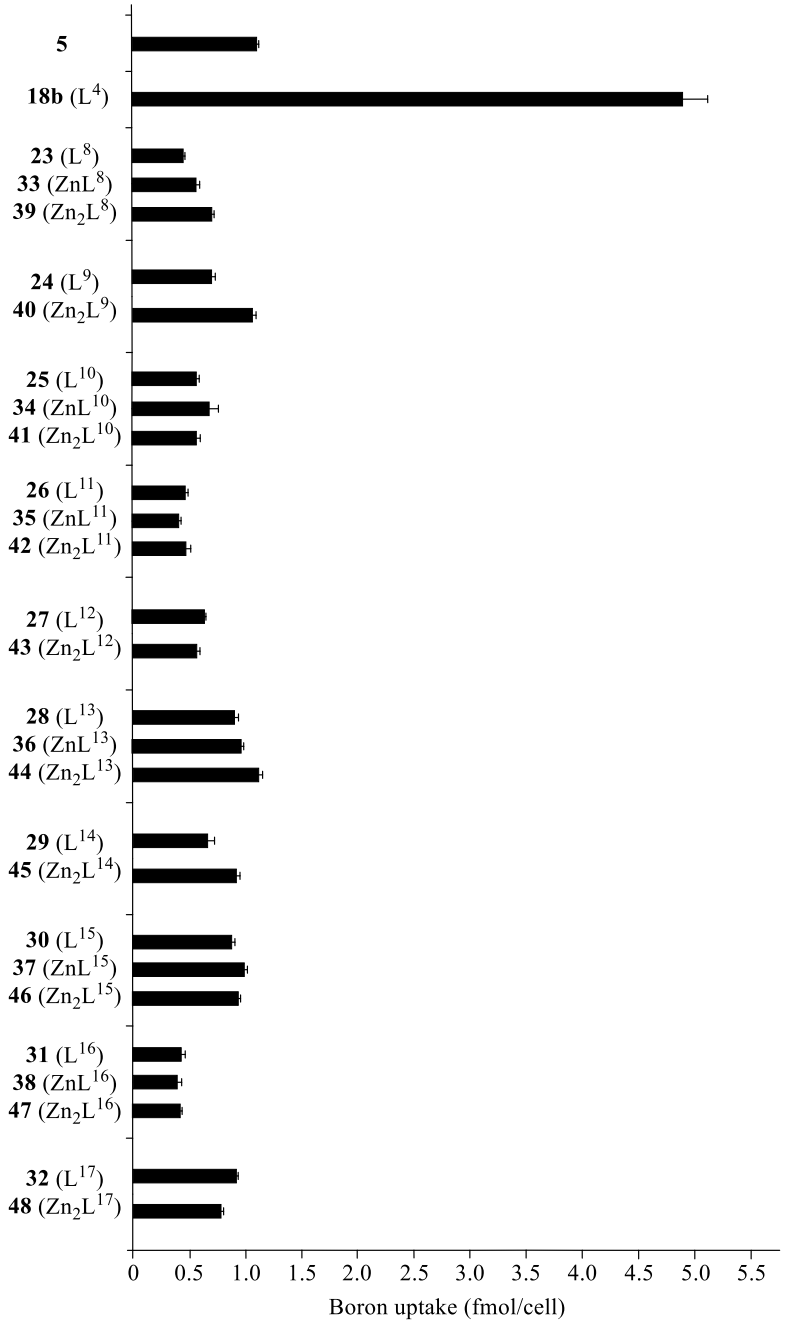

Figure 3-6. Intracellular uptake of boron compounds by A549 cells as determined by ICP-MS. A549 cells were treated with boron compounds **5**, **18b** (L^4) and **23**–**48** (L^8–L^{17}, ZnL^8–ZnL^{16} and Zn_2L^8–Zn_2L^{17}) (100 μM) in culture medium at 37 °C for 24 h. Data represent the mean ± SD of at least three replicates.

[3-2-5] Evaluation of the cytotoxic effect of ^{10}B-enriched macrocyclic polyamine dimers with thermal neutron irradiation by a colony formation assay

Because our previous work indicated that the BNCT effect of ^{10}B carriers is not always parallel to their intracellular boron uptake, we decided to synthesize the ^{10}B-enriched compounds, as shown in Schemes 3-10 and 3-11. The ^{10}B-enriched form of **81** (**^{10}B-81**) was prepared by the reaction of **90** with ^{10}B-enriched trimethyl borate (>99.5% of ^{10}B),[88] followed by treatment with aqueous HCl, and esterification with pinacol. The bromination of **^{10}B-81** was conducted using *N*-bromosuccinimide (NBS) to afford **^{10}B-82**, and the following conversions were carried out to obtain **^{10}B-23**–**^{10}B-47**, as described in Schemes 3-7 and 3-8.

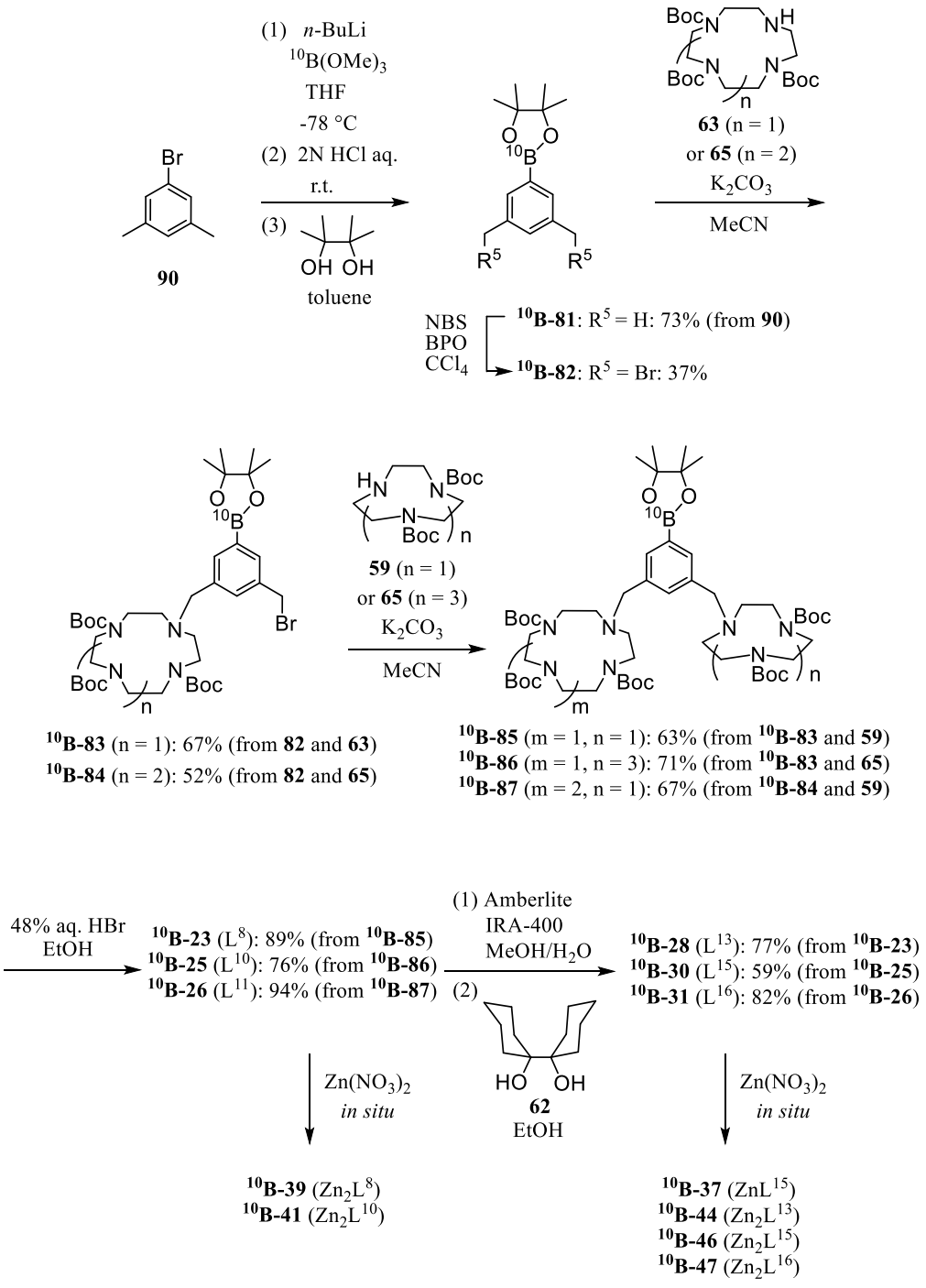

Scheme 3-10. Synthesis of ^{10}B-enriched heterodimers and their Zn^{2+} complexes.

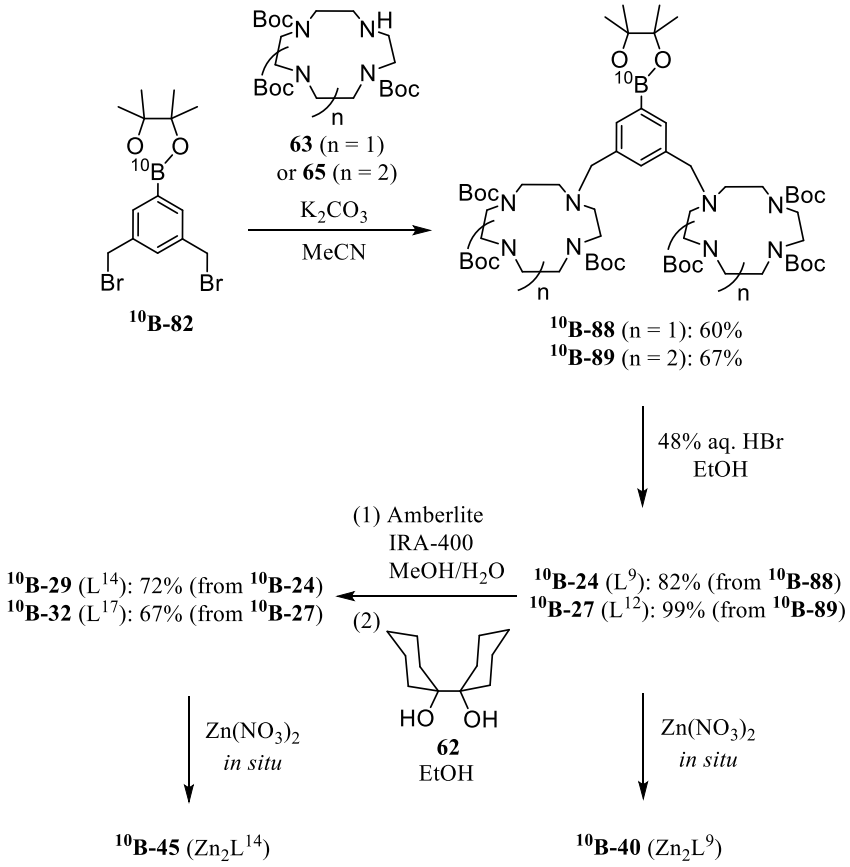

Scheme 3-11. Synthesis of ^{10}B-enriched homodimers **^{10}B-24**, **^{10}B-27**, **^{10}B-29** and **^{10}B-32**, and their Zn^{2+} complexes **^{10}B-40** and **^{10}B-45**.

The A549 cells were irradiated with thermal neutrons in the absence and presence of the ^{10}B-enriched compounds of **23**–**47** at the Institute for Integrated Radiation and Nuclear Science, Kyoto University (KURNS) and the effect of these ^{10}B drugs was evaluated by colony formation assay. After the treatment with the boron compounds (100 μM) at 37 °C in a 5% CO_2 environment for 24 h, suspensions (5×10^4 cells/mL) of A549 cells were irradiated with thermal neutrons (average thermal neutron flux: (1.2 ± 0.1) $\times10^9$ n/cm^2·s) at room temperature for given times (0, 15, 30, and 45 min). The irradiated cells were incubated for 7 days, fixed with EtOH and stained with crystal violet.

The surviving fractions were examined using the "ImageJ-plugin Colony Area"[77] software. The results shown in Figure 3-7 suggest that the cytotoxic activity of **^{10}B-23**–**^{10}B-47** is somewhat weaker than that of **5** and **^{10}B-18b**. These results might be explained by much lower uptake of these B drugs in comparison with previous monomeric polyamine derivatives and/or nonspecific ionic interactions with intracellular biomolecules such as enzymes, proteins, phospholipids and related biomolecules.

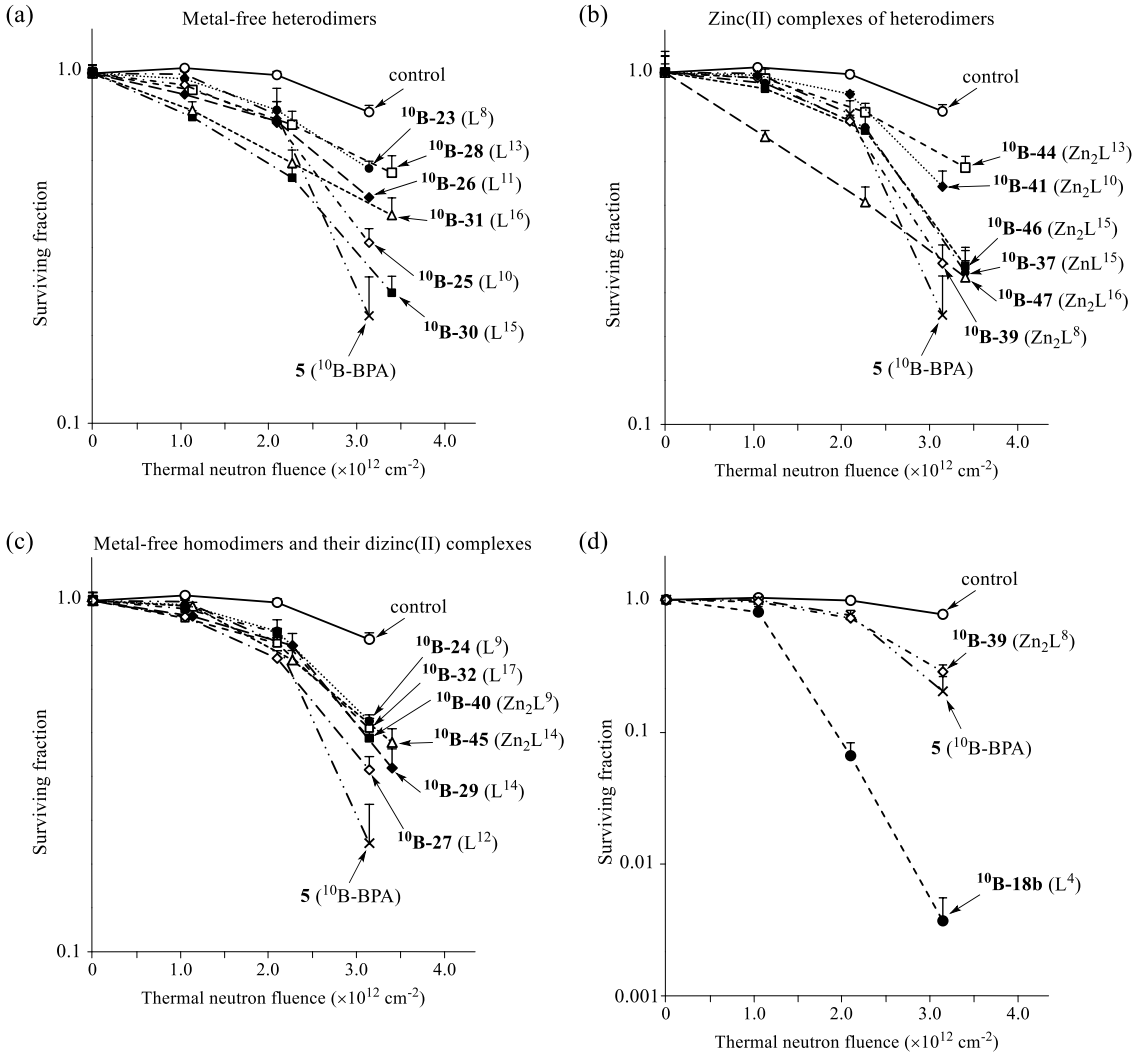

Figure 3-7. BNCT effect of ^{10}B-enriched compounds against A549 cells was examined by a colony formation assay: (a) control (in the absence of boron compound) (○), **5** (×), **^{10}B-23** (●), **^{10}B-25** (◇), **^{10}B-26** (◆), **^{10}B-28** (□), **^{10}B-30** (■), and **^{10}B-31** (△), (b) control (○), **5** (×), **^{10}B-37** (●), **^{10}B-39** (◇), **^{10}B-41** (◆), **^{10}B-44** (□), **^{10}B-46** (■), and **^{10}B-47**

(△), (c) control (○), **5** (×), **^{10}B-24** (●), **^{10}B-27** (◇), **^{10}B-29** (◆), **^{10}B-32** (□), **^{10}B-40** (■), and **^{10}B-45** (△), (d) control (○), **5** (×), **^{10}B-18b** (●) and **^{10}B-39** (◇). Note that y-axis of Figure 3-7d is wider than that of Figure 3-7a, 3-7b and 3-7c. After treatment with ^{10}B-enriched compounds (100 μM) for 24 h, the cells were irradiated with thermal neutrons for 0, 15, 30, and 45 min and then incubated without neutron irradiation for 7 days. The averaged thermal neutron flux was 1.2×10^9 n/cm^2·s for control (in the absence of boron compound), **5**, **^{10}B-18b**, **^{10}B-23**, **^{10}B-24**, **^{10}B-25**, **^{10}B-26**, **^{10}B-27**, **^{10}B-32**, **^{10}B-39**, **^{10}B-40**, and **^{10}B-41** and 1.3×10^9 n/cm^2·s for **^{10}B-28**, **^{10}B-29**, **^{10}B-30,** **^{10}B-31**, **^{10}B-37**, **^{10}B-44**, **^{10}B-45**, **^{10}B-46**, and **^{10}B-47**, respectively. The surviving fraction was determined by ImageJ-plugin Colony Area. Data represent the mean ± SD of at least three replicates.

[3-3] Conclusions

In conclusion, we report on the design and synthesis of novel DNA-binding BNCT agents that are equipped with homo- and hetero-dimers of macrocyclic polyamines such as [9]aneN$_3$, [12]aneN$_4$ and [15]aneN$_5$ and their Zn^{2+} complexes in an attempt to achieve a higher BNCT effect. The results of DNA interaction studies indicate that **28**–**31** (L^{13}–L^{16}) and **37** (ZnL^{15}) would stabilize dsDNA by electrostatic interactions, and that **44** and **45** (Zn_2L^{13} and Zn_2L^{14}) interact with DNA by coordination bonding between its Zn^{2+}–[12]aneN$_4$ complex unit and the dT^- in DNA. It was also found that the metal-free ligands **23**, **24**, **26**, and **28**–**31** and Zn^{2+} complexes **33**–**38**, **40**, **41**, **45**, and **46** were much less cytotoxic than that of monomeric macrocyclic polyamines **17b**, **18b**, **19a**, **20b**, **21b**, and **22a**. In addition, BNCT experiments using ^{10}B-enriched compounds suggest that the BNCT activities of **^{10}B-23**–**^{10}B-47** were lower than that of **^{10}B-18b**, possibly due to their lower boron uptake and interaction not only with DNA but also with intracellular biomolecules. We therefore conclude that monomeric polyamine-type ^{10}B carriers such as **18b** and **19a** are more preferable for BNCT among the boron–macrocyclic polyamine conjugates that were synthesized in our previous publication and in this study. We believe that these results provide useful information for the design of more efficient and less toxic boron delivery agents for use in cancer treatment and the development of more effective boron carriers is currently underway.

Chapter 4.

Concluding Remarks

In this thesis, we report on the novel DNA-targeting boron carriers based on monomeric macrocyclic polyamines (Chapter 2), and homo- and hetero-dimers of macrocyclic polyamines (Chapter 3) for boron neutron capture therapy (Scheme 4-1).

In Chapter 2, we report on the design and synthesis of boron carriers equipped with 9-, 12-, and 15-membered macrocyclic polyamines and the corresponding Zn^{2+} complexes. It was expected that macrocyclic polyamines having boron units would be efficiently uptaken into cancer cells and that the thermal neutron irradiation would induce effective DNA damage when ^{10}B atoms are accumulated near DNA molecules. In this study, we synthesized monomeric [9]aneN_3, [12]aneN_4, and [15]aneN_5 compounds containing cyclic boron ester units **17**–**22** in natural abundant ratio ($^{10}B/^{11}B$ = 19.9/ 80.1) and examined their biological activities such as cytotoxicity and intracellular uptake (Scheme 4-1). Thereafter, three promising compounds (**17b**, **18b**, and **19a**) were selected and their corresponding ^{10}B-enriched forms were prepared for BNCT experiments. It was found that these monomeric ^{10}B carriers were efficiently taken up to cancer cells (A549 and HeLa S3 cells) possibly via polyamine transport system. In addition, the results of in vitro BNCT studies indicate that [12]aneN_4- and [15]aneN_5-type ^{10}B-enriched macrocycles (**^{10}B-18b** and **^{10}B-19a**) effectively inhibit the proliferation of cancer cells upon thermal neutron irradiation, possibly via the interaction with DNA.

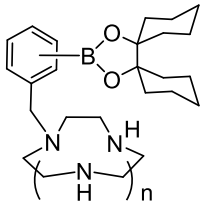

17a (L^1): n = 1, *p*-form
17b (L^2): n = 1, *m*-form
18a (L^3): n = 2, *p*-form
18b (L^4): n = 2, *m*-form
19a (L^5): n = 3, *p*-form
19b (L^6): n = 3, *m*-form
19c (L^7): n = 3, *o*-form

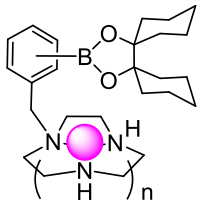

20a (ZnL^1): n = 1, *p*-form
20b (ZnL^2): n = 1, *m*-form
21a (ZnL^3): n = 2, *p*-form
21b (ZnL^4): n = 2, *m*-form
22a (ZnL^5): n = 3, *p*-form
22b (ZnL^6): n = 3, *m*-form
22c (ZnL^7): n = 3, *o*-form

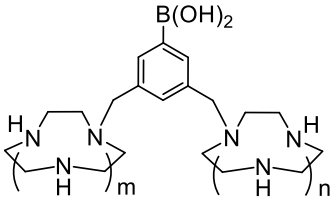

23 (L^8): m = 2, n = 1
24 (L^9): m = 2, n = 2
25 (L^{10}): m = 2, n = 3
26 (L^{11}): m = 3, n = 1
27 (L^{12}): m = 3, n = 3

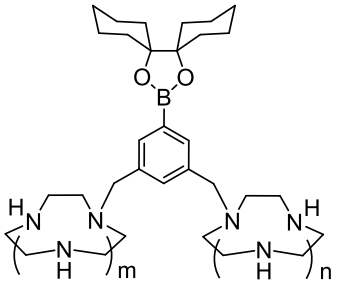

28 (L^{13}): m = 2, n = 1
29 (L^{14}): m = 2, n = 2
30 (L^{15}): m = 2, n = 3
31 (L^{16}): m = 3, n = 1
32 (L^{17}): m = 3, n = 3

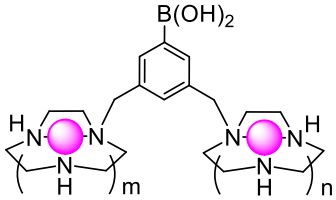

39 (Zn_2L^8): m = 2, n = 1
40 (Zn_2L^9): m = 2, n = 2
41 (Zn_2L^{10}): m = 2, n = 3
42 (Zn_2L^{11}): m = 3, n = 1
43 (Zn_2L^{12}): m = 3, n = 3

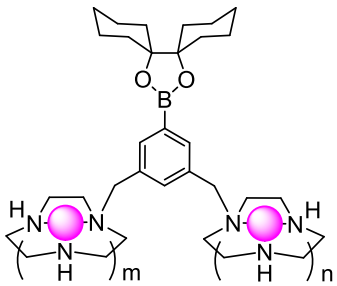

44 (Zn_2L^{13}): m = 2, n = 1
45 (Zn_2L^{14}): m = 2, n = 2
46 (Zn_2L^{15}): m = 2, n = 3
47 (Zn_2L^{16}): m = 3, n = 1
48 (Zn_2L^{17}): m = 3, n = 3

Scheme 4-1. Structure of monomeric- and dimeric-macrocyclic polyamines and their Zn^{2+} complexes for boron neutron capture therapy.

In Chapter 3, the design and synthesis of DNA-targeting boron agents that are conjugated with homo- and hetero-dimers of macrocyclic polyamines and their corresponding Zn^{2+} complexes are reported. We anticipated that the dizinc(II) complexes of these ligands would interact with two adjacent thymidine (thymidyl(3′–5′)thymidine, d(TpT)) units, resulting in more efficient contact with DNA and its more efficient breakdown upon thermal neutron irradiation and synthesized the boron-containing macrocyclic polyamine dimers (**23**–**32**) and the corresponding Zn^{2+} complexes (**39**–**48**) (Scheme 4-1). It was found that homo- and heterodimers of macrocyclic polyamines and their Zn^{2+} complexes interact with double-stranded DNA and that they are much less cytotoxic than the monomeric macrocycles. The results of in vitro BNCT experiments using ^{10}B-enriched forms of selected compounds indicate that the cytotoxic effect of dimeric ^{10}B carriers is almost same as that of ^{10}B-BPA and weaker than that of the monomeric [12]aneN$_4$- and [15]aneN$_5$-type macrocycles reported in Chapter 2, possibly due to their lower boron uptake and unexpected interactions with intracellular biomolecules. These data suggest that the ^{10}B carriers based on monomeric [12]aneN$_4$ and [15]aneN$_5$ (**^{10}B-18b** and **^{10}B-19a**) described in Chapter 2 are more preferable for BNCT than ditopic macrocyclic polyamine-type ^{10}B carriers.

We believe that these findings afford important and useful information regarding the fundamental chemistry of boron containing drugs and the design and synthesis of safer and more effecient BNCT agents.

Chapter 5.

Experimental Section

[5] Experimental section

General information

All reagents and solvents were purchased at the highest commercial quality and were used without further purification. 3-(4,5-Di-methylthiazol-2yl)-2,5-diphenyltetrazolium bromide (MTT) was purchased from Dojindo Laboratories. Spermidine was purchased from WAKO Pure Chemical Industries Ltd. Methyl-β-cyclodextrin, amiloride, and calf thymus DNA (ctDNA) were purchased from Sigma-Aldrich. Dynasore was purchased from Tokyo Chemical Industry. ^{10}B-B(OMe)$_3$ was purchased from Katchem Ltd. Anhydrous tetrahydrofuran (THF) was prepared by distillation from sodium and benzophenone. All aqueous solutions were prepared using deionized water. Minimum Essential Medium (MEM), Dulbecco's Modified Eagle's Medium (DMEM), phosphate buffer saline (PBS) without Ca and Mg, trypsin, and crystal violet were purchased from Nacalai tesque. Fetal bovine serum (FBS) was purchased from Chemical Dojin Co., Ltd. Streptomycin sulphate and benzylpenicillin potassium were purchased from WAKO Pure Chemical Industries Ltd. The cell lines, HeLa S3 cells (human cervical carcinoma) were provided by Dr. Tomoko Okada (National Institute of Advanced Industrial Science and Technology), A549 cells (human caucasian lung carcinoma) were provided by Prof. Dr. Mitsutoshi Tsukimoto (Tokyo University of Science), and IMR-90 cells were provided by Dr. Eiko Yoshida (Tokyo University of Science). ^{1}H (300 and 400 MHz), ^{13}C (100 MHz), and ^{11}B (128 MHz) NMR spectra were recorded on a JEOL Always 300 (JEOL, Tokyo, Japan) and a JEOL Lamda 400 (JEOL, Tokyo, Japan) spectrometer. Tetramethylsilane (TMS) was used as an internal reference (0 ppm) for ^{1}H and ^{13}C NMR measurements in $CDCl_3$, and acetone-d_6 and DMSO-d_6. 3-(Trimethylsilyl)propionic-2,2,3,3-d_4 acid sodium (TSP) was used as an internal reference (0 ppm) for ^{1}H NMR measurements in D_2O. 1,4-Dioxane was used as an internal reference (67.19 ppm) for ^{13}C NMR measurements in D_2O. ^{11}B NMR spectra were measured in quartz NMR tubes using boron trifluoride diethyl ether complex ($BF_3 \cdot OEt_2$) in $CDCl_3$ as an internal

reference (0 ppm). IR spectra were recorded on Perkin-Elmer FTIR Spectrum 100 (ATR) (PerkinElmer, Massachusetts, USA). Melting points were measured on a Yanaco Micro Melting Point apparatus and are uncorrected. MS measurements were performed on a Sciex X500R QTOF (AB SCIEX, Framingham, Massachusetts, USA) and Varian 910-MS (Varian Medical Systems, California, USA) spectrometer. Elemental analyses were performed on a 2400 series II CHNS elemental analyzer (PerkinElmer, Massachusetts, USA) to determine the purity (> 95%) of all compounds. Isotopic purity of ^{10}B were determined on ICP-MS (NexION300S, PerkinElmer, Waltham, Massachusetts, USA). Thin-layer chromatography (TLC) and silica gel column chromatography were performed using Merck Silica gel 60 F_{254} plate (Merck KGaA, Darmstadt, Germany) and Fuji Silysia Chemical FL-100D (Fuji Silysia Chemical, Aichi, Japan), Fuji Silysia Chromatorex NH-DM1020 Silica Gel for chromatography (Fuji Silysia Chemical, Aichi, Japan), respectively.

1-[(4-Boronopheny)methyl]-4,7-bis(*tert*-butoxycarbonyl)-1,4,7-triazacyclononane (61a)

To a solution of 4-(bromomethyl)phenylboronic acid **60a**[68] (66.1 mg, 0.308 mmol, 1.2 equiv) in MeCN (2.5 mL), 2Boc-tacn **59**[67] (84.7 mg, 0.257 mmol) and potassium carbonate (44.0 mg, 0.318 mmol, 1.2 equiv) were added and the resulting mixture was stirred at reflux for 4 h. After adding H_2O, the reaction mixture was extracted with $CHCl_3$. The organic layer was washed with brine, dried over Na_2SO_4, and concentrated under reduced pressure. The resulting residue was purified by silica gel column chromatography ($CHCl_3$/MeOH = 50/1) to afford **61a** (122.3 mg, 0.264 mmol, quant.) as a colorless amorphous solid: mp 106–110 °C; ^1H NMR (400 MHz, acetone-d_6, TMS): δ = 1.44 (s, 9H), 1.51 (d, J = 5.2 Hz, 9H), 2.64–2.72 (m, 4H), 3.18–3.31 (m, 4H), 3.47–3.54 (m, 4H), 3.66–3.74 (m, 2H), 7.07–7.10 (m, 2H), 7.39–7.42 (m, 2H), 7.76–7.86 (m, 2H); ^{13}C NMR (100 MHz, acetone-d_6, TMS): δ = 27.86, 48.29–49.84 (m), 50.15–51.53 (m),

52.89–54.34 (m), 60.39–60.58 (m), 78.6–78.69 (m), 128.02–128.41 (m), 133.97–134.16 (m), 142.53, 155.02, 155.20; ^{11}B NMR (128 MHz, acetone-d_6, $BF_3 \cdot OEt_2$): δ = 29.3 (brs); IR (ATR): ν = 3407, 2974, 1668, 1462, 1410, 1365, 1247, 1143, 999, 856, 752, 648, 532, 491, 458, 436 cm^{-1}; HRMS (ESI$^+$): *m*/*z* calcd for $[M+H]^+$, $C_{23}H_{39}{}^{10}BN_3O_6$, 463.2963; found, 463.2976; Anal. Calcd (%) for $C_{23}H_{38}BN_3O_6 \cdot 0.2CHCl_3$: C, 57.19; H, 7.90; N, 8.62. found: C, 57.32; H, 7.66; N, 8.42.

1-[(3-Boronopheny)methyl]-4,7-bis(*tert*-butoxycarbonyl)-1,4,7-triazacyclononane (61b)

To a solution of 3-(bromomethyl)phenylboronic acid **60b**[70] (70.1 mg, 0.326 mmol, 1.2 equiv) in MeCN (2.5 mL), 2Boc-tacn **59**[67] (90.1 mg, 0.273 mmol) and potassium carbonate (46.0 mg, 0.333 mmol, 1.2 equiv) were added and the mixture was stirred at reflux for 26 h. After adding H_2O, the reaction mixture was extracted with $CHCl_3$. The organic layer was washed with brine, dried over Na_2SO_4 and concentrated under reduced pressure. The resulting residue was purified by silica gel column chromatography (hexanes/AcOEt = 1/1 to $CHCl_3$/MeOH = 50/1) to afford **61b** (120.8 mg, 0.261 mmol, 95%) as a colorless amorphous solid: mp 95–97 °C; ^{1}H NMR (400 MHz, acetone-d_6, TMS): δ = 1.43 (*J* = 3.6 Hz, 9H), 1.50 (*J* = 3.6 Hz, 9H), 2.67–2.74 (m, 4H), 3.21–3.26 (m, 4H), 3.47–3.51 (m, 4H), 3.66–3.76 (m, 2H), 7.13 (s, 2H), 7.26–7.34 (m, 1H), 7.49–7.57 (m, 1H), 7.73–7.86 (m, 2H); ^{13}C NMR (100 MHz, acetone-d_6, TMS): δ = 28.70, 49.38–50.24 (m), 50.70–51.33 (m), 52.18, 53.75–53.98 (m), 55.09–55.25 (m), 61.89–61.98 (m), 79.54–79.68 (m), 128.11–128.19 (m), 131.96–132.13 (m), 133.62, 135.77–135.90 (m), 139.92, 155.88–156.13 (m); ^{11}B NMR (128 MHz, acetone-d_6, $BF_3 \cdot OEt_2$): δ = 29.0 (brs); IR (ATR): ν = 3407, 2974, 2931, 1669, 1460, 1413, 1364, 1246, 1142, 1093, 997, 856, 751, 710, 665, 621, 527, 459, 436 cm^{-1}; HRMS (ESI$^+$): *m*/*z* calcd for $[M+H]^+$, $C_{23}H_{39}{}^{10}BN_3O_6$, 463.2968; found, 463.2963; Anal. Calcd (%) for $C_{23}H_{38}BN_3O_6$: C, 59.62; H, 8.27; N, 9.07. found: C, 59.93; H, 8.24; N, 8.81.

1-[(4-Boronopheny)methyl]-1,4,7-triazacyclononane Trifluoroacetic Acid Salt (2TFA) (14a)

TFA (1.5 mL) was added to a solution of **61a** (122.3 mg, 0.264 mmol) in CH_2Cl_2 (1.5 mL), and the resulting mixture was stirred at room temperature for 1 h. After evaporation, the resulting residue was dissolved in MeCN and reprecipitated with Et_2O to afford **14a** (95.7 mg, 0.195 mmol, 74%) as colorless powder, which was determined to be the 2TFA salt by elemental analysis: mp 138–141 °C; ^{1}H NMR (400 MHz, D_2O, TSP): δ = 3.06 (t, *J* = 5.6 Hz, 4H), 3.24 (t, *J* = 5.6 Hz, 4H), 3.64 (s, 4H), 3.95 (s, 2H), 7.49 (d, *J* = 7.6 Hz, 2H), 7.83 (d, *J* = 7.6 Hz, 2H); ^{13}C NMR (100 MHz, D_2O, 1,4-dioxane): δ = 42.84, 44.32, 48.35, 59.57, 116.93, 130.33, 134.65, 138.81, 163.43; ^{11}B NMR (128 MHz, D_2O, $BF_3{\cdot}OEt_2$): δ = 29.0 (brs); IR (ATR): *ν* = 3005, 2774, 1665, 1610, 1485, 1420, 1397, 1384, 1353, 1183, 1130, 1083, 1055, 1004, 875, 841, 795, 723, 696, 654, 518, 410 cm^{-1}; HRMS (ESI$^+$): *m*/*z* calcd for $[M+H]^+$, $C_{13}H_{23}{}^{10}BN_3O_2$, 263.1920; found, 263.1914; Anal. Calcd (%) for $C_{13}H_{22}BN_3O_2{\cdot}2TFA$: C, 41.57; H, 4.93; N, 8.55. found: C, 41.72; H, 4.85; N, 8.54.

1-[(3-Boronopheny)methyl]-1,4,7-triazacyclononane Trifluoroacetic Acid Salt (2TFA) (14b)

TFA (1.0 mL) was added to a solution of **61b** (81.4 mg, 0.174 mmol) in CH_2Cl_2 (1.0 mL), and the mixture was stirred at room temperature for 1 h. After evaporation, the resulting residue was dissolved in MeCN and reprecipitated with Et_2O to afford **14b** (60.9 mg, 0.124 mmol, 71%) as colorless powder, which was determined to be the 2TFA salt by elemental analysis: mp 136–138 °C; ^{1}H NMR (400 MHz, D_2O, TSP): δ = 3.00 (t, *J* = 6.0 Hz, 4H), 3.15 (brs, 4H), 3.51 (brs, 4H), 3.94 (s, 2H), 7.51 (t, *J* = 8.0 Hz, 1H), 7.57 (d, *J* = 8.0 Hz, 1H), 7.79–7.80 (m, 2H); ^{13}C NMR (100 MHz, D_2O, 1,4-dioxane): δ = 42.84, 44.17, 48.42, 59.82, 116.94, 129.02, 133.21, 133.94, 135.85, 136.01; ^{11}B NMR (128 MHz,

D_2O, $BF_3 \cdot OEt_2$): δ = 29.3 (brs); IR (ATR): *v* = 2810, 1667, 1429, 1337, 1180, 1126, 1010, 834, 797, 719, 582, 515, 441, 414 cm^{-1}; HRMS (ESI^+): *m*/*z* calcd for $[M+H]^+$, $C_{13}H_{23}{}^{10}BN_3O_2$, 263.1920; found, 263.1914; Anal. Calcd (%) for $C_{13}H_{22}BN_3O_2 \cdot 2TFA – 0.8H_2O$: C, 42.83; H, 4.74; N, 8.81. found: C, 42.88; H, 5.04; N, 8.81.

1-[4-(13,15-Dioxa-15-boradispiro[5.0.5.3]pentadec-14-yl)phenyl]methyl-1,4,7-triazacyclononane (17a)

A mixture of **14a** (30.0 mg, 0.0611 mmol) and bicyclohexyl-1,1′-diol **62**[69] (15.7 mg, 0.0792 mmol, 1.3 equiv) in EtOH (0.8 mL) was refluxed for 6 h. After evaporation, the resulting residue was purified by NH silica gel column chromatography ($CHCl_3$/MeOH = 20/1) to afford **17a** (24.8 mg, 0.0583 mmol, 95%) as a colorless amorphous solid: mp 65–67 °C; ^1H NMR (400 MHz, $CDCl_3$, TMS): δ = 1.13–1.32 (m, 6H), 1.63–1.81 (m, 14H), 2.61–2.67 (m, 8H), 2.78 (s, 4H), 3.73 (s, 2H), 7.34 (d, *J* = 8.0 Hz, 2H), 7.82 (d, *J* = 7.6 Hz, 2H); ^{13}C NMR (100 MHz, $CDCl_3$, TMS): δ = 22.32, 25.81, 32.47, 46.40, 46.54, 52.76, 61.71, 84.64, 128.33, 134.92, 142.61; ^{11}B NMR (128 MHz, $CDCl_3$, $BF_3 \cdot OEt_2$): δ = 31.5 (brs); IR (ATR): *v* = 2929, 2851, 1611, 1449, 1398, 1356, 1284, 1238, 1131, 1087, 1018, 937, 822, 750, 652, 506, 418 cm^{-1}; HRMS (ESI^+): *m*/*z* calcd for $[M+H]^+$, $C_{25}H_{41}{}^{10}BN_3O_2$, 425.3328; found, 425.3322; Anal. Calcd (%) for $C_{25}H_{40}BN_3O_2 \cdot 0.2CHCl_3 \cdot 0.6MeOH$: C, 66.14; H, 9.17; N, 8.97. found: C, 66.05; H, 8.98; N, 8.70.

1-[3-(13,15-Dioxa-15-boradispiro[5.0.5.3]pentadec-14-yl)phenyl]methyl-1,4,7-triazacyclononane (17b)

A mixture of **14b** (20.0 mg, 0.041 mmol) and bicyclohexyl-1,1′-diol **62**[69] (10.5 mg, 0.053 mmol, 1.3 equiv) in EtOH (0.5 mL) was refluxed for 6 h. After evaporation, the resulting residue was purified by NH silica gel column chromatography ($CHCl_3$/MeOH = 20/1) to afford **17b** (11.8 mg, 0.028 mmol, 68%) as a colorless amorphous solid: mp

57–58 °C; ^{1}H NMR (400 MHz, $CDCl_3$, TMS): δ = 1.14–1.33 (m, 6H), 1.63–1.84 (m, 14H), 2.65–2.69 (m, 8H), 2.83 (s, 4H), 3.74 (s, 2H), 7.34 (t, *J* = 7.6 Hz 1H), 7.46 (d, *J* = 8.0 Hz 1H), 7.75 (d, *J* = 7.6 Hz 1H), 7.79 (s, 1H); ^{13}C NMR (100 MHz, $CDCl_3$, TMS): δ = 22.34, 25.81, 32.48, 46.58, 46.86, 52.95, 61.54, 84.71, 127.75, 131,66, 133.64, 135.24, 138.84; ^{11}B NMR (128 MHz, $CDCl_3$, $BF_3{\cdot}OEt_2$): δ = 30.8 (brs); IR (ATR): *v* = 2928, 2852, 1448, 1353, 1285, 1239, 1200, 1145, 1131, 1076, 1040, 939, 779, 751, 708, 615, 507, 409 cm^{-1}; HRMS (ESI$^+$): *m*/*z* calcd for $[M+H]^+$, $C_{25}H_{41}{}^{10}BN_3O_2$, 425.3323; found, 425.3327; Anal. Calcd (%) for $C_{25}H_{40}BN_3O_2{\cdot}0.1CHCl_3{\cdot}MeOH$: C, 66.78; H, 9.47; N, 8.95. found: C, 66.88; H, 9.29; N, 8.57.

1-[(4-Boronopheny)methyl]-4,7,10-tris(*tert*-butoxycarbonyl)-1,4,7,10-tetraazacyclododecane (64a)

To a solution of 4-(bromomethyl)phenylboronic acid **60a**[68] (66.4 mg, 0.309 mmol, 1.5 equiv) in MeCN (2.0 mL), 3Boc-cyclen **63**[72] (100 mg, 0.212 mmol) and potassium carbonate (58.1 mg, 0.420 mmol, 2.0 equiv) were added and the mixture was stirred at reflux for 4 h. After adding H_2O, the reaction mixture was extracted with $CHCl_3$. The organic layer was washed with brine, dried over Na_2SO_4, and concentrated under reduced pressure. The resulting residue was purified by silica gel column chromatography ($CHCl_3$/MeOH = 100/1) to afford **64a** (108.3 mg, 0.179 mmol, 84%) as a colorless amorphous solid: mp 112–115 °C; ^{1}H NMR (300 MHz, $CDCl_3$, TMS): δ = 1.44–1.49 (m, 27H), 2.71 (brs, 4H), 3.30–3.40 (m, 8H), 3.59 (brs, 4H), 3.70–3.74 (m, 2H), 7.29 (d, *J* = 8.0 Hz, 1H), 7.40 (d, *J* = 8.0 Hz, 1H), 7.70 (d, *J* = 8.0 Hz, 1H), 8.18 (d, *J* = 7.6 Hz, 1H); ^{13}C NMR (100 MHz, $CDCl_3$, TMS): δ = 18.45, 28.49, 28.72, 2872, 29.70, 47.39, 49.82, 58.50, 79.68, 129.46, 129.97, 133.59, 135.61, 139.38, 155.34, 156.18, 158.78, 163.43, 196.70, 209.38, 210.84; ^{11}B NMR (128 MHz, $CDCl_3$, $BF_3{\cdot}OEt_2$): δ = 29.1 (brs); IR (ATR): *v* = 3397, 2975, 2931, 1682, 1668, 1611, 1478, 1457, 1412, 1364, 1341, 1249, 1151, 1109, 1019, 979, 856, 770, 754, 734, 649, 555, 516, 458 cm^{-1}; HRMS (ESI$^+$): *m*/*z*

calcd for $[M+H]^+$, $C_{30}H_{52}{}^{10}BN_4O_8$, 606.3909; found, 606.3917; Anal. Calcd (%) for $C_{30}H_{51}BN_4O_8 \cdot 0.3CHCl_3$: C, 56.65; H, 8.05; N, 8.72. found: C, 56.73; H, 8.10; N, 8.66.

1-[(3-Boronopheny)methyl]-4,7,10-tris(*tert*-butoxycarbonyl)-1,4,7,10-tetraazacyclododecane (64b)[54]

To a solution of 3-(bromomethyl)phenylboronic acid **60b**[70] (67.8 mg, 0.316 mmol, 1.5 equiv) in MeCN (2.0 mL), 3Boc-cyclen **63**[72] (100 mg, 0.212 mmol) and potassium carbonate (58.4 mg, 0.423 mmol, 2.0 equiv) were added and the mixture was stirred at reflux for 3 h. After adding H_2O, the reaction mixture was extracted with $CHCl_3$. The organic layer was washed with brine, dried over Na_2SO_4, and concentrated under reduced pressure. The resulting residue was purified by silica gel column chromatography ($CHCl_3$/MeOH = 100/1) to afford **64b** (121.8 mg, 0.201 mmol, 95%) as a colorless amorphous solid: The ^1H and ^{13}C and ^{11}B NMR spectra of product were identical to previously reported data.[54]

1-[(4-Boronopheny)methyl]-1,4,7,10-tetraazacyclododecane Trifluoroacetic Acid Salt (2TFA) (15a)

TFA (1.0 mL) was added to a solution of **64a** (94.2 mg, 0.155 mmol) in CH_2Cl_2 (1.0 mL), and the mixture was stirred at room temperature for 1 h. After evaporation, the resulting residue was dissolved in AcOEt and reprecipitated with hexanes to afford **15a** (72.5 mg, 0.136 mmol, 88%) as colorless powder, which were determined to be the 2TFA salt by elemental analysis: mp 172–175 °C; ^1H NMR (400 MHz, D_2O, TSP): δ = 2.93–3.01 (m, 8H), 3.17–3.25 (m, 8H), 3.88 (s, 2H), 7.44 (d, J = 8.0 Hz, 2H), 7.83 (d, J = 8.0 Hz, 2H); ^{13}C NMR (100 MHz, D_2O, 1,4-dioxane): δ = 42.31, 42.46, 44.78, 48.38, 57.18, 129.96, 134.87, 138.74; ^{11}B NMR (128 MHz, D_2O, $BF_3 \cdot OEt_2$): δ = 29.05 (brs); IR (ATR): ν = 3301, 3088, 2856, 1668, 1610, 1454, 1409, 1343, 1196, 1176, 1120, 1052, 1017, 829, 796, 719, 693, 651, 596, 516, 435, 414 cm^{-1}; HRMS (ESI^+): m/z calcd for $[M+H]^+$,

$C_{15}H_{28}{}^{10}BN_4O_2$, 306.2342; found, 306.2336; Anal. Calcd (%) for $C_{15}H_{27}BN_4O_2 \cdot 2TFA$: C, 42.71; H, 5.47; N, 10.49. found: C, 42.75; H, 5.38; N, 10.44.

1-[(3-Boronopheny)methyl]-1,4,7,10-tetraazacyclododecane (15b)[54]

TFA (2.0 mL) was added to a solution of **64b** (110.2 mg, 0.182 mmol) in CH_2Cl_2 (2.0 mL), and the mixture was stirred at room temperature for 1 h. After evaporation, the resulting residue was purified by NH silica gel column chromatography ($CHCl_3$/MeOH = 20/1) to afford **15b** (50.4 mg, 0.165 mmol, 91%) as a colorless amorphous solid: The ^1H, ^{13}C and ^{11}B NMR spectra of product were identical to previously reported data.[54]

1-[4-(13,15-Dioxa-15-boradispiro[5.0.5.3]pentadec-14-yl)phenyl]methyl-1,4,7,10-tetraazacyclododecane (18a)

A mixture of **15a** (40.0 mg, 0.0748 mmol) and bicyclohexyl-1,1′-diol **62**[69] (15.2 mg, 0.0766 mmol, 1.0 equiv) in EtOH (1.0 mL) was refluxed for 6 h. After evaporation, the resulting residue was dissolved in EtOH and reprecipitated with hexanes, and the resulting precipitate was purified by NH silica gel column chromatography ($CHCl_3$/MeOH = 20/1) to afford **18a** (34.5 mg, 0.0736 mmol, 98%) as a colorless solid: mp 129–131 °C; ^1H NMR (300 MHz, $CDCl_3$, TMS): δ = 1.13–1.31 (m, 6H), 1.62–1.83 (m, 14H), 2.57 (t, *J* = 5.2 Hz, 8H), 2.67 (t, *J* = 5.2 Hz, 4H), 2.81 (t, *J* = 5.6 Hz, 4H), 3.63 (s, 2H), 7.31 (d, *J* = 8.0 Hz, 2H), 7.81 (d, *J* = 8.0 Hz, 2H); ^{13}C NMR (100 MHz, $CDCl_3$, TMS): δ = 22.31, 25.81, 32.45, 45.09, 46.34, 47.14, 51.26, 59.33, 84.51, 128.36, 134.95, 141.93; ^{11}B NMR (128 MHz, $CDCl_3$, $BF_3 \cdot OEt_2$): δ = 31.1 (brs); IR (ATR): *v* = 2933, 2856, 2811, 1610, 1450, 1403, 1356, 1319, 1284, 1272, 1239, 1131, 1088, 1041, 1020, 937, 911, 822, 801, 746, 725, 653, 540, 507 cm^{-1}; HRMS (ESI^+): *m/z* calcd for $[M+H]^+$, $C_{27}H_{46}{}^{10}BN_4O_2$, 468.3750; found, 468.3745; Anal. Calcd (%) for $C_{27}H_{45}BN_4O_2 \cdot 0.5MeOH$: C, 68.17; H, 9.78; N, 11.56. found: C, 68.35; H, 9.79; N, 11.26.

1-[3-(13,15-Dioxa-15-boradispiro[5.0.5.3]pentadec-14-yl)phenyl]methyl-1,4,7,10-tetraazacyclododecane (18b)

A mixture of **15b** (27.0 mg, 0.0882 mmol) and bicyclohexyl-1,1′-diol **62**[69] (17.5 mg, 0.0882 mmol, 1.0 equiv) in EtOH (0.9 mL) was refluxed for 3 h. After evaporation, the resulting residue was purified by NH silica gel column chromatography ($CHCl_3$/MeOH = 20/1) to afford **18b** (33.5 mg, 0.0714 mmol, 81%) as a colorless amorphous solid: mp 46–48 °C; ^{1}H NMR (400 MHz, $CDCl_3$, TMS): δ = 1.22–1.32 (m, 6H), 1.63–1.83 (m, 14H), 2.56–2.59 (m, 8H), 2.67 (t, *J* = 4.4 Hz, 4H), 2.81 (t, *J* = 4.4 Hz, 4H), 3.64 (s, 2H), 7.32 (t, *J* = 7.6 Hz, 1H), 7.41 (d, *J* = 8.0 Hz, 1H), 7.74 (d, *J* = 7.2 Hz, 1H), 7.77 (s, 1H); ^{13}C NMR (100 MHz, $CDCl_3$, TMS): δ = 22.31, 25.80, 32.45, 45.34, 46.40, 47.39, 51.38, 59.26, 84.57, 127.71, 131.79, 133.80, 135.43, 138.04; ^{11}B NMR (128 MHz, $CDCl_3$, $BF_3{\cdot}OEt_2$): δ = 30.8 (brs); IR (ATR): *ν* = 2929, 2851, 1604, 1448, 1429, 1392, 1352, 1320, 1284, 1272, 1253, 1239, 1200, 1146, 1131, 1114, 1077, 1039, 939, 909, 834, 803, 747, 707, 681, 658, 541, 507 cm^{-1}; HRMS (ESI$^+$): *m*/*z* calcd for $[M+H]^+$, $C_{27}H_{46}{}^{10}BN_4O_2$, 468.3750; found, 468.3745; Anal. Calcd (%) for $C_{27}H_{45}BN_4O_2{\cdot}0.1CHCl_3{\cdot}2.4MeOH$: C, 63.58; H, 9.89; N, 10.05. found: C, 63.90; H, 9.63; N, 9.65.

1-[(4-Boronopheny)methyl]-4,7,10,13-tetra(*tert*-butoxycarbonyl)-1,4,7,10,13-pentaazacyclopentadecane (66a)

To a solution of 4-(bromomethyl)phenylboronic acid **60a**[68] (48.3 mg, 0.225 mmol, 1.2 equiv) in MeCN (1.5 mL), **65**[73] (113.9 mg, 0.185 mmol) and potassium carbonate (38.1 mg, 0.276 mmol, 1.5 equiv) were added and the mixture was stirred at reflux for 2 h. After adding H_2O, the reaction mixture was extracted with $CHCl_3$. The organic layer was washed with brine, dried over Na_2SO_4, and concentrated under reduced pressure. The resulting residue was purified by silica gel column chromatography ($CHCl_3$/MeOH = 100/1) to afford **66a** (115.0 mg, 0.153 mmol, 83%) as a colorless amorphous solid: mp 94–96 °C; ^{1}H NMR (400 MHz, acetone-*d*$_6$, TMS): δ = 1.30 (s, 9H), 1.44 (s, 9H), 1.48 (s,

18H), 2.74 (s, 4H), 3.47 (s, 16H), 3.67 (s, 2H), 7.09 (s, 2H), 7.34 (d, J = 8.0 Hz, 2H), 7.83 (d, J = 8.0 Hz, 2H); ^{13}C NMR (100 MHz, acetone-d_6, TMS): δ = 28.63, 31.99, 47.35, 53.23, 55.49, 60.21, 69.71, 79.56, 79.89, 128.59, 135.05, 142.72, 155.59, 155.72; ^{11}B NMR (128 MHz, acetone-d_6, $BF_3{\cdot}OEt_2$): δ = 29.7 (brs); IR (ATR): v = 3420, 2976, 1682, 1465, 1411, 1365, 1245, 1155, 1018, 858, 753, 648, 559, 458 cm^{-1}; HRMS (ESI$^+$): m/z calcd for $[M+H]^+$, $C_{37}H_{65}{}^{10}BN_5O_{10}$, 749.4861; found, 749.4855; Anal. Calcd (%) for $C_{37}H_{64}BN_5O_{10}{\cdot}0.3H_2O$: C, 58.85; H, 8.62; N, 9.27. found: C, 58.88; H, 8.56; N, 9.06.

1-[(3-Boronopheny)methyl]-4,7,10,13-tetra(*tert*-butoxycarbonyl)-1,4,7,10,13-pentaazacyclopentadecane (66b)

To a solution of 3-(bromomethyl)phenylboronic acid **60b**[70] (51.6 mg, 0.240 mmol, 1.2 equiv) in MeCN (2.0 mL), **65**[73] (121.0 mg, 0.196 mmol) and potassium carbonate (40.6 mg, 0.294 mmol, 1.5 equiv) were added and the mixture was stirred at reflux for 4 h. After adding H_2O, the reaction mixture was extracted with $CHCl_3$. The organic layer was washed with brine, dried over Na_2SO_4, and concentrated under reduced pressure. The resulting residue was purified by silica gel column chromatography ($CHCl_3$/MeOH = 100/1) to afford **66b** (127.4 mg, 0.170 mmol, 87%) as a colorless amorphous solid: mp 106–110 °C; ^{1}H NMR (400 MHz, acetone-d_6, TMS): δ = 1.29 (s, 9H), 1.45 (s, 9H), 1.47 (s, 18H), 2.74 (s, 4H), 3.47 (s, 16H), 3.68 (s, 2H), 7.15 (s, 2H), 7.29 (t, J = 7.2 Hz, 1H), 7.40 (d, J = 6.8 Hz, 1H), 7.72 (d, J = 5.6 Hz, 1H), 7.82 (s, 1H); ^{13}C NMR (100 MHz, acetone-d_6, TMS): δ = 28.61, 31.99, 46.54, 47.34, 53.22, 55.44, 60.19, 79.65, 79.89, 128.26, 131.44, 133.58, 135.15, 155.74; ^{11}B NMR (128 MHz, acetone-d_6, $BF_3{\cdot}OEt_2$): δ = 30.0 (brs); IR (ATR): v = 3419, 2976, 1682, 1464, 1413, 1365, 1244, 1155, 1043, 860, 770, 710, 558, 462, 418 cm^{-1}; HRMS (ESI$^+$): m/z calcd for $[M+H]^+$, $C_{37}H_{65}{}^{10}BN_5O_{10}$, 749.4861; found, 749.4855; Anal. Calcd (%) for $C_{37}H_{64}BN_5O_{10}{\cdot}0.25CHCl_3$: C, 57.39; H, 8.31; N, 8.92. found: C, 57.67; H, 8.21; N, 8.72.

1-[(2-Boronopheny)methyl]-4,7,10,13-tetra(*tert*-butoxycarbonyl)-1,4,7,10,13-pentaazacyclopentadecane (66c)

To a solution of 2-(bromomethyl)phenylboronic acid **60c**[71] (55.1 mg, 0.256 mmol, 1.2 equiv) in MeCN (2.0 mL), **65**[73] (129.8 mg, 0.211 mmol) and potassium carbonate (44.3 mg, 0.32 mmol, 1.5 equiv) were added and the mixture was stirred at reflux for 10 h. After adding H_2O, the reaction mixture was extracted with $CHCl_3$. The organic layer was washed with brine, dried over Na_2SO_4, and concentrated under reduced pressure. The resulting residue was purified by silica gel column chromatography ($CHCl_3$/MeOH = 100/1) to afford **66c** (115.7 mg, 0.154 mmol, 73%) as a colorless amorphous solid: mp 105–109 °C; ^{1}H NMR (400 MHz, acetone-d_6, TMS): δ = 1.47 (s, 36H), 2.82 (s, 4H), 3.45 (s, 16H), 3.82 (s, 2H), 7.25–7.36 (m, 4H), 7.87 (br, 1H), 8.78 (br, 1H); ^{13}C NMR (100 MHz, acetone-d_6, TMS): δ = 28.39, 28.63, 47.12, 50.94, 51.42, 55.49, 62.29, 79.77, 79.94, 127.94, 130.61, 131.96, 137.26, 142.60, 155.44, 155.62; ^{11}B NMR (128 MHz, acetone-d_6, $BF_3{\cdot}OEt_2$): δ = 29.7 (brs); IR (ATR): ν = 2975, 2932, 1692, 1463, 1412, 1391, 1365, 1309, 1244, 1156, 1032, 947, 894, 860, 770, 653, 550, 460 cm^{-1}; HRMS (ESI$^+$): *m*/*z* calcd for $[M+H]^+$, $C_{37}H_{65}{}^{10}BN_5O_{10}$, 749.4861; found, 749.4864; Anal. Calcd (%) for $C_{37}H_{64}BN_5O_{10}{\cdot}1.5MeOH$: C, 57.96; H, 8.84; N, 8.78. found: C, 57.84; H, 9.06; N, 9.07.

1-[(4-Boronopheny)methyl]-1,4,7,10,13-pentaazacyclopentadecane Trifluoroacetic Acid Salt (3TFA) (16a)

TFA (1.5 mL) was added to a solution of **66a** (111.0 mg, 0.148 mmol) in CH_2Cl_2 (1.5 mL), and the mixture was stirred at room temperature for 30 min. After evaporation, the resulting residue was dissolved in MeCN and reprecipitated with Et_2O to afford **16a** (90.0 mg, 0.130 mmol, 88%) as colorless powder, which was determined to be the 3TFA salt by elemental analysis: mp 136–137 °C; ^{1}H NMR (400 MHz, D_2O, TSP): δ = 3.01 (t, *J* = 6.0 Hz, 4H), 3.17 (s, 4H), 3.26–3.33 (m, 8H), 3.38 (t, *J* = 6.0 Hz, 4H), 3.95 (s, 2H), 7.43 (d, *J* = 8.0 Hz, 2H), 7.83 (d, *J* = 8.0 Hz, 2H); ^{13}C NMR (100 MHz, D_2O, 1,4-dioxane):

δ = 44.31, 45.30, 45.81, 50.24, 56.73, 116.92, 130.56, 134.66, 137.03, 163.59; ^{11}B NMR (128 MHz, D_2O, $BF_3{\cdot}OEt_2$): δ = 29.2 (brs); IR (ATR): *v* = 3029, 1668, 1410, 1382, 1359, 1178, 1129, 1055, 1018, 888, 838, 798, 720, 698, 654, 517 cm^{-1}; HRMS (ESI$^+$): *m*/*z* calcd for $[M+H]^+$, $C_{17}H_{33}{}^{10}BN_5O_2$, 349.2764 ; found, 349.2770; Anal. Calcd (%) for $C_{17}H_{32}BN_5O_2{\cdot}3TFA$: C, 39.96; H, 5.10; N, 10.13. found: C, 39.97; H, 4.98; N, 10.05.

1-[(3-Boronopheny)methyl]-1,4,7,10,13-pentaazacyclopentadecane Trifluoroacetic Acid Salt (3TFA) (16b)

TFA (1.5 mL) was added to a solution of **66b** (127.2 mg, 0.170 mmol) in CH_2Cl_2 (1.5 mL), and the mixture was stirred at room temperature for 1 h. After evaporation, the resulting residue was dissolved in MeCN and reprecipitated with Et_2O to afford **16b** (107.1 mg, 0.155 mmol, 91%) as colorless powder, which was determined to be the 3TFA salt by elemental analysis: mp 106–108 °C; ^{1}H NMR (400 MHz, D_2O, TSP): δ = 3.03 (t, *J* = 5.2 Hz 4H), 3.18 (s, 4H), 3.27–3.29 (m, 4H), 3.33 (t, *J* = 5.2 Hz 4H), 3.37–3.40 (m, 4H), 3.98 (s, 2H), 7.48–7.55 (m, 2H), 7.73 (s, 1H), 7.80–7.83 (m, 1H); ^{13}C NMR (100 MHz, D_2O, 1,4-dioxane): δ = 44.34, 45.21, 45.49, 45.79, 50.27, 56.94, 116.92, 129.09, 133.53, 133.62, 134.35, 136.20, 163.58; ^{11}B NMR (128 MHz, D_2O, $BF_3{\cdot}OEt_2$): δ = 28.6 (brs); IR (ATR): *v* = 3030, 2856, 1666, 1426, 1337, 1179, 1123, 834, 797, 719, 597, 517 cm^{-1}; HRMS (ESI$^+$): *m*/*z* calcd for $[M+H]^+$, $C_{17}H_{33}{}^{10}BN_5O_2$, 349.2764; found, 349.2758; Anal. Calcd (%) for $C_{17}H_{32}BN_5O_2{\cdot}3.4TFA$: C, 38.79; H, 4.82; N, 9.43. found: C, 38.66; H, 4.95; N, 9.33.

1-[(2-Boronopheny)methyl]-1,4,7,10,13-pentaazacyclopentadecane Trifluoroacetic Acid Salt (3TFA) (16c)

TFA (1.5 mL) was added to a solution of **66c** (115.7 mg, 0.154 mmol) in CH_2Cl_2 (1.5 mL), and the mixture was stirred at room temperature for 1 h. After evaporation, the resulting residue was dissolved in AcOEt and reprecipitated with hexanes to afford **16c**

(94.8 mg, 0.137 mmol, 89%) as colorless powder, which was determined to be the 3TFA salt by elemental analysis: mp 118–120 °C; ^{1}H NMR (400 MHz, D_2O, TSP): δ = 2.99 (t, *J* = 4.8 Hz 4H), 3.11 (m, *J* = 5.6 Hz 4H), 3.17 (s, 12H), 4.02 (s, 2H), 7.40 (d, *J* = 6.8 Hz 1H), 7.47–7.51 (m, 2H), 7.70 (d, *J* = 7.2 Hz 1H); ^{13}C NMR (100 MHz, D_2O, 1,4-dioxane): δ = 44.60, 44.86, 45.50, 51.06, 60.39, 116.91, 128.88, 130.75, 131.36, 134.06, 138.21, 163.60; ^{11}B NMR (128 MHz, D_2O, $BF_3{\cdot}OEt_2$): δ = 29.7 (brs); IR (ATR): *v* = 3023, 2843, 1668, 1440, 1359, 1193, 1147, 1126, 1050, 1032, 836, 797, 767, 719, 624, 588, 517, 443, 420 cm^{-1}; HRMS (ESI^{+}): *m*/*z* calcd for $[M+H]^{+}$, $C_{17}H_{33}{}^{10}BN_5O_2$, 349.2764; found, 349.2769; Anal. Calcd (%) for $C_{17}H_{32}BN_5O_2{\cdot}3TFA$: C, 39.96; H, 5.10; N, 10.13. found: C, 39.67; H, 4.87; N, 9.84.

1-[4-(13,15-Dioxa-15-boradispiro[5.0.5.3]pentadec-14-yl)phenyl]methyl-1,4,7,10,13-pentaazacyclopentadecane (19a)

A mixture of **16a** (30.4 mg, 0.044 mmol) and bicyclohexyl-1,1′-diol **62**[69] (9.4 mg, 0.0474 mmol, 1.1 equiv) in EtOH (0.8 mL) was refluxed for 2 h. After evaporation, the resulting residue was purified by NH silica gel column chromatography ($CHCl_3$/MeOH = 100/1) to afford **19a** (21.4 mg, 0.0419 mmol, 88%) as a colorless amorphous solid: mp 43–44 °C; ^{1}H NMR (400 MHz, $CDCl_3$, TMS): δ = 1.16–1.31 (m, 6H), 1.73–1.80 (m, 14H), 2.65 (s, 12H), 2.79 (s, 8H), 3.62 (s, 2H), 7.32 (d, *J* = 8.0 Hz, 2H), 7.81 (d, *J* = 7.6 Hz, 2H); ^{13}C NMR (100 MHz, $CDCl_3$, TMS): δ = 22.31, 25.81, 32.47, 47.29, 47.79, 48.24, 49.00, 54.55, 59.62, 84.68, 128.36, 134.93, 142.52; ^{11}B NMR (128 MHz, $CDCl_3$, $BF_3{\cdot}OEt_2$): δ = 30.3 (brs); IR (ATR): *v* = 3287, 2930, 2849, 1610, 1449, 1399, 1356, 1284, 1238, 1130, 1087, 937, 823, 727, 652, 507 cm^{-1}; HRMS (ESI^{+}): *m*/*z* calcd for $[M+Na]^{+}$, $C_{29}H_{50}{}^{10}BN_5O_2Na$, 533.3986; found, 533.4010; Anal. Calcd (%) for $C_{29}H_{50}BN_5O_2{\cdot}CHCl_3$: C, 57.11; H, 8.15; N, 11.10. found: C, 57.46; H, 8.13; N, 10.79.

1-[3-(13,15-Dioxa-15-boradispiro[5.0.5.3]pentadec-14-yl)phenyl]methyl-

1,4,7,10,13-pentaazacyclopentadecane (19b)

A mixture of **16b** (30.2 mg, 0.0437 mmol) and bicyclohexyl-1,1′-diol **62**[69] (8.7 mg, 0.0439 mmol, 1.0 equiv) in EtOH (0.6 mL) was refluxed for 5 h. After evaporation, the resulting residue was purified by NH silica gel column chromatography ($CHCl_3$/MeOH = 20/1) to afford **19b** (15.6 mg, 0.0305 mmol, 70%) as a colorless amorphous solid: ^{1}H NMR (400 MHz, $CDCl_3$, TMS): δ = 1.17–1.33 (m, 6H), 1.76–1.80 (m, 14H), 2.62–2.80 (m, 20H), 3.60 (s, 2H), 7.33 (t, *J* = 7.6 Hz, 1H), 7.47 (d, *J* = 8.0 Hz, 1H), 7.68 (s, 1H), 7.76 (d, *J* = 7.6 Hz, 1H); ^{13}C NMR (100 MHz, $CDCl_3$, TMS): δ = 22.33, 25.78, 32.48, 47.30, 47.85, 48.33, 48.96, 54.84, 59.63, 84.79, 127.70, 132.04, 133.90, 135.45, 138.83; ^{11}B NMR (128 MHz, $CDCl_3$, $BF_3{\cdot}OEt_2$): δ = 30.2 (brs); IR (ATR): *v* = 3281, 2929, 2849, 1550, 1449, 1353, 1272, 1238, 1201, 1130, 1077, 1041, 939, 910, 807, 760, 708, 611, 540, 509 cm^{-1}; HRMS (ESI$^+$): *m*/*z* calcd for $[M+Na]^+$, $C_{29}H_{50}{}^{10}BN_5O_2Na$, 533.3986; found, 533.4010; Anal. Calcd (%) for $C_{29}H_{50}BN_5O_2$: C, 68.09; H, 9.85; N, 13.69. found: C, 68.06; H, 10.15; N, 13.77.

1-[2-(13,15-Dioxa-15-boradispiro[5.0.5.3]pentadec-14-yl)phenyl]methyl-1,4,7,10,13-pentaazacyclopentadecane (19c)

A mixture of **16c** (26.5 mg, 0.0383 mmol) and bicyclohexyl-1,1′-diol **62**[69] (7.6 mg, 0.0383 mmol, 1.0 equiv) in EtOH (0.4 mL) was refluxed for 6 h. After evaporation, the resulting residue was purified by NH silica gel column chromatography ($CHCl_3$/MeOH = 30/1) to afford **19c** (15 mg, 0.0293 mmol, 77%) as a colorless solid: mp 78–80 °C; ^{1}H NMR (400 MHz, $CDCl_3$, TMS): δ = 1.14–1.33 (m, 6H), 1.64–1.81 (m, 14H), 2.58–2.77 (m, 20H), 3.94 (s, 2H), 7.23 (t, *J* = 7.2 Hz, 1H), 7.42 (td, *J* = 7.6, 1.2 Hz, 1H), 7.59 (d, *J* = 7.2 Hz,1H), 7.82 (dd, *J* = 7.2, 1.6 Hz, 1H); ^{13}C NMR (100 MHz, $CDCl_3$, TMS): δ = 22.52, 25.78, 32.48, 47.57, 48.03, 48.52, 49.16, 55.40, 57.57, 84.76, 125.97, 129.34, 130.78, 135.91, 147.03; ^{11}B NMR (128 MHz, $CDCl_3$, $BF_3{\cdot}OEt_2$): δ = 30.4 (brs); IR (ATR): *v* = 3285, 2932, 2814, 1598, 1568, 1439, 1345, 1311, 1284, 1272, 1236, 1132,

1110, 1064, 1039, 938, 805, 749, 733, 655, 545, 507 cm^{-1}; HRMS (ESI^+): *m*/*z* calcd for $[M+H]^+$, $C_{29}H_{51}{}^{10}BN_5O_2$, 511.4167; found, 511.4173; Anal. Calcd (%) for $C_{29}H_{50}BN_5O_2 \cdot 0.25CHCl_3$: C, 64.89; H, 9.36; N, 12.94. found: C, 65.04; H, 9.60; N, 12.82.

Complexation of 18a with Zn^{2+} (21a)

To a solution of **18a** (10.8 mg, 0.023 mmol) in EtOH (0.3 mL), $Zn(NO_3)_2 \cdot 6H_2O$ (6.9 mg, 0.0232 mmol, 1.0 equiv) in EtOH (0.2 mL) was added at room temperature. After evaporation, the resulting residue was recrystallized from EtOH (0.1 mL) to provide colorless crystals of **21a** (10.1 mg, 0.015 mmol, 67%): mp 257–259 °C; ^1H NMR (400 MHz, D_2O, TSP): δ =1.26 (br, 2H), 1.49 (br, 4H), 1.66–1.81 (m, 14H), 2.73 (br, 2H), 2.86 (br, 8H), 2.99 (br, 4H), 3.24 (br, 2H), 3.84 (br, 1H), 4.05 (s, 2H), 4.10 (brs, 2H), 7.46 (d, *J* = 7.6 Hz, 2H), 7.90 (d, *J* = 7.6 Hz, 2H); ^{13}C NMR (100 MHz, D_2O, 1,4-dioxane): δ = 22.44, 25.51, 32.00, 42.75, 44.17, 45.09, 49.73, 56.24, 87.52, 131.42, 134.44, 135.30; ^{11}B NMR (128 MHz, D_2O, $BF_3 \cdot OEt_2$): δ = 29.3 (brs); IR (ATR): *v* = 3243, 2928, 1611, 1482, 1449, 1354, 1284, 1238, 1131, 1088, 992, 935, 856, 819, 730, 702, 673, 644, 538, 473 cm^{-1}; HRMS (ESI^+): *m*/*z* calcd for $[M]^{2+}$, $C_{27}H_{45}{}^{10}BN_4O_2{}^{64}Zn$, 265.6476 ; found, 265.6474; Anal. Calcd (%) for $C_{27}H_{45}BN_6O_8Zn \cdot 0.5H_2O$: C, 48.63; H, 6.95; N, 12.60. found: C, 48.58; H, 6.88; N, 12.47.

Complexation of 18b with Zn^{2+} (21b)

To a solution of **18b** (15.5 mg, 0.0331 mmol) in EtOH (0.3 mL), $Zn(NO_3)_2 \cdot 6H_2O$ (9.8 mg, 0.033 mmol, 1.0 equiv) in EtOH (0.2 mL) was added at room temperature. The generated crystalline sample of **21b** was recrystallized from EtOH (0.5 mL) and Et_2O (0.5 mL) to provide colorless crystals (10.6 mg, 0.016 mmol, 49%): mp 208–210 °C; ^1H NMR (400 MHz, D_2O, TSP): δ =1.44–1.83 (m, 20H), 2.74 (br, 2H), 2.87 (br, 8H), 3.00 (br, 4H), 3.26 (br, 2H), 3.83 (br, 1H), 4.04–4.11 (m, 4H), 7.52–7.57 (m, 2H), 7.74–7.92 (m, 2H); ^{13}C NMR (100 MHz, D_2O, 1,4-dioxane): δ = 21.90, 25.84, 30.08, 42.77, 44.17, 45.09,

49.67, 56.33, 77.05, 128.85, 131.42, 134.24, 134.52, 136.86; ^{11}B NMR (128 MHz, D_2O, $BF_3 \cdot OEt_2$): δ = 28.3 (brs); IR (ATR): ν = 3211, 2927, 1495, 1432, 1349, 1283, 1238, 1204, 1131, 1092, 961, 937, 909, 808, 708, 694, 641, 614, 565, 502 cm^{-1}; HRMS (ESI$^+$): *m*/*z* calcd for $[M]^{2+}$, $C_{27}H_{45}{}^{10}BN_4O_2{}^{64}Zn$, 265.6476 ; found, 265.6475; Anal. Calcd (%) for $C_{27}H_{45}BN_6O_8Zn \cdot 0.5H_2O$: C, 48.63; H, 6.95; N, 12.60. found: C, 48.73; H, 7.11; N, 12.37.

Synthesis of ^{10}B-enriched compounds

4-(Bromomethyl)phenylboronic acid (^{10}B-60a)[68]

To a solution of 4-bromotoluene **72a** (904 mg, 5.28 mmol, 1.3 equiv) in THF (10 mL), 1.6 N of *n*-butyllithium (*n*-BuLi) in hexanes (3.3 mL, 5.28 mmol, 1.3 equiv) was added at –78 °C and the reaction mixture was stirred at the same temperature for 1 h, after which, ^{10}B-enriched trimethylborate (> 99.5% of ^{10}B) (450 μL, 4.06 mmol, 1.0 equiv) was slowly added. After stirring at –78 °C to room temperature overnight, 2N aqueous HCl was added to the reaction mixture, which was further stirred at 0 °C for 3 h. After extraction with $CHCl_3$, the organic layer was washed with brine, dried over Na_2SO_4, and concentrated under reduced pressure. The resulting residue was recrystallized from hexanes to afford **^{10}B-73a** (279 mg, 2.06 mmol, 51%) as a colorless needle crystal.

A mixture of **^{10}B-73a** (270mg, 2.00 mmol), *N*-bromosuccinimide (NBS) (390 mg, 2.19 mmol, 1.1 equiv), and benzoyl peroxide (BPO) (16 mg, 0.066 mmol, 0.03 equiv) in CCl_4 (13 mL) was refluxed for 6 h and then diluted with $CHCl_3$. The reaction mixture was washed with H_2O and brine, dried over Na_2SO_4 and evaporated. The resulting residue was recrystallized from hexanes/AcOEt to give **^{10}B-60a** (281mg, 1.31 mmol, 66%) as a colorless solid: isotopic purity of ^{10}B: 98.5 ± 0.3%; mp 159–162 °C; ^{1}H NMR (400 MHz, DMSO-*d*$_6$, TMS): δ = 4.69 (s, 2H), 7.40 (d, *J* = 8.4 Hz, 2H), 7.76 (d, *J* = 7.6 Hz, 2H), 8.09 (s, 2H); ^{13}C NMR (100 MHz, DMSO-*d*$_6$, TMS): δ = 34.53, 125.42, 128.26, 134.39, 139.62; IR (ATR): ν = 3268, 1613, 1518, 1398, 1373, 1230, 1178, 1110, 1094, 1028, 1014, 844, 803, 744, 691, 659, 633, 601, 500, 442 cm^{-1}; HRMS (ESI$^+$): *m*/*z* calcd for $[M+Na]^+$,

$C_7H_8{}^{10}BBrO_2Na$, 235.9729; found, 235.9735; Anal. Calcd (%) for $C_7H_8{}^{10}BBrO_2 \cdot 0.1H_2O$: C, 38.95; H, 3.83. found: C, 38.56; H, 3.52.

3-(Bromomethyl)phenylboronic acid (^{10}B-60b)[70]

To a solution of 3-bromotoluene **72b** (916 mg, 5.36 mmol, 1.7 equiv) in THF (6 mL), 1.6 N of *n*-butyllithium (*n*-BuLi) in hexanes (3.5 mL, 5.6 mmol, 1.8 equiv) was added at –78 °C and the reaction mixture was stirred at the same temperature for 1 h, after which, ^{10}B-enriched trimethylborate (> 99.5% of ^{10}B) (350 μL, 3.16 mmol, 1.0 equiv) was slowly added. After stirring at –78 °C to room temperature overnight, 2N aqueous HCl was added to the reaction mixture, which was further stirred at 0 °C for 3 h. After extraction with $CHCl_3$, the organic layer was washed with brine, dried over Na_2SO_4 and concentrated under reduced pressure. The resulting residue was recrystallized from hexanes to afford **^{10}B-73b** (103 mg, 0.762 mmol, 24%) as a colorless needle crystal.

A mixture of **^{10}B-73b** (98 mg, 0.721 mmol), *N*-bromosuccinimide (NBS) (140 mg, 0.787 mmol, 1.1 equiv), and benzoyl peroxide (BPO) (6.0 mg, 0.025 mmol, 0.03 equiv) in CCl_4 (4 mL) was refluxed for 7 h and then diluted with $CHCl_3$. The reaction mixture was washed with H_2O and brine, dried over Na_2SO_4, and evaporated. The resulting residue was recrystallized from hexanes/AcOEt to give **^{10}B-60b** (110.2 mg, 0.515 mmol, 71%) as a colorless solid: isotopic purity of ^{10}B: 98.8 ± 0.1%; mp 208–211 °C; ^{1}H NMR (400 MHz, DMSO-d_6, TMS): δ = 4.70 (s, 2H), 7.33 (t, J = 8.0 Hz, 1H), 7.48 (d, J = 7.6 Hz, 1H), 7.73 (d, J = 7.6 Hz, 1H), 7.84 (s, 1H), 8.12 (s, 2H); ^{13}C NMR (100 MHz, DMSO-d_6, TMS): δ = 34.90, 127.63, 130.81, 133.92, 134.95, 136.79; IR (ATR): ν = 3054, 1693, 1604, 1486, 1434, 1370, 1331, 1222, 1200, 1079, 999, 926, 806, 739, 696, 612, 597, 553, 431 cm^{-1}; HRMS (ESI$^+$): m/z calcd for $[M+Na]^+$, $C_7H_8{}^{10}BBrO_2Na$, 235.9729; found, 235.9739; Anal. Calcd (%) for $C_7H_8{}^{10}BBrO_2 \cdot 0.3AcOEt–3H_2O$: C, 43.39; H, 3.35. found: C, 43.66; H, 3.01.

1-[(3-Boronopheny)methyl]-1,4,7-triazacyclononane Trifluoroacetic Acid Salt (2TFA) (^{10}B-14b)

A mixture of 3-(bromomethyl)phenylboronic acid **^{10}B-60b**[70] (35 mg, 0.164 mmol, 1.1 equiv), 2Boc-tacn **59**[67] (50 mg, 0.152 mmol), and potassium carbonate (25.1 mg, 0.182 mmol, 1.2 equiv) in MeCN (1.5 mL) were refluxed for 16 h. After adding H_2O, the reaction mixture was extracted with $CHCl_3$. The organic layer was washed with brine, dried over Na_2SO_4, and concentrated under reduced pressure. The resulting residue was purified by silica gel column chromatography ($CHCl_3$/MeOH = 50/1) to afford **^{10}B-61b** (62.1 mg) as a colorless amorphous solid.

TFA (1.0 mL) was added to a solution of **^{10}B-61b** in CH_2Cl_2 (1.0 mL), and the mixture was stirred at room temperature for 1 h. After evaporation, the resulting residue was dissolved in MeCN and reprecipitated with Et_2O to afford **^{10}B-14b** (55.6 mg, 0.113 mmol, 74%) as colorless powder: mp 134–136 °C; ^{1}H NMR (400 MHz, D_2O, TSP): δ = 3.03 (t, *J* = 6.0 Hz, 4H), 3.19 (brs, 4H), 3.57 (brs, 4H), 3.95 (s, 2H), 7.51 (t, *J* = 7.6 Hz, 1H), 7.57 (d, *J* = 7.6 Hz, 1H), 7.78–7.80 (m, 2H); ^{13}C NMR (100 MHz, D_2O, 1,4-dioxane): δ = 42.77, 44.17, 48.29, 59.74, 116.92, 129.03, 133.26, 134.00, 135.70, 135.91, 163.61; IR (ATR): *v* = 2808, 1667, 1489, 1439, 1366, 1313, 1180, 1126, 1012, 834, 797, 719, 591, 517, 417 cm^{-1}; HRMS (ESI$^+$): *m*/*z* calcd for $[M+H]^+$, $C_{13}H_{23}{}^{10}BN_3O_2$, 263.1914; found, 263.1922; Anal. Calcd (%) for $C_{13}H_{22}{}^{10}BN_3O_2 \cdot 2TFA$: C, 41.64; H, 4.93; N, 8.57. found: C, 41.94; H, 5.02; N, 8.50.

1-[3-(13,15-Dioxa-15-boradispiro[5.0.5.3]pentadec-14-yl)phenyl]methyl-1,4,7-triazacyclononane (^{10}B-17b)

A mixture of **^{10}B-14b** (24 mg, 0.049 mmol) and bicyclohexyl-1,1′-diol **62**[69] (10.1 mg, 0.043 mmol, 1.0 equiv) in EtOH (0.7 mL) was refluxed for 13 h. After evaporation, the resulting residue was purified by NH silica gel column chromatography ($CHCl_3$/MeOH = 20/1) to afford **^{10}B-17b** (18.7 mg, 0.051 mmol, 90%) as a colorless amorphous solid:

mp 58–59 °C; ^{1}H NMR (400 MHz, $CDCl_3$, TMS): δ = 1.16–1.33 (m, 6H), 1.71–1.84 (m, 14H), 2.63–2.69 (m, 8H), 2.81 (s, 4H), 3.74 (s, 2H), 7.33 (t, *J* = 7.6 Hz 1H), 7.46 (d, *J* = 7.6 Hz 1H), 7.74 (d, *J* = 7.2 Hz 1H), 7.80 (s, 1H); ^{13}C NMR (100 MHz, $CDCl_3$, TMS): δ = 22.33, 25.80, 32.45, 46.51, 46.86, 52.95, 61.54, 84.69, 127.73, 131,66, 133.59, 135.22, 138.86; IR (ATR): *v* = 2930, 2854, 1612, 1449, 1397, 1372, 1284, 1242, 1146, 1132, 1091, 1020, 937, 823, 750, 727, 678, 662,616, 495, 404 cm^{-1}; HRMS (ESI^{+}): *m*/*z* calcd for $[M+H]^{+}$, $C_{25}H_{41}{}^{10}BN_3O_2$, 425.3323; found, 425.3323; Anal. Calcd (%) for $C_{25}H_{40}{}^{10}BN_3O_2 \cdot 0.4CHCl_3 \cdot 1.6MeOH$: C, 61.93; H, 9.01; N, 8.02. found: C, 61.66; H, 8.65; N, 7.65.

1-[(3-Boronopheny)methyl]-1,4,7,10-tetraazacyclododecane Trifluoroacetic Acid Salt (2TFA) (^{10}**B-15b)**[54]

A mixture of 3-(bromomethyl)phenylboronic acid **^{10}B-60b**[70] (25.7 mg, 0.12 mmol, 1.1 equiv), 3Boc-cyclen **63**[72] (51.2 mg, 0.108 mmol), and potassium carbonate (18.5 mg, 0.134 mmol, 1.2 equiv) in MeCN (1.5 mL) was refluxed for 10 h. After adding H_2O, the reaction mixture was extracted with $CHCl_3$. The organic layer was washed with brine, dried over Na_2SO_4, and concentrated under reduced pressure. The resulting residue was purified by silica gel column chromatography ($CHCl_3$/MeOH = 50/1) to afford **^{10}B-64b** (83.2 mg) as a colorless amorphous solid.

TFA (1.0 mL) was added to a solution of **^{10}B-64b** in CH_2Cl_2 (1.0 mL), and the mixture was stirred at room temperature for 1 h. After evaporation, the resulting residue was dissolved in MeCN and reprecipitated with Et_2O to afford **^{10}B-15b** (54.4 mg, 0.102 mmol, 94%) as colorless powder: mp 113–117 °C; ^{1}H NMR (400 MHz, D_2O, TSP): δ = 2.93–3.02 (m, 8H), 3.16–3.23 (m, 8H), 3.89 (s, 2H), 7.51–7.53 (m, 2H), 7.75 (s, 1H), 7.79–7.81 (m, 1H); ^{13}C NMR (100 MHz, D_2O, 1,4-dioxane): δ = 42.33, 42.45, 44.75, 48.37, 57.23, 116.91, 129.22, 132.98, 134.07, 135.47, 135.53, 163.60; IR (ATR): *v* = 3018, 2859, 1668, 1404, 1175, 1123, 1064, 830, 796, 718, 629, 593, 517, 411 cm^{-1}; HRMS (ESI^{+}):

m/*z* calcd for $[M+H]^+$, $C_{15}H_{28}{}^{10}BN_4O_2$, 306.2336; found, 306.2334; Anal. Calcd (%) for $C_{15}H_{27}{}^{10}BN_4O_2 \cdot 2.4TFA$: C, 41.07; H, 5.12; N, 9.68. found: C, 40.84; H, 5.32; N, 9.79.

1-[3-(13,15-Dioxa-15-boradispiro[5.0.5.3]pentadec-14-yl)phenyl]methyl-1,4,7,10-tetraazacyclododecane (^{10}**B-18b)**

A mixture of **^{10}B-15b** (26 mg, 0.049 mmol) and bicyclohexyl-1,1′-diol **62**[69] (10.1 mg, 0.051 mmol, 1.0 equiv) in EtOH (1.0 mL) was refluxed for 8 h. After evaporation, the resulting residue was purified by NH silica gel column chromatography ($CHCl_3$/MeOH = 20/1) to afford **^{10}B-18b** (16.1 mg, 0.034 mmol, 71%) as a colorless amorphous solid: mp 56–58 °C; ^{1}H NMR (400 MHz, $CDCl_3$, TMS): δ = 1.13–1.32 (m, 6H), 1.62–1.80 (m, 14H), 2.56–2.59 (m, 8H), 2.67 (t, *J* = 4.8 Hz, 4H), 2.81 (t, *J* = 4.8 Hz, 4H), 3.65 (s, 2H), 7.32 (t, *J* = 8.0 Hz, 1H), 7.40 (d, *J* = 8.0 Hz, 1H), 7.74 (d, *J* = 7.2 Hz, 1H), 7.77 (s, 1H); ^{13}C NMR (100 MHz, $CDCl_3$, TMS): δ = 22.31, 25.81, 32.44, 45.30, 46.43, 47.37, 51.38, 59.18, 84.57, 127.69, 131.77, 133.77, 135.43, 138.06; IR (ATR): *v* = 2930, 2851, 1579, 1435, 1392, 1371, 1347, 1272, 1243, 1201, 1131, 1076, 1040, 939, 808, 748, 713, 660, 618, 507, 412 cm^{-1}; HRMS (ESI^+): *m*/*z* calcd for $[M+H]^+$, $C_{27}H_{46}{}^{10}BN_4O_2$, 468.3745; found, 468.3741; Anal. Calcd (%) for $C_{27}H_{45}{}^{10}BN_4O_2 \cdot 0.5CHCl_3 \cdot MeOH$: C, 61.19; H, 8.92; N, 10.02. found: C, 61.27; H, 9.08; N, 9.64.

1-[(4-Boronopheny)methyl]-1,4,7,10,13-pentaazacyclopentadecane Trifluoroacetic Acid Salt (3TFA) (^{10}**B-16a)**

A mixture of 4-(bromomethyl)phenylboronic acid **^{10}B-60a**[68] (38.2 mg, 0.178 mmol, 1.2 equiv), **65**[73] (92.1 mg, 0.150 mmol), and potassium carbonate (25.5 mg,0.184 mmol, 1.2 equiv) in MeCN (1.5 mL) was refluxed for 11 h. After adding H_2O, the reaction mixture was extracted with $CHCl_3$. The organic layer was washed with brine, dried over Na_2SO_4 and concentrated under reduced pressure. The resulting residue was purified by silica gel column chromatography ($CHCl_3$/MeOH = 50/1) to afford **^{10}B-66a** (112.2 mg) as a

colorless amorphous solid.

TFA (1.5 mL) was added to a solution of **^{10}B-66a** in CH_2Cl_2 (1.5 mL), and the mixture was stirred at room temperature for 1 h. After evaporation, the resulting residue was dissolved in MeCN and reprecipitated with Et_2O to afford **^{10}B-16a** (79.1 mg, 0.115 mmol, 77%) as colorless powder: mp 136–140 °C; ^{1}H NMR (400 MHz, D_2O, TSP): δ = 2.99 (t, *J* = 5.2 Hz,4H), 3.16 (s, 4H), 3.24–3.33 (m, 12H), 3.95 (s, 2H), 7.45 (d, *J* = 8.0 Hz, 2H), 7.84 (d, *J* = 7.6 Hz, 2H); ^{13}C NMR (100 MHz, D_2O, 1,4-dioxane): δ = 44.29, 45.29, 45.78, 50.21, 56.67, 116.90, 130.55, 134.65, 137.01, 163.59; IR (ATR): *v* = 3045, 2852, 1671, 1610, 1421, 1391, 1200, 1177, 1126, 1060, 1016, 836, 799, 735, 720, 699, 666, 518, 503, 413 cm^{-1}; HRMS (ESI$^+$): *m*/*z* calcd for $[M+H]^+$, $C_{17}H_{33}{}^{10}BN_5O_2$, 349.2758 ; found, 349.2754; Anal. Calcd (%) for $C_{17}H_{32}{}^{10}BN_5O_2 \cdot 3TFA$: C, 40.00; H, 5.11; N, 10.14. found: C, 40.13; H, 5.03; N, 10.07.

1-[4-(13,15-Dioxa-15-boradispiro[5.0.5.3]pentadec-14-yl)phenyl]methyl-1,4,7,10,13-pentaazacyclopentadecane (^{10}B-19a)

A mixture of **^{10}B-16a** (32.5 mg, 0.047 mmol) and bicyclohexyl-1,1′-diol **62**[69] (9.7 mg, 0.049 mmol, 1.0 equiv) in EtOH (0.7 mL) was refluxed for 7 h. After evaporation, the resulting residue was purified by NH silica gel column chromatography ($CHCl_3$/MeOH = 20/1) to afford **^{10}B-19a** (20.9 mg, 0.041 mmol, 87%) as a colorless amorphous solid: mp 47–49 °C; ^{1}H NMR (400 MHz, $CDCl_3$, TMS): δ = 1.16–1.32 (m, 6H), 1.62–1.83 (m, 14H), 2.64 (s, 12H), 2.78 (s, 8H), 3.61 (s, 2H), 7.33 (d, *J* = 7.6 Hz, 2H), 7.80 (d, *J* = 8.0 Hz, 2H); ^{13}C NMR (100 MHz, $CDCl_3$, TMS): δ = 22.29, 25.80, 32.45, 47.34, 47.91, 48.41, 49.14, 54.66, 59.54, 84.61, 128.30, 134.90, 142.52; IR (ATR): *v* = 2929, 2849, 1612, 1517, 1448, 1396, 1373, 1243, 1131, 1091, 1040, 1020, 937, 823, 747, 730, 677, 661, 507 cm^{-1}; HRMS (ESI$^+$): *m*/*z* calcd for $[M+H]^+$, $C_{29}H_{51}{}^{10}BN_5O_2$, 511.4167; found, 511.4166; Anal. Calcd (%) for $C_{29}H_{50}{}^{10}BN_5O_2 \cdot 0.3CHCl_3 \cdot 2MeOH$: C, 61.56; H, 9.62; N, 11.47. found: C, 61.77; H, 9.25; N, 11.15.

General procedure A

An aqueous 48% solution of HBr (1.0 mL) was added to a solution of Boc-protected macrocyclic polyamine dimers in EtOH (4.0 mL), and the reaction mixture was stirred overnight at room temperature. The resulting colorless solids were isolated on a filter, washed with Et_2O and dried *in vacuo*.

General procedure B

A solution of boron-containing macrocyclic polyamine dimers in MeOH/H_2O (2/1) was passed through an anion exchange resin column (Amberlite IRA-400) to produce the acid-free forms, and the solvent was evaporated under reduced pressure. The mixture of intermediates and bicyclohexyl-1,1′-diol **62**[69] (1.0 equiv) in EtOH was refluxed for 2 h. After evaporation, the resulting residue was purified by column chromatography using Fuji Silysia Chromatorex NH-DM1020 Silica Gel ($CHCl_3$/MeOH = 100/1 to 20/1).

3,5-Dimethylphenylboronic acid pinacol ester (81)

Pinacol (1650 mg, 13.96 mmol, 1.0 equiv) was added to a solution of 3,5-Dimethylphenylboronic acid **80** (2021 mg, 13.48 mmol) in toluene (60 mL), and the reaction mixture was refluxed for 2 h. After evaporation, the residue was recrystallized from MeOH to afford **81** (3022 mg, 13.02 mmol, 97%) as colorless crystals; the ^1H and ^{13}C NMR spectra of the product were identical to previously reported data.[85]

3,5-Bis(bromomethyl)phenylboronic acid pinacol ester (82)

A mixture of **81** (3000 mg, 12.92 mmol), *N*-bromosuccinimide (NBS) (4600 mg, 25.85 mmol, 2.0 equiv) and benzoyl peroxide (BPO) (150 mg, 0.619 mmol, 0.05 equiv) in CCl_4 (70 mL) was refluxed for 9 h. After adding hexanes, the resulting precipitate was

removed by filtration, and the solvent was evaporated under reduced pressure. The residue was purified by silica gel column chromatography (hexanes/CH_2Cl_2 = 8/1 to 1/2) to afford **82** as a colorless syrup, which was further purified by recrystallization from $CHCl_3$/MeOH at 0 °C to –78 °C to give **82** (1572 mg, 4.03 mmol, 31%) as a colorless needle crystal: mp 76–77 °C; ^{1}H NMR (400 MHz, $CDCl_3$, TMS): δ = 1.35 (s, 12H), 4.48 (s, 4H), 7.53 (t, *J* = 1.6 Hz, 1H), 7.75 (d, *J* = 1.6 Hz, 2H); ^{13}C NMR (100 MHz, $CDCl_3$, TMS): δ = 24.88, 32.78, 84.18, 132.51, 135.26, 137.86; ^{11}B NMR (128 MHz, $CDCl_3$, BF_3·OEt_2): δ = 30.6 (brs); IR (ATR): *v* = 2977, 1605, 1470, 1427, 1370, 1328, 1274, 1244, 1215, 1167, 1138, 1109, 965, 898, 845, 705, 665, 601, 577, 552 cm^{-1}; HRMS (ESI$^+$): *m*/*z* calcd for $[M+NH_4]^+$, $C_{14}H_{23}{}^{10}B^{79}Br_2NO_2$, 405.0219; found, 405.0239; Anal. Calcd (%) for $C_{14}H_{19}BBr_2O_2$: C, 43.13; H, 4.91. found: C, 43.14; H, 4.81.

1-[(3-(Bromomethyl)-5-(4,4,5,5-tetramethyl-1,3,2-dioxaborolan-2-yl)phenyl)methyl]-4,7,10-tris(*tert*-butoxycarbonyl)-1,4,7,10-tetraazacyclododecane (83)

To a solution of 3,5-Bis(bromomethyl)phenylboronic acid pinacol ester **82** (1050 mg, 2.69 mmol, 1.5 equiv) in MeCN (18 mL), 3Boc-cyclen **63**[72] (848 mg, 1.79 mmol) and potassium carbonate (302 mg, 2.19 mmol, 1.2 equiv) were added, and the mixture was stirred at room temperature for 24 h. After adding H_2O, the reaction mixture was extracted with $CHCl_3$. The organic layer was washed with brine, dried over Na_2SO_4 and concentrated under reduced pressure. The resulting residue was purified by silica gel column chromatography (hexanes/AcOEt = 10/1 to 3/1) to afford **83** (940 mg, 1.20 mmol, 67%) as a colorless amorphous solid: mp 81–83 °C; ^{1}H NMR (400 MHz, $CDCl_3$, TMS): δ = 1.34 (s, 12H), 1.43–1.47 (m, 27H), 2.66 (br, 4H), 3.14–3.48 (m, 8H), 3.62 (s, 4H), 3.72 (s, 2H), 4.46 (s, 2H), 7.42 (s, 1H), 7.62 (s, 1H), 7.71 (s, 1H); ^{13}C NMR (100 MHz, $CDCl_3$, TMS): δ = 24.87, 28.50, 28.69, 33.23, 47.63, 47.87, 48.40, 50.07, 55.70, 56.51, 58.08, 79.19, 79.41, 83.97, 129.53, 133.97, 134.26, 136.70, 137.34, 155.30, 155.75,

156.21; ^{11}B NMR (128 MHz, $CDCl_3$, $BF_3 \cdot OEt_2$): δ = 31.0 (brs); IR (ATR): *v* = 2975, 1682, 1457, 1412, 1363, 1323, 1245, 1144, 1107, 969, 850, 771, 712, 558, 510 cm^{-1}; HRMS (ESI^+): *m*/*z* calcd for $[M+H]^+$, $C_{37}H_{63}{}^{10}BBrN_4O_8$, 780.3953; found, 780.3953; Anal. Calcd (%) for $C_{37}H_{62}BBrN_4O_8$: C, 56.86; H, 8.00; N, 7.17. found: C, 56.88; H, 8.23; N, 6.96.

1-[(3-(Bromomethyl)-5-(4,4,5,5-tetramethyl-1,3,2-dioxaborolan-2-yl)phenyl)methyl]-4,7,10,13-tetrakis(*tert*-butoxycarbonyl)-1,4,7,10,13-pentaazacyclopentadecane (84)

To a solution of 3,5-Bis(bromomethyl)phenylboronic acid pinacol ester **82** (614 mg, 1.58 mmol, 1.5 equiv) in MeCN (10 mL), **65**[73] (632 mg, 1.03 mmol) and potassium carbonate (171 mg, 1.24 mmol, 1.2 equiv) were added, and the reaction mixture was stirred at room temperature for 24 h. After adding H_2O, the reaction mixture was extracted with $CHCl_3$. The organic layer was washed with brine, dried over Na_2SO_4 and concentrated under reduced pressure. The resulting residue was purified by silica gel column chromatography (hexanes/AcOEt = 10/1 to 3/1) to give **84** (677 mg, 0.733 mmol, 71%) as a colorless amorphous solid: mp 69–71 °C; ^{1}H NMR (400 MHz, $CDCl_3$, TMS): δ = 1.24 (s, 9H), 1.35 (s, 12H), 1.43–1.47 (m, 27H), 2.64 (br, 4H), 3.40 (br, 16H), 3.60 (s, 2H), 4.50 (s, 2H), 7.47 (s, 1H), 7.59 (s, 1H), 7.68 (s, 1H); ^{13}C NMR (100 MHz, $CDCl_3$, TMS): δ = 24.89, 28.44, 33.60, 46.82 (br), 53.20 (br), 59.27, 79.59, 80.03, 83.96, 129.53, 132.39, 134.17, 135.09, 137.29, 139.34, 155.25; ^{11}B NMR (128 MHz, $CDCl_3$, $BF_3 \cdot OEt_2$): δ = 30.1 (brs); IR (ATR): *v* = 2976, 1689, 1464, 1411, 1365, 1320, 1240, 1144, 967, 950, 892, 850, 772, 711, 560, 501, 458 cm^{-1}; HRMS (ESI^+): *m*/*z* calcd for $[M+H]^+$, $C_{44}H_{76}{}^{10}BBrN_5O_{10}$, 923.4899; found, 923.4897; Anal. Calcd (%) for $C_{44}H_{75}BBrN_5O_{10}$: C, 57.14; H, 8.17; N, 7.57. found: C, 57.26; H, 8.53; N, 7.29.

1-[(3-(1,4,7-Triazacyclononan-1-ylmethyl)-5-boronophenyl)methyl]-1,4,7,10-tetraazacyclododecane heptahydrobromic acid salt (7HBr) (23)

A mixture of **83** (515 mg, 0.659 mmol), 2Boc-tacn **59**[67] (254 mg, 0.771 mmol, 1.2 equiv) and potassium carbonate (111 mg, 0.802 mmol, 1.2 equiv) in MeCN (6.0 mL) was refluxed for 6 h. After adding H_2O, the reaction mixture was extracted with $CHCl_3$. The organic layer was washed with brine, dried over Na_2SO_4 and concentrated under reduced pressure. The resulting residue was purified by silica gel column chromatography (hexanes/AcOEt = 4/1 to 2/1) to afford **85** (439 mg, 0.426 mmol, 65%) as a colorless amorphous solid.

Using general procedure A, compound **85** (335 mg, 0.325 mmol) gave **23** (306 mg, 0.301 mmol, 93%) as colorless powder, which was determined to be the 7HBr salt by elemental analysis: mp 213–215 °C; ^{1}H NMR (400 MHz, D_2O, TSP): δ = 2.99 (t, *J* = 4.8 Hz, 4H), 3.06 (t, *J* = 5.6 Hz, 8H) 3.21 (t, *J* = 5.2 Hz, 4H) 3.27 (t, *J* = 4.8 Hz, 8H), 3.66 (s, 4H), 3.99 (s, 2H), 4.00 (s, 2H), 7.56 (s, 1H), 7.75 (s, 1H), 7.79 (s, 1H); ^{13}C NMR (100 MHz, D_2O, 1,4-dioxane): δ = 42.54, 42.66, 44.16, 44.82, 47.92, 48.42, 57.22, 59.06, 134.84, 135.08, 135.54, 135.94, 136.03; ^{11}B NMR (128 MHz, D_2O, $BF_3{\cdot}OEt_2$): δ = 29.5 (brs); IR (ATR): *v* = 3390, 2934, 2612, 1567, 1489, 1441, 1375, 1251, 1186, 1138, 1041, 1005, 947, 912, 880, 757, 713, 678, 583, 560, 487, 439 cm^{-1}; HRMS (ESI$^+$): *m*/*z* calcd for $[M+2H]^{2+}$, $C_{22}H_{44}{}^{10}BN_7O_2$, 224.1837; found, 224.1837; Anal. Calcd (%) for $C_{22}H_{42}BN_7O_2{\cdot}7HBr{\cdot}0.2EtOH$: C, 26.30; H, 4.95; N, 9.58. found: C, 26.30; H, 5.33; N, 9.35.

1-[(3-(1,4,7-Triazacyclononan-1-ylmethyl)-5-boronophenyl)methyl]-1,4,7,10,13-pentaazacyclopentadecane octahydrobromic acid salt (8HBr) (26)

A mixture of **84** (677 mg, 0.733 mmol), 2Boc-tacn **59**[67] (270 mg, 0.820 mmol, 1.1 equiv) and potassium carbonate (123 mg, 0.886 mmol, 1.2 equiv) in MeCN (7.0 mL) was refluxed for 21 h. After adding H_2O, the reaction mixture was extracted with $CHCl_3$. The organic layer was washed with brine, dried over Na_2SO_4 and concentrated under reduced pressure. The resulting residue was purified by silica gel column

chromatography (hexanes/AcOEt = 4/1 to 2/1) to afford **87** (551 mg, 0.469 mmol, 64%) as a colorless amorphous solid.

Using general procedure A, compound **87** (234 mg, 0.199 mmol) gave **26** (198 mg, 0.174 mmol, 87%) as colorless powder, which was determined to be the 8HBr salt by elemental analysis: mp 229–231 °C; ^{1}H NMR (400 MHz, D_2O, TSP): δ = 3.05–3.09 (m, 8H), 3.24 (s, 4H), 3.27–3.47 (m, 16H), 3.67 (s, 4H), 4.00 (s, 2H), 4.07 (s, 2H), 7.59 (s, 1H), 7.76 (s, 1H), 7.81 (s, 1H); ^{13}C NMR (100 MHz, D_2O, 1,4-dioxane): δ = 42.68, 44.21, 44.25, 45.11, 45.61, 47.93, 50.00, 56.63, 58.97, 133.56, 135.40, 135.93, 136.10, 136.20; ^{11}B NMR (128 MHz, D_2O, $BF_3{\cdot}OEt_2$): δ = 28.6 (brs); IR (ATR): *ν* = 3362, 2971, 2640, 1571, 1435, 1343, 1245, 1146, 1040, 878, 758, 716, 427 cm^{-1}; HRMS (ESI^{+}): *m*/*z* calcd for $[M+2H]^{2+}$, $C_{24}H_{49}{}^{10}BN_8O_2$, 245.7048; found, 245.7048; Anal. Calcd (%) for $C_{24}H_{47}BN_8O_2{\cdot}8HBr{\cdot}EtOH$: C, 26.38; H, 5.19; N, 9.47. found: C, 26.17; H. 5.41; N, 9.21.

1-[(3-(1,4,7,10-Tetraazacyclododecan-1-ylmethyl)-5-boronophenyl)methyl]-1,4,7,10,13-pentaazacyclopentadecane nonahydrobromic acid salt (9HBr) (25)

A mixture of **83** (236 mg, 0.301 mmol), **65**[73] (210 mg, 0.341 mmol, 1.1 equiv) and potassium carbonate (50 mg, 0.362 mmol, 1.2 equiv) in MeCN (3.0 mL) was refluxed for 16 h. After adding H_2O, the reaction mixture was extracted with $CHCl_3$. The organic layer was washed with brine, dried over Na_2SO_4 and concentrated under reduced pressure. The resulting residue was purified by silica gel column chromatography (hexanes/AcOEt = 4/1 to 2/1) to afford **86** (300 mg, 0.228 mmol, 76%) as a colorless amorphous solid.

Using general procedure A, compound **86** (257 mg, 0.195 mmol) gave **25** (222 mg, 0.176 mmol, 90%) as colorless powder, which was determined to be the 9HBr salt by elemental analysis: mp 224–226 °C; ^{1}H NMR (400 MHz, D_2O, TSP): δ = 2.95–3.21 (m, 16H), 3.26 (s, 8H), 3.37–3.47 (m, 12H), 3.98 (s, 2H), 4.09 (s, 2H), 7.56 (s, 1H), 7.77 (s, 1H), 7.78 (s, 1H); ^{13}C NMR (100 MHz, D_2O, 1,4-dioxane): δ = 42.48, 42.64, 44.15, 44.85, 44.93, 45.37, 48.35, 49.94, 56.91, 57.07, 133.50, 135.20, 135.49, 136.00, 136.33; ^{11}B

NMR (128 MHz, D_2O, $BF_3{\cdot}OEt_2$): δ = 29.2 (brs); IR (ATR): *v* = 3362, 2929, 2638, 1568, 1435, 1343, 1246, 1035, 754, 717, 442, 426, 414 cm^{-1}; HRMS (ESI^+): *m*/*z* calcd for $[M+2H]^{2+}$, $C_{26}H_{54}{}^{10}BN_9O_2$, 267.2259; found, 267.2259; Anal. Calcd (%) for $C_{26}H_{52}BN_9O_2{\cdot}9HBr{\cdot}0.3EtOH$: C, 25.05; H, 4.96; N, 9.88. found: C, 25.23; H. 5.32; N, 9.70.

1-[(3-(1,4,7-Triazacyclononan-1-ylmethyl)-5-(13,15-dioxa-15-boradispiro[5.0.5.3]pentadec-14-yl)phenyl)methyl]-1,4,7,10-tetraazacyclododecane (28)

Using general procedure B, compound **23** (110 mg, 0.109 mmol) gave **28** (49 mg, 0.0808 mmol, 74%) as a colorless amorphous solid: mp 65–67 °C; ^1H NMR (400 MHz, $CDCl_3$, TMS): δ =1.16–1.33 (m, 6H), 1.62–1.81 (m, 14H), 2.56–2.80 (m, 28H), 3.63 (s, 2H), 3.72 (s, 2H), 7.44 (s, 1H), 7.65 (s, 2H); ^{13}C NMR (100 MHz, $CDCl_3$, TMS): δ = 22.33, 25.80, 32.44, 45.06, 46.34, 46.57, 47.15, 51.30, 52.67, 59.01, 61.52, 84.68, 132.38, 134.34, 138.40, 138.96; ^{11}B NMR (128 MHz, $CDCl_3$, $BF_3{\cdot}OEt_2$): δ = 30.2 (brs); IR (ATR): *v* = 3296, 2927, 2849, 1602, 1449, 1354, 1272, 1231, 1146, 1130, 1115, 1041, 960, 940, 910, 875, 832, 746, 712, 505 cm^{-1}; HRMS (ESI^+): *m*/*z* calcd for $[M+2H]^{2+}$, $C_{34}H_{62}{}^{10}BN_7O_2$, 305.2542; found, 305.2542; Anal. Calcd (%) for $C_{34}H_{60}BN_7O_2{\cdot}0.2MeOH{\cdot}0.4CHCl_3$: C, 62.60; H, 9.29; N,14.77. found: C, 62.65; H, 9.29; N,14.49.

1-[(3-(1,4,7-Triazacyclononan-1-ylmethyl)-5-(13,15-dioxa-15-boradispiro[5.0.5.3]pentadec-14-yl)phenyl)methyl]-1,4,7,10,13-pentaazacyclopentadecane (31)

Using general procedure B, compound **26** (120 mg, 0.106 mmol) gave **31** (58 mg, 0.0891 mmol, 84%) as a colorless amorphous solid: mp 69–71 °C; ^1H NMR (400 MHz, $CDCl_3$, TMS): δ = 1.17–1.33 (m, 6H), 1.64–1.81 (m, 14H), 2.65 (br, 20H), 2.71–2.77 (m,

8H), 2.80 (s, 4H), 3.58 (s, 2H), 3.73 (s, 2H), 7.39 (s, 1H), 7.57 (s, 1H), 7.72 (s, 1H); ^{13}C NMR (100 MHz, $CDCl_3$, TMS): δ = 22.34, 25.77, 32.47, 46.63, 47.02, 47.26, 47.86, 48.41, 49.02, 53.23, 54.55, 59.40, 61.71, 84.76, 132.73, 134.36, 134.47, 138.68, 139.06; ^{11}B NMR (128 MHz, $CDCl_3$, $BF_3 \cdot OEt_2$): δ = 31.0 (brs); IR (ATR): *v* = 3293, 2927, 2812, 1602, 1449, 1354, 1271, 1231, 1130, 1062, 960, 940, 910, 874, 832, 746, 713, 657, 542, 507 cm^{-1}; HRMS (ESI$^+$): *m*/*z* calcd for $[M+H]^+$, $C_{36}H_{66}{}^{10}BN_8O_2$, 652.5433; found, 652.5434; Anal. Calcd (%) for $C_{36}H_{65}BN_8O_2 \cdot MeOH \cdot 0.5CHCl_3$: C, 60.50; H, 9.41; N,15.05. found: C, 60.46; H, 9.35; N,14.85.

1-[(3-(1,4,7,10-Tetraazacyclododecan-1-ylmethyl)-5-(13,15-dioxa-15-boradispiro[5.0.5.3]pentadec-14-yl)phenyl)methyl]-1,4,7,10,13-pentaazacyclopentadecane (30)

Using general procedure B, compound **25** (150 mg, 0.119 mmol) gave **30** (64 mg, 0.0917 mmol, 77%) as a colorless amorphous solid: mp 44–46 °C; ^{1}H NMR (400 MHz, $CDCl_3$, TMS): δ = 1.17–1.32 (m, 6H), 1.64–1.79 (m, 14H), 2.54–2.59 (m, 8H), 2.64 (br, 16H), 2.71 (s, 4H), 2.74–2.79 (m, 8H), 3.58 (s, 2H), 3.61 (s, 2H), 7.32 (s, 1H), 7.57 (s, 1H), 7.70 (s, 1H); ^{13}C NMR (100 MHz, $CDCl_3$, TMS): δ = 22.31, 25.78, 32.45, 45.18, 46.33, 47.23, 47.85, 48.39, 49.01, 51.44, 54.34, 59.15, 59.34, 84.66, 133.00, 134.60, 134.72, 138.28, 138.38; ^{11}B NMR (128 MHz, $CDCl_3$, $BF_3 \cdot OEt_2$): δ = 31.3 (brs); IR (ATR): *v* = 3290, 2929, 2810, 1602, 1449, 1353, 1271, 1231, 1130, 1040, 959, 941, 910, 876, 833, 745, 712, 657, 542, 507 cm^{-1}; HRMS (ESI$^+$): *m*/*z* calcd for $[M+H]^+$, $C_{38}H_{71}{}^{10}BN_9O_2$, 695.5855; found, 695.5855; Anal. Calcd (%) for $C_{38}H_{70}BN_9O_2 \cdot MeOH \cdot 0.6CHCl_3$: C, 59.49; H, 9.41; N,15.77. found: C, 59.34; H, 9.46; N, 15.74.

1-[(3-(4,7,10-Tris(*tert*-butoxycarbonyl)-1,4,7,10-tetraazacyclododecan-1-ylmethyl)-5-(4,4,5,5-tetramethyl-1,3,2-dioxaborolan-2-yl)phenyl)methyl]-4,7,10-

tris(*tert*-butoxycarbonyl)-1,4,7,10-tetraazacyclododecane (88)

A mixture of 3,5-Bis(bromomethyl)phenylboronic acid pinacol ester **82** (107 mg, 0.275 mmol), 3Boc-cyclen **63**[72] (260 mg, 0.551 mmol, 2.0 equiv) and potassium carbonate (96 mg, 0.691 mmol, 2.5 equiv) in MeCN (2.5 mL) was refluxed for 8 h. After adding H_2O, the reaction mixture was extracted with $CHCl_3$. The organic layer was washed with brine, dried over Na_2SO_4 and concentrated under reduced pressure. The resulting residue was purified by silica gel column chromatography (hexanes/AcOEt = 4/1 to 1/1) to afford **88** (217 mg, 0.185 mmol, 67%) as a colorless amorphous solid: mp 105–107 °C; ^{1}H NMR (400 MHz, $CDCl_3$, TMS): δ = 1.32 (s, 12H), 1.42–1.48 (m, 54H), 2.64–2.68 (m, 8H), 3.17–3.42 (m, 16H), 3.62 (s, 8H), 3.73 (s, 4H), 7.15 (s, 1H), 7.62 (s, 2H); ^{13}C NMR (100 MHz, $CDCl_3$, TMS): δ = 24.89, 28.54, 28.74, 47.49, 47.78, 48.17, 48.59, 50.01, 54.90, 55.94, 57.33, 79.21, 79.44, 83.83, 128.94, 135.32, 135.92, 155.33, 155.73, 156.15; ^{11}B NMR (128 MHz, $CDCl_3$, $BF_3{\cdot}OEt_2$): δ = 31.1 (brs); IR (ATR): ν = 2975, 1684, 1458, 1412, 1390, 1363, 1316, 1246, 1146, 978, 887, 852, 770, 751, 718, 555, 514 cm^{-1}; HRMS (ESI$^+$): *m*/*z* calcd for $[M+2H]^{2+}$, $C_{60}H_{107}{}^{10}BN_8O_{14}$, 586.9013; found, 586.9012; Anal. Calcd (%) for $C_{60}H_{105}BN_8O_{14}{\cdot}1.5H_2O$: C, 60.04; H, 9.07; N, 9.34. found: C, 59.99; H, 8.85; N, 9.10.

1-[(3-(4,7,10,13-Tetrakis(*tert*-butoxycarbonyl)-1,4,7,10,13-pentaazacyclopentadecan-1-ylmethyl)-5-(4,4,5,5-tetramethyl-1,3,2-dioxaborolan-2-yl)phenyl)methyl]-4,7,10,13-tetrakis(*tert*-butoxycarbonyl)-1,4,7,10,13-pentaazacyclopentadecane (89)

A mixture of 3,5-Bis(bromomethyl)phenylboronic acid pinacol ester **82** (76 mg, 0.196 mmol), **65**[73] (240 mg, 0.39 mmol, 2.0 equiv) and potassium carbonate (68 mg, 0.492 mmol, 2.5 equiv) in MeCN (2.0 mL) was refluxed for 16 h. After adding H_2O, the reaction mixture was extracted with $CHCl_3$. The organic layer was washed with brine, dried over Na_2SO_4 and concentrated under reduced pressure. The resulting residue was

purified by silica gel column chromatography (hexanes/AcOEt = 3/1 to 1/1) to afford **89** (211 mg, 0.145 mmol, 74 %) as a colorless amorphous solid: mp 89–91 °C; ^{1}H NMR (400 MHz, $CDCl_3$, TMS): δ = 1.28–1.47 (m, 84H), 2.63 (br, 8H), 3.39 (br, 32H), 3.59 (s, 4H), 7.28 (s, 1H), 7.57 (s, 2H); ^{13}C NMR (100 MHz, $CDCl_3$, TMS): δ = 24.91, 28.40, 46.74 (br), 52.85 (br), 59.45, 79.44, 79.90, 83.66, 128.78, 132.65, 134.12, 138.14, 155.14; ^{11}B NMR (128 MHz, $CDCl_3$, $BF_3{\cdot}OEt_2$): δ = 31.9 (brs); IR (ATR): *v* = 2975, 1690, 1463, 1410, 1390, 1364, 1303, 1239, 1156, 1044, 949, 894, 852, 771, 714, 554, 461 cm^{-1}; HRMS (ESI^{+}): *m*/*z* calcd for $[M+H]^{+}$, $C_{74}H_{132}{}^{10}BN_{10}O_{18}$, 1458.9845; found, 1458.9843

1-[(3-(1,4,7,10-Tetraazacyclododecan-1-ylmethyl)-5-boronophenyl)methyl]-1,4,7,10-tetraazacyclododecane heptahydrobromic acid salt (7HBr) (24)

Using general procedure A, compound **88** (165 mg, 0.141 mmol) gave **24** (119 mg, 0.104 mmol, 74%) as colorless powder, which was determined to be the 7HBr salt by elemental analysis: mp 241–243 °C; ^{1}H NMR (400 MHz, D_2O, TSP): δ = 2.97 (t, *J* = 4.8 Hz, 8H), 3.07 (br, 8H), 3.23 (t, *J* = 4.8 Hz, 8H), 3.31 (br, 8H), 3.99 (s, 4H), 7.49 (s, 1H), 7.80 (s, 2H); ^{13}C NMR (100 MHz, D_2O, 1,4-dioxane): δ = 42.42, 42.59, 44.88, 48.26, 56.99, 135.07, 135.39, 135.47; ^{11}B NMR (128 MHz, D_2O, $BF_3{\cdot}OEt_2$): δ = 30.3 (brs); IR (ATR): *v* = 3374, 2949, 2644, 1602, 1434, 1344, 1242, 1065, 1002, 967, 849, 757, 717, 439 cm^{-1}; HRMS (ESI^{+}): *m*/*z* calcd for $[M+2H]^{2+}$, $C_{24}H_{49}{}^{10}BN_8O_2$, 245.7048; found, 245.7049; Anal. Calcd (%) for $C_{24}H_{47}BN_8O_2{\cdot}7HBr{\cdot}0.5EtOH$: C, 27.81; H, 5.32; N, 10.38. found: C, 27.86; H, 5.68; N, 10.11.

1-[(3-(1,4,7,10,13-Pentaazacyclopentadecan-1-ylmethyl)-5-boronophenyl)methyl]-1,4,7,10,13-pentaazacyclopentadecane decahydrobromic acid salt (10HBr) (27)

Using general procedure A, compound **89** (150 mg, 0.103 mmol) gave **27** (115 mg, 0.083 mmol, 81%) as colorless powder, which was determined to be the 10HBr salt by elemental analysis: mp 240–242 °C; ^{1}H NMR (400 MHz, D_2O, TSP): δ = 3.11 (t, *J* = 5.6

Hz, 8H), 3.27 (s, 8H), 3.37–3.48 (m, 24H), 4.09 (s, 4H), 7.63 (s, 1H), 7.78 (s, 2H); ^{13}C NMR (100 MHz, D_2O, 1,4-dioxane): δ = 44.24, 45.12, 45.55, 45.59, 50.00, 56.66, 133.73, 135.89, 136.55; ^{11}B NMR (128 MHz, D_2O, $BF_3 \cdot OEt_2$): δ = 30.2 (brs); IR (ATR): ν = 3360, 2957, 2650, 1574, 1435, 1342, 1238, 1064, 941, 750, 720, 500 cm^{-1}; HRMS (ESI$^+$): *m*/*z* calcd for $[M+2H]^{2+}$, $C_{28}H_{59}{}^{10}BN_{10}O_2$, 288.7470; found, 288.7470; Anal. Calcd (%) for $C_{28}H_{57}BN_{10}O_2 \cdot 10HBr \cdot EtOH$: C, 25.17; H, 5.14; N, 9.78. found: C, 25.38; H. 5.48; N, 10.06.

1-[(3-(1,4,7,10-Tetraazacyclododecan-1-ylmethyl)-5-(13,15-dioxa-15-boradispiro[5.0.5.3]pentadec-14-yl)phenyl)methyl]-1,4,7,10-tetraazacyclododecane (29)

Using general procedure B, compound **24** (110 mg, 0.0969 mmol) gave **29** (32 mg, 0.0489 mmol, 50%) as a colorless amorphous solid: mp 83–85 °C; ^{1}H NMR (400 MHz, $CDCl_3$, TMS): δ = 1.16–1.32 (m, 6H), 1.65–1.79 (m, 14H), 2.52–2.57 (m, 16H), 2.65 (br, 8H), 2.79 (br, 8H), 3.60 (s, 4H), 7.38 (s, 1H), 7.64 (s, 2H); ^{13}C NMR (100 MHz, $CDCl_3$, TMS): δ = 22.33, 25.82, 32.45, 45.12, 46.52, 47.24, 51.26, 58.97, 84.59, 132.90, 134.83, 138.36; ^{11}B NMR (128 MHz, $CDCl_3$, $BF_3 \cdot OEt_2$): δ = 30.9 (brs); IR (ATR): ν = 3286, 2929, 2811, 1602, 1460, 1353, 1272, 1231, 1146, 1130, 1114, 1041, 940, 910, 832, 746, 712, 658, 543, 505, 420 cm^{-1}; HRMS (ESI$^+$): *m*/*z* calcd for $[M+H]^+$, $C_{36}H_{66}{}^{10}BN_8O_2$, 652.5433; found, 652.5432; Anal. Calcd (%) for $C_{36}H_{65}BN_8O_2 \cdot MeOH \cdot 0.5CHCl_3$: C, 60.50; H, 9.41; N, 15.05. found: C, 60.39; H, 9.54; N, 14.97.

1-[(3-(1,4,7,10,13-Pentaazacyclopentadecan-1-ylmethyl)-5-(13,15-dioxa-15-boradispiro[5.0.5.3]pentadec-14-yl)phenyl)methyl]-1,4,7,10,13-pentaazacyclopentadecane (32)

Using general procedure B, compound **27** (90 mg, 0.0651 mmol) gave **32** (37 mg, 0.0496 mmol, 76%) as a colorless amorphous solid: mp 98–100 °C; ^{1}H NMR (400 MHz,

$CDCl_3$, TMS): δ = 1.21–1.34 (m, 6H), 1.64–1.80 (m, 14H), 2.61–2.65 (m, 20H), 2.71 (s, 8H), 2.73–2.78 (m, 12H), 3.59 (s, 4H), 7.35 (s, 1H), 7.60 (s, 2H); ^{13}C NMR (100 MHz, $CDCl_3$, TMS): δ = 22.33, 25.75, 32.48, 47.28, 47.83, 48.38, 49.03, 54.51, 59.57, 84.80, 133.04, 134.60, 138.57; ^{11}B NMR (128 MHz, $CDCl_3$, $BF_3{\cdot}OEt_2$): δ = 31.6 (brs); IR (ATR): *v* = 3284 2930, 2885, 2813, 1449, 1369, 1340, 1285, 1270, 1233, 1129, 1040, 941, 874, 831, 756, 713 cm^{-1}; HRMS (ESI$^+$): *m*/*z* calcd for $[M+H]^+$, $C_{40}H_{76}{}^{10}BN_{10}O_2$, 738.6277; found, 738.6277; Anal. Calcd (%) for $C_{40}H_{75}BN_{10}O_2{\cdot}0.2CHCl_3$: C, 63.30; H, 9.94; N, 18.36. found: C, 63.55; H, 9.95; N, 18.07.

Synthesis of ^{10}B-enriched compounds

3,5-Dimethylphenylboronic acid pinacol ester (^{10}B-81)[85,88]

To a solution of 5-bromo-*m*-xylene **90** (2724 mg, 14.72 mmol) in THF (40 mL), 1.6 N of *n*-butyllithium in hexanes (10 mL, 16.0 mmol, 1.1 equiv) was added at –78 °C and the reaction mixture was stirred at the same temperature for 1 h, after which, a solution of ^{10}B-enriched trimethyl borate (>99.5% of ^{10}B) (2000 μL, 18.04 mmol, 1.2 equiv) in THF (30 mL) was slowly added. After allowing the stirred solution to warm from –78 °C to room temperature overnight, 2N aqueous HCl was added to the reaction mixture, which was then stirred for a further 2 h. After extraction with $CHCl_3$, the organic layer was washed with brine, dried over Na_2SO_4 and concentrated under reduced pressure. The resulting residue (2.1 g) was dissolved in toluene (60 mL) and treated with pinacol (1740 mg, 14.72 mmol, 1.0 equiv) at reflux for 2 h. After evaporation, the resulting residue was recrystallized from MeOH to afford **^{10}B-81** (2493 mg, 10.78 mmol, 73%) as a colorless crystal: isotopic purity of ^{10}B: 98.4 ± 0.8%: mp 98–99 °C; ^{1}H NMR (400 MHz, $CDCl_3$, TMS): δ = 1.34 (s, 12H), 2.32 (s, 6H), 7.10 (s, 1H), 7.44 (s, 2H); ^{13}C NMR (100 MHz, $CDCl_3$, TMS): δ = 21.13, 24.85, 83.68, 132.38, 132.98, 137.16; IR (ATR): *v* = 2977, 1601, 1422, 1402, 1389, 1371, 1347, 1248, 1139, 1117, 964, 849, 719. 498 cm^{-1}; HRMS (ESI$^+$): *m*/*z* calcd for $[M+H]^+$, $C_{14}H_{22}{}^{10}BO_2$, 232.1744; found, 232.1744; Anal. Calcd (%)

for $C_{14}H_{21}{}^{10}BO_2$: C, 72.69; H, 9.15. found: C, 72.80; H, 9.25.

3,5-Bis(bromomethyl)phenylboronic acid pinacol ester (^{10}**B-82)**

A mixture of **^{10}B-81** (2450 mg, 10.59 mmol), *N*-bromosuccinimide (NBS) (3750 mg, 21.07 mmol, 2.0 equiv) and benzoyl peroxide (BPO) (122 mg, 0.504 mmol, 0.05 equiv) in CCl_4 (60 mL) was refluxed overnight. After adding hexanes, the precipitate was removed by filtration, and the solvent was evaporated under reduced pressure. The resulting residue was purified by silica gel column chromatography (hexanes/CH_2Cl_2 = 8/1 to 1/2) to afford **^{10}B-82** as a colorless syrup, which was further purified by recrystallization from $CHCl_3$/MeOH at 0 °C to –78 °C to give **^{10}B-82** (1519 mg, 3.9 mmol, 37%) as a colorless needle crystal: mp 79–80 °C; ^{1}H NMR (400 MHz, $CDCl_3$, TMS): δ = 1.35 (s, 12H), 4.48 (s, 4H), 7.53 (t, *J* = 1.6 Hz, 1H), 7.75 (d, *J* = 1.6 Hz, 2H); ^{13}C NMR (100 MHz, $CDCl_3$, TMS): δ = 24.89, 32.78, 84.19, 132.52, 135.27, 137.87; IR (ATR): *ν* = 2977, 1604, 1471, 1462, 1430, 1396, 1372, 1353, 1251, 1215, 1138, 966, 845, 713, 666, 602, 578, 552 cm^{-1}; HRMS (ESI$^+$): *m*/*z* calcd for $[M+NH_4]^+$, $C_{14}H_{23}{}^{10}BBr_2NO_2$, 405.0219; found, 405.0218; Anal. Calcd (%) for $C_{14}H_{19}{}^{10}BBr_2O_2$: C, 43.21; H, 4.92. found: C, 43.18; H, 4.93.

1-[(3-(Bromomethyl)-5-(4,4,5,5-tetramethyl-1,3,2-dioxaborolan-2-yl)phenyl)methyl]-4,7,10-tris(*tert*-butoxycarbonyl)-1,4,7,10-tetraazacyclododecane (^{10}**B-83)**

To a solution of **^{10}B-82** (770 mg, 1.98 mmol, 1.5 equiv) in MeCN (13 mL), 3Boc-cyclen **63**[72] (620 mg, 1.32 mmol) and potassium carbonate (220 mg, 1.59 mmol, 1.2 equiv) were added and the mixture was stirred at room temperature for 24 h. After adding H_2O, the reaction mixture was extracted with $CHCl_3$. The organic layer was washed with brine, dried over Na_2SO_4 and concentrated under reduced pressure. The resulting residue was purified by silica gel column chromatography (hexanes/AcOEt =

10/1 to 3/1) to afford **^{10}B-83** (686 mg, 0.879 mmol, 67%) as a colorless amorphous solid: mp 77–79 °C; ^{1}H NMR (400 MHz, $CDCl_3$, TMS): δ = 1.34 (s, 12H), 1.43–1.47 (m, 27H), 2.66 (br, 4H), 3.14–3.41 (m, 8H), 3.62 (br, 4H), 3.72 (s, 2H), 4.46 (s, 2H), 7.42 (s, 1H), 7.62 (s, 1H), 7.71 (s, 1H); ^{13}C NMR (100 MHz, $CDCl_3$, TMS): δ = 24.89, 28.52, 28.71, 33.27, 47.66, 48.37, 50.10, 55.71, 56.50, 58.03, 79.22, 79.45, 84.02, 129.59, 133.94, 134.28, 136.68, 137.37, 155.34, 155.78, 156.24; IR (ATR): *ν* = 2975, 1682, 1461, 1405, 1363, 1248, 1145, 969, 890, 850, 771, 719, 612, 557 cm^{-1}; HRMS (ESI^{+}): *m*/*z* calcd for $[M+H]^{+}$, $C_{37}H_{63}{}^{10}BBrN_4O_8$, 780.3953; found, 780.3952; Anal. Calcd (%) for $C_{37}H_{62}{}^{10}BBrN_4O_8 \cdot 0.5H_2O$: C, 56.26; H, 8.04; N, 7.09. found: C, 56.43; H, 8.02; N, 6.78.

1-[(3-(Bromomethyl)-5-(4,4,5,5-tetramethyl-1,3,2-dioxaborolan-2-yl)phenyl)methyl]-4,7,10,13-tetrakis(*tert*-butoxycarbonyl)-1,4,7,10,13-pentaazacyclopentadecane (^{10}B-84)

To a solution of **^{10}B-82** (360 mg, 0.925 mmol, 1.5 equiv) in MeCN (6.0 mL), **65**[73] (370 mg, 0.601 mmol) and potassium carbonate (101 mg, 0.724 mmol, 1.2 equiv) were added and the mixture was stirred at room temperature for 24 h. After adding H_2O, the reaction mixture was extracted with $CHCl_3$. The organic layer was washed with brine, dried over Na_2SO_4 and concentrated under reduced pressure. The resulting residue was purified by silica gel column chromatography (hexanes/AcOEt = 10/1 to 3/1) to afford **^{10}B-84** (291 mg, 0.315 mmol, 52%) as a colorless amorphous solid: mp 67–68 °C; ^{1}H NMR (400 MHz, $CDCl_3$, TMS): δ = 1.35 (s, 12H), 1.44–1.47 (m, 36H), 2.64 (br, 4H), 3.40 (br, 16H), 3.60 (s, 2H), 4.50 (s, 2H), 7.47 (s, 1H), 7.60 (s, 1H), 7.68 (s, 1H); ^{13}C NMR (100 MHz, $CDCl_3$, TMS): δ = 24.89, 28.46, 33.60, 46.86 (br), 53.24, 59.27, 80.05, 83.98, 129.47, 132.39, 134.17, 135.09, 137.35, 139.34, 155.23; IR (ATR): *ν* = 2976, 1690, 1465, 1406, 1364, 1306, 1245, 1144, 1044, 967, 894, 850, 772, 718, 561, 460 cm^{-1}; HRMS (ESI^{+}): *m*/*z* calcd for $[M+H]^{+}$, $C_{44}H_{76}{}^{10}BBrN_5O_{10}$, 923.4899; found, 923.4901; Anal. Calcd (%) for $C_{44}H_{75}{}^{10}BBrN_5O_{10} \cdot 0.5H_2O$: C, 56.64; H, 8.21; N, 7.51. found: C, 56.62; H, 8.36; N, 7.17.

1-[(3-(1,4,7-Triazacyclononan-1-ylmethyl)-5-boronophenyl)methyl]-1,4,7,10-tetraazacyclododecane heptahydrobromic acid salt (7HBr) (^{10}B-23)

A mixture of **^{10}B-83** (330 mg, 0.432 mmol), 2Boc-tacn **59**[67] (170 mg, 0.516 mmol, 1.2 equiv) and potassium carbonate (71 mg, 0.510 mmol, 1.2 equiv) in MeCN (4.0 mL) was refluxed for 11 h. After adding H_2O, the reaction mixture was extracted with $CHCl_3$. The organic layer was washed with brine, dried over Na_2SO_4 and concentrated under reduced pressure. The resulting residue was purified by silica gel column chromatography (hexanes/AcOEt = 4/1 to 2/1) to afford **^{10}B-85** (272 mg, 0.264 mmol, 63%) as a colorless amorphous solid.

Using general procedure A, compound **^{10}B-85** (225 mg, 0.219 mmol) gave **^{10}B-23** (197 mg, 0.194 mmol, 89%) as colorless powder, which was determined to be the 7HBr salt by elemental analysis: mp 214–215 °C; ^{1}H NMR (400 MHz, D_2O, TSP): δ = 2.92 (t, *J* = 5.6 Hz, 4H), 3.05 (t, *J* = 5.6 Hz, 8H) 3.18 (br, 4H) 3.28 (t, *J* = 6.4 Hz, 8H), 3.66 (s, 4H), 3.94 (s, 2H), 3.98 (s, 2H), 7.48 (s, 1H), 7.76 (s, 1H), 7.79 (s, 1H); ^{13}C NMR (100 MHz, D_2O, 1,4-dioxane): δ = 42.39, 42.58, 42.68, 44.19, 44.90, 47.93, 48.20, 56.94, 59.05, 134.05, 134.99, 135.34, 135.87, 135.97; IR (ATR): *ν* = 3379, 2934, 2609, 1605, 1567, 1489, 1452, 1401, 1254, 1186, 1137, 1006, 947, 912, 880, 844, 756, 715, 585, 561 cm^{-1}; HRMS (ESI$^+$): *m*/*z* calcd for $[M+2H]^{2+}$, $C_{22}H_{44}{}^{10}BN_7O_2$, 224.1837; found, 224.1836; Anal. Calcd (%) for $C_{22}H_{42}{}^{10}BN_7O_2 \cdot 7HBr \cdot 2H_2O$: C, 25.19; H, 5.09; N, 9.35. found: C, 25.03; H. 5.21; N, 9.12.

1-[(3-(1,4,7-Triazacyclononan-1-ylmethyl)-5-boronophenyl)methyl]-1,4,7,10,13-pentaazacyclopentadecane octahydrobromic acid salt (8HBr) (^{10}B-26)

A mixture of **^{10}B-84** (280 mg, 0.303 mmol), 2Boc-tacn **59**[67] (116 mg, 0.353 mmol, 1.2 equiv) and potassium carbonate (52 mg, 0.373 mmol, 1.2 equiv) in MeCN (3.0 mL) was refluxed for 18 h. After adding H_2O, the reaction mixture was extracted with $CHCl_3$.

The organic layer was washed with brine, dried over Na_2SO_4 and concentrated under reduced pressure. The resulting residue was purified by silica gel column chromatography (hexanes/AcOEt = 4/1 to 2/1) to afford **^{10}B-87** (238 mg, 0.203 mmol, 67%) as a colorless amorphous solid.

Using general procedure A, compound **^{10}B-87** (210 mg, 0.179 mmol) gave **^{10}B-26** (192 mg, 0.169 mmol, 94%) as colorless powder, which was determined to be the 8HBr salt by elemental analysis: mp 217–218 °C; ^{1}H NMR (400 MHz, D_2O, TSP): δ = 3.00–3.06 (m, 8H), 3.21 (s, 4H), 3.27–3.43 (m, 16H) 3.67 (s, 4H), 3.99 (s, 2H), 4.02 (s, 2H), 7.50 (s, 1H), 7.75 (s, 1H), 7.82 (s, 1H); ^{13}C NMR (100 MHz, D_2O, 1,4-dioxane): δ = 42.70, 44.21, 44.31, 45.21, 45.73, 47.93, 50.02, 56.50, 58.97, 133.73, 135.36, 135.93, 136.07; IR (ATR): ν = 3363, 2934, 2642, 1570, 1498, 1446, 1385, 1254, 1041, 947, 759, 714, 444, 418 cm^{-1}; HRMS (ESI$^+$): *m*/*z* calcd for $[M+2H]^{2+}$, $C_{24}H_{49}{}^{10}BN_8O_2$, 245.7048; found, 245.7048; Anal. Calcd (%) for $C_{24}H_{47}{}^{10}BN_8O_2 \cdot 8HBr \cdot 2H_2O$: C, 24.57; H, 5.07; N, 9.55. found: C, 24.63; H. 5.29; N, 9.30.

1-[(3-(1,4,7,10-Tetraazacyclododecan-1-ylmethyl)-5-boronophenyl)methyl]-1,4,7,10,13-pentaazacyclopentadecane nonahydrobromic acid salt (9HBr) (^{10}B-25)

A mixture of **^{10}B-83** (320 mg, 0.410 mmol), **65**[73] (280 mg, 0.455 mmol, 1.1 equiv) and potassium carbonate (68 mg, 0.493 mmol, 1.2 equiv) in MeCN (4.0 mL) was refluxed for 14 h. After adding H_2O, the reaction mixture was extracted with $CHCl_3$. The organic layer was washed with brine, dried over Na_2SO_4 and concentrated under reduced pressure. The resulting residue was purified by silica gel column chromatography (hexanes/AcOEt = 4/1 to 2/1) to afford **^{10}B-86** (385 mg, 0.292 mmol, 71%) as a colorless amorphous solid.

Using general procedure A, compound **^{10}B-86** (265 mg, 0.201 mmol) gave **^{10}B-25** (192 mg, 0.152 mmol, 76%) as colorless powder, which was determined to be the 9HBr salt by elemental analysis: mp 218–220 °C; ^{1}H NMR (400 MHz, D_2O, TSP): δ = 2.94 (t, J = 5.2 Hz, 4H), 3.06 (t, J = 5.2 Hz, 8H), 3.19 (t, J = 4.8 Hz, 4H), 3.22 (s, 4H), 3.26–3.45 (m,

16H), 3.96 (s, 2H), 4.05 (s, 2H), 7.51 (s, 1H), 7.76 (s, 1H), 7.78 (s, 1H); ^{13}C NMR (100 MHz, D_2O, 1,4-dioxane): δ = 42.37, 42.58, 44.29, 44.92, 45.19, 45.69, 45.73, 48.20, 50.04, 56.57, 56.88, 133.86, 135.41, 135.49, 135.70, 136.14; IR (ATR): *v* = 3369, 2934, 2641, 1570, 1440, 1370, 1251, 1039, 756, 719, 423, 406 cm^{-1}; HRMS (ESI$^+$): *m*/*z* calcd for $[M+2H]^{2+}$, $C_{26}H_{54}{}^{10}BN_9O_2$, 267.2259; found, 267.2259; Anal. Calcd (%) for $C_{26}H_{52}{}^{10}BN_9O_2 \cdot 9HBr \cdot H_2O$: C, 24.42; H, 4.97; N, 9.86. found: C, 24.51; H. 5.27; N, 9.59.

1-[(3-(1,4,7-Triazacyclononan-1-ylmethyl)-5-(13,15-dioxa-15-boradispiro[5.0.5.3]pentadec-14-yl)phenyl)methyl]-1,4,7,10-tetraazacyclododecane (^{10}B-28)

Using general procedure B, compound **^{10}B-23** (102 mg, 0.101 mmol) gave **^{10}B-28** (47 mg, 0.0777 mmol, 77%) as a colorless amorphous solid: mp 74–76 °C; ^{1}H NMR (400 MHz, $CDCl_3$, TMS): δ = 1.16–1.32 (m, 6H), 1.63–1.81 (m, 14H), 2.65 (br, 20H), 2.81 (br, 8H), 3.61 (s, 2H), 3.71 (s, 2H), 7.45 (s, 1H), 7.63 (s, 2H); ^{13}C NMR (100 MHz, $CDCl_3$, TMS): δ = 22.35, 25.80, 32.46, 44.50 (br), 46.32 (br), 51.17, 58.97, 61.10, 84.71, 129.38, 133.19, 134.82, 138.35, 139.38; IR (ATR): *v* = 3286, 2930, 2851, 1557, 1463, 1399, 1348, 1272, 1237, 1146, 1130, 1040, 961, 940, 910, 810, 748, 721, 600, 505, 415 cm^{-1}; HRMS (ESI$^+$): *m*/*z* calcd for $[M+2H]^{2+}$, $C_{34}H_{62}{}^{10}BN_7O_2$, 305.2542; found, 305.2542; Anal. Calcd (%) for $C_{34}H_{60}{}^{10}BN_7O_2 \cdot 0.7MeOH \cdot 0.7CHCl_3$: C, 59.48; H, 8.95; N, 13.72. found: C, 59.43; H, 9.17; N, 13.41.

1-[(3-(1,4,7-Triazacyclononan-1-ylmethyl)-5-(13,15-dioxa-15-boradispiro[5.0.5.3]pentadec-14-yl)phenyl)methyl]-1,4,7,10,13-pentaazacyclopentadecane (^{10}B-31)

Using general procedure B, compound **^{10}B-26** (120 mg, 0.106 mmol) gave **^{10}B-31** (57 mg, 0.0866 mmol, 82%) as a colorless amorphous solid: mp 71–73 °C; ^{1}H NMR (400 MHz, $CDCl_3$, TMS): δ = 1.17–1.33 (m, 6H), 1.64–1.78 (m, 14H), 2.65 (br, 20H), 2.72 (s,

4H), 2.74 (br, 4H), 2.80 (s, 4H), 3.58 (s, 2H), 3.72 (s, 2H), 7.39 (s, 1H), 7.56 (s, 1H), 7.72 (s, 1H); ^{13}C NMR (100 MHz, $CDCl_3$, TMS): δ = 22.35, 25.78, 32.46, 46.86, 47.49, 48.35, 54.27, 59.75, 61.31, 84.76, 129.26, 132.98, 134.45, 134.63, 138.75; IR (ATR): *v* = 3290, 2928, 2848, 1552, 1463, 1400, 1371, 1272, 1237, 1130, 962, 940, 910, 875, 832, 810, 747, 720, 658, 507 cm^{-1}; HRMS (ESI$^+$): *m*/*z* calcd for $[M+H]^+$, $C_{36}H_{66}{}^{10}BN_8O_2$, 652.5433; found, 652.5433; Anal. Calcd (%) for $C_{36}H_{65}{}^{10}BN_8O_2$·MeOH·0.5$CHCl_3$: C, 60.56; H, 9.42; N, 15.07. found: C, 60.54; H, 9.58; N, 15.03.

1-[(3-(1,4,7,10-Tetraazacyclododecan-1-ylmethyl)-5-(13,15-dioxa-15-boradispiro[5.0.5.3]pentadec-14-yl)phenyl)methyl]-1,4,7,10,13-pentaazacyclopentadecane (^{10}B-30)

Using general procedure B, compound **^{10}B-25** (130 mg, 0.103 mmol) gave **^{10}B-30** (42 mg, 0.0609 mmol, 59%) as a colorless amorphous solid: mp 69–71 °C; ^{1}H NMR (400 MHz, $CDCl_3$, TMS): δ = 1.17–1.32 (m, 6H), 1.65–1.79 (m, 14H), 2.55–2.58 (m, 8H), 2.64 (br, 16H), 2.71 (s, 4H), 2.74–2.79 (m, 8H), 3.58 (s, 2H), 3.61 (s, 2H), 7.32 (s, 1H), 7.57 (s, 1H), 7.70 (s, 1H); ^{13}C NMR (100 MHz, $CDCl_3$, TMS): δ = 22.33, 25.80, 32.46, 45.15, 46.32, 47.24, 47.87, 48.41, 49.02, 51.44, 54.37, 59.12, 59.35, 84.69, 133.02, 134.61, 134.72, 138.29, 138.40; IR (ATR): *v* = 3281, 2929, 2848, 1555, 1462, 1401, 1372, 1272, 1237, 1130, 1040, 961, 940, 909, 809, 758, 720, 505, 422 cm^{-1}; HRMS (ESI$^+$): *m*/*z* calcd for $[M+H]^+$, $C_{38}H_{71}{}^{10}BN_9O_2$, 695.5855; found, 695.5855; Anal. Calcd (%) for $C_{38}H_{70}{}^{10}BN_9O_2$·0.5MeOH·1.5$H_2O$: C, 62.65; H, 10.24; N, 17.08. found: C, 62.49; H, 10.38; N, 16.79.

1-[(3-(4,7,10-Tris(*tert*-butoxycarbonyl)-1,4,7,10-tetraazacyclododecan-1-ylmethyl)-5-(4,4,5,5-tetramethyl-1,3,2-dioxaborolan-2-yl)phenyl)methyl]-4,7,10-tris(*tert*-butoxycarbonyl)-1,4,7,10-tetraazacyclododecane (^{10}B-88)

A mixture of **^{10}B-82** (140 mg, 0.360 mmol), 3Boc-cyclen **63**[72] (340 mg, 0.719 mmol,

2.0 equiv) and potassium carbonate (126 mg, 0.914 mmol, 2.5 equiv) in MeCN (3.5 mL) was refluxed for 24 h. After adding H_2O, the reaction mixture was extracted with $CHCl_3$. The organic layer was washed with brine, dried over Na_2SO_4 and concentrated under reduced pressure. The resulting residue was purified by silica gel column chromatography (hexanes/AcOEt = 4/1 to 1/1) to afford **^{10}B-88** (255 mg, 0.217 mmol, 60%) as a colorless amorphous solid: mp 104–106 °C; ^{1}H NMR (400 MHz, $CDCl_3$, TMS): δ = 1.32 (s, 12H), 1.42–1.47 (m, 54H), 2.63–2.68 (m, 8H), 3.17–3.41 (m, 16H), 3.62 (br, 8H), 3.73 (br, 4H), 7.15 (s, 1H), 7.62 (s, 2H); ^{13}C NMR (100 MHz, $CDCl_3$, TMS): δ = 24.88, 28.52, 28.73, 47.48, 47.76, 48.11, 48.61, 50.01, 54.92, 55.95, 57.38, 79.19, 79.42, 79.52, 83.82, 128.85, 135.31, 135.94, 155.31, 155.70, 156.15; IR (ATR): *v* = 2976, 1682, 1457, 1410, 1391, 1363, 1315, 1246, 1146, 969, 887, 852, 751, 723, 666, 555, 515 cm^{-1}; HRMS (ESI$^+$): *m*/*z* calcd for $[M+H]^+$, $C_{60}H_{106}{}^{10}BN_8O_{14}$, 1172.7952; found, 1172.7952; Anal. Calcd (%) for $C_{60}H_{105}{}^{10}BN_8O_{14}\cdot 0.5H_2O$: C, 60.99; H, 9.04; N, 9.48. found: C, 60.98; H, 8.66; N, 9.31.

1-[(3-(4,7,10,13-Tetrakis(*tert*-butoxycarbonyl)-1,4,7,10,13-pentaazacyclopentadecan-1-ylmethyl)-5-(4,4,5,5-tetramethyl-1,3,2-dioxaborolan-2-yl)phenyl)methyl]-4,7,10,13-tetrakis(*tert*-butoxycarbonyl)-1,4,7,10,13-pentaazacyclopentadecane (^{10}B-89**)**

A mixture of **^{10}B-82** (108 mg, 0.278 mmol), **65**[73] (340 mg, 0.552 mmol, 2.0 equiv) and potassium carbonate (96 mg, 0.695 mmol, 2.5 equiv) in MeCN (2.5 mL) was refluxed for 16 h. After adding H_2O, the reaction mixture was extracted with $CHCl_3$. The organic layer was washed with brine, dried over Na_2SO_4 and concentrated under reduced pressure. The resulting residue was purified by silica gel column chromatography (hexanes/AcOEt = 3/1 to 1/1) to afford **^{10}B-89** (272 mg, 0.186 mmol, 67%) as a colorless amorphous solid: mp 88–90 °C; ^{1}H NMR (400 MHz, $CDCl_3$, TMS): δ = 1.28–1.47 (m, 84H), 2.63 (br, 8H), 3.39 (br, 32H), 3.59 (s, 4H), 7.28 (s, 1H), 7.57 (s, 2H); ^{13}C NMR (100 MHz, $CDCl_3$,

TMS): δ = 24.91, 28.41, 46.74 (br), 52.86 (br), 59.46, 79.93, 83.68, 128.78, 132.63, 134.16, 138.15, 155.15; IR (ATR): *v* = 2975, 1691, 1464, 1409, 1364, 1305, 1241, 1157, 1044, 949, 895, 852, 771, 721, 548, 463 cm^{-1}; HRMS (ESI^+): *m*/*z* calcd for $[M+2H]^{2+}$, $C_{74}H_{133}{}^{10}BN_{10}O_{18}$, 729.9959; found, 729.9959; Anal. Calcd (%) for $C_{74}H_{131}{}^{10}BN_{10}O_{18}\cdot 0.5H_2O$: C, 60.55; H, 9.06; N, 9.54. found: C, 60.34; H, 9.08; N, 9.32.

1-[(3-(1,4,7,10-Tetraazacyclododecan-1-ylmethyl)-5-boronophenyl)methyl]-1,4,7,10-tetraazacyclododecane heptahydrobromic acid salt (7HBr) (^{10}B-24)

Using general procedure A, compound **^{10}B-88** (180 mg, 0.154 mmol) gave **^{10}B-24** (144 mg, 0.127 mmol, 82%) as colorless powder, which was determined to be the 7HBr salt by elemental analysis: mp 214–216 °C; ^{1}H NMR (400 MHz, D_2O, TSP): δ = 2.95 (t, *J* = 5.2 Hz, 8H), 3.04 (br, 8H), 3.20 (t, *J* = 5.2 Hz, 8H), 3.27 (br, 8H), 3.97 (s, 4H), 7.49 (s, 1H), 7.76 (s, 2H); ^{13}C NMR (100 MHz, D_2O, 1,4-dioxane): δ = 42.41, 42.58, 44.90, 48.22, 56.96, 135.05, 135.41; IR (ATR): *v* = 3425, 2992, 2907, 2775, 2611, 1568, 1488, 1455, 1417, 1351, 1249, 1026, 998, 954, 930, 889, 829, 759, 740, 721, 546, 437 cm^{-1}; HRMS (ESI^+): *m*/*z* calcd for $[M+2H]^{2+}$, $C_{24}H_{49}{}^{10}BN_8O_2$, 245.7048; found, 245.7048; Anal. Calcd (%) for $C_{24}H_{47}{}^{10}BN_8O_2\cdot 7HBr\cdot 3H_2O$: C, 25.97; H, 5.45; N, 10.09. found: C, 25.85; H. 5.14; N, 9.72.

1-[(3-(1,4,7,10,13-Pentaazacyclopentadecan-1-ylmethyl)-5-boronophenyl)methyl]-1,4,7,10,13-pentaazacyclopentadecane decahydrobromic acid salt (10HBr) (^{10}B-27)

Using general procedure A, compound **^{10}B-89** (220 mg, 0.151 mmol) gave **^{10}B-27** (207 mg, 0.149 mmol, 99%) as colorless powder, which was determined to be the 10HBr salt by elemental analysis: mp 242–244 °C; ^{1}H NMR (400 MHz, D_2O, TSP): δ =3.08 (t, *J* = 4.8 Hz, 8H), 3.25 (s, 8H), 3.35–3.47 (m, 24H), 4.08 (s, 4H), 7.60 (s, 1H), 7.78 (s, 2H); ^{13}C NMR (100 MHz, D_2O, 1,4-dioxane): δ = 44.27, 45.19, 45.67, 50.02, 56.55, 133.86, 135.84, 136.45; IR (ATR): *v* = 3377, 2951, 2649, 1567, 1440, 1372, 1250, 1036, 756, 720

cm^{-1}; HRMS (ESI^+): *m*/*z* calcd for $[M+2H]^{2+}$, $C_{28}H_{59}{}^{10}BN_{10}O_2$, 288.7470; found, 288.7470; Anal. Calcd (%) for $C_{28}H_{57}{}^{10}BN_{10}O_2 \cdot 10HBr$: C, 24.28; H, 4.88; N, 10.11. found: C, 24.50; H, 4.61; N, 9.75.

1-[(3-(1,4,7,10-Tetraazacyclododecan-1-ylmethyl)-5-(13,15-dioxa-15-boradispiro[5.0.5.3]pentadec-14-yl)phenyl)methyl]-1,4,7,10-tetraazacyclododecane (^{10}B-29)

Using general procedure B, compound **^{10}B-24** (100 mg, 0.088 mmol) gave **^{10}B-29** (41 mg, 0.0629 mmol, 72%) as a colorless amorphous solid: mp 80–82 °C; ^{1}H NMR (400 MHz, $CDCl_3$, TMS): δ = 1.16–1.31 (m, 6H), 1.62–1.79 (m, 14H), 2.52–2.57 (m, 16H), 2.65 (br, 8H), 2.79 (br, 8H), 3.60 (s, 4H), 7.38(s, 1H), 7.64 (s, 2H); ^{13}C NMR (100 MHz, $CDCl_3$, TMS): δ = 22.33, 25.83, 32.45, 45.25, 46.66, 47.37, 51.25, 58.99, 84.53, 132.81, 134.86, 138.19; IR (ATR): *v* = 3274, 2929, 2849, 1557, 1462, 1399, 1346, 1272, 1236, 1146, 1130, 1041, 960, 940, 811, 748, 720, 601, 501, 408 cm^{-1}; HRMS (ESI^+): *m*/*z* calcd for $[M+H]^+$, $C_{36}H_{66}{}^{10}BN_8O_2$, 652.5433; found, 652.5433; Anal. Calcd (%) for $C_{36}H_{65}{}^{10}BN_8O_2 \cdot MeOH \cdot 0.5CHCl_3$: C, 60.56; H, 9.42; N, 15.07. found: C, 60.66; H, 9.65; N, 15.01.

1-[(3-(1,4,7,10,13-Pentaazacyclopentadecan-1-ylmethyl)-5-(13,15-dioxa-15-boradispiro[5.0.5.3]pentadec-14-yl)phenyl)methyl]-1,4,7,10,13-pentaazacyclopentadecane (^{10}B-32)

Using general procedure B, compound **^{10}B-27** (125 mg, 0.0904 mmol) gave **^{10}B-32** (45 mg, 0.0608 mmol, 67%) as a colorless amorphous solid: mp 88–90 °C; ^{1}H NMR (400 MHz, $CDCl_3$, TMS): δ = 1.18–1.34 (m, 6H), 1.64–1.80 (m, 14H), 2.62–2.65 (m, 20H), 2.71 (s, 8H), 2.73–2.78 (m, 12H), 3.59 (s, 4H), 7.34 (s, 1H), 7.60 (d, *J* = 1.6 Hz, 2H); ^{13}C NMR (100 MHz, $CDCl_3$, TMS): δ = 22.33, 25.75, 32.47, 47.24, 47.82, 48.36, 49.00, 54.51, 59.55, 84.84, 133.05, 134.61, 138.60; IR (ATR): *v* = 3286, 2927, 2812, 1599, 1447, 1402,

1360, 1272, 1236, 1129, 1063, 940, 876, 720 cm^{-1}; HRMS (ESI^+): *m*/*z* calcd for $[M+2H]^{2+}$, $C_{40}H_{77}{}^{10}BN_{10}O_2$, 369.8175; found, 369.8175; Anal. Calcd (%) for $C_{40}H_{75}{}^{10}BN_{10}O_2 \cdot 0.2MeOH \cdot 0.3CHCl_3$: C, 62.34; H, 9.83; N, 17.95. found: C, 62.48; H, 10.23; N, 17.60.

X-ray data collection and refinement

The crystals of **21a** (ZnL^3) were suitable for a single-crystal X-ray structure analysis, which were performed on a Bruker APEX CCD diffractometer equipped with a Rigaku Instruments low-temperature attachment. Data were collected at 93K using monochromated Mo-Kα radiation (λ = 0.71073 Å). The frames were indexed, integrated, and scaled using the SMART and SAINT software packages. An empirical absorption correction was applied to the collection reflections with SADABS using XPREP. The structure was solved by the direct method and refined on F^2 by the full-matrix least squares technique using the SHELX-2015 program package. All non-hydrogen atoms were refined anisotropically. The crystal data in this manuscript can be obtained free of change from The Cambridge Crystallographic Data Centre via www.cccdc.cam.ac.uk/data_request/cif. Crystal data for **21a** $C_{29}H_{51}BN_6O_9Zn$, M_r = 703.93, orthorhombic, P 2_1 2_1 2_1, a = 10.008 (4), b = 10.967 (4), c = 30.483 (12) Å, V = 3346 (2) $Å^3$, Z = 4, ρ_{calc} = 1.397 $g \cdot cm^{-3}$, R = 0.0553 (7083 reflections), R_w = 0.1229 (7656 reflections), GOF = 1.195. CCDC 2058200 contains the supplementary crystallographic data for the paper.

Cell cultures

HeLa S3 cells (human cervical carcinoma) were cultured in Minimum Essential Medium (MEM) containing 10% fetal bovine serum (FBS), penicillin, and streptomycin. A549 cells (human caucasian lung carcinoma) and IMR-90 cells (normal human

fibroblast) were cultured in Dulbecco's modified Eagle's medium (DMEM) with 10% FBS, penicillin and streptomycin. All cells were cultured at 37 °C in a humidified atmosphere containing 5% CO_2.

MTT assays

HeLa S3, A549, and IMR-90 cells (1×10^4 cells/well) were seeded on 96-well plates (Watson) in cell culture medium. After incubation overnight at 37 °C under 5% CO_2., the cells were treated with ^{10}B-BSH **4** (Stella Chemifa, Japan, ^{10}B-enrichment ≥ 95%), BPA **5** (Fluka, USA)-D-fructose complex, **14**–**22** (0–200 μM), and **23**–**48** (0–400 μM) in cell culture medium under same conditions for 24 h, and then, 0.5% MTT (3-(4,5-dimethylthiazol-2yl)-2,5-diphenyltetrazolium bromide) reagent in PBS (10 μL) was added to each well. After incubation for 4 h, a formazan lysis solution (10% sodium dodecyl sulfate (SDS) in 0.01 N HCl aq.) (100 μL) was added and the resulting solution was incubated under same conditions overnight. The absorbance at λ = 570 nm was measured with a microplate reader (Bio-Rad).

Measurement of intracellular uptake of boron compounds into HeLa S3, A549, and IMR-90 cells evaluated by ICP-MS

HeLa S3, A549, and IMR-90 cells (5×10^5 cells/well) were seeded on 6-well plates (TrueLine, USA) in cell culture medium. After incubation overnight at 37 °C under 5% CO_2. and 18–20% O_2 (normoxic conditions), the cells were washed gently with PBS (1 mL) and treated with the boron compounds **4**, **5**, and **14**–**22** (30 μM), and **23**–**48** (100 μM) in cell culture medium (2 mL) under same conditions for 24 h (n = 4). To count the number of cells after treatment with the boron compounds, the cells (n = 1) were washed with PBS, detached by trypsin, and counted with a hemocytometer. For measurement of boron uptake, the cells (n = 3) were washed with PBS (1 mL×3) and digested with 60% HNO_3 aq. (0.5 mL) at room temperature for 24 h, which were

transferred to 15 mL centrifuge tubes with Milli-Q water (3.5 mL). These tubes were centrifuged at 3000 rpm and 4 °C for 10 min, and the resulting sample solutions were filtered. The concentration of boron atoms was determined by ICP-MS (NexION300S, PerkinElmer, Waltham, Massachusetts, USA).

Active energy-dependent uptake of boron-containing macrocyclic polyamine derivatives into HeLa S3 and A549 cells

HeLa S3 and A549 cells (5×10^5 cells/well) were seeded on 6-well plates (TrueLine, USA) and incubated in cell culture medium at 37 °C under 5% CO_2 (n = 4). After incubation for 2 days, the cells were washed with PBS (1 mL) and treated with boron compounds **5** and **17a**–**19a** (30 μM) in cell culture medium (2 mL) at 37 °C or 4 °C for 1 h (n = 4). To count the number of cells after treatment with the boron compounds, the cells (n = 1) were washed with PBS, detached by trypsin, and counted with a hemocytometer. For measurement of boron uptake, the cells (n = 3) were washed with PBS (1 mL×3) and digested with 60% HNO_3 aq. (0.5 mL) at room temperature for 24 h, and then transferred to 15 mL centrifuge tubes with Milli-Q water (3.5 mL). These tubes were centrifuged at 3000 rpm and 4 °C for 10 min and then sample solution was filtered. The concentration of boron atoms was determined by ICP-MS (NexION300S, PerkinElmer, Waltham, Massachusetts, USA).

Effect of inhibitors on the intracellular uptake of 19a

HeLa S3 and A549 cells (5×10^5 cells/well) were seeded on 6-well plates (TrueLine, USA) and incubated in cell culture medium at 37 °C under 5% CO_2 for 2 days (n = 4). After preincubation with inhibitors in cell culture medium (2 mL) at 37 °C for 1 h, the cells were treated with boron compounds **5** and **19a** (30 μM) in the presence of inhibitors at 37 °C for 1 h. To count the number of cells after treatment with the boron compounds, the cells (n = 1) were washed with PBS, detached by trypsin, and counted with a

hemocytometer. For measurement of boron uptake, the cells (n = 3) were washed with PBS (1 mL×3) and digested with 60% HNO_3 aq. (0.5 mL) at room temperature for 24 h, which were transferred to 15 mL centrifuge tubes with Milli-Q water (3.5 mL). These tubes were centrifuged at 3000 rpm and 4 °C for 10 min and then sample solutions were filtered. The concentration of boron atoms was determined by ICP-MS (NexION300S, PerkinElmer, Waltham, Massachusetts, USA).

Evaluation of the anti-tumor effect of boron-containing macrocyclic polyamine derivatives with thermal neutron irradiation (colony formation assay)

A549 cells (5×10^5 cells/well) were seeded on 6-well plates (TrueLine, USA) and incubated in cell culture medium at 37 °C under 5% CO_2 for 1 day. After removing the cell culture medium, the cells were washed gently with PBS. Cell culture medium containing boron compounds **4**, **5**, **17**–**22** (30 μM), and **23**–**47** (100 μM) (2 mL) was added to the wells, which was incubated for 24 h under same conditions. After removing the medium, the cells were washed twice with PBS (1.0 mL) and collected by trypsinization. After centrifugation, the supernatant was removed, and cell culture medium was added to prepare a cell suspension (5×10^4 cells/mL). The cells (5×10^4 cells/mL, 1 mL) in 1.5 mL tubes were irradiated with thermal neutrons (Institute for Integrated Radiation and Nuclear Science, Kyoto University, Osaka, Japan) for 0, 15, 30, and 45 min, respectively. The thermal neutron flux (1.5×10^9 n/cm^2·s) was measured by two gold foils which were attached to the surface of the 1.5 mL tube. To evaluate the cell proliferation, the irradiated cells (3×10^3 cells/well, 1.0 mL) were seeded on 12-well plates (TrueLine, USA) and incubated for 7 days at 37 °C under 5% CO_2 in cell culture medium. After removing the medium, the attached cells were washed gently with PBS, fixed with EtOH, stained by 0.1% crystal violet and washed with PBS three times.

For analyzing the cell proliferation, images of the stained colony were acquired using a Bio-Rad Chemidoc^{TM} MP Imaging System (Bio-Rad, Hercules, CA, USA), which were

automatically examined by ImageJ-plugin Colony Area to determine the percentage of colony area of each wells.[77] The surviving fractions were calculated as the colony area and normalized by the result for non-irradiated condition.

Effect of boron-containing macrocyclic polyamine derivatives on the melting temperature of ctDNA

Thermal denaturation experiments of ctDNA (50 μM in phosphate) in 10 mM HEPES buffer (pH 7.4) with I = 0.02 ($NaNO_3$) were performed on a JASCO V-550 UV/vis spectrophotometer (JASCO, Tokyo, Japan) equipped with a thermoelectric temperature controller (± 0.5 °C), a stirring unit, and a 10 mm quartz cuvette. All aqueous solutions were made with purified water. The concentration of ctDNA was determined by UV absorption spectroscopy based on its molar extinction coefficient at 253 nm (ε_{253} = 6.6×10^3).[65d,79] Thermal melting curves for ctDNA with and without additives (**49**, **18b**, **21b**, **19a**, **22a**, **28**–**32**, **37**, **44**–**46**, and **48**) were obtained by following the absorption change at 260 nm as a function of the temperature (the temperature was raised at the rate of 1 °C/min). The T_m value was graphically determined from the spectral data, and the ΔT_m value for each condition was calculated from the results in the presence and absence of additives.

Chapter 6.

References and Notes

References and notes

(1) Sung, H.; Ferlay, J.; Siegel, R. L.; Laversanne, M.; Soerjomataram, I.; Jemal, A.; Bray, F. Global Cancer Statistics 2020: GLOBOCAN Estimates of Incidence and Mortality Worldwide for 36 Cancers in 185 Countries. *CA Cancer J. Clin*. **2021**, *71*, 209–249.

(2) Hosmane, N. S.; Maguire, J. A.; Zhu, Y.; Takagaki, M. Boron and Gadolinium Neutron Capture Therapy for Cancer Treatment. World Scientific Publishing: Singapore, 2012.

(3) (a) Taylor, H. J.; Goldhaber, M. Detection of Nuclear Disintegration in a Photographic Emulsion. *Nature* **1935**, *135*, 341. (b) Barth, R. F.; Soloway, A. H.; Fairchild, R. G. Boron Neutron Capture Therapy of Cancer. *Cancer Res*. **1990**, *50*, 1061–1070. (c) Hu, K.; Yang, Z.; Zhang, L.; Xie, L.; Wang, L.; Xu, H.; Josephson, L.; Liang, S. H.; Zhang, M.-R. Boron Agents for Neutron Capture Therapy. *Coord. Chem. Rev*. **2020**, *405*, 213139.

(4) (a) Rinard, P. M. Neutron Interactions with Matter. In Reilly, D.; Ensslin, N.; Smith, H.; Kreiner, S., editors, Passive Nondestructive Assay of Nuclear Materials. Nuclear Regulatory Commission, 1991. (b) Salt, C.; Lennox, A. J.; Takagaki, M.; Maguire, J. A.; Hosmane, N. S. Boron and Gadolinium Neutron Capture Therapy. *Russ. Chem. Bull., Int. Ed*. **2004**, *53*, 1871–1888.

(5) Suzuki, M. Boron Neutron Capture Therapy (BNCT): a Unique Role in Radiotherapy with a View to Entering the Accelerator-based BNCT era. *Int. J. Clin. Oncol.* **2020**, *25*, 43–50.

(6) Kanno, H.; Nagata, H.; Ishiguro, A.; Tsuzuranuki, S.; Nakano, S.; Nonaka, T.; Kiyohara, K.; Kimura, T.; Sugawara, A.; Okazaki, Y.; Takae, S.; Nakabayashi, T.; Arai, H.; Suzuki, H. Designation Products: Boron Neutron Capture Therapy for Head and Neck Carcinoma. *The Oncologist* **2021**, *26*, e1250–1255.

(7) (a) Suzuki, M.; Sakurai, Y.; Hagiwara, S.; Masunaga, S.; Kinashi, Y.; Nagata, K.; Maruhashi, A.; Kudo, M.; Ono, K. First Attempt of Boron Neutron Capture Therapy (BNCT) for Hepatocellular Carcinoma. *Jpn. J. Clin. Oncol.* **2007**, *37*, 376–381. (b)

Suzuki, M.; Suzuki, O.; Sakurai, Y.; Tanaka, H.; Kondo, N.; Kinashi, Y.; Masunaga, S.; Maruhashi, A.; Ono, K. Reirradiation for Locally Recurrent Lung Cancer in the Chest Wall with Boron Neutron Capture Therapy (BNCT). *Int. Canc. Conf. J.* **2012**, *1*, 235–238. (c) Suzuki, M. New Application for Boron Neutron Capture Therapy. *Radioisotopes* **2015**, *64*, 59–66. (d) Malouff, T. D.; Seneviratne, D. S.; Ebner, D. K.; Stross, W. C.; Waddle, M. R.; Trifiletti, D. M.; Krishnan, S. Boron Neutron Capture Therapy: A Review of Clinical Applications. *Front. Oncol.* **2021**, *11*, 601820.

(8) (a) Hawthorne, M. F. The Role of Chemistry in the Development of Boron Neutron Capture Therapy of Cancer. *Angew. Chem. Int. Ed. Engl.* **1993**, *32*, 950–984. (b) Morin, C. The Chemistry of Boron Analogues of Biomolecules. *Tetrahedron* **1994**, *50*, 12521–12569. (c) Soloway, A. H.; Tjarks, W.; Barnum, B. A.; Rong, F.-G.; Barth, R. F.; Codogni, I. M.; Wilson, J. G. The Chemistry of Neutron Capture Therapy. *Chem. Rev.* **1998**, *98*, 1515–1562. (d) Barth, R. F.; Coderre, J. A.; Vicente, M. G. H.; Blue, T. E. Boron Neutron Capture Therapy of Cancer: Current Status and Future Prospects. *Clin. Cancer Res*. **2005**, *11*, 3987–4002. (e) Luderer, M. J.; de la Puente, P.; Azab, A. K. Advancements in Tumor Targeting Strategies for Boron Neutron Capture Therapy. *Pharm. Res.* **2015**, *32*, 2824–2836. (f) Barth, R. F.; Mi, P.; Yang, W. Boron Delivery Agents for Boron Neutron Capture Therapy of Cancer. *Canc. Commun.* **2018**, *38*, 35. (g) Cerecetto, H.; Couto, M. Medicinal Chemistry of Boron-Bearing Compounds for BNCT-Glioma Treatment: Current Challenges and Perspectives. In Glioma – Contemporary Diagnostic and Therapeutic Approaches, Omerhodžić, I.; Arnautović, K. Eds., IntechOpen, U.K. **2018**.

(9) Kruger, P. G. Some Biological Effects of Nuclear Disintegration Products on Neoplastic Tissue. *Proc. Natl. Acad. Sci.* **1940**, *26*, 181–192.

(10) (a) Godwin, J. T.; Farr, L. E.; Sweet, W. H.; Robertson, J. S. Pathological Study of Eight Patients with Glioblastoma Multiforme Treated by Neutron Capture Therapy Using Boron 10. *Cancer* **1955**, *8*, 601–615. (b) Sweet, W. H.; Soloway, A. H.;

Brownell, G. L. Boron-Slow Neutron Capture Therapy of Gliomas. *Acta Radiol. Ther. Phys*. **1963**, *1*, 114–121. (c) Slatkin, D. N. A History of Boron Neutron Capture Therapy of Brain Tumors. *Brain* **1991**, *114*, 1609–1629.

(11) Knoth, W. H.; Sauer, J. C.; England, D. C.; Hertler, W. R.; Muetterties, E. L. Chemistry of Boranes. XIX. Derivative Chemistry of $B_{10}H_{10}^{-2}$ and $B_{12}H_{12}^{-2}$. *J. Am. Chem. Soc.* **1964**, *89*, 3973–3983.

(12) Soloway, A. H.; Hatanaka, H.; Davis, M. A. Penetration of Brain and Brain Tumor. VII. Tumor-Binding Sulfhydryl Boron Compounds. *J. Med. Chem.* **1967**, *10*, 714–717.

(13) (a) Hatanaka, H. A Revised Boron-Neutron Capture Therapy for Malignant Brain Tumors. *J. Neurol.* **1975**, *209*, 81–94. (b) Hatanaka, H.; Nakagawa, Y. Clinical Results of Long-Surviving Brain Tumor Patients Who Underwent Boron Neutron Capture Therapy. *Int. J. Radiat. Oncol. Biol. Phys.* **1994**, *28*, 1061–1066.

(14) Snyder, H. R.; Reedy, A. J.; Lennarz, W. J. Synthesis of Aromatic Boronic Acids. Aldehydo Boronic Acids and a Boronic Acid Analog of Tyrosine. *J. Am. Chem. Soc.* **1958**, *80*, 835–838.

(15) (a) Ichihashi, M.; Nakanishi, T.; Mishima, Y. Specific Killing Effect of ^{10}B-Para-boronophenylalanine in Thermal Neutron Capture Therapy of Malignant Melanoma: In Vitro Radiobiological Evaluation. *J. Invest. Dermatol*. **1982**, *78*, 215–218. (b) Mishima, Y.; Ichihashi, M.; Tsuji, M.; Hatta, S.; Ueda, M.; Honda, C.; Suzuki, T. Treatment of Malignant Melanoma by Selective Thermal Neutron Capture Therapy Using Melanoma-Seeking Compound. *J. Invest. Dermatol*. **1989**, *92*, 312S–325S.

(16) Mishima, Y.; Honda, C.; Ichihashi, M.; Obara, H.; Hiratsuka, J.; Fukuda, H.; Karashima, H.; Kobayashi, T.; Kanda, K.; Yoshino, K. Treatment of Malignant Melanoma by Single Thermal Neutron Capture Therapy with Melanoma-Seeking ^{10}B-Compound. *The Lancet* **1989**, *334*, 388–389.

(17) (a) Coderre, J. A.; Button, T. M.; Micca, P. L.; Fisher, C. D.; Nawrocky, M. M.; Liu,

H. B. Neutron Capture Therapy of The 9L Rat Gliosarcoma Using The *p*-Boronophenylalanine-fructose Complex. *Int. J. Radiat. Oncol. Biol. Phys.* **1994**, *30*, 643–652. (b) Shull, B. K.; Spielvogel, D. E.; Head, G.; Gopalaswamy, R.; Sankar, S.; Devito, K. Studies on the Structure of the Complex of the Boron Neutron Capture Therapy Drug, L-*p*-Boronophenylalanine, with Fructose and Related Carbohydrates: Chemical and ^{13}C NMR Evidence for the β-D-Fructofuranose 2,3,6-(*p*-Phenylalanylorthoboronate) Structure. *J. Pharm. Sci.* **2000**, *89*, 215–222.

(18) (a) Kato, I.; Ono, K.; Sakurai, Y.; Ohmae, M.; Maruhashi, A.; Imahori, Y.; Kirihata, M.; Nakazawa, M.; Yura, Y. Effectiveness of BNCT for Recurrent Head and Neck Malignancies. *Appl. Radiat. Isot.* **2004**, *61*, 1069–1073. (b) Kankaanranta, L.; Seppälä, T.; Koivunoro, H.; Saarilahti, K.; Atula, T.; Collan, J.; Salli, E.; Kortesniemi, M.; Uusi-Simola, J.; Välimäki, P.; Mäkitie, A.; Seppänen, M.; Minn, H.; Revitzer, H.; Kouri, M.; Kotiluoto, P.; Seren, T.; Auterinen, I.; Savolainen, S.; Joensuu, H. Boron Neutron Capture Therapy in the Treatment of Locally Recurred Head and Neck Cancer: Final Analysis of a Phase I/II Trial. *Int. J. Radiat. Oncol. Biol. Phys.* **2012**, *82*, e67–e75. (c) Barth, R. F.; Vicente, M. G. H.; Harling, O. K.; Kinger III, W. S.; Riley, K. J.; Binns, P. J.; Wagner, F. M.; Suzuki, M.; Aihara, T.; Kato, I.; Kawabata, S. Current Status of Boron Neutron Capture Therapy of High Grade Gliomas and Recurrent Head and Neck Cancer. *Radiat. Oncol.* **2012**, *7*, 146. (d) Suzuki, M.; Kato, I.; Aihara, T.; Hiratsuka, J.; Yoshimura, K.; Niimi, M.; Kimura, Y.; Ariyoshi, Y.; Haginomori, S.; Sakurai, Y.; Kinashi, Y.; Masunaga, S.; Fukushima, M.; Ono, K.; Maruhashi, A. Boron Neutron Capture Therapy Outcomes for Advanced or Recurrent Head and Neck Cancer. *J. Radiat. Res.* **2014**, *55*, 146–153.

(19) Ishiwata, K.; Ido, T.; Mejia, A. A.; Ichihashi, M.; Mishima, Y. Synthesis and Radiation Dosimetry of 4-Boron-2-[^{18}F]fluoro-D,L-phenylalanine: a Target Compound for PET and Boron Neutron Capture Therapy. *Appl. Radiat. Isot.* **1991**, *42*, 325–328.

(20) (a) Kabalka, G. W.; Smith, G. T.; Dyke, J. P.: Reid, W. S.; Desmond Longford, C. P.; Roberts, T. G.; Reddy, N. K.; Buonocore, E.; Hübner, K. F. Evaluation of Fluorine-18-BPA-Fructose for Boron Neutron Capture Treatment Planning. *J. Nucl. Med.* **1997**, *38*, 1762–1767. (b) Aihara, T.; Hiratsuka, J.; Morita, N.; Uno, M.; Sakurai, Y.; Maruhashi, A.; Ono, K.; Harada, T. First Clinical Case of Boron Neutron Capture Therapy for Head and Neck Cancer Malignancies using ^{18}F-BPA PET. *Head Neck* **2006**, *28*, 850–855. (c) Barth, R. F.; Zhang, Z.; Liu, T. A Realistic Appraisal of Boron Neutron Capture Therapy as a Cancer Treatment Nodality. *Canc. Commun.* **2018**, *38*, 36.

(21) Wongthai, P.; Hagiwara, K.; Miyoshi, Y.; Wiriyasermkul, P.; Wei, L.; Ohgaki, R.; Kato, I.; Hamase, K.; Nagamori, S.; Kanai, Y. Boronophenylalanine, a Boron Delivery agent for Boron Neutron Capture Therapy, is Transported by ATB$^{0,+}$, LAT1 and LAT2. *Cancer Sci.* **2015**, *106*, 279–286.

(22) Watanabe. T.; Hattori, Y.; Ohta, Y.; Ishimura, M.; Nakagawa, Y.; Sanada, Y.; Tanaka, H.; Fukutani, S.; Masunaga, S.; Hiraoka, M.; Ono, K.; Suzuki, M.; Kirihata, M. Comparison of the Pharmacokinetics Between L-BPA and L-FBPA Using the Same Administration Dose and Protocol: a Validation Study for the Theranostic Approach Using [^{18}F]-L-BPA Positron Emission Tomography in Boron Neutron Capture Therapy. *BMC Canc.* **2016**, *16*, 859.

(23) Yokoyama, K.; Miyatake, S.; Kajimoto. Y.; Kawabata, S.; Doi, A.; Yoshida, T.; Asano, T.; Kirihata, M.; Ono, K.; Kuroiwa, T. Pharmacokinetic Study of BSH and BPA in Simultaneous Use for BNCT. *J. Neuro. Oncol.* **2006**, *78*, 227–232.

(24) (a) Woodburn, K.; Phadke, A. S.; Morgan, A. R. An *in Vitro* Study of Boronated Porphyrins for Potential Use in Boron Neutron Capture Therapy. *Bioorg. Med. Chem. Lett.* **1993**, *3*, 2017−2022. (b) Toi, H.; Nagai, Y.; Aoyama,Y.; Kawabe, H.; Aizawa, K.; Ogoshi, H. Preparation of Porphyrins Having Phenylboronic Acid Groups. *Chem. Lett.* **1993**, *22*, 1043–1046. (c) Miura, M.; Micca, P. L.; Fisher, C. D.; Heinrichs, J.

C.; Donaldson, J. A.; Finkel, G. C.; Slatkin, D. N. Synthesis of a Nickel Tetracarboranylphenylporphyrin for Boron Neutron Capture Therapy: Biodistribution and Toxicity in Tumor-bearing Mice. *Int. J. Cancer* **1996**, *68*, 114−119. (d) Chayer, S.; Jaquinod, L.; Smith, K. M.; Vicente, M. G. H. Synthesis of Carboranylpyrroles. *Tetrahedron Lett.* **2001**, *42*, 7759−7761. (e) Sibrian-Vazquez, M.; Hao, E.; Jensen, T. J.; Vicente, G. H. Enhanced Cellular Uptake with a Cobaltacarborane-Porphyrin-HIV-1 Tat 48–60 Conjugate. *Bioconjugate Chem.* **2006**, *17*, 928–934. (f) Koo, M.-S.; Ozawa, T.; Santos, R. A.; Lamborn, K. R.; Bollen, A. W.; Deen, D. F.; Kahl, S. B. Synthesis and Comparative Toxicology of a Series of Polyhedral Borane Anion-Substituted Tetraphenyl Porphyrins. *J. Med. Chem.* **2007**, *50*, 820–827. (g) El-Zaria, M. E.; Ban, H. S.; Nakamura, H. Boron-Containing Protoporphyrin IX Derivatives and Their Modification for Boron Neutron Capture Therapy: Synthesis, Characterization, and Comparative In Vitro Toxicity Evaluation. *Chem. Eur. J.* **2010**, *16,* 1543–1552. (h) Bhupathiraju, N. V. S. D. K.; Vicente, M. G. H. Synthesis and Cellular Studies of Polyamine Conjugates of a Mercaptomethyl-carboranylporphyrin. *Bioorg. Med. Chem.* **2013**, *21*, 485–495.

(25) Kahl, S. B.; Koo, M.-S. Synthesis of Tetrakis-carborane-carboxylate Esters of 2,4-Bis-(α,β-dihydroxyethyl)-deuteroporphyrin IX. *J. Chem. Soc., Chem. Commun.* **1990**, 1769–1771.

(26) (a) Hill, J. S.; Kahl, S. B.; Kaye, A. H.; Stylli, S. S.; Koo, M.-S.; Gonzales, M. F.; Vardaxis, N. J.; Johnson, C. I. Selective Tumor Uptake of a Boronated Porphyrin in an Animal Model of Cerebral Glioma. *Proc. Natl. Acad. Sci.* **1992**, *89*, 1785–1789. (b) Dagrosa, M. A.; Viaggi, M.; Rebagliati, R. J.; Batistoni, D.; Kahl, S. B.; Juvenal, G. J.; Pisarev, M. A. Biodistribution of Boron Compounds in as Animal Model of Human Undifferentiated Thyroid Cancer for Boron Neutron Capture Therapy. *Mol. Pharm.* **2005**, *2*, 151–156.

(27) Dagrosa, M. A.; Crivello, M.; Perona, M.; Thorp, S.; Cruz, G. A. S.; Pozzi, E.; Casal,

M.; Thomasz, L.; Cabrini, R.; Kahl, S.; Juvenal, G. J.; Pisarev, M. A. First Evaluation of the Biologic Effectiveness Factors of Boron Neutron Capture Therapy (BNCT) in a Human Colon Carcinoma Cell Line. *Int. J. Radiat. Oncol. Biol. Phys.* **2011**, *79*, 262–268.

(28) Rosenthal, M. A.; Kavar, B.; Hill, J. S.; Morgan, D. J.; Nation, R. L.; Stylli, S. S.; Basser, R. L.; Uren, S.; Geldard, H.; Green, M. D.; Kahl, S. B.; Kaye, A. H. Phase I and Pharmacokinetic Study of Photodynamic Therapy for High-Grade Gliomas Using a Novel Boronated Porphyrin. *J. Clin. Oncol.* **2001**, *19*, 519–524.

(29) Arnér, E. J.; Eriksson, S. Mammalian Deoxyribonucleoside Kinase. *Pharmac. Ther.* **1995**, *67*, 155–186.

(30) (a) Jagarlamudi, K. K.; Shaw, M. Thymidine Kinase 1 as Tumor Biomarker: Technical Advances Offer New Potential to An Old Biomarker. *Biomark. Med.* **2018**, *12*, 1035–1048. (b) Bitter, E. E.; Townsend, M. H.; Erickson, R.; Allen, C.; O´Neill, K. L. Thymidine Kinase 1 Through The Ages: A Comprehensive Review. *Cell Biosci.* **2020**, *10*, 138.

(31) (a) Liao, T. K.; Podrebarac, E. G.; Cheng, C. C. Boron-Substituted Pyrimidines. *J. Am. Chem. Soc.* **1964**, *86*, 1869−1870. (b) Schinazi, R. F.; Prusoff, W. H. Synthesis and Properties of Boron and Silicon Substituted Uracil or 2'-Deoxyuridine. *Tetrahedron Lett.* **1978**, *50*, 4981−4984. (c) Schinazi, R. F.; Prusoff, W. H. Synthesis of 5-(Dihydroxyboryl)-2´-deoxyuridine and Related Boron-Containing Pyrimidines. *J. Org. Chem.* **1985**, *50*, 841–847. (d) Reynolds, R. C.; Trask, T. W.; Sedwick, W. D. 2,4-Dichloro-5-(1-*o*-carboranylmethyl)-6-methylpyrimidine: A Potential Synthon for 5-(1-*o*-carboranylmethyl)pyrimidines. *J. Org. Chem.* **1991**, *56*, 2391−2395. (e) Tjarks, W.; Anisuzzaman, A. K. M.; Liu, L.; Soloway, A. H.; Barth, R. F.; Perkins, D. J.; Adams, D. M. Synthesis and in Vitro Evaluation of Boronated Uridine and Glucose Derivatives for Boron Neutron Capture Therapy. *J. Med. Chem.* **1992**, *35*, 1628–1633. (f) Wyzlic, I. M.; Tjarks, W.; Soloway, A. H.; Anisuzzaman, A. K. M.; Rong, F.-G.;

Barth, R. F. Strategies for the Design and Synthesis of Boronated Nucleic Acid and Protein Components as Potential Delivery Agents for Neutron Capture Therapy. *Int. J. Radiat. Oncol. Biol. Phys.* **1994**, *28*, 1203–1213. (g) Goudgaon, N. M.; El-Kattan, G. F.; Schinazi, R. F. Boron Containing Pyrimidines, Nucleosides, and Oligonucleotides for Neutron Capture Therapy. *Nucleosides Nucleotides* **1994**, *13*, 849–880. (h) Kattan, G. F.; Lesnikowski, Z. J.; Yao, S.; Tanious, F.; Wilson, W. D.; Schinazi, R. F. Carboranyl Oligonucleotides. 2. Synthesis and Physicochemical Properties of Dodecathymidylate Containing 5-(*o*-Carboran-1-yl)-2′-deoxyuridine. *J. Am. Chem. Soc.* **1994**, *116*, 7494−7501. (i) Tjarks, W. The Use of Boron Clusters in The Rational Design of Boronated Nucleosides for Boron Neutron Capture Therapy. *J. Organomet. Chem.* **2000**, *614*–615, 37–47. (j) Al-Madhoun, A. S.; Tjarks, W.; Eriksson, S. The Role of Thymidine Kinases in the Activation of Pyrimidine Nucleoside Analogues. *Mini-Rev. Med. Chem.* **2004**, *4*, 341–350. (k) Nizioł, J.; Zieliński, Z.; Leś, A.; Dąbrowska, M.; Rode, W.; Ruman, T. Synthesis, Reactivity and Biological Activity of N(4)-Boronated Derivatives of 2'-Deoxycytidine. *Bioorg. Med. Chem.* **2014**, *22*, 3906–3912. (l) Nizioł, J.; Uram, Ł.; Szuster, M.; Sekuła, J.; Ruman, T. Biological Activity of N(4)-boronated Derivatives of 2'-Deoxycytidine, Potential Agents for Boron Neutron Capture Therapy. *Bioorg. Med. Chem.* **2015**, *23*, 6297–6304. (m) Novopashina, D. S.; Vorobyeva, M. A.; Venyaminova, A. Recent Advances in the Synthesis of High Boron-Loaded Nucleic Acids for BNCT. *Front. Chem.* **2021**, *9*, 619052.

(32) Al-Madhoun, A. S.; Johnsamuel, J.; Yan, J.; Ji, W.; Wang, J.; Zhuo, J.-C.; Lunato, A. J.; Woollard, J. E.; Hawk, A. E.; Cosquer, G. Y.; Blue, T. E.; Eriksson, S.; Tjarks, W. Synthesis of a Small Library of 3-(Carboranylalkyl)thymidines and Their Biological Evaluation as Substrates for Human Thymidine Kinase 1 and 2. *J. Med. Chem.* **2002**, *45*, 4018–4028.

(33) (a) Al-Madhoun, A. S.; Johnsamuel, J.; Barth, R. F.; Tjarks, W.; Eriksson, S.

Evaluation of Human Thymidine Kinase 1 Substrates as New Candidates for Boron Neutron Capture Therapy. *Cancer Res.* **2004**, *64*, 6280–6286. (b) Barth, R. F.; Yang, W.; Al-Madhoun, A. S.; Johnsamuel, J.; Byun, Y.; Chandra, S.; Smith, D. R.; Tjarks, W.; Eriksson, S. Boron Containing Nucleosides as Potential Delivery Agents for Neutron Capture Therapy of Brain Tumors. *Cancer Res.* **2004**, *64*, 6287–6295. (c) Byun, Y.; Thirumamagal, B. T. S.; Yang, W.; Eriksson, S.; Barth, R. F.; Tjarks, W. Preparation and Biological Evaluation of ^{10}B-Enriched 3-[5-{2-(2,3-dihydroxyprop-1-yl)-o-carboran-1-yl}pentan-1-yl]thymidine (N5-2OH), a New Boron Delivery Agent for Boron Neutron Capture Therapy of Brain Tumors. *J. Med. Chem.* **2006**, *49*, 5513–5523. (d) Tjarks, W.; Tiwari, R.; Byun, Y.; Narayanasamy, S.; Barth, R. F. Carboranyl Thymidine Analogues for Neutron Capture Therapy. *Chem. Commun.* **2007**, 4978–4991. (e) Barth, R. F.; Yang, W.; Wu, G.; Swindall, M.; Byun, Y.; Narayanasamy, S.; Tjarks, W.; Tordoff, K.; Moeschberger, M. L.; Eriksson, S.; Binns, P. J.; Riley, K. J. Thymidine Kinase 1 as a Molecular Target for Boron Neutron Capture Therapy of Brain Tumors. *Proc. Natl. Acad. Sci.* **2008**, *105*, 17493–17497.

(34) (a) Gerner, E. W.; Meyskens, F. L. Polyamines and Cancer: Old Molecules, New Understanding. *Nat. Rev. Cancer*, **2004**, *4*, 781–792. (b) Miller-Fleming, L.; Olin-Sandoval, V.; Campbell, K.; Ralser, M. Remaining Mysteries of Molecular Biology: The Role of Polyamines in the Cell. *J. Mol. Biol.* **2015**, *427*, 3389–3406.

(35) (a) Palmer, A. J.; Wallace, H. M. The Polyamine Transport System as a Target for Anticancer Drug Development. *Amino Acids*, **2010**, *38*, 415–422. (b) Nowotarski, S. L.; Woster, P. M.; Casero, R. A. Polyamines and Cancer: Implications for Chemoprevention and Chemotherapy. *Expert Rev. Mol. Med.* **2013**, *15*, e3. (c) Murray-Stewart, T. R.; Woster, P. M.; Casero, R. A. Targeting Polyamine Metabolism for Cancer Therapy and Prevention. *Biochem. J.* **2016**, *473*, 2937–2953.

(36) (a) Edwards, M. L.; Snyder, R. D.; Stemerick, D. M. Synthesis and DNA-Binding Properties of Polyamine Analogues. *J. Med. Chem.* **1991**, *34*, 2414–2420. (b)

Bergeron, R. J.; McManis, J. S.; Liu, C. Z.; Feng, Y.; Weimar, W. R.; Luchetta, G. R.; Wu, Q.; Ortiz-Ocasio, J.; Vinson, J. R. T.; Kramer, D.; Porter, C. Antiproliferative Properties of Polyamine Analogues: A Structure–Activity Study. *J. Med. Chem.* **1994**, *37*, 3464–3476. (c) Casero, R. A.; Woster, P. M. Terminally Alkylated Polyamine Analogues as Chemotherapeutic Agents. *J. Med. Chem.* **2001**, *44*, 1–26. (d) Casero, R. A.; Marton, L. J. Targeting Polyamine Metabolism and Function in Cancer and Other Hyperproliferative Diseases. *Nat. Rev. Drug Discovery* **2007**, *6*, 373–390. (e) Casero, R. A.; Woster, P. M. Recent Advances in the Development of Polyamine Analogues as Antitumor Agents. *J. Med. Chem.* **2009**, *52*, 4551–4573.

(37) (a) Cai, J.; Soloway, A. H. Synthesis of Carboranyl Polyamines for DNA Targeting. *Tetrahedron Lett.* **1996**, *37*, 9283–9286. (b) Cai, J.; Soloway, A. H.; Barth, R. F.; Adams, D. M.; Hariharan, J. R.; Wyzlic, I. M.; Radcliffe, K. Boron-Containing Polyamines as DNA Targeting Agents for Neutron Capture Therapy of Brain Tumors: Synthesis and Biological Evaluation. *J. Med. Chem.* **1997**, *40*, 3887–3896. (c) Ghaneolhosseini, H.; Tjarks, W.; Sjöberg, S. Synthesis of Novel Boronated Acridines-and Spermidines as Possible Agents for BNCT. *Tetrahedron* **1998**, *54*, 3877–3884. (d) Martin, B.; Possémé, F.; Le Barbier, C.; Carreaux, F.; Carboni, B.; Seiler, N.; Moulinoux, J.-P.; Delcros, J-G. *N*-Benzylpolyamines as Vectors of Boron and Fluorine for Cancer Therapy and Imaging: Synthesis and Biological Evaluation. *J. Med. Chem.* **2001**, *44*, 3653–3664. (e) Pan, X. Q.; Wang, H.; Shukla, S.; Sekido, M.; Adams, D. M.; Tjarks, W.; Barth, R. F.; Lee, R. J. Boron-Containing Folate Receptor-Targeted Liposomes as Potential Delivery Agents for Neutron Capture Therapy. *Bioconjugate Chem.* **2002**, *13*, 435–442. (f) El-Zaria, M. E.; Dörfler, U.; Gabel, D. Synthesis of (Aminoalkylamine)-*N*-aminoalkyl)azanonaborane(11)-Derivatives for Boron Neutron Capture Therapy. *J. Med. Chem.* **2002**, *45*, 5817–5819. (g) Lee, J.-D.; Lee, Y.-J.; Jeong, H.-J.; Lee, J. S.; Lee, C.-H.; Ko, J.; Kang, S. O. Practical Synthesis of Aminoethyl-*o*-carboranes. *Organometallics* **2003**, *22*, 445–449. (h) El-Zaria, M. E.

Synthesis and Biological Evaluation of Novel Azanonaboranes as Potential Agents for Boron Neutron Capture Therapy. *Appl. Organomet. Chem.* **2005**, *19*, 683–689. (i) El-Zaria, M. E.; Genady, A. R.; Gabel, D. Azanonaboranes Containing Imidazole Derivatives for Boron Neutron Capture Therapy: Synthesis, Cheracterization, and In Vitro Toxicity Evaluation. *Chem. Eur. J.* **2006**, *12*, 8084–8089.

(38) Zhuo, J.-C.; Cai, J.; Soloway, A. H.; Barth, R. F.; Adams, D. M.; Ji, W.; Tjarks, W. Synthesis and Biological Evaluation of Boron-Containing Polyamines as Potential Agents for Neutron Capture Therapy of Brain Tumors. *J. Med. Chem.* **1999**, *42*, 1282–1292.

(39) Hattori, Y.; Kusaka, S.; Mukumoto, M.; Ishimura, M.; Ohta, Y.; Takenaka, H.; Uehara, K.; Asano, T.; Suzuki, M.; Masunaga, S.; Ono, K.; Tanimori, S.; Kirihata, M. Synthesis and in Vitro Evaluation of Thiododecaborated α, α-Cycloalkylamino Acids for the Treatment of Malignant Brain Tumors by Boron Neutron Capture Therapy. *Amino Acids* **2014**, *46*, 2715–2720.

(40) Futamura, G.; Kawabata, S.; Nonoguchi, N.; Hiramatsu, R.; Toho, T.; Tanaka, H.; Masunaga, S.; Hattori, Y.; Kirihata, M.; Ono, K.; Kuroiwa, T. Evaluation of a Novel Sodium Borocaptate-Containing Unnatural Amino Acid as a Boron Delivery Agent for Neutron Capture Therapy of the F98 Rat Glioma. *Radiat. Oncol.* **2017**, *12*, 26.

(41) (a) Srivastava, R. R.; Singhaus, R. R.; Kabalka, G. W. 4-Dyhidroxyborylphenyl Analogues of 1-Aminocyclobutanecarboxylic Acids: Potential Boron Neutron Capture Therapy Agents. *J. Org. Chem.* **1999**, *64*, 8495–8500. (b) Kabalka, G. W.; Das, B. C.; Das, S. Synthesis of Novel Boron Containing Unnatural Cyclic Amino Acids as Potential Therapeutic Agents. *Tetrahedron Lett.* **2001**, *42*, 7145–7146. (c) Das, B. C.; Das, S.; Li, G.; Bao, W.; Kabalka, G. W. Synthesis of a Water Soluble Carborane Containing Amino Acid as a Potential Therapeutic Agent. *Synlett* **2001**, *9*, 1419–1420. (d) Kabalka, G. W.; Yao, M.-L. Synthesis of a Potential Boron Neutron Capture Therapy Agent: 1-Aminocyclobutane-1-carboxylic Acid Bearing a

Butylboronic Acid Side Chain. *Synthesis* **2003**, *18*, 2890–2893. (e) Kabalka, G. W.; Yao, M.-L. Synthesis of a Novel Boronated 1-Aminocyclobutanecarboxylic Acid as a Potential Boron Neutron Capture Therapy Agent. *Appl. Organometal. Chem.* **2003**, *17*, 398–402. (f) Kabalka, G. W.; Yao, M.-L.; Navarane, A. Synthesis of a Boronated Amino Acid as a Potential Neutron Therapy Agent: 1-Amino-3-[(dihydroxyboryl)ethyl]-cyclobutanecarboxylic Acid. *Tetrahedron Lett.* **2005**, *46*, 4915–4917. (g) Kabalka, G. W.; Yao, M.-L.; Wu, Z. Hydroboration of Alkene-Containing Hydantoins. *Org. Process Res. Dev.* **2006**, *10*, 1059–1061. (h) Kabalka, G. W.; Yao, M. -L.; Marepally, S. R.; Chandra, S. Biological Evaluation of Boronated Unnatural Amino Acids as New Boron Carriers. *Appl. Radiat. Isot*. **2009**, *67*, S374–S379. (i) Chandra, S.; Barth, R. F.; Haider, S. A.; Yang, W.; Huo, T.; Shaikh, A. L.; Kabalka, G. W. Biodistribution and Subcellular Localization of an Unnatural Boron-Containing Amino Acid (*Cis*-ABCPC) by Imaging Secondary Ion Mass Spectrometry for Neutron Capture Therapy of Melanomas and Gliomas. *PloS One* **2013**, *8*, No. e75377.

(42) (a) Warburg, O. On the Origin of Cancer Cells. *Science* **1956**, *123*, 309-314. (b) Heiden, M. G. V.; Cantley, L. C.; Thompson, C. B. Understanding the Warburg Effect: The Metabolic Requirements of Cell Proliferation. *Science* **2009**, *324*, 1029–1033.

(43) (a) Maurer, J. L.; Serino, A. J.; Hawthorne, M. F. Hydrophilically Augmented Glycosyl Carborane Derivatives for Incorporation in Antibody Conjugation Reagents. *Organometallics.* **1988**, *7*, 2519−2524. (b) Tietze, L. F.; Bothe, U. *Ortho*-Carboranyl Glycosides of Glucose, Mannose, Maltose and Lactose for Cancer Treatment by Boron Neutron-Capture Therapy. *Chem. Eur. J.* **1998**, *7*, 1179−1183. (c) Giovenzana, G. B.; Lay, L.; Monti, D.; Palmisano, G.; Panza, L. Synthesis of Carboranyl Derivatives of Alkynyl Glycosides as Potential BNCT Agents. *Tetrahedron* **1999**, *55*, 14123–14136. (d) Tietze, L. F.; Bothe, U.; Schuberth, I. Preparation of a New Carboranyl Lactoside for the Treatment of Cancer by Boron Neutron Capture

Therapy: Synthesis and Toxicity of Fluoro Carboranyl Glycosides for in Vivo ^{19}F-NMR Spectroscopy. *Chem. Eur. J.* **2000**, *6*, 836−842. (e) Tietze, L. F.; Bothe, U.; Griesbach, U.; Nakaichi, M.; Hasegawa, T.; Nakamura, H.; Yamamoto, Y. Carboranyl Bisglycosides for the Treatment of Cancer by Boron Neutron Capture Therapy. *ChemBioChem* **2001**, *2*, 326−334. (f) Tietze, L. F.; Bothe, U.; Griesbach, U.; Nakaichi, M.; Hasegawa, T.; Nakamura, H.; Yamamoto, Y. *ortho*-Carboranyl Glycosides for the Treatment of Cancer by Boron Neutron Capture Therapy. *Bioorg. Med. Chem.* **2001**, *9*, 1747–1752. (g) Tietze, L. F.; Griesbach, U.; Schuberth, I.; Bothe, U.; Marra, A.; Dondoni, A. Novel Carboranyl *C*-Glycosides for the Treatment of Cancer by Boron Neutron Capture Therapy. *Chem. Eur. J.* **2003**, *9*, 1296–1302. (h) Ronchi, S.; Prosperi, D.; Compostella, F.; Panza, L. Synthesis of Novel Carborane-hybrids Based on a Trizine Scaffold for Boron Neutron Capture Therapy. *Synlett* **2004**, *6*,1007−1010. (i) Orlova, A. V.; Kononov, L. O.; Kimel, B. G.; Sivaev, I. B.; Bregadze, V. I. Conjugates of Polyhedral Boron Compounds with Carbohydrates. 4. Hydrolytic Stability of Carborane-Lactose Conjugates Depends on the Structure of a Spacer between Carborane Cage and Sugar Moiety. *Appl. Organomet. Chem.* **2006**, *20*, 416–420. (j) Satapathy, R.; Dash, B. P.; Bode, B. P.; Byczynski, E. A.; Hosmane, S. N.; Bux, S.; Hosmane, N. S. New Classes of Carborane-appended 5-Thio-D-glucopyranose Derivatives. *Dalton Trans.* **2012**, *41*, 8982–8988.

(44) (a) Thimon, C.; Panza, L.; Morin, C. Synthesis of a Glycosylated *ortho*-Carboranyl Amino Acid. *Synlett* **2003**, *34*, 1399−1402. (b) Ronchi, S.; Prosperi, D.; Thimon, C.; Morin, C.; Panza, L. Synthesis of Mono- and Bisglucuronoylated Carboranes. *Tetrahedron Asymmetry* **2005**, *16*, 39−44. (c) Imperio, D.; Del Grosso, E. D.; Fallarini, S.; Lombardi, G.; Panza, L. Synthesis of Suger-Boronic Acid Derivatives: A Class of Potential Agents for Boron Neutron Capture Therapy. *Org. Lett.* **2017**, *19*, 1678–1681. (d) Imperio, D.; Muz, B.; Azab, A. K.; Fallarini, S.; Lombardi, G.; Panza, L. A Short and Convenient Synthesis of *closo*-Dodecaborate Sugar Conjugates. *Eur. J. Org.*

Chem. **2019**, 7228–7232. (e) Imperio, D.; Del Grosso, E.; Fallarini, S.; Lombardi, G.; Panza, L. Anomeric Sugar Boronic Acid Analogues as Potential Agents for Boron Neutron Capture Therapy. *Beilstein J. Org. Chem.* **2019**, *15*, 1355–1359.

(45) (a) Lechtenberg, B.; Gabel, D. Synthesis of $(B_{12}H_{11}S)^{2-}$ Containing Glucuronoside as Potential Prodrug for BNCT. *J. Organomet. Chem.* **2005**, *690*, 2780–2782. (b) Genady, A. R.; El-Zaria, M. E. Novel Glycosylated Carboranylquinazolines for Boron Neutron Capture Therapy of Tumors: Synthesis, Characterization, and *in Vitro* Toxicity Studies. *Appl. Organomet. Chem.* **2008**, *22*, 227–232. (c) Tsurubuchi, T.; Shirakawa, M.; Kurosawa, W.; Matsumoto, K.; Ubagai, R.; Umishio, H.; Suga, Y.; Yamazaki, J.; Arakawa, A.; Maruyama, Y.; Seki, T.; Shibui, Y.; Yoshida, F.; Zaboronok, A.; Suzuki, M.; Sakurai, Y.; Tanaka, H.; Nakai, K.; Ishikawa, E.; Matsumura, A. Evaluation of a Novel Boron-Containing α-D-Mannopyranoside for BNCT. *Cells* **2020**, *9*, 1277.

(46) Tanaka, T.; Sawamoto, Y.; Aoki, S. Concise and Versatile Synthesis of Sulfoquinovosyl Acyl Glycerol Derivatives for Biological Applications. *Chem. Pharm. Bull.* **2017**, *65*, 566–572.

(47) Itoh, T.; Tamura, K.; Ueda, H.; Tanaka, T.; Sato, K.; Kuroda, R.; Aoki, S. Design and Synthesis of Boron Containing Monosaccharides by the Hydroboration of D-Glucal for Use in Boron Neutron Capture Therapy (BNCT). *Bioorg. Med. Chem.* **2018**, *26*, 5922–5933.

(48) (a) Ahrens, V. M.; Frank, R.; Boehnke, S.; Schütz, C. L.; Hampel, G.; Iffland, D. S.; Bings, N. H.; Hey-Hawkins, E.; Beck-Sickinger, A. G. Receptor-Mediated Uptake of Boron-Rich Neuropeptide Y Analogues for Boron Neutron Capture Therapy. *ChemMedChem* **2015**, *10*, 164–172. (b) Isono, A.; Tsuji, M.; Sanada, Y.; Matsushita, A.; Masunaga, S.; Hirayama, T.; Nagasawa, H. Design, Synthesis, and Evaluation of Lipopeptide Conjugates of Mercaptoundecahydrododecaborate for Boron Neutron Capture Therapy. *ChemMedChem* **2019**, *14*, 823–832. (c) Nakase, I.; Katayama, M.;

Hattori, Y.; Ishimura, M.; Inaura, S.; Fujiwara, D.; Takatani-Nakase, T.; Fujii, I.; Futaki, S.; Kirihata, M. Intracellular Target Delivery of Cell-penetrating Peptide-conjugated Dodecaborate for Boron Neutron Capture Therapy (BNCT). *Chem. Commun.* **2019**, *55*, 13955–13958. (d) Kawai, K.; Nishimura, K.; Okada, S.; Sato, S.; Suzuki, M.; Takata, T.; Nakamura, H. Cyclic RGD-Functionalized *closo*-Dodecaborate Albumine Conjugates as Integrin Targeting Boron Carriers for Neutron Capture Therapy. *Mol. Pharmaceutics* **2020**, *17*, 3740–3747.

(49) (a) Miyajima, Y.; Nakamura, H.; Kuwata, Y.; Lee, J.-D.; Masunaga, S.; Ono, K.; Maruyama, K. Transferrin-Loaded *nido*-Carborane Liposomes: Tumor-Targeting Boron Delivery System for Neutron Capture Therapy. *Bioconjugate Chem.* **2006**, *17*, 1314–1320. (b) Nakamura, H. Liposomal Boron Delivery for Neutron Capture Therapy. *Academic Press,* **2009**, *465*, 179–208. (c) Ueno, M.; Ban, H. S.; Nakai, K.; Inomata, R.; Kaneda, Y.; Matsumura, A.; Nakamura, H. Dodecaborate Lipid Liposomes as New Vehicles for Boron Delivery System of Neutron Capture Therapy. *Bioorg. Med. Chem.* **2010**, *18*, 3059–3065. (d) Koganei, H.; Tachikawa, S.; El-Zaria, M. E.; Nakamura, H. Synthesis of Oligo-*closo*-dodecaborates by Hüisgen Click Reaction as Encapsulated Agents for the Preparation of High-boron-content Liposomes for Neutron Capture Therapy. *New J. Chem.* **2015**, *39*, 6388–6394. (e) Luderer, M. J.; Muz, B.; Alhallak, K.; Sun, J.; Wasden, K.; Guenther, N.; Puente, P.; Federico, C.; Azab, A. K. Thermal Sensitive Liposomes Improve Delivery of Boronated Agents for Boron Neutron Capture Therapy. *Pharm. Res.* **2019**, *36*, 144.

(50) (a) Ali, F.; Hosmane, N. S.; Zhu, Y. Boron Chemistry for Medical Applications. *Molecules* **2020**, *25*, 828. (b) Pitto-Barry, A. Polymers and Boron Neutron Capture Therapy (BNCT): A Potent Combination. *Polym. Chem.* **2021**, *12*, 2035–2044.

(51) (a) Paxton, R. J.; Beatty, B. G.; Varadarajan, A.; Hawthorne, M. F. Carboranyl Peptide-Antibody Conjugates for Neutron Capture Therapy: Preparation, Characterization, and in Vivo Evaluation. *Bioconjugate Chem.* **1992**, *3*, 241–247. (b)

Barth, R. F.; Adams, D. M.; Soloway, A. H.; Alam, F.; Darby, M. V. Boronated Starburst Dendrimer-Monoclonal Antibody Immunoconjugates: Evaluation as a Potential Delivery System for Neutron Capture Therapy. *Bioconjugate Chem.* **1994**, *5*, 58–66. (c) Wu, G.; Barth, R. F.; Yang, W.; Chatterjee, M.; Tjarks, W.; Ciesielski, M. J.; Fenstermaker, R. A. Site-Specific Conjugation of Boron-Containing Dendrimers to Anti-EGF Receptor Monoclonal Antibody Cetuximab (IMC-C225) and Its Evaluation as a Potential Delivery Agent for Neutron Capture Therapy. *Bioconjugate Chem.* **2004**, *15*, 185–194.

(52) (a) Wyzlic, I. M.; Soloway, A. H. A General, Convenient Way to Carborane-Containing Amino Acids for Boron Neutron Capture Therapy. *Tetrahedron Lett.* **1992**, *33*, 7489−7490. (b) Nemoto, H.; Iwamoto, S.; Nakamura, H.; Yamamoto, Y. A New Water-soluble p-Boronophenylalanine Derivatives for Neutron Capture Therapy. *Chem. Lett.* **1993**, *22*, 465−468. (c) Prashar, J. K.; Moore, D. E. Synthesis of Carboranyl Phenylalanine for Potential Use in Neutron Capture Therapy of Melanoma. *J. Chem. Soc., Perkin. Trans. 1* **1993**, 1051−1053. (d) Karnbrock, W.; Musiol, H.-J.; Moroder, L. Enantioselective Synthesis of *S*-*o*-Carboranylalanine via Methylated Bislactim Ethers of 2,5-Diketopiperazines. *Tetrahedron* **1995**, *51*, 1187–1196. (e) Denniel, V.; Bauchat, P.; Danion, D.; Danion-Bougot, R. Hydroboration of Vinylglycine and Allylglycine as a Route to Boron-derivatives of α-Amino Acids. *Tetrahedron Lett.* **1996**, *37*, 5111–5114. (f) Radel, P. A.; Kahl, S. B. Enantioselective Synthesis of L- and D-Carboranylalanine. *J. Org. Chem.* **1996**, *61*, 4582–4588. (g) Hattori, Y.; Kusaka, S.; Mukumoto, M.; Uehara, K.; Asano, T.; Suzuki, M.; Masunaga, S.; Ono, K.; Tanimori, S.; Kirihata, M. Biological Evaluation of Dodecaborate-Containing L-Amino Acids for Boron Neutron Capture Therapy. *J. Med. Chem*. **2012**, *55*, 6980–6984. (h) Li, R.; Zhang, J.; Guo, J.; Xu, Y.; Duan, K.; Zheng, J.; Wan, H.; Yuan, Z.; Chen, H. Application of Nitroimidazole–Carborane-Modified Phenylalanine Derivatives as Dual-Target Boron Carriers in Boron Neutron Capture

Therapy. *Mol. Pharmaceutics.* **2020**, *17*, 202–211. (i) Laskova, J.; Kosenko, I.; Ananyev, I.; Stogniy, M.; Sivaev, I.; Bregadze, V. ″Free of Base″ Sulfa-Michael Addition for Novel *o*-Carboranyl-DL-Cysteine Synthesis. *Crystals.* **2020**, *10*, 1133.

(53) (a) Danhier, F.; Feron, O.; Préat, V. To Exploit The Tumor Microenvironment: Passive and Active Tumor Targeting of Nanocarriers for Anti-Cancer Drug Delivery. *J. Contr. Rel.* **2010**, *148*, 135–146. (b) Kikuchi, S.; Kanoh, D.; Sato, S.; Sakurai, Y.; Suzuki, M.; Nakamura, H. Maleimide-Functionalized *closo*-Dodecaborate Albumin Conjugates (MID-AC): Unique Ligation at Cysteine and Lysine Residues Enables Efficient Boron Delivery to Tumor for Neutron Capture Therapy. *J. Control. Release* **2016**, *237*, 160–167. (c) Sato, S.; Ishii, S.; Nakamura, H. Development of Albumin-closo-Dodecaborate Conjugates as Boron Carriers for Neutron-Capture Therapy Ru(bpy)3-Photocatalyzed Modification of Thyrosin. *Eur. J. Inorg. Chem.* **2017**, 4406–4410. (d) Nakamura, H.; Kikuchi, S.; Kawai, K.; Ishii, S.; Sato, S. *closo*-Dodecaborate-Conjugated Human Serum Albumins: Preparation and in vivo Selective Boron Delivery to Tumor. *Pure Appl. Chem.* **2018**, *90*, 745–753. (e) Ishii, S.; Sato, S.; Asami, H.; Hasegawa, T.; Kohno, J.; Nakamura, H. Design of S–S Bond Containing Maleimide-Conjugated *closo*-Dodecaborate (SSMID): Identification of Unique Modification Sites on Albumin and Investigation of Intracellular Uptake. O*rg. Biomol. Chem.* **2019**, *17*, 5496–5499. (f) Matsumura, Y. Cancer Stromal Targeting Therapy to Overcome The Pitfall of EPR Effect. *Adv. Drug Deliv. Rev.* **2020**, *154–*155, 142–150.

(54) Kitamura, M.; Suzuki, T.; Abe, R.; Ueno, T.; Aoki, S. ^{11}B NMR Sensing of d-Block Metal Ions in Vitro and in Cells Based on the Carbon-Boron Bond Cleavage of Phenylboronic Acid-Pendant Cyclen (Cyclen = 1,4,7,10-Tertaazacyclododecane). *Inorg. Chem*. **2011**, *50*, 11568–11580.

(55) (a) Tanaka, T.; Nishiura, Y.; Araki, R.; Saido, T.; Abe, R.; Aoki, S. ^{11}B NMR Probes of Copper(II): Finding and Implications of the Cu^{2+}-Promoted Decomposition of

ortho-Carborane Derivatives. *Eur. J. Inorg. Chem.* **2016**, 1819–1834. (b) Tanaka, T.; Araki, R.; Saido, T.; Abe, R.; Aoki, S. ^{11}B NMR/MRI Sensing of Copper(II) Ions In Vitro by the Decomposition of a Hybrid Compound of a *nido*-*o*-Carborane and a Metal Chelator. *Eur. J. Inorg. Chem.* **2016**, 3330–3337.

(56) (a) Mislick, K. A.; Baldeschwieler, J. D. Evidence for the Role of Proteoglycans in Cation-Mediated Gene Transfer. *Proc. Natl. Acad. Sci. U.S.A.* **1996**, *93*, 12349–12354. (b) Belting, M.; Persson, S.; Fransson, L.-Å. Proteoglycan Involvement in Polyamine Uptake. *Biochem. J.* **1999**, *338*, 317–323. (c) Belting, M.; Mani, K.; Jönsson, M.; Cheng, F.; Sandgren, S.; Jonsson, S.; Ding, K.; Delcros, J.-G.; Fransson, L.-Å. Glypican-1 Is a Vehicle for Polyamine Uptake in Mammalian Cells. *J. Biol. Chem.* **2003**, *278*, 47181–47189. (d) Welch, J. E.; Bengtson, P.; Svensson, K.; Wittrup, A.; Jenniskens, G. J.; Ten Dam, G. B.; Van Kuppevelt, T. H.; Belting, M. Single Chain Fragment Anti-heparan Sulfate Antibody Targets the Polyamine Transport System and Attenuates Polyamine-Dependent Cell Proliferation. *Int. J. Oncol.* **2008**, *32*, 749–756. (e) Uemura, T.; Stringer, D. E.; Blohm-Mangone, K. A.; Gerner, E. W. Polyamine Transport is Mediated by Both Endocytic and Solute Carrier Transport Mechanisms in the Gastrointestinal Tract. *Am. J. Physiol.: Gastrointest. Liver Physiol.* **2010**, *299*, G517–G522. (f) Christianson, H. C.; Belting, M. Heparin Sulfate Proteoglycan as a Cell-surface Endocytosis Receptor. *Matrix Biol.* **2014**, *35*, 51–55. (g) Abdulhussein, A. A.; Wallace, H. M. Polyamines and Membrane Transporters. *Amino Acids* **2014**, *46*, 655–660. (h) Nikitovic, D.; Berdiaki, A.; Spyridaki, I.; Krasanakis, T.; Tsatsakis, A.; Tzanakakis, G. N. Proteoglycans–Biomarkers and Targets in Cancer Therapy. *Front. Endocrinol.* **2018**, *9*, 69.

(57) It is reported that macrocyclic polyamine-modified lipids and chitosan are utilized for gene transfection. See: (a) Li, C.; Tian, H.; Rong, N.; Liu, K.; Liu, F.; Zhu, Y.; Qiao, R.; Jiang, Y. Chitosan Grafted with Macrocyclic Polyamines on C-2 and C-6 Positions as Nonviral Gene Vectors: Preparation, Characterization, and In Vitro

Transfection Studies. *Biomacromolecules* **2011**, *12*, 298–305. (b) Li, L.; Zhao, F.; Zhao, B.; Zhang, J.; Li, C.; Qiao, R. Chitosan Grafted with Phosphorylcholine and Macrocyclic Polyamine as an Effective Gene Delivery Vector: Preparation, Characterization, and In Vitro Transfection. *Macromol. Biosci.* **2015**, *15*, 912–926. (c) Chang, D.-C.; Zhang, Y.-M.; Zhang, J.; Liu, Y.-H.; Yu, X.-Q. Cationic Lipids with a Cyclen Headgroup: Synthesis and Structure–Activity Relationship Studies as Non-viral Gene Vectors. *RSC Adv.* **2017**, *7*, 18681–18689.

(58) (a) Yang, R.; Zompa, L. J. Metal Complexes of Cyclic Triamines. 1. Complexes of 1,4,7-Triazacyclononane ([9]aneN_3) with Nickel(II), Copper(II), and Zinc(II). *Inorg. Chem.* **1976**, *15*, 1499–1502. (b) Kimura, E. Macrocyclic Polyamines as Biological Cation and Anion Complexones – An Application to Calculi Dissolution. *Biomimetic and Bioorganic Chemistry: Topics in Current Chemistry:* Springer, **1985**; Vol. 128, 113–141.

(59) (a) Kodama, M.; Kimura, E. Thermodynamic and Kinetic Effects of 12-Membered Macrocycles Polarographic Studies of 1,4,7,10-Tetra-azacyclododecanecopper(II). *J. Chem. Soc., Dalton Trans.* **1976**, 116–120. (b) Ohshima, R.; Kitamura, M.; Morita, A.; Shiro, M.; Yamada, Y.; Ikekita, M.; Kimura, E.; Aoki, S. Design and Synthesis of a Fluorescent Probe for Zn^{2+}, 5,7-Bis(*N*,*N*-dimethylaminosulfonyl)-8-hydroxyquinoline-Pendant 1,4,7,10-Tetraazacyclododecane and Zn^{2+}-Dependent Hydrolytic and Zn^{2+}-Independent Photochemical Reactivation of Its Benzenesulfonyl-Caged Derivative. *Inorg. Chem*. **2010**, *49*, 888–899.

(60) Kodama, M.; Kimura, E. Effects of Cyclization and Ring Size on Complex Formation Between Penta-amine Ligands and Copper(II). *J. Chem. Soc., Dalton Trans.* **1978**, 104–110.

(61) (a) Kodama, M.; Kimura, E. Equilibria of Complex Formation Between Several Bivalent Metal Ions and Macrocyclic Tri- and Penta-amines. *J. Chem. Soc., Dalton Trans.* **1978**, 1081–1085. (b) Kimura, E.; Yatsunami, T. Synthesis of Some Cyclic

Derivatives of Spermidine and Spermine. *Chem. Pharm. Bull.* **1980**, *28*, 994–997. (c) Diez-Castellnou, M.; Salassa, G.; Mancin, F.; Scrimin, P. The Zn(II)-1,4,7-Trimethyl-1,4,7-Triazacyclononane Complex: A Monometallic Catalyst Active in Two Protonation States. *Front. Chem.* **2019**, *7*, 469. (d) Savastano, M.; Fiaschi, M.; Ferraro, G.; Gratteri, P.; Mariani, P.; Bianchi, A.; Bazzicalupi, C. Sensing Zn^{2+} in Aqueous Solution with a Fluorescent Scorpiand Macrocyclic Ligand Decorated with an Anthracene Bearing Tail. *Molecules.* **2020**, *25*, 1355.

(62) (a) Kimura, E. Model Studies for Molecular Recognition of Carbonic Anhydrase and Carboxypeptidase. *Acc. Chem. Res.* **2001**, *34*, 171–179. (b) Aoki, S.; Kagata, D.; Shiro, M.; Takeda, K.; Kimura, E. Metal Chelation-Controlled Twisted Intramolecular Charge Transfer and Its Application to Fluorescent Sensing of Metal Ions and Anions. *J. Am. Chem. Soc.* **2004**, *126*, 13377–13390. (c) Aoki, S.; Zulkefeli, M.; Kitamura, M.; Hisamatsu, Y. Supramolecular Host and Catalysts Formed by the Synergistic Molecular Assembly of Multinuclear Zinc(II) Complexes in Aqueous Solution. In *Synergy in Supramolecular Chemistry;* Nabeshima, T., Ed.; CRC: Boca Raton, FL, USA, 2015; pp 33–56. (d) Kimura, E.; Koike, T.; Aoki, S. Evolution of Zn^{II}–Macrocyclic Polyamines to Biological Probes and Supramolecular Assembly. In *Macrocyclic and Supramolecular Chemistry: How Izatt-Christensen Award Winners Shaped the Field*; Izatt, R. M., Ed.; John Wiley & Sons: Hoboken, NJ, USA, 2016; pp 417–445.

(63) (a) Kimura, E. Evolution of Macrocyclic Polyamines from Molecular Science to Supramolecular Science. *Bull. Jpn. Soc. Coord. Chem.* **2012**, *59*, 26–47. (b) Itoh, S.; Sonoike, S.; Kitamura, M.; Aoki, S. Design and Synthesis of Chiral Zn^{2+} Complexes Mimicking Natural Aldolases for Catalytic C–C Bond Forming Reactions in Aqueous Solution. *Int. J. Mol. Sci.* **2014**, *15*, 2087–2118.

(64) (a) Inouye, Y.; Kanamori, T.; Yoshida, T.; Bu, X.; Shionoya, M.; Koike, T.; Kimura, E. Inhibition of Human Immunodeficiency Virus Proliferation by Macrocyclic

Polyamines and Their Metal Complexes. *Biol. Pharm. Bull.*, **1994**, *17*, 243–250. (b) Inouye, Y.; Kanamori, T.; Yoshida, T.; Koike, T.; Shionoya, M.; Fujioka, H.; Kimura, E. Differential Contribution of Metal Complexation and Dimerization to the Chemotherapeutic Potential of Bicyclen-Zn^{II}_2 Complex against Human Immunodeficiency Virus. *Biol. Pharm. Bull.*, **1996**, *19*, 456–458.

(65) (a) Shionoya, M.; Kimura, E.; Shiro, M. A New Ternary Zinc(II) Complex with [12]aneN_4 (= 1,4,7,10-Tetraazacyclododecane) and AZT (= 3'-Azido-3'-deoxythymine). Highly Selective Recognition of Thymidine and Its Related Nucleosides by a Zinc(II) Macrocyclic Tetraamine Complex with Novel Complementary Associations. *J. Am. Chem. Soc*. **1993**, *115*, 6730–6737. (b) Kikuta, E.; Murata, M.; Katsube, N.; Koike, T.; Kimura, E. Novel Recognition of Thymine Base in Double-Stranded DNA by Zinc(II)–Macrocyclic Tetraamine Complexes Appended with Aromatic Groups. *J. Am. Chem. Soc*. **1999**, *121*, 5426–5436. (c) Kimura, E.; Kikuta, E. Why Zinc in Zinc Enzymes? From Biological Roles to DNA Based-Selective Recognition. *J. Biol. Inorg. Chem.* **2000**, *5*, 139–155. (d) Kimura, E.; Kikuta, E. Macrocyclic Zinc(II) Complexes for Selective Recognition of Nucleobases in Single- and Double-Stranded Polynucleotides. *Prog. React. Kinet. Mech.* **2000**, *25*, 1–64. (e) Aoki, S.; Kimura, E. Zinc–Nucleic Acid Interaction. *Chem. Rev*. **2004**, *104*, 769–788. (f) del Mundo, I. M.; Siters, K. E.; Fountain, M. A.; Morrow, J. R. Structural Basis for Bifunctional Zinc(II) Macrocyclic Complex Recognition of Thymine Bulges in DNA. *Inorg. Chem.* **2012**, *51*, 5444–5457.

(66) (a) Richman, J. E.; Atkins, T. J. Nitrogen Analogs of Crown Ethers. *J. Am. Chem. Soc.* **1974**, *96*, 2268–2270. (b) Atkins, T. J.; Richman, J. E.; Oettle, W. F. Macrocyclic Polyamines: 1,4,7,10,13,16-Hexaazacyclooctadecane. *Org. Synth.* **2003**, *6*, 652. (c) Cao, R.; Müller, P.; Lippard, S. J. Tripodal Tris-tacn and Tris-dpa Platforms for Assembling Phosphate-Templated Trimetallic Centers. *J. Am. Chem. Soc.* **2010**, *132*, 17366–17369. (d) Brown, A; Bunchuay, T.; Crane, C. G.; White, N.

G.; Thompson, A. L.; Beer, P. D. A Bis-Triazacyclononane Tris-Pyridyl N_9-Azacryptand "Beer Can" Receptor for Completion of Alkali Metal and Lead(II) Cations. *Chem. Eur. J*. **2018**, *24*, 10434–10442.

(67) Pieters, G.; Cazzolaro, A.; Bonomi, R.; Prins, L. J. Self-assembly and Selective Exchange of Oligoanions on the Surface of Monolayer Protected Au Nanoparticles in Water. *Chem. Commun*. **2012**, *48*, 1916–1918.

(68) (a) Qu, D.-H.; Wang, Q.-C.; Ren, J.; Tian, H. A Light-Driven Rotaxane Molecular Shuttle with Dual Fluorescence Addresses. *Org. Lett.* **2004***, 6,* 2085–2088. (b) Liu, Y.; Zhang, S.; Miao, Q.; Zheng, L.; Zong, L.; Cheng, Y. Fluorescent Chemosensory Conjugated Polymers Based on Optically Active Polybinaphthyls and 2,2'-Bipyridyl Units. *Macromolecules* **2007**, *40*, 4839–4847.

(69) (a) Corey, E. J.; Danheiser, R. L.; Chandrasekaran, S. New Reagents for the Intermolecular Pinacolic Coupling of Ketones and Aldehydes. *J. Org. Chem.* **1976**, *41*, 260–265. (b) Chen, C.-Y.; Chen, C.-T. Reaction-Based and Single Fluorescent Emitter Decorated Ratiometric Nanoprobe to Detect Hydrogen Peroxide. *Chem. Eur. J*. **2013**, *19*, 16050–16057.

(70) Cappuccio, F. E.; Suri, J. T.; Cordes, D. B.; Wessling, R. A.; Singaram, B. Evaluation of Pyranine Derivatives in Boronic Acid Based Saccharide Sensing: Significance of Charge Interaction Between Dye and Quencher in Solution and Hydrogel. *J. Fluoresc.* **2004***, 14,* 521–533.

(71) (a) Takeuchi, M.; Mizuno, T.; Shinmori, H.; Nakashima, M.; Shinkai, S. Fluorescence and CD Spectroscopic Sugar Sensing by a Cyanine-appended Diboronic Acid Probe. *Tetrahedron* **1996***, 52,* 1195–1204. (b) Pathak, R.; Nhlapo, J. M.; Govender, S.; Michael, J. P.; van Otterlo, W. A. L.; de Koning, C. B. A Concise Synthesis of Novel Naphtho[α]carbazoles and Benzo[*c*]carbazoles. *Tetrahedron* **2006***, 62,* 2820–2830.

(72) Kimura, E.; Aoki, S.; Koike, T.; Shiro, M. A Tris(Zn^{II}–1,4,7,10-

tetraazacyclododecane) Complex as a New Receptor for Phosphate Dianions in Aqueous Solution. *J. Am. Chem. Soc.* **1997**, *119*, 3068–3076.

(73) (a) Itoh, S.; Kitamura, M.; Yamada, Y.; Aoki, S. Chiral Catalysts Dually Functionalized with Amino Acid an Zn^{2+} Complex Components for Enantioselective Direct Aldol Reactions Inspired by Natural Aldolases: Design, Synthesis, Complexation Properties, Catalytic Activities, and Mechanistic Study. *Chem. Eur. J.* **2009**, *15*, 10570–10584. (b) Itoh, S.; Sonoike, S.; Kitamura, M.; Aoki, S. Design and Synthesis of Chiral Zn^{2+} Complexes Mimicking Natural Aldolases for Catalytic C–C Bond Forming Reactions in Aqueous Solution. *Int. J. Mol. Sci.* **2014**, *15*, 2087–2118.

(74) Rodal, S. K.; Skretting, G.; Garred, Ø.; Vilhardt, F.; van Deurs, B.; Sandvig, K. Extraction of Cholesterol with Methyl-β-Cyclodextrin Perturbs Formation of Clathrin-Coated Endocytic Vesicles. *Mol. Biol. Cell.* **1999**, *10*, 961–974.

(75) (a) Macia, E.; Ehrlich, M.; Massol, R.; Boucrot, E.; Brunner, C.; Kirchhausen, T. Dynasore, a Cell-Permeable Inhibitor of Dynamin. *Dev. Cell* **2006**, *10*, 839–850. (b) Dutta, D.; Donaldson, J. G. Search for Inhibitors of Endocytosis. *Cell. Logist.* **2012**, *2*, 203–208.

(76) (a) Lagana, A.; Vadnais, J.; Le, P. U.; Nguyen, T. N.; Laprade, R.; Nabi, I. R.; Noël, J. Regulation of the Formation of Tumor Cell Pseudopodia by the Na^+/H^+ Exchanger NHE1. *J. Cell Sci*. **2000**, *113*, 3649–3662. (b) Koivusalo, M.; Welch, C.; Hayashi, H.; Scott, C. C.; Kim, M.; Alexander, T.; Touret, N.; Hahn, K. M.; Grinstein, S. Amiloride Inhibits Micropinocytosis by Lowering Submembranous pH and Preventing Rac1 and Cdc42 Signaling. *J. Cell Biol.* **2010**, *188*, 547–563.

(77) (a) Schneider, C. A.; Rasband, W. S.; Eliceiri, K. W. NIH Image to ImageJ: 25 Years of Image Analysis. *Nat. Methods.* **2012**, *9*, 671–675. (b) Guzmán, C.; Bagga, M.; Kaur, A.; Westermarck, J.; Abankwa, D. ColonyArea: An ImageJ Plugin to Automatically Quantify Colony Formation in Clonogenic Assays. *PloS One* **2014**, *9*,

No. e92444.

(78) (a) Hartman, T.; Carlsson, J. Radiation Dose Heterogeneity in Receptor and Antigen Mediated Boron Neutron Capture Therapy. *Radiother. Oncol.* **1994**, *31*, 61–75. (b) Ono, K.; Tanaka, H.; Tamari, Y.; Watanabe, T.; Suzuki, M.; Masunaga, S. Proposal for Determining Absolute Biological Effectiveness of Boron Neutron Capture Therapy—the Effect of $^{10}B(n,\alpha)^{7}Li$ Dose can be Predicted from the Nucleocytoplasmic Ratio or the Cell Size. *J. Radiat. Res.* **2019**, *60*, 29–36.

(79) (a) Kimura, E.; Ikeda, T.; Aoki, S.; Shionoya, M. Macrocylic Zinc(II) Complexes for Selective Recognition of Nucleobases in Single- and Double-Stranded Polynucleotides. *J. Biol. Inorg. Chem.* **1998**, *3*, 259–267. (b) Zulkefeli, M.; Sogon, T.; Takeda, K.; Kimura, E.; Aoki, S. Design and Synthesis of a Stable Supramolecular Trigonal Prism Formed by the Self-Assembly of a Linear Tetrakis(Zn^{2+}—cyclen) Complex and Trianionic Trithiocyanuric Acid in Aqueous Solution and Its Complexation with DNA (Cyclen = 1,4,7,10-Tetraazacyclododecane). *Inorg. Chem.* **2009**, *48*, 9567–9578. (c) Kimura, E.; Kitamura, H.; Ohtani, K.; Koike, T. Elaboration of Selective and Efficient Recognition of Thymidine Beas in Dinucleotides (TpT, ApT, CpT, and GpT), Single-Stranded d(GTGACGCC), and Double-Stranded $d(CGCTAGCG)_2$ by Zn^{2+}—Acridinylcyclen (Acridinylcyclen = (9-Acridinyl)methyl-1,4,7,10-tetraazacyclododecane) *J. Am. Chem. Soc.* **2000**, *122*, 4668–4677.

(80) Aoki, S.; Kikuchi, C.; Kitagawa, Y.; Hasegawa, Y.; Sonoike, S.; Saga, Y.; Hatanaka, M. Evaluation of Zn^{2+} Coordination Structures in Chiral Zn^{2+} Complexes Based on Shape Measurement Factors: Relationships between Activity and the Coordination Structure. *Eur. J. Inorg. Chem.* **2019**, 4740–4751.

(81) The complexation properties of metal-free [15]aneN_5 and larger macrocyclic polyamines with organic anions were reported in Refs. 58b, 63 and 82. On the other hand, the complexation of their Zn^{2+} complexes with dT and other imide-type

guest molecules is yet to be studied. To the best of our knowledge, this is the first observation of the electrostatic interaction of Zn^{2+}–[15]aneN_5 complexes with the double-stranded DNA and the details will be reported elsewhere (we consider that it is not easy to directly and quantitatively compare the affinity of ctDNA with these B-carriers, which exhibit different interaction modes with DNA).

(82) (a) Lehn, J. M. *Supramolecular Chemistry: Concepts and Perspectives*; VCH: Weinheim, New York, 1995. (b) Kimura, E. Macrocyclic Polyamines as Biological Cation and Anion Complexones: An Application to Calculi Dissolution, Biomimetic and Bioorganic Chemistry; Topics in Current Chemistry; Springer-Verlag Berlin: Heidelberg, 1985; Vol. 128, pp 113–141. (c) Kimura, E. Macrocyclic Polyamines with Intelligent Functions, *Tetrahedron*, **1992**, *48*, 6175–6217.

(83) Hawthorne, M. F.; Lee, M. W. A Critical Assessment of Boron Target Compounds for Boron Neutron Capture Therapy. *J. Neuro. Oncol.* **2003**, *62*, 33–45.

(84) (a) Aoki, S.; Sugimura, C.; Kimura, E. Efficient Inhibition of Photo[2 + 2]cycloaddition of Thymidilyl(3′–5′)thymidine and Promotion of Photosplitting of the *cis-syn*-Cyclobutane Thymine Dimer by Dimeric Zinc(II)–Cyclen Complexes Containing *m*- and *p*-Xylyl Spacers. *J. Am. Chem. Soc*. **1998**, *120*, 10094–10102. (b) Kimura, E.; Kikuchi, M.; Kitamura, H.; Koike, T. Selective and Efficient Recognition of Thymidylylthymidine (TpT) by Bis(Zn^{II}–Cyclen) and Thymidylylthymidylylthymidine (TpTpT) by Tris(Zn^{II}–Cyclen) at Neutral pH in Aqueous Solution. *Chem. Eur. J.* **1999**, *5*, 3113–3123. (c) Aoki, S.; Kimura, E. Highly Selective Recognition of Thymidine Mono- and Diphosphate Nucleotides in Aqueous Solution by Ditopic Receptors Zinc(II)–Bis(cyclen) Complexes (Cyclen = 1,4,7,10-Tetraazacyclododecane). *J. Am. Chem. Soc*. **2000**, *122*, 4542–4548. (d) Kikuta, E.; Aoki, S.; Kimura, E. A New Type of Potent Inhibitors of HIV-1 TAR RNA–Tat Peptide Binding by Zinc(II)–Macrocyclic Tetraamine Complexes. *J. Am. Chem. Soc*. **2001**, *123*, 7911–7912.

(85) (a) Harrisson, P.; Morris, J.; Marder, T. B.; Steel, P. G. Microwave-Accelerated Iridium-Catalyzed Borylation of Aromatic C–H Bonds. *Org. Lett.* **2009**, *11*, 3586–3589. (b) Wang, Z.; Sun, J.; Jia, X. Self-Immolative Nanoparticles Triggered by Hydrogen Peroxide and pH. *J. Polym. Sci., Part A: Polym. Chem.* **2014**, *52*, 1962–1969.

(86) Cao, S.; Wang, Y.; Peng, X. The Leaving Group Strongly Affects H_2O_2-Induced DNA Cross-Linking by Arylboronates. *J. Org. Chem.* **2014**, *79*, 501–508.

(87) Notni, J.; Görls, H.; Anders, E. Zinc Thiolate Complexes $[ZnL_n(SR)]^+$ with Azamacrocyclic Ligands: Synthesis and Structural Properties. *Eur. J. Inorg. Chem.* **2006**, *48*, 1444–1455.

(88) Wiedemann, T.; Voit, G.; Tchernook, A.; Roesle, P.; Göttker-Schnetmann, I.; Mecking, S. Monofunctional Hyperbranched Ethylene Oligomers. *J. Am. Chem. Soc.* **2014**, *136*, 2078–2085.

Acknowledgement

本研究の遂行ならびに本論文の執筆に際して、６年間終始熱心な御指導、御鞭撻を賜りました東京理科大学薬学部　青木 伸 教授に深謝申し上げます。

本論文の副査をして頂き、適切な御助言を賜りました東京理科大学薬学部　秋本 和憲 教授、月本 光俊 教授、和田 猛 教授、ならびに東京理科大学理学部　倉持 幸司 教授に厚く御礼申し上げます。

前 東京理科大学薬学部助教 久松 洋介 先生（現 名古屋市立大学医薬学総合研究院（薬学）講師）ならびに、嵯峨 裕 先生（現 大阪大学大学院工学研究科 助教）には数々のご指導、御助言をいただきました。心より感謝申し上げます。

東京理科大学薬学部助教　田中 智博 先生には研究遂行にあたり数々のご指導ならびに貴重な御助言をいただきました。心より感謝申し上げます。

前 東京理科大学薬学部ポストドクトラルフェロー Babita Shashni 先生（現 筑波大学数理物質系 特任助教）、Chandrasekar Balachandran 先生（現 東京理科大学生命医科学研究所助教）には細胞実験に関するご指導や英語でのディスカッションを行っていただきました。心より感謝申し上げます。

前 日本学術振興会 外国人特別研究員 Jebiti Haribabu 先生（現 University of Atacama ポストドクトラルフェロー）には英語でのディスカッションを行っていただきました。心より感謝申し上げます。

中性子線照射実験に関する御助言ならびに新型コロナウィルス感染拡大に伴いメールインサービスでの細胞照射実験を快く引き受けていただきました京都大学複合原子力科学研究所 鈴木 実 教授、櫻井 良憲 准教授に深く感謝申し上げます。

細胞内ホウ素量の測定においてICP-MSの使用方法・サンプル調製に関する御助言をいただきました東京理科大学薬学部 鍜冶 利幸 教授、前 東京理科大学薬学部助教 吉田 映子 先生（現 電力中央研究所 主任研究員）に深く感謝申し上げます。

質量分析を引き受けてくださいました前 東京理科大学薬学部質量分析室 長谷川 富貴子 技術専門職員、東京理科大学薬学部質量分析室 吉村 弥生 技術専門職員に深く感謝申し上げます。

NMR 測定法をご教示いただきました前 東京理科大学薬学部核磁気共鳴分析室 澤邉

紀子 技術専門職員、松田 諭 技術専門職員、東京理科大学薬学部核磁気共鳴分析室 飯田 基雄 技術専門職員に深く感謝申し上げます。

元素分析を引き受けてくださいました前 東京理科大学研究推進機構研究機器センター 中村 里子 技術専門職員、東京理科大学研究推進機構研究機器センター 倉持 裕生 技術専門職員に深く感謝申し上げます。

私の研究生活を支えていただきました同級生（今福 浩輝氏、萱野 蒔人氏、関根 禎亮氏、内藤 佳奈氏、横井 健汰氏）に心より御礼申し上げます。

多くの有益な御助言を賜り、研究生活を支えていただきました先輩方（Abdullah Masum 博士、伊藤 太基博士、染谷 英寿博士、宮澤 有哉博士、Akib Bin Rahman 博士、関口 康氏、西 友里恵氏、松本 和恵氏、宮内 美樹氏、朱 俊傑氏、加藤 萌氏、菊池 千陽氏、田村 佳氏、田村 裕一氏、寺岡 達朗氏）に深く感謝申し上げます。

いつも温かく接して私の研究生活を支えていただきました後輩たち（2017 年度: 水野 皓介氏、安藤 涼輔氏、風間 彩水氏、口石 博斗氏、小林 由佳氏、佐藤 秀哉氏、直井 竜大氏、廣瀬 真澄氏、2018 年度: 川端 凌矢氏、清水 舜氏、関 健仁氏、中川 聖也氏 2019 年度: 石上 剛大氏、内山 遥氏、小山田 有沙氏、芝内 涼太氏、山口 晃平氏、2020 年度: 藤田 絢子氏、森田 都望恵氏、岡本 紘知氏、笠井 貴文氏、神戸 梓氏、2021 年度: 磯部 理沙氏、宮内 奈津子氏、垣花 真輝氏、川本 健太氏、新居 真由香氏）に心より感謝申し上げます。

筆末ながら、私の研究活動を温かく応援し支えてくださいました家族、友人に厚く御礼申し上げます。

2022 年（令和 4 年）2 月

東京理科大学大学院　薬学研究科薬科学専攻

生物有機化学研究室

上田 大貴

List of Publications

主論文を構成する論文

1. Design, Synthesis, and Biological Evaluation of Boron-Containing Macrocyclic Polyamines and Their Zinc(II) Complexes for Boron Neutron Capture Therapy
（ホウ素中性子捕捉療法のための含ホウ素大環状ポリアミン誘導体と亜鉛錯体の設計、合成および生物学的評価）
Hiroki Ueda, Minoru Suzuki, Reiko Kuroda, Tomohiro Tanaka, and Shin Aoki
Journal of Medicinal Chemistry, Vol. 64, 8523–8544 (2021 年 6 月)
DOI: 10.1021/acs.jmedchem.1c00445

2. Design, Synthesis and Biological Evaluation of Boron-Containing Macrocyclic Polyamine Dimers and Their Zinc(II) Complexes for Boron Neutron Capture Therapy
（ホウ素中性子捕捉療法のための含ホウ素大環状ポリアミン二量体と亜鉛錯体の設計、合成および生物学的評価）
Hiroki Ueda, Minoru Suzuki, Yoshinori Sakurai, Tomohiro Tanaka, and Shin Aoki
European Journal of Inorganic Chemistry, 2022, e202100949 (2022 年 2 月)
DOI: 10.1002/ejic.202100949

参考論文

1. Design and synthesis of boron containing monosaccharides by the hydroboration of D-glucal for use in boron neutron capture therapy (BNCT)
（D-グルカールのヒドロホウ素化を利用した、ホウ素中性子捕捉療法のための含ホウ素単糖誘導体の設計および合成）
Taiki Itoh, Kei Tamura, Hiroki Ueda, Tomohiro Tanaka, Kyouhei Sato, Reiko Kuroda, and Shin Aoki
Bioorganic & Medicinal Chemistry, Vol. 26, No. 22, 5922-5933 (2018 年 10 月)
DOI: 10.1016/j.bmc.2018.10.041